UNIVERSITÀ DEGLI STUDI DI MILANO

FACOLTÀ DI SCIENZE MATEMATICHE, FISICHE E NATURALI

DIPARTIMENTO DI CHIMICA

DOCTORATE COURSE IN CHEMISTRY

XXIX CYCLE, CHIM/06

DESIGN AND SYNTHESIS OF MODIFIED PEPTIDE NUCLEIC ACID (PNAs) WITH IMPROVED PHYSICO-CHEMICAL PROPERTIES FOR DNA, RNA AND MICRO RNA TARGETING

PRAMOD R. THAKARE

Matr. N. R10770

TUTOR: PROF. SSA EMANUELA LICANDRO

CO-TUTOR: DR. SILVIA CAUTERUCCIO

CO-ORDINATOR: PROF. SSA EMANUELA LICANDRO

2014-2016

UNIVERSITÀ DEGLI STUDI DI MILANO
DIPARTIMENTO DI CHIMICA

CERTIFICATE

This is to certify that the work incorporated in the thesis entitled ***"Design and synthesis of modified Peptide Nucleic Acid (PNAs) with improved physico-chemical properties for DNA, RNA and Micro RNA targeting"*** which is being submitted to the ***University of Milan*** for the award of ***Doctor of Philosophy*** in ***Chemistry*** by ***Mr. Pramod R. Thakare*** was carried out by him under my supervision at the University of Milan, Milan. Research material obtained from other sources has been duly acknowledged in the thesis.

Emanuela Licandro

December 2016 **Prof.ssa Emanuela Licandro**

Milan (Research Supervisor)

Dipartimento di Chimica, Prof.ssa Emanuela Licandro, Via Golgi, 19 – 20133 Milano (Italy)
Tel: +39.0250314143 Fax: +39.0250314139, E-mail: emanuela.licandro@unimi.it

CANDIDATE'S DECLARATION

I hereby declare that the thesis entitled ***"Design and synthesis of modified Peptide Nucleic Acid (PNAs) with improved physico-chemical properties for DNA, RNA and Micro RNA targeting"*** submitted for the degree of ***Doctor of Philosophy*** in ***Chemistry*** to the ***University of Milan*** has been carried out at Chemistry department, University of Milan, under the supervision of Prof.ssa Emanuela Licandro. This work is original and has not been submitted in part or full by me for any degree or diploma to this or any other university.

December 2016

Milan

Pramod R. Thakare

Department of Chemistry

University of Milan,

Via Camillo Golgi 19, 20133

Milan, Italy

Dedicated to…

My beloved Parents, sister

and to my lovely wife…

Acknowledgements

Though only my name appears on the cover of this dissertation, many others have contributed to its production. I therefore take this opportunity to thanks all those people from the bottom of my soul, who have made this thesis possible and because of whom my Ph.D. experience has been one that I will cherish for the rest of my life.

First and foremost, my hearty thanks and deep sense of gratitude to my research supervisor ***Prof. Emanuela Licandro*** *at the first place for believing in my abilities and providing me an incredible opportunity to pursue my career as a Ph.D. student. I thank her for excellent guidance, constant encouragement, motivation, sincere advice, understanding and unstinted support during all the times of my Ph.D. life. My interactions with her have improved my belief towards research as well as real life. I consider very fortunate for my association with her, which has given a decisive turn and a significant boost in my career. I can never forget* ***Prof. Stefano Maiorana,*** *for his valuable suggestions and encouragement. He has helped me many occasions including inviting some non-lab friends to give me company. He also invited us to visit his company Promidis and allowed us to interact with their research group and also organise a wonderful lunch party @ chinese restaurant.*

I am also grateful to my co-tutor ***Dr. Silvia Cauteruccio*** *without her support; this thesis would not have been possible. Her suggestions and encouragement has been an immense help during my research period.*

I am indebted in gratitude to ***Dr. Clara Baldoli****. Apart from the scientific front, I have really enjoyed our day by day discussions, her constant support and presence, a witty remark and lots more. She taught me Italian words like "Ciao...Buongiorno…come va…Buonasera…Buon appetito." She always created a sweet and friendly atmosphere in the lab and has never stopped going farther to help especially in difficult times.*

I have been extremely fortunate to have supervisors who not only educated me in chemistry; but also taught me discipline and shown unique ways to achieve my goals. This has helped me to overcome many obstacles along the path of my Ph.D. The humanity and scientific curiosity were a constant source of inspiration. I am grateful to have been part of Prof.

Licandro, Prof. Maiorana and Dr. Baldoli research group; I feel so lucky to do work with those great scientists as well as great human being.

I would like to thanks our collaborators Prof. Guido Viscardi and Dr. Nadia Barbero (Department of Chemistry and NIS Interdepartmental Centre, University of Torino, Italy) for performing the kinetic studies by stopped-flow fluorescence instrument, Dr. Daniela Maggioni and her groups (Department of Chemistry, University of Milano, Italy) for studying and characterization of MNP with PNA and Dr. Alberto Bossi (CNR-ISTM, Milano) for performing the optical characterization and photoluminescence emission studies.

I would like to thanks to Lara de Benassuti for teaching me NMR instrument from the beginning and she always helped me for performing the Mass spectra and equally thanks to Teresa Recca for analysing the Q-Tof analysis also thanks to Dr. Anna Daghetti and Manuela Gilberti for MALDI-TOF analysis.

I express my profound gratitude to Prof. Sabrina Dallavalle and Dr. Loana Musso for their support to get the documents from university of Milan, for my visa to get into Italy.

I would like to thanks to Dr. Giulia M. Rossignolo. She has helped me do get my Italian codice fiscale and other important documentation. She also helped me in many circumstances at different times as a colleague in laboratory.

I extend my thanks to Dr. Claudio Carrara who helped me in many occasions as a translator and for being such a nice colleague. I thanks to for all my colleagues in the laboratory for their valuable discussions, suggestions, support and their friendly nature in laboratory, especially Dr. Davide Dova he always helped me in lab and Dr. Lucia Viglianti as a best colleague.

With much appreciation I would like to mention the crucial role of my charming labmates Chiara Briguori, Silvia Farina, Susan Sammak, Kasia Fidecka, Valentina Pelliccioli, Federica Campanella, Simona Todisco, Maryam Fallah, Laura Libani, Andrea Ghiglioni, Luigi Menduti, Alessandro Gotti, Ivan Andreosso for their cooperation, friendly attitude and cheerful atmosphere in lab. It has been a great learning experience for me through our group seminar.

I would like to thanks to Technical and Administrative Staff, Chemistry Department, University of Milan for their cooperation.

I am also sincerely thankful to my friends Atul, Chetan, Harsha and Rahul from Milan. Sagar, Suresh, Rakesh and his family and remaining friends in Italy which made my stay in Italy, very enjoyable and memorable.

It gives me great pleasure to express my deep sense of esteem gratitude to my supervisors in India. Specially ***Dr. Subhash Chavan*** *(Senior Scientist, NCL, Pune) and* ***Dr. Santosh Mhaske*** *(Scientist, NCL, Pune) for their inspiring guidance, never diminishing encouragement, support and their complete dedication during the progress of my research project. They provide me excellent environment in research which creates an enthusiasm in me to do further research. I also would like to thanks* ***Dr. Sharad Shelke*** *(Assistant Professor, S.S.G.M. College, Kopargaon) for gave me nice opportunity to do work under his valuable guidance during my master degree.*

My feeling go beyond the limit in acknowledging ***Dr. H. B. Borate*** *and* ***Dr. Vandana S. Pore*** *(Senior Scientists, NCL, Pune), who indeed patiently helped me in research as with their expertise. I owe a very special word of gratitude to* ***Dr. U. R. Kalkote*** *(Former Scientist, NCL, Pune) for his time to time suggestions, help and encouragement.*

I also consider myself blessed because; I spend a major time for almost four years in National Chemical Laboratory (NCL), which is one of the finest and immense research institute in India. I would like to thanks all my seniors and friends from NCL who directly and indirectly play important role in my life, particularly I would like to thanks to Dr. Lalit Khairnar, Dr. Kishor Harale, Dr. Nilesh Dumare, Dr. Sumanta Garai, Dr. Pradeep Lasonkar, Dr. Prakash Chavan, Dr. Kailash Pawar, Dr. Harshali Khatod and Mr. Pankaj Mahajan, Mr. Sanket, Appasaheb, Nitin, Dinesh, Sandip, Ranjeet, Yogeshwar, Jaysingh and Mrs. Jyoti with whom I started my research experience.

I would like to acknowledge my Teachers from Kopargaon and Satana College during my post graduation and graduation for their inspiring guidance and support Dr. Karale, Dr. Nikumbh, Dr. Kulkarni, Dr. Sangle, Mr. Chaudhary, Mr. Chavan, Mrs. Randhavane, Dr. Pawar, Dr. Shah, Dr. Pagar, Mr. Gunjal, Mr. Hire and Mr. Zoman throughout my tenure in Kopargaon and Satana College. No words can suffice to acknowledge my prized friends, classmates & best buddies Dr. Bhushan, Mr. Dinesh, Narendra, Amol, Yogesh, Rahul, Sandip, Nilesh, Jalindar and Muralidhar for helping me in various aspects of life as well as work.

My family is always source of inspiration and great moral support for me in perceiving my education, it is impossible to express my sense of gratitude for my family, ***AAI*** *and* ***AANNA****. Whatever I am and whatever I will be in future is because of their enormous blessings, hard work, commitments to my ambitions, and their selfless sacrifices. It was their single minded pursuit of the cause of my education that gave me the strength and will continue to guide my future. Although this eulogy is insufficient, I preserve an everlasting gratitude for them. Words fall short to thank my sister Mrs. Madhuri (Mai) for her support, help and never ending encouragement. I really grateful to have nephews like Siddhesh (siddhu) and Gauri (didi) who are full of happiness, Joy and Curiosity, they brought everlasting cheerfulness in my life. I wish to thank Dhanashri, my wife, for her love, affection and support extended to me during last year and she has brought a great deal of happiness and positive change to my life. Her patience and selfless sacrifice will remain my inspiration throughout my life. Without her help, I would not have been able to complete much of what I have done and become who I am.*

I wish to thanks to the coordinator Prof. Emanuela Licandro and head of the chemistry department Prof. Francesco Demartin for giving me the opportunity and providing all necessary infrastructure and facilities. I acknowledge the University of Milan for providing me financial support.

It has never been my intention to hurt anyone's feeling knowingly and unknowingly. In spite of my efforts, if I have caused any inconvenience to anyone, my apologies for the same.

Pramod Ramesh Thakare

Department of Chemistry,
University of Milan, ITALY.

CONTENTS

Chapter 2: Design and synthesis of modified peptide nucleic acids (PNAs) with and without fluorescein isothiourea and its kinetic studies by using stopped-flow technique.

Chapter 4: Design and synthesis of modified thymine monomer PNA and homothymine decamer PNA sequence with gold(I) complexes for cellular imaging.

Abbreviations

A:	Adenine
Ac:	Acetyl
Ac_2O:	Acetic anhydride
aeg:	Aminoethylglycine
aeg[STD]-PNA:	Aminoethylglycine standard sequence PNA
aeg[T]10-PNA:	Aminoethylglycine homothymine PNA
aq.:	Aqueous
Boc:	tert-Butyloxycarbonyl
Boc-aeg-PNA-OH:	N(Boc)-aminoethylglycine PNA monomer carboxylic acid
Boc-Lys(Fmoc)-OH:	N(α)Boc-N(ε)Fmoc-lysine carboxylic acid
C:	Cytosine
Cbz:	Benzyloxycarbonyl
$CDCl_3$:	Deuterated chloroform
COSY:	Correlation spectroscopy
Cys:	Cysteine
cm:	Centimetre
DCM:	Dichloromethane
DMF:	Dimethylformamide
DMSO:	Dimethylsulfoxide
DIPEA:	N,N-Diisopropylethylamine
DMAP:	N,N-Dimethyl-4-aminopyridine
DMSO-d_6:	Deuterated dimethylsulfoxide
DNA:	Deoxyribonucleic acid
E.S.I.:	Elemental analysis
Et_2O:	Diethyl ether
EtOAc:	Ethyl acetate
EDC.HCl:	N-(3-Dimethylaminopropyl)-N′-ethylcarbodiimide hydrochloride
FG:	Functional group
FITC:	Fluorescein isothiocyanate
FITU:	Fluorescein isothiourea

Fmoc:	9-Fluorenylmethoxycarbonyl
FTIR:	Fourier transform infrared spectroscopy
G:	Guanine
Gm:	gram
Hr:	Hour
HATU:	O-(7-Azabenzotriazol-1-yl)-N,N,N',N'-tetramethyluronium hexafluorophosphate
HBTU:	O-(Benzotriazol-1-yl)-N,N,N',N'-tetramethyluronium Hexafluorophosphate
HOBt:	N-Hydroxybenzotriazole
HPLC:	High performance liquid chromatography
HSQC:	Heteronuclear single quantum correlation
KF:	Potassium fluoride
Lys:	Lysine
MALDI-TOF:	Matrix assisted laser desorption ionization – Time of flight
MBHA:	4-Methylbenzhydrylamine hydrochloride salt
MFH:	Magnetic fluid hyperthermia
MNP:	Magnetic nanoparticle
MP:	Melting point
MW:	Molecular weight
MRI:	Magnetic resonance imaging
miRNA:	Micro ribonucleic acid
mg:	milligram
MHz:	Megahertz
Min:	minutes
µL:	Microliter
µM:	Micromolar
mL:	milliliter
mM:	millimolar
mmol:	millimoles
mm:	Millimetre
MeOH:	Methanol
NCO:	Isocyanate
NMP:	*N*-Methylpirrolidone

NMR:	Nuclear magnetic resonance
NP:	Nanoparticle
Nm:	nanometre
NHS:	*N*-Hydroxysuccinimide
PABA:	*p*-Aminobenzoic acid
PCR:	Polymerase chain reaction
$PhCH_3$:	Toluene
PMBA:	*p*-Maleimidobenzoic acid
PMB-Cl:	*p*-Maleimidobenzoyl chloride
PMP-AZIDE:	*p*-Maleimidobenzoyl azide
PMPI:	*p*-Maleimidophenyl isocyanate
PNA:	Peptide nucleic acid
Py:	Pyridine
Q-TOF MS:	Quadrupole time-of-flight mass spectrometer
RNA:	Ribonucleic acid
Rf:	Retention factor
RP:	Reverse Phase (-HPLC)
Rt:	Room temperature
RT:	Retention time
SPION:	Superparamagnetic iron oxide nanoparticle
SPR:	Surface Plasmon resonance
SPPS:	Solid Phase Peptide Synthesis
T:	Thymine
TEA/Et3N:	Triethylamine
TFA:	Trifluoroacetic acid
TFMSA:	Trifluoromethanesulfonic acid
THF:	Tetrahydrofuran
Tm:	Melting temperature
TPP:	Triphenylphosphine (PPh3)
TPPTS:	Triphenylphosphine-3,3′,3″-trisulfonic acid trisodium salt
TMSCl:	Trimethylsilyl chloride
UV-Vis:	Ultraviolet-visible spectroscopy

Abstract of the thesis

Note: Compound numbers in the abstract are different from those in the thesis.

Abstract

The thesis entitled **"Design and synthesis of modified Peptide Nucleic Acid (PNAs) with improved physico-chemical properties for DNA, RNA and Micro RNA targeting"** is divided into four chapters. Chapter one deals with the introduction to Peptide Nucleic Acid (PNA) its properties and its applications. The second chapter deals with the synthesis of modified PNAs with and without fluorescein isothiourea and its kinetic studies by using stopped-flow technique. The third chapter deals with the design, synthesis and characterization of functionalized PNAs with heterobifunctional linker and their conjugation with magnetic nanoparticles (MNPs) for miRNA targeting. The fourth chapter deals with design and synthesis of modified thymine monomer PNA and homothymine decamer PNA sequence with gold(I) complexes for cellular imaging.

Chapter 1: Peptide Nucleic Acid (PNA)

Peptide nucleic acids (PNA) are DNA analogues in which the sugar phosphate backbone is replaced by repetitive units of *N*-(2-aminoethyl) glycine subunits. PNAs exhibit unique properties that set them apart from other traditional DNA analogues they are achiral, neutral with high chemical and biochemical stability. They hybridize to complementary DNA, RNA or PNA sequences according to the Watson-Crick base-pairing rules and leading to PNA-DNA duplexes are more stable than DNA-DNA duplexes. These favourable features have led to application of PNAs in various research areas such as antisense and antigene therapies, molecular biology and functional genomics, PNA as a probe for diagnosis and detection and PNA as a biosensor (Figure 1)

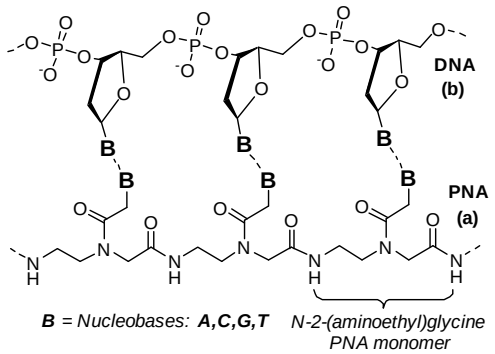

Figure 1: Peptide Nucleic Acid oligomer (a) with its complementary DNA (b)

PNA Applications

The potential applications of PNAs can be divided in three different fields like diagnostics, molecular biology and therapy. It is important to notice that new techniques are continuously being developed. However, some techniques are very important because they represent "historically" steps in the development and use of PNAs. The stability of PNA/DNA complexes makes PNAs powerful tools in antisense and antigene applications, and as markers in DNA screening assays. The major drawbacks of PNA are like poor water solubility, inefficient cell uptake, self-aggregation and uncertainty in directionality of binding restricts PNA extensive applications.

Chemical Modifications of PNA

The major limitations of the therapeutic applications of PNAs are their poor solubility in aqueous media due to self-aggregation and an insufficient cellular uptake. In order to improve PNA solubility in aqueous media, the cellular uptake, the binding selectivity towards RNA versus DNA, or to stabilise duplex or triplex structures, several analogues of modified PNA have been synthesised over the years.

Aim of the thesis

This research work concerns with the design, synthesis, characterization and analytical studies of newly modified Peptide Nucleic Acids (PNAs), [which is mimic of DNA and RNA] in non conventional manner for the applications in DNA interactions, RNA targeting and cellular imaging.

Chapter 2: Design and synthesis of modified peptide nucleic acids (PNAs) with and without fluorescein isothiourea and its kinetic studies by using stopped-flow technique.

Synthesis of aminoethylglycine PNA monomer and PNA decamers

In the present section, the synthesis of newly modified lysine based Peptide Nucleic Acids (PNA) decamer **1**, with the TCACTAGATG sequence of nucleobases, and the corresponding fluorescent PNA-FITU (fluorescein isothiourea) decamer **2** were synthesized with standard manual Boc-based chemistry using MBHA resin loaded with the N(α)-Boc-N(ε)-Fmoc-*L*-lysine (Figure 2) The interaction of both decamers **1** and **2** with the complementary parallel and antiparallel DNA was followed by steady-state and stopped-flow fluorescence intensity. The kinetics of the PNA-DNA duplex formation has been studied. In particular, fluorescence stopped-flow technique has been exploited to compare the affinity of two PNA-DNA

duplexes: using parallel and antiparallel DNA, such data would be very important for the evaluation and improvement of antisense reagents and of diagnostic probes based on PNA.

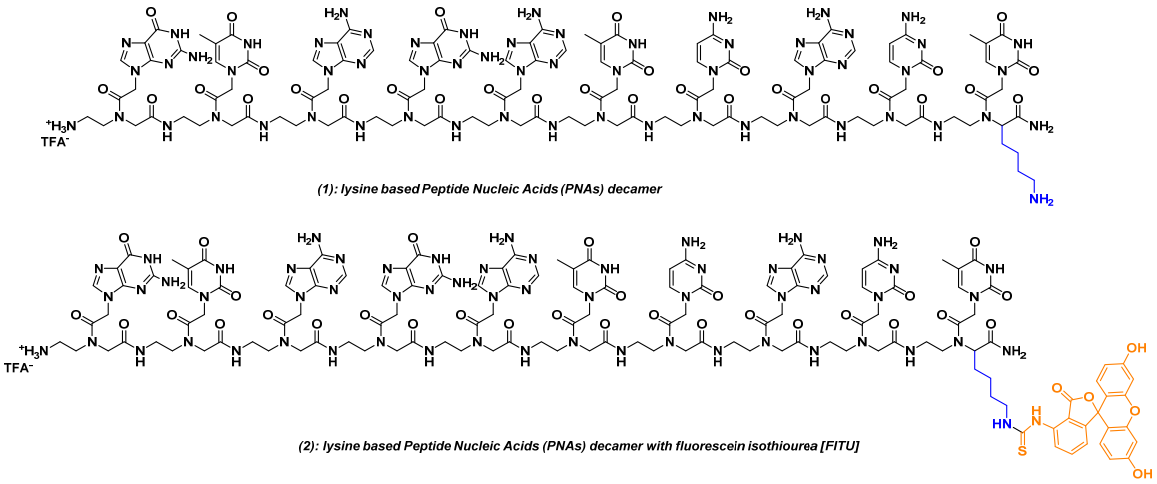

Figure 2: Synthesis of Peptide Nucleic Acids (PNAs) decamer **(1)** and **(2)**

Kinetic studies of PNA: DNA duplexes by fluorescence Stopped-flow technique

The interaction of both decamers **1** and **2** with the complementary parallel and antiparallel DNA was followed by steady-state and stopped-flow fluorescence intensity. The kinetics of the PNA-DNA duplex formation has been studied. In particular, fluorescence stopped-flow technique has been exploited to compare the affinity of two PNA-DNA duplexes: using parallel and antiparallel DNA, such data would be very important for the evaluation and improvement of antisense reagents and of diagnostic probes based on PNA.

Chapter 3: Design, synthesis and characterization of functionalized PNAs with heterobifunctional linker and their conjugation with magnetic nanoparticles (MNPs) for miRNA targeting.

Introduction to Magnetic nanoparticles and its properties

Magnetic nanoparticles (MNPs) are a class of nanoparticles which can be manipulated using magnetic fields. The particles are made of magnetic elements such as iron, nickel and cobalt or their chemical compounds. During the past decade magnetic nanoparticles have been intensively studied, not only for general scientific interest but also due to the large number of their possible applications, such as catalysis, biomedicine, magnetic resonance imaging, data storage and environmental remediation.

The physical and chemical properties of magnetic nanoparticles largely depend on the synthesis method and on their chemical structure. In most cases, their size range from 1 to

100 nm, that is the size range necessary for them to display superparamagnetism. In a more general way, the properties of the nanocrystals strongly depend upon the dimension of the nanoparticles. Therefore it is important to control their proprieties and studies related to fluid stability, control of surfactants, particle sizes, materials, and physical behaviour are essential to understand ferrofluid behaviour to improve applications or develop new nanoparticles (Figure 3).

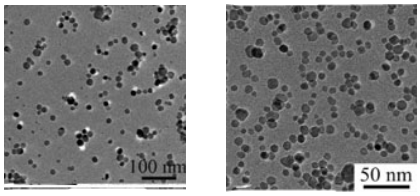

Figure 3: TEM imaging of iron nanoparticles.

In the present section we focused our attention on to the design, synthesis and characterization of functionalized PNA **3** with heterobifunctional linker and their conjugation with magnetic nanoparticles **4** (MNPs) for miRNA targeting. The MNPs bound to PNA can be exploited both as contrast agents for magnetic resonance imaging (MRI) and as sources of local overheating through the application of an alternating magnetic field (Magnetic Fluid Hyperthermia, MFH). Moreover, the microRNAs targeting ability of these tools for selectively delivering magnetic nanoparticles and destroying, by hyperthermia, targeted cells in multicellular organisms. (Figure 4)

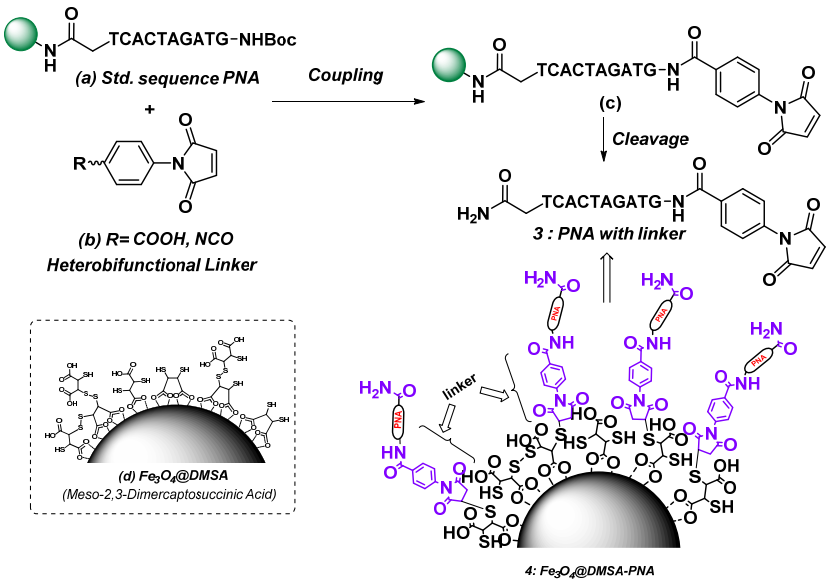

Figure 4: Functionalisation of magnetic nanoparticles with PNA through heterobifunctional linker.

Chapter 4: Design and synthesis of modified thymine monomer PNA and homothymine decamer PNA sequence with gold(I) complexes for cellular imaging.

In the present section we focused our attention on to the design and synthesis of modified Thymine monomer and PNA decamer with simple organometallic gold(I) complexes which is applicable for cellular imaging. Here we introduce Phosphine gold(I) on to the thymine monomer **5** and homothymine decamer PNA containing the triple bond **6** at the terminal position (Figure 5). The development of gold (I)-acetylide complexes has led to several novel compounds. Most notably they have been investigated for their interesting photochemical properties or rich luminescence properties. Luminescence from gold-acetylide complexes typically results from "aurophilicity".

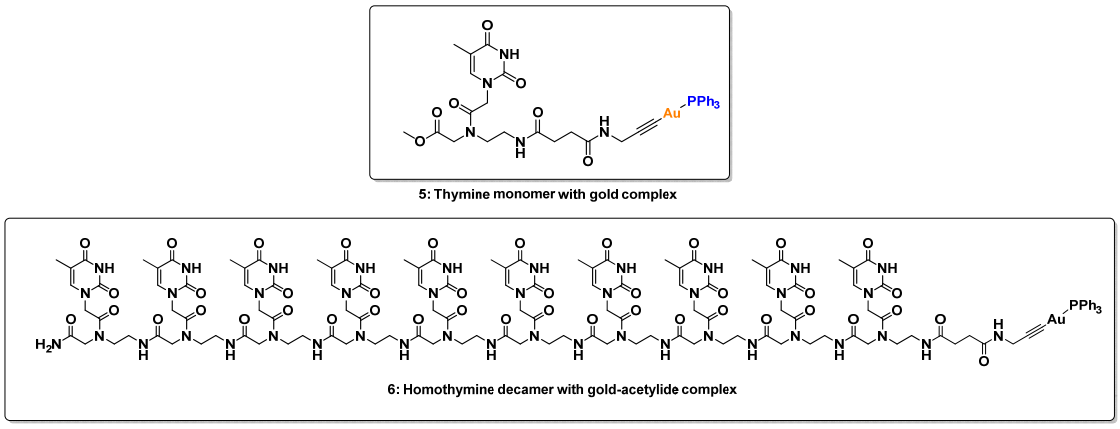

Figure 5: Thymine monomer **5** and homothymine 10-mer PNA **6** with gold complex

Synthesis of modified thymine PNA monomer (5)

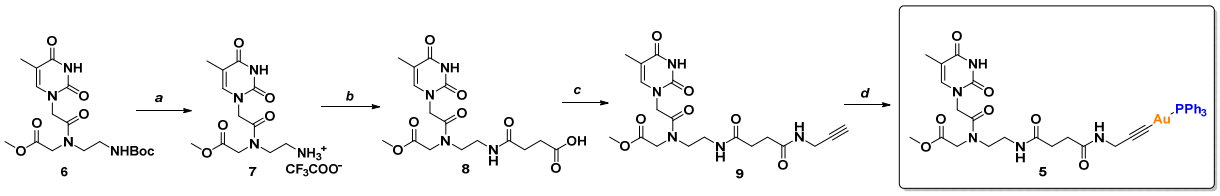

Scheme 1: Reagents and conditions: *a) 20% TFA, DCM, 0 ^{o}C - rt, 12 hr, 96%; b) succinic anhydride, DIPEA, DMF, 0 ^{o}C - rt, 12 hr, 70%; c) propargyl amine, EDC.HCl, DMF, rt., 12 hr, 82% ; d) Phosphine gold chloride, KOtBu, MeOH, rt, 12 hr, 24%.*

Synthesis of gold complex with homothymine PNA oligomer (6) on solid support

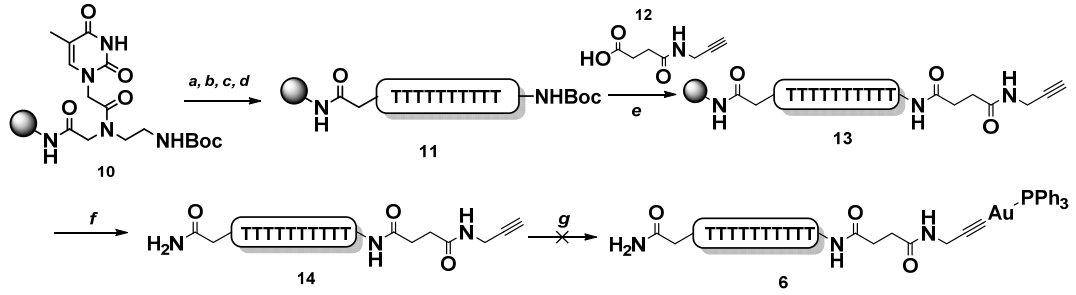

Scheme 2: Reagents and conditions: *a) TFA/m-cresol, 95:5; b) CH_2Cl_2/DIPEA, 95:5; c) thymine monomer, HATU, DIPEA, NMP; d) Ac2O/Pyridine/NMP 1:25:25; e) 12, HATU, DIPEA, NMP, 12 hr; f) Cleavage; g) PPh_3AuCl, KOtBu, MeOH, rt.*

We have successfully synthesized phosphine gold complex of thymine monomer **5** in solution phase and studied its photoluminescence emission properties and which are applicable in cellular imaging.

Chapter 1: Peptide Nucleic Acid (PNA)

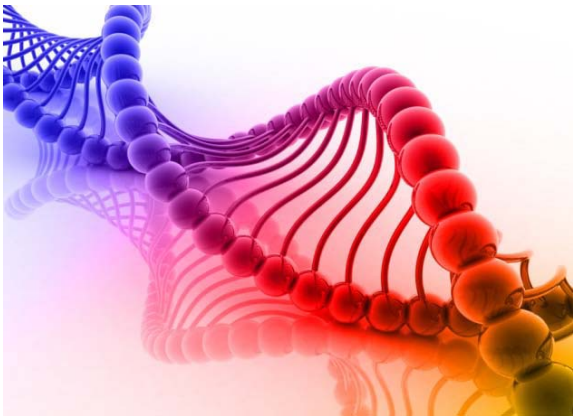

Section 1: Introduction to Peptide Nucleic Acid (PNA) and its properties

1.1.1. Introduction

Peptide nucleic acids (PNAs), first introduced in 1991 by Nielsen and co-workers[1] at Copenhagen University, are a remarkable example of a simple, neutral and achiral whole backbone replacement, that has suppressed, in many ways, other attempts to mimic the native nucleic acid structures in terms of molecular recognition properties. PNAs are synthetic nucleic acid analogues with an achiral pseudopeptide backbone in which the phosphodiester backbone is replaced by repetitive units of *N*-(2- aminoethyl) glycine. On the backbone the purine and pyrimidine bases are attached *via* a methyl carbonyl linker. Usually, PNA is an oligomer of 6-15 monomeric units (Figure 1.1).

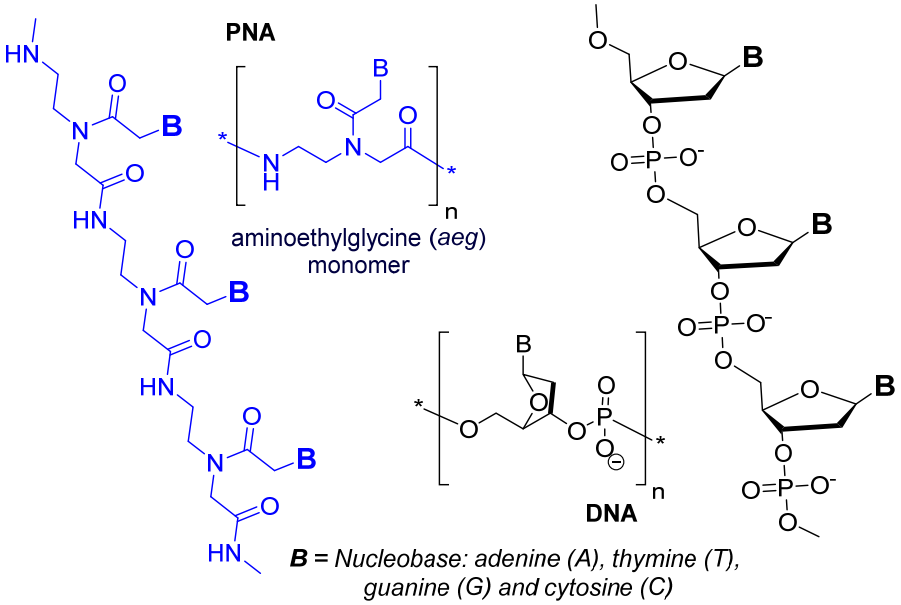

Figure 1.1: PNA (blue) versus **DNA** (black) oligomeric structures and in squared brackets are shown the repeating units

The PNA backbone maintains approximately the same length per repeating unit as in DNA or RNA. The appended nucleobases projects from the backbone to form stable double or triple helical complexes with target nucleic acids[2]. The internucleobase distance in PNA is conserved, so that it can bind to the target DNA or RNA sequences with high sequence specificity and affinity. Therefore, chemical terms they are neither proteins nor nucleic acids. The amide (or peptide) bonds in PNA are sufficiently different from the α-amino acid peptide bonds present in proteins, resulting that PNA is biologically stable. These non-natural characteristics make PNA oligomers highly resistant to protease and nuclease attacks[3]. Because PNAs have a neutral backbone, hybridization with target nucleic acids is not

affected by the interstrand negative charge electrostatic repulsions[4]. In addition, the absence of a repetitive charged backbone prevents PNAs from binding to proteins that normally recognize polyanions, avoiding a major source of nonspecific interactions and it is also found that PNAs are charge-neutral compounds and hence have poor water solubility compared with DNA. PNA solubility is also related to the length of the oligomers and to the purine/pyrimidine ratio. Some recent modifications, including the incorporation of positively charged lysine residues (carboxyl-terminal or backbone modification in place of glycine), have shown improvements in solubility while negative charges may also be introduced, especially in PNA/DNA chimeras, which will enhance the water solubility[5].

1.1.2. PNA interactions with single strand nucleic acids

a) Duplex

PNAs are able to hybridize to both complementary DNA and RNA targets in a sequence-specific manner to form PNA/DNA[6] (Figure 1.2) or PNA/RNA duplex structures, according to Watson-Crick hydrogen binding rules (Figure 1.3)[2, 7, 8]

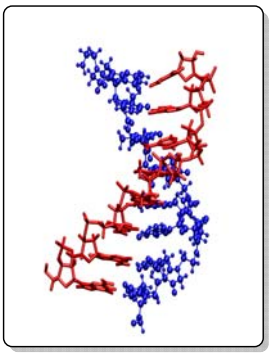

Figure 1.2: PNA/DNA duplex

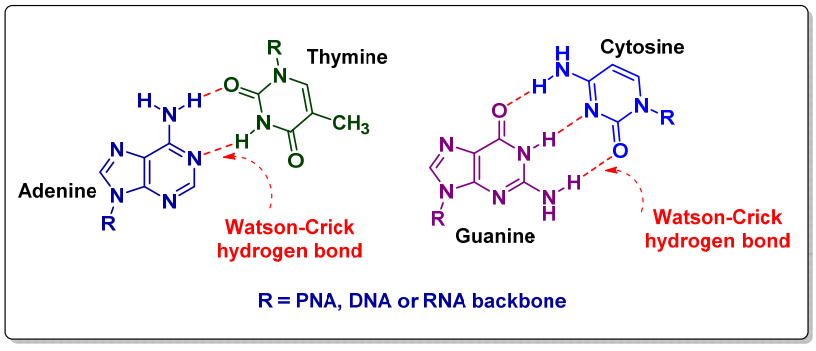

Figure 1.3: PNA/DNA duplex Watson-Crick hydrogen bonding paring rules

PNAs bind DNA/RNA in either parallel or antiparallel modes, the later being slightly preferred over the former. The antiparallel mode refers to the instance when the PNA 'N' terminus lies towards the 3'-end and the 'C' terminus lies towards the 5'-end of the complementary DNA/RNA oligonucleotides. Similarly, the parallel mode of binding is said to occur when the PNA 'N' terminus lies towards the 5'-end and the 'C' terminus towards the 3'-end of the complementary DNA/RNA oligonucleotide (Figure 1.4).

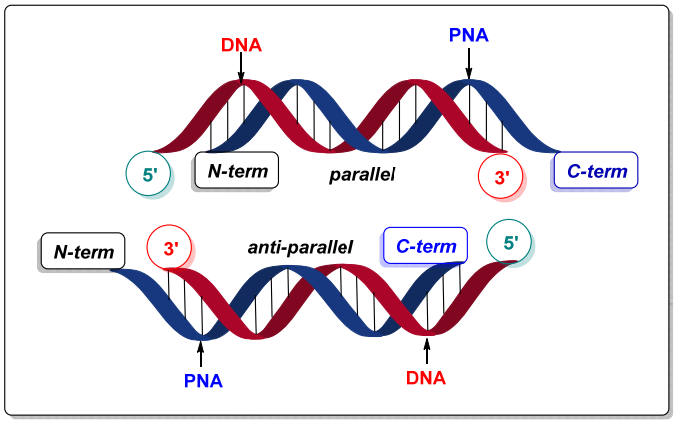

Figure 1.4: PNA/DNA binding in parallel (top) and antiparallel (bottom) modes.

b) Triplex

Homopyrimidinic PNAs strongly bind to target homopurine nucleic acids and sequence Specifically, forming of 2:1 PNA_2/DNA triplex (Figure 1.5).[9]

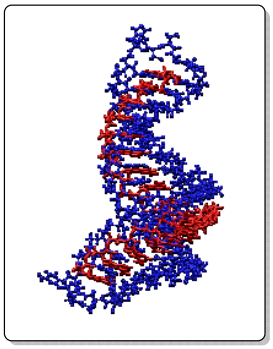

Figure 1.5: $(PNA)_2$/DNA triplex

This complex can be formed thanks to the ability of the homopyrimidine strand to bind PNA/DNA duplex by Hoogsteen hydrogen bonding scheme (Figure 1.6)

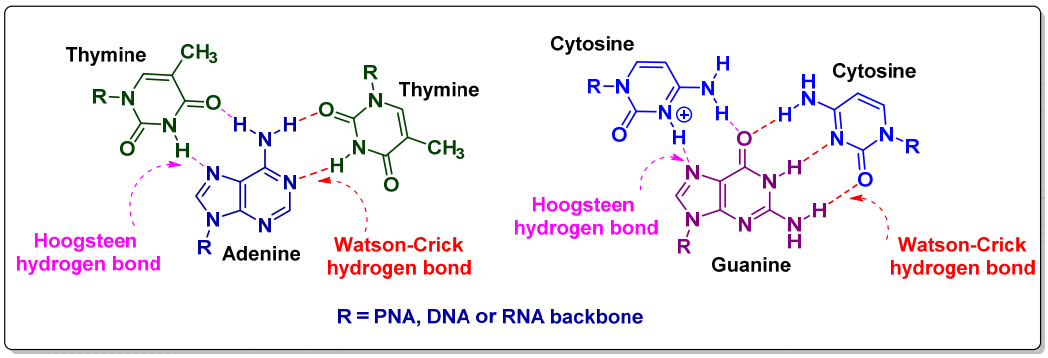

Figure 1.6: PNA/DNA triplex Hoogsteen and Watson-Crick hydrogen bonding paring rules.

c) Quadruplex

G-quadruplexes are four-stranded structures formed from DNA sequences that contain stretches of contiguous guanine bases, usually in the presence of alkali metal cations[10]. G-quadruplex DNA has been recently in focus because of its putative existence and its biological function at telomeres, which affects replication[11, 12], and in promoter sites influencing transcription[13]. The guanine bases in G-quadruplexes form G-tetrads where four G bases hydrogen bond via the Hoogsteen sites in a cyclic fashion (Figure 1.7)

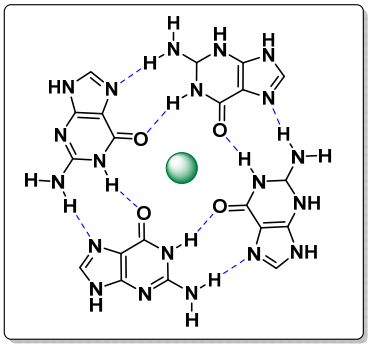

Figure 1.7: G-quadruplex in presence of an alkali metal cation.

In 2003 Prof. Datta reported[14] that homologous G-rich PNA and DNA oligomers hybridize to form a PNA_2-DNA_2 quadruplex. The hybrid quadruplex exhibits high thermodynamic stability and expands the range of molecular recognition motifs for PNA beyond duplex and triplex formation. After this study many research groups have reported the synthesis of PNA based G-quadruplex structures with different topologies, [15, 16] for instance a PNA_4 G-quadruplex,[17] a structure obtained from PNA-DNA chimeras[18] and even a PNA/RNA quadruplex.[19]

1.1.3. PNA interactions with double strands nucleic acids

The interaction of single-stranded PNA with double-stranded DNA is interesting not only because of his potential applications in antigene strategy but also for the possible use of PNA in different biotechnological applications (as discussed later). Various modes of interaction are possible, depending on sequences and conditions. (Figure 1.8) illustrates the triplex and duplex invasion modes, in which the targeting PNA breaks up the double helix and complexes with the complementary DNA strand.

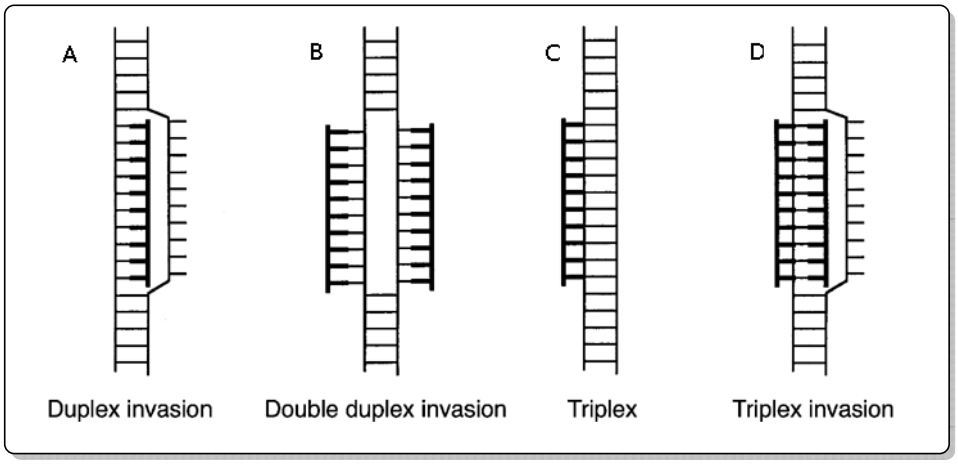

Figure 1.8: Duplex and triplex invasion modes.

Duplex invasion (Figure 1.8 A) can result if the target DNA is a homopyrimidine and the PNA has a homopurine sequence. Instead, if the DNA target is a homopurine sequence, it can result a very stable triplex invasion (Figure 1.8 D) complex. Synthesizing pyrimidine-PNAs as a palindrome sequence with a flexible linker in the middle creates a so-called bisPNA or "PNA clamp", allowing triplex formation in optimal directions with the Watson-Crick base pairing in an antiparallel and Hoogsteen bonding in a parallel orientation[20, 21]. However, the triplex invasion complex is very slow to form at neutral pH, unless the cytosine's in the "Hoogsteen-pairing" strand are exchanged to pseudo-isocytosines, also called J bases[20]. For practical applications, the rate of formation can be increased by using cationic PNAs (e.g., with extra lysine's linked) or by linking the PNA to an intercalating molecule such as 9-aminoacridine[22]. The most successful method to obtain a double-duplex invasion (Figure 1.8 B) is to use a pseudo-complementary PNA ($_{pc}$PNA) in which nucleobases adenine (A) and thymine (T) in conventional PNA are replaced with modified bases 2,6-diaminopurine (D) and 2-thiouracil (Us)[23].

1.1.4. Stability of PNAs and PNA complexes

Compared to normal DNA and RNA oligonucleotides, PNAs are much more stable inside cells. PNAs are very resistant to nuclease and protease digestion since nuclease cannot digest their altered backbones[3]. Furthermore, duplexes between PNA and DNA or RNA are in general more thermally stable than the corresponding DNA/DNA or DNA/RNA duplexes[24, 25]. The stability of PNA/DNA duplexes was studied by differential scanning calorimetry[26]. PNA/DNA duplexes show increased stability when the purines are in the PNA strand. It is also observed that the thermal stability of PNA/PNA duplexes exceeds that of PNA/RNA duplexes, that are already more stable than PNA/DNA duplexes. As a general rule, the ***Melting Temperature Tm*** (the temperature at which half of the PNA or DNA strands are in the double-helical state and half are in the random coil state) of a PNA/DNA duplex is 1 °C higher per base pair than the Tm of the corresponding DNA/DNA duplex. Very important, the stability of PNA/DNA duplexes are almost unaffected by the ionic strength of the medium.[2] PNA/DNA/PNA triplexes exhibit extraordinarily high stability (the thermal stability for a decamer is typically up to 70 °C).

1.1.5. Solubility of PNAs

As it said, PNAs are charge-neutral compounds and hence have poor water solubility compared with DNA. Neutral PNA molecules tend to aggregate, depending on the sequence of the oligomer. PNA solubility is also related to the length of the oligomer and to the purine/pyrimidine ratio[24]. Some recent modifications, including the incorporation of positively charged lysine residues (carboxyl-terminal or backbone modification in place of glycine), have shown improvements in solubility[27]. Negative charges may also be introduced, especially in PNA/DNA chimeras, which will enhance the water solubility[28].

1.1.5. Bibliography

1. Nielsen, P.; Egholm, M.; Berg, R.; Buchardt, O. *Science*. **1991**, *254*, 1497-1500.
2. Egholm, M.; Buchardt, O.; Christensen, L.; Behrens, C.; Freier, S. M.; Driver, D. A.; Berg, R. H.; Kim, S. K.; Norden, B.; Nielsen, P. E. *Nature*. **1993**, *365*, 566-8.
3. Demidov, V. V.; Potaman, V. N.; Frank-Kamenetskii, M. D.; Egholm, M.; Buchard, O.; Sonnichsen, S. H.; Nielsen, P. E. *Biochem Pharmacol.* **1994**, *48*, 1310-3.
4. Smulevitch, S. V.; Simmons, C. G.; Norton, J. C.; Wise, T. W.; Corey, D. R. *Nat Biotech.* **1996**, *14*, 1700-1704.

5. Shakeel, S.; Karim, S.; Ali, A. *J. Chem. Tech. & Biotech*. **2006**, *81*, 892-899.
6. Eriksson, M.; Nielsen, P. E. *Nat. Struct. Biol*. **1996**, *3*, 410-3.
7. Egholm, M.; Nielsen, P. E.; Buchardt, O.; Berg, R. H. *J. Am. Chem. Soc*. **1992**, *114*, 9677-9678.
8. Brown, S.; Thomson, S.; Veal, J.; Davis, D. *Science*. **1994**, *265*, 777-780.
9. Betts, L.; Josey, J. A.; Veal, J. M.; Jordan, S. R. *Science.* **1995**, *270*, 1838-1841
10. Gellert, M.; Lipsett, M. N.; Davies, D. R. *Proc. Natl. Acad. Sci. USA*. **1962**, *48*, 2013‑2018.
11. Hurley, L. H. *Nat. Rev. Cancer.* **2002**, *2,* 188-200.
12. Neidle, S.; Parkinson, G. *Nat. Rev. Drug. Discov.* **2002**, *1*, 383-393.
13. Siddiqui-Jain, A.; Grand, C. L.; Bearss, D. J.; Hurley, L. H. *Proc. Natl. Acad. Sci. USA.* **2002**, *99*, 11593-11598.
14. Datta, B.; Schmitt, C.; Armitage, B. *J. Am. Chem. Soc.* **2003**, *125*, 4111-4118.
15. Ghosh, Y.K.; Liu, D.; Balasubramanian, S. *J Am Chem Soc.* **2004**, *126*, 11009-16
16. Datta, B.; Bier, M. E.; Roy, S.; Armitage, B. *J Am Chem Soc.* **2005**, *127*, 4199-207.
17. Ghosh, Y. K.; Stephens, E.; Balasubramanian, S. *J Am Chem Soc.* **2004**, *126*, 5944-5.
18. Petraccone, L.; Pagano, B.; Esposito, V.; Randazzo, A.; Piccialli, G.; Barone, G.; Mattia, C.; Giancola, C. *J. Am. Chem. Soc.* **2005**, *127*, 16215-16223..
19. Marin, V.; Armitage, B.; *Biochemistry.* **2006**, *45*, 1745-1754.
20. Egholm, M.; Christensen, L.; Dueholm, K. L.; Buchardt, O.; Coull, J.; Nielsen, P. E. *Nucleic Acids Res.* **1995**, *23*, 217‑222.
21 Kuhn, H.; Demidov, V. V.; Nielsen, P. E.; Frank-Kamenetskii, M. D. *J. Mol. Biol.* **1999**, *286*, 1337-45.
22. Kuhn, H.; Demidov, V. V.; Frank-Kamenetskii, M. D.; Nielsen, P. E. *Nucleic Acids Res.* **1998**, *26*, 582-587.
23. Lohse, J.; Dahl, O.; Nielsen, P. E. *Proc Natl. Acad. Sci. USA*.**1999**, *96*, 11804‑11808.
24. Hyrup, B.; Nielsen, P. E. *Bioorg. Med. Chem*. **1996**, *4*, 5-23.
25 Nielsen, P. *Pure Appl. Chem.* **1998**, *70*, 105-110.
26. Chakrabarti, M.; Schwarz, F. *Nucl. Acids Res*. **1999**, *27*, 4801-4806.
27. Shakeel, S.; Karim, S.; Ali, A. Journal of Chemical Technology & Biotechnology. 2006, 81, 892- 899.
28 Gildea, B. D.; Casey, S.; MacNeill, J.; Perry-O'Keefe, H.; Sorensen, D.; Coull, J. M. Tetrahedron Letters. 1998, 39, 7255-7258.

Chapter 1: Peptide Nucleic Acid (PNA)

Section 2: PNA applications

Section 2: PNA applications

The present section deals with brief discussion about some important applications of PNAs. The potential applications of PNAs can be divided in three different fields:

1.2.1 Diagnostics

1.2.2 Molecular biology

1.2.3 Therapy

It is important to notice that new techniques are continuously being developed and that this section could not be exhaustive. However, some techniques are very important because they represent "historically" step in the development and use of PNAs. These techniques will be described more exhaustively than others.

1.2.1 Diagnostics

PNAs have found application to detect genetic mutations and to analyse of mismatches in the Watson & Creek hydrogen bonding. Their particular affinity towards DNA and RNA, their high sequence specificity and their capacity to perform strand displacements make PNAs powerful tools for diagnostic purposes. One of the best features of PNAs is the possibility to detect the Single Nucleotide Polymorphism (SNP) by measuring the variations of the melting temperature. Some techniques have been developed for this target, for example the PCR and capillary electrophoresis.[1]

1.2.1.1 Single Base Polymorphism: "PCR clamping"

The Polymerase Chain Reaction (PCR) technique is considered one of the most valuable step in the detection of genetic diseases. The high specificity of PNA to bind DNA, the greater stability of PNA-DNA duplexes than DNA-DNA ones and the inefficiency of PNA to act as primer for DNA polymerases are the bases for this novel techniques.

This strategy includes a distinct annealing step involving the PNA targeted against one of the PCR primer sites. This step is carried out at a higher temperature than that for conventional PCR primer annealing where the PNA is selectively bound to the DNA molecule. The PNA/DNA complex formed at one of the primer sites effectively blocks the formation of a PCR product.[2] PNA is also able to discriminate between fully complementary and single

mismatch targets in a mixed target PCR. Sequence-selective blockage by PNA allows suppression of target sequences that differ by only one base pair. Also, this PNA clamping was able to discriminate three different point mutations at a single position.[3]

1.2.1.2 Screening for genetic mutations by capillary electrophoresis

In capillary electrophoresis, the separation is generally carried out using a long, thin fused silica capillary (typically 50–80 cm long, inner diameter; 10-300 mm). A portion of the coating, closed at one end of the capillary, is removed to allow optical detection of the analyte. The analyte passes the detection window during a separation process and can be visualized by online, automated UV, or laser-induced fluorescence (LIF) detection systems. Capillary electrophoresis is capable of analyzing minute amounts of sample (typically in the order of picograms to femtograms). However, it is not possible to analyze more than one sample at a time, which is regarded as the major disadvantage compared to slab gel electrophoresis.

A new diagnostic method for the detection of genetic mutations using PNA as a probe for capillary electrophoresis has been reported by Carlsson *et al*.[4] The method is sensitive enough to detect a single mismatch in the sample DNA. The model system consisted of four 50-mer, single-stranded DNA fragments representing a part of the cystic fibrosis transmembrane conductance regulator gene, one wild-type and three mutant sequences, and a 15-mer PNA probe having a sequence complementary to the wild-type oligomer.

The probe PNA only binds the fully matched DNA, and the presence of this duplex is detected using free solution capillary electrophoresis. Separation of full-match from mismatch duplexes was accomplished at a high temperature (70°C) and 50 mM ionic strength. At this temperature and ionic strength, only the hybrid duplex carrying the wild-type DNA sequences remains stable, while the hybrid complex carrying single mismatch DNA will be melted. Free PNA binds to the capillary wall and is not detected.[4]

Another application involves the use of fluorescent labelled PNAs. PNA probes with fluorescent tags offer sensitive detection and require only a very low concentration of the sample. At high temperatures (as described above), the LIF detection system will generate a signal for the bound PNAs, since free PNA is efficiently removed. Maybe it will be possible in the future to establish a universal screening strategy for any genetic disease with a known spectrum of mutations by developing a PNA probe library, possibly using multiple

fluorescent tags for multiplex testing of one or more exons. Other electrophoretic techniques (also in gel phase) are possible: the RNA binding properties of PNAs have also been characterized using capillary gel electrophoresis.[5,6]

1.2.1.3 PNA as a probe for nucleic acid biosensor

The DNA biosensor technology holds promises for a rapid and cost-effective detection of specific DNA sequences. A single-stranded nucleic acid probe is immobilized onto optical, electrochemical, or mass-sensitive transducers to detect the complementary (or mismatch) strand in a sample solution. The response from the hybridization event is converted into a useful electrical signal by the transducer. The use of PNAs based probes is a powerful alternative to DNAs based ones in different techniques:

1.2.1.3.1 BIAcore (Biomolecular Interaction Analysis)

The main background of this technique is the effect called SPR (Surface Plasmon Resonance). The PNA hybridization and corresponding mismatch analysis can be studied using a BIAcore instrument, which can evaluate a real-time biomolecular interaction analysis using optical detection technology. The real-time interactions are monitored on a sensor (surface) chip, which constitutes the core part of a BIAcore instrument. The probe molecule is attached directly to the surface and the analyte molecule is free in solution. The detection principle in BIA uses surface plasmon resonance. The response signal of the BIAcore apparatus is proportional to the change in the refractive index at the surface and is assumed to be proportional to the mass of substance bound to the chip (Figure 1.9).[7]

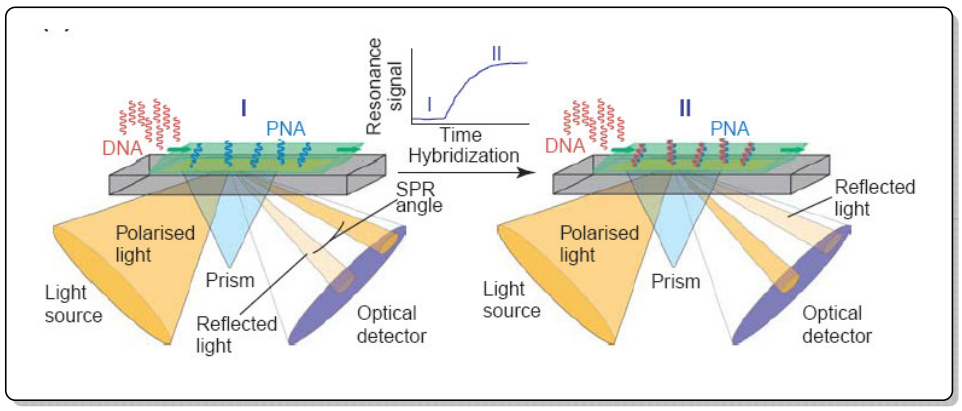

Figure 1.9: Schematic representation of BIAcore.

Jensen *et al*. used this technique to study the interactions between PNA and DNA or RNA. The sensor chip used in this case was basically a thin gold surface covered with a layer of dextran and containing streptavidin chemically coupled to the dextran. A biotinylated PNA probe was immobilized on the surface by using the strong coupling between biotin and streptavidin. The amount of bound substance (fully complementary as well as various singly mismatched RNA and DNA oligonucleotides) was measured as a function of time when a solution containing the complementary strands passed over the chip surface. In this way both the association (*annealing*) and dissociation (*melting*) kinetics could be studied.[8]

1.2.1.3.2 QCM (Quartz Crystal Microbalance)

The quartz crystal microbalance has been used for some time to monitor the mass or the thickness of thin films deposited on surfaces, to study gas adsorption and the deposition on surfaces in the monolayer and sub monolayer regimes[9]. Only recently, this sensitive mass measuring device has begun to be used in the area of biochemistry and biotechnology, such as for studying the hybridization of nucleic acids on surface. [10,11,12] The resonant frequency of the crystal changes due to a minute weight increases on the surface. It is expected that immobilized PNA strands (or probes) would show an improved distinction between the closely related target sequences compared to an immobilized DNA probe. A recent report by Wang and co-workers on quartz crystal microbalance biosensor, based on peptide nucleic acid probes, showed that the system can differentiate between a full complementary and single mismatch oligonucleotide. A rapid and sensitive detection of mismatch sequences is possible by monitoring the frequency/time response of the PNA-QCM biosensor. The PNA probes used in the abovementioned study, which formed the monolayer onto the gold QCM surface, contained a cysteine attached to the PNA core with the help of an ethylene glycol unit.[13] The remarkable specificity of the immobilized probe provides a rapid hybridization with corresponding oligonucleotides. Such a mismatch sensitivity of PNA-immobilized QCM biosensors could be of great importance for diagnostic applications, particularly for genetic screening and diagnosis of malignant diseases.

1.2.1.3.3 MALDI-TOF mass spectrometry

MALDI-TOF mass spectrometry has been used successfully in PNA-based diagnostic research to study discrimination of single-nucleotide polymorphisms (SNPs) in human DNA. The human genome and the mitochondrial DNA contain many SNPs that may be linked to diseases.[14] Rapid and accurate screening of important SNPs, based on high-affinity binding of

PNA probes to DNA, is possible by using MALDI-TOF mass spectroscopy. The captured, single-stranded DNA molecules are PCR-amplified and thereafter hybridized with PNA probes in an allele-specific fashion. MALDITOF can rapidly and accurately detect (identify) these hybridized PNA probes. This provides a straightforward, rapid, accurate, and specific detection of SNPs in amplified DNA.[15] The detection of multiple point mutations using allele-specific, mass-labelled PNA hybridization probes is also possible by using a direct MALDI-TOF-MS analysis method.[16] The mass spectra will show peaks of distinct masses corresponding to each allele, and in this way a mass spectral 'fingerprint' of each DNA sample can be obtained.[1] This technique can also be applied to analyse microarrays (Figure 1.10).

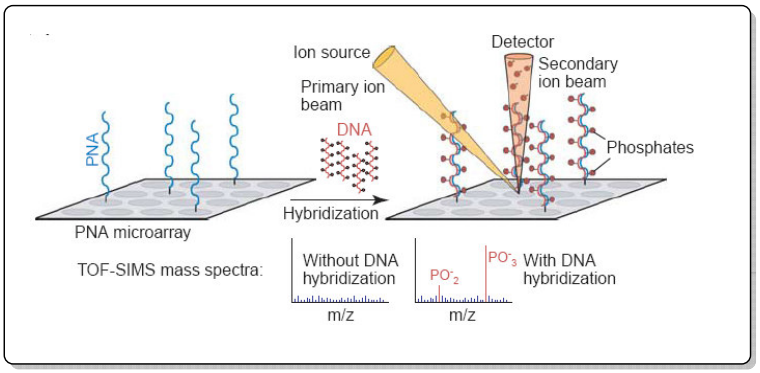

Figure 1.10: Application of MALDI-TOF in the analysis of microarrays.

Wang *et al.*[17] have also reported the use of PNA as a recognition probe for the electrochemical detection of the hybridization event using chronopotentiometric measurements. The method consists of four steps: probe (PNA) immobilization onto the transducer surface, hybridization, indicator binding, and chronopotentiometric transduction. A carbon paste electrode contains the immobilized DNA or PNA probe. The hybridization experiment was carried out by immersing the electrode into the stirred buffer solution containing a desired target, followed by measurement of signal. It is important to remember that similar techniques could be used to prepare microarray with electrochemical detection systems.

1.2.1.4 Microarray

Microarrays are small chips carrying on their surface row and column of ordered molecular probes (spot). Each of them is able to bind a specific target molecule. The success of microarrays in screening *m*RNA expression profiles of thousands of genes simultaneously

has prompted researchers in bioorganic chemistry to explore this format for screening small molecules. From an analytical perspective, the prospect of screening thousand of analytes in a few micro litres is attractive. Microarrays can be prepared by several techniques including photolithography, contact printing and inkjet to generate arrays with densities ranging from 1000 to 500 000 features per square centimetre. To date, a number of chemistries have been developed to derivatize glass surfaces to immobilize proteins, oligosaccharides, and small molecules in the microarray format. Many of these methods require the attachment of the protein or small molecule to the glass slide and likewise require that screening with the biological sample would also be performed on the surface. A supramolecular attachment, based on sequence specific hybridization of peptide nucleic acid (PNA), allows the use of the libraries as a mixture in solution that can then be converted to an organized microarray in one step by a self-sorting process.[18]

The microarray could be treated with the sample and the entity of the response of every single spot leads to the determination of the sample structure. This technique is already successfully applied for nucleic acids sequences screening: in this case the complementary DNA sequences of all known polymorphism are spotted on the chip[19] (Figure 1.11).

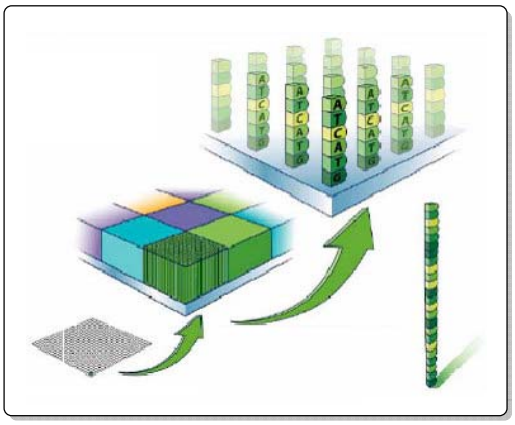

Figure 1.11: Schematic representation of microarrays

The microarrays technology is very interesting in biochemistry especially because it can be miniaturized; this feature makes the microarray the best choice to study the interaction between proteins and ligands or to check enzymatic activities in biological unpurified mixtures.

PNAs can represent an useful and advantageous probe, expecially for their peculiar chemical, physical and biochemical properties. Different type of PNA based microarrays have been

developed, with a variety in terms of its modes of action, especially with respect to detection.[20]

1.2.2 Tools in molecular biology

PNAs show good features to be used as new tools in molecular biology. Some examples are illustrated in the following sub-sections;

1.2.2.1 Polymerase Chain Reaction (PCR)

The polymerase chain reaction (PCR) has been widely used for various molecular genetic applications including the amplification of variable number of tandem repeat (VNTR) loci for the purpose of genetic typing.[1] However, in some cases preferential amplification of small allelic products relative to large allelic products may be problematic. This results in an incorrect typing in a heterozygous sample.[21] PNA has been used to achieve an enhanced amplification of VNTR locus D1S80.[22] Small PNA oligomers are used to block the template, and the latter becomes unavailable for intra and interstrand interaction during re-association. On the other hand, the primer extension is not blocked; during this extension, the polymerase displaces the PNA molecules from the template and the primer is extended toward completion of reaction. This approach shows the potential of PNA application for PCR amplification where fragments of different sizes are more accurately and evenly amplified. Since the probability of differential amplification is less, the risk of misclassification is greatly reduced. Misra *et al.* demonstrated that PNA-DNA chimera lacking the true phosphate backbone are capable of acting as primers for polymerase reactions catalyzed by DNA polymerases.[23,24]

The chimera $(PNA)_{19}$-TPG-OH, consisting of a 19 base PNA part linked to a single phosphate-containing dinucleotide (TPG-OH) with a free 3'-OH terminus, when annealed with a complementary RNA or DNA template strand works as an efficient primer to catalyze the addition of nucleotide by polymerase enzymes. The primer is also recognized by reverse transcriptase and by the Klenow fragment of *E. coli* DNA polymerase - I. The results suggested that the diameter of the duplex region rather than the presence of phosphate backbone of the template primer is the critical factor for a proper template-primer reaction and accommodating the enzyme within the binding domain. It also appears that the primer phosphate backbone may not be essential, at least not in this case, for the polymerase recognition and binding.

1.2.2.2 PNA hybridization as alternative to Southern hybridization

Southern hybridization is perhaps one of the most widely used techniques in molecular biology. Despite its great potential to predict both size and sequence information and information regarding the genetic context, there are certain disadvantages of this process. It requires a laborious multistep washing procedure and sometimes the sequence discrimination between closely related species. PNA pre-gel hybridization simplifies the process of Southern hybridization by reducing the required time, as the cumbersome post separation, probing, and washing steps are eliminated. Labelled (fluoresceinated) PNA oligomers are used as probes and allowed to hybridize to a denatured DNA sample at low ionic strength. The mixture is thereafter subjected directly to electrophoresis for size separation and single stranded DNA fragments separated on the basis of length. The charge-neutral PNA allows hybridization at low ionic strength and renders higher mobility to the complex, compared to the excess unbound PNA. The DNA-PNA hybrids are blotted (transferred) onto a nylon membrane, dried, UV cross-linked, and detected using standard chemiluminescent techniques.[25] Alternatively, the bound PNA can be detected by using capillary electrophoresis (vide infra), which uses the direct fluorescence detection method. Under the same conditions, a normal DNA-DNA duplex will tend to disrupt, here as the PNA-DNA duplex will remain intact due to the strong binding of PNA to DNA. This allows specific sequence detection with simultaneous size separation of the target DNA following a simple and straightforward protocol. Consequently, the analysis is much faster than conventional the Southern hybridization technique.[1]

1.2.2.3 PNA-assisted rare cleavage

The DNAs of bacteria have specific sites that are the target of restriction enzymes and methylases. Methylases are particular enzymes that can add a methyl group to a specific DNA site to protect that site against the cutting by some endonucleases.

Peptide nucleic acids, in combination with methylases and other restriction endonucleases, can act as rare genome cutters.[26] The method is called PNA-assisted rare cleavage (PARC) technique. It uses the strong sequence-selective binding of PNAs, preferably bis-PNAs, to short homopyrimidine sites on large DNA molecules, *e.g.*, yeast or λ DNA.[1] The PNA target site is experimentally designed to overlap with the methylation/ restriction enzyme site on the DNA, so that a bound PNA molecule will efficiently shield the host site from enzymatic methylation whereas the other unprotected methylation/ restriction sites will be methylated.

After the removal of bis-PNA, followed by restriction digestions, it is possible to cleave the whole DNA by enzymes into limited number of pieces.[26] DNA is efficiently protected from enzymatic digestion due to methylation in most of the sites except for those previously bound to PNA. Thus, short PNA sequences, particularly positively charged bis-PNAs, in combination with various methylation/restriction enzyme pairs can constitute an extraordinary new class of genome rare cutters.

1.2.2.4 Artificial restriction enzyme

S1 nuclease cleaves single-stranded nucleic acids releasing 5'-phosphoryl mono- or oligonucleotides. It removes the single-stranded overhangs of DNA fragments and can be used in RNA transcript mapping and construction of unidirectional deletions. PNA in combination with S1 nuclease can work as an "artificial restriction enzyme" system. Homopyrimidine PNA oligomers hybridize to the complementary targets on dsDNA *via* a strand invasion mechanism, leading to the formation of looped-out non complementary DNA strands. The enzyme nuclease S1 can degrade this single-stranded DNA part into well defined fragments. If two PNAs are used for this purpose and allowed to bind to two adjacent targets on either the same or opposite DNA strands, it will essentially open up the entire region, making the substrate accessible for the nuclease digestion and thereby increasing the cleavage efficiency.[27]

1.2.2.5 Determination of telomere size

The conventional method for the determination of telomere length involves Southern blot analysis of genomic DNA and provides a range for the telomere length of all chromosomes present. The modern approach uses fluorescein-labelled oligonucleotides and monitor *in situ* hybridization to telomeric repeats. However, a more delicate approach resulting in better quantitative results is possible by using fluorescein-labelled PNAs, as shown by Lansdorp *et al*.[28] This PNA-mediated approach permits accurate estimates of telomeric length. *In situ* hybridization of fluorescein-labelled PNA probes to telomeres is faster and requires a lower concentration of the probe compared to its DNA counterpart. Low photo bleaching and an excellent signal-to-noise ratio make it possible to quantitative telomeric repeats on individual chromosomes in this way. Experiments suggest that variations of this approach can possibly be applied to other repetitive sequences.

1.2.2.6 Nucleic acids purification

Based on its unique hybridization properties, PNAs can also be used to purify target nucleic acids. PNAs carrying six histidine residues have been used to purify target nucleic acids using nickel affinity chromatography.[29] Also, biotinylated PNAs in combination with streptavidin-coated magnetic beads may be used to purify *Chlamydia trachomatis* genomic DNA directly from urine samples. However, it appears that this simple, fast, and straightforward "purification by hybridization" approach has certain drawbacks. It requires the knowledge of the target sequence and depends on a capture oligomer to be synthesized for each different target nucleic acid. Such target sequences for the short pyrimidine PNA, i.e., the most efficient probe for strand invasion, are prevalent in large nucleic acids. Thus, short PNAs can also be used as generic capture probes for purification of large nucleic acids. It has been shown that a biotin tagged PNA-thymine heptamer could be used to efficiently purify human genomic DNA from whole blood by a simple and rapid procedure.[1]

1.2.2.7 Gene expression induction

Although most of the focuses on PNA applications have revolved around antisense strategies, several groups have studied the ability of PNAs to turn on gene expression. When PNA triplex structures are formed on one strand of the DNA duplex, the opposing DNA strand is displaced to form a D-loop. When sufficiently large, this D-loop resembles a transcriptional bubble or an initiation/elongation loop. Using bacterial and rat spleen-cell nuclear extracts and triplex-forming PNAs that bound to adjacent sites on a DNA template, Møllegaard and colleagues found that transcription was more efficient if two adjacent PNAs were bound to the same strand of DNA, thus giving rise to a 26 base D-loop. In this case, transcript initiation sites mapped to a site just downstream of PNA binding.[30,31]

More recently, the work form the Wang laboratory has extended these findings and has shown that PNAs can be used in cultural cells to activate endogenous gene expression.[32] Using promoter-less GFP reporter constructs containing homopurine PNA target sites just upstream of the GFP initiation codon, Wang was able to demonstrate specific transcriptional initiation *in vitro* using HeLa cell extracts. In these experiments, designed to explore gene therapy approaches for Sickle cell disease (SCD) and Thalassemia, the homopurine target sequence was from the 300 region of the human Gγ-globin promoter. As seen by Møllegaard[30], transcript start sites mapped to the PNA target site and used the D-loop strand as template. When the PNAs were hybridized to the reporter plasmid under low salt

conditions and microinjected into the nuclei of cells, GFP expression was detected within 20 hr of injection. By contrast, no GFP expression was detected in cells microinjected with plasmid alone. Wang also demonstrated that K562 erythroleukemia cells could be efficiently transfected with PNAs using electroporation and inducing the endogenous γ-globin gene threefold over background.

Up regulation of γ -globin gene expression, normally suppressed in adults to <1%, can help in the treatment of β-Thalassemia disease, in which it may partially act in place of the mutated defective γ-globin. Moreover, this induction was clearly a specific effect of the PNAs since the start sites for the transcripts mapped to both the endogenous promoter and to the PNA binding sites, 300 bp upstream.

Thus, despite the presence of physiological salt concentrations and potential chromatin structures, the PNAs were able to bind to their target sites in the chromosome and promote transcription initiation, providing proof of principle for this approach of gene therapy. It is somewhat surprising that γ-globin transcription was induced not only at the PNA binding site, but also from its native promoter region.[32] Probably the transcription of the γ-globin gene from the sequences upstream also makes the native promoter more accessible for RNA polymerase. In the cellular context PNA-mediated arrest of transcription is interpreted as an inability of the transcription machinery to dissociate PNA/DNA or PNA_2/DNA helices, more specifically, by the inability of the DNA helicase to unwind these structures. Indeed, specific studies show that bis-PNAs can significantly reduce DNA unwinding activity of the UL9 helicase.[33,34]

1.2.3 Gene therapy

Peptide nucleic acids have promise as candidates for gene therapeutic drugs design. They require well identified targets and a well-characterized mechanism for their cellular delivery. In principle, two general strategies can be adapted to design gene therapeutic drugs. Oligonucleotides or their potential analogs are designed to recognize and hybridize to complementary sequences in a particular gene whereby they should interfere with the transcription of that particular gene (antigene strategy, Figure 1.12).

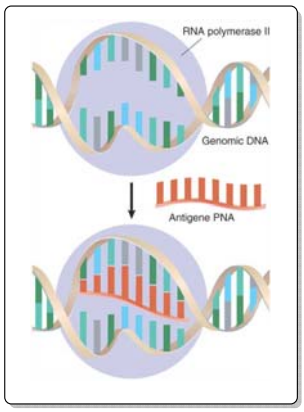

Figure 1.12: Antigene strategy

Alternatively, nucleic acid analogs can be designed to recognize and hybridize to complementary sequences in *m*RNA and thereby inhibit its translation (antisense strategy, Figure 1.13). PNAs are chemically and biologically stable molecules and have significant effects on replication, transcription, and translation processes, as revealed from *in vitro* experiments. Moreover, no sign of any general toxicity of PNA has so far been observed.[1a]

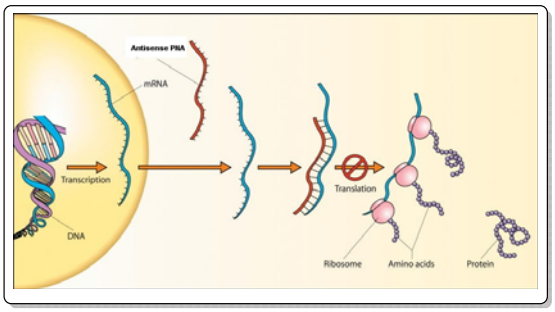

Figure 1.13: Antisense strategy

MicroRNAs are short non-coding RNAs expressed in different tissue and cell types that suppress the expression of target genes. As such, microRNAs are critical cogs in numerous biological processes[1b, c] and dysregulated microRNA expression is correlated with many human diseases.

Very recently in 2015 Cheng *et al* reported, MicroRNA (miRNAs) applicable for cancer therapy in tumour microenvironment. They introduce a novel antimiR delivery platform that targets the acidic tumour microenvironment, evades systemic clearance by the liver and facilitates cell entry *via* a non-endocytic pathway and they find that the attachment of peptide nucleic acid antimiRs to a peptide with a low pH-induced transmembrane structure (pHLIP) produces a novel construct that could target the tumour microenvironment, transport antimiRs

across plasma membranes under acidic conditions such as those found in solid tumours (pH ~6), and effectively inhibit themiR-155 oncomiRin a mouse model of lymphoma. This study introduces a new model for using antimiRs as anti-cancer drugs, which can have broad impacts on the field of targeted drug delivery.[1d]

The blood disorder, β-thalassaemia, is considered an attractive target for gene correction. 1e Site-specific triplex formation has been shown to induce DNA repair and thereby catalyse genome editing. In 2016 Bahal *et al* reported that triplex-forming peptide nucleic acids (PNAs) substituted at the γ position plus stimulation of the stem cell factor (SCF)/c-Kit pathway yielded high levels of gene editing in haematopoietic stem cells (HSCs) in a mouse model of human β-thalassaemia. Injection of thalassemic mice with SCF plus nanoparticles containing γPNAs and donor DNAs ameliorated the disease phenotype, with sustained elevation of blood haemoglobin levels into the normal range, reduced reticulocytosis, reversal of splenomegaly and up to 7% β-globin gene correction in HSCs, with extremely low off-target effects. The combination of nanoparticle delivery, next generation γPNAs and SCF treatment may offer a minimally invasive treatment for genetic disorders of the blood that can be achieved safely and simply by intravenous administration.

1.2.3.1 Antigene strategy

Peptide nucleic acids should be capable of arresting transcriptional processes thanks to of their ability to form a stable triplex structure or a strand-invaded or strand displacement complex with DNA. Such complexes can create a structural hindrance to block the stable function of RNA polymerase and thus are capable of working as antigene agents. Evidence from *in vitro* studies supports the idea that such complexes are indeed capable of affecting the process of transcription involving both prokaryotic and eukaryotic RNA polymerases. PNA targeted against the promoter region can form a stable PNA–DNA complex that restricts the DNA access of the corresponding polymerase. PNA strand displacement complexes, located far downstream from the promoter, can also efficiently block polymerase progression and transcription elongation and thereby produce truncated RNA transcripts; the PNA (DNA poly-purine) target must be present in the gene of interest.,[35] Nielsen *et al*. have demonstrated that even an 8-mer PNA (T8) is capable of blocking phage T3 polymerase activity.[36] The presence of a PNA target within the promoter region of IL-2Ra gene has been used to understand the effect of PNA binding to its target on this gene expression.[37,38] The PNA_2/DNA triplex arrests transcription *in vitro* and it is capable of acting as an antigene

agent. Unfortunately one of the major obstacles to use PNA as an antigene agent is that the strand invasion or the formation of strand displacement complex is rather slow at physiological salt concentrations.[39] Several modifications of PNA have shown improvements in terms of binding. Modifications of PNA by chemically linking the ends of the Watson-Crick and Hoogsteen PNA strands to each other, introducing pH-independent pseudoisocytosines into the Hoogsteen strand,[40] incorporating intercalators,[41] or positively charged lysine residues [40,42] in PNA strands can drastically increase the association rates with dsDNA. Lee *et al.* have demonstrated that PNA, as well as the PNA–DNA chimera, complementary to the primary site of the HIV-I genome can completely block priming by *t*RNA3Lys.[43] Consequently, *in vitro* initiation of the reverse transcription by HIV-1 RT is blocked. Thus, oligomeric PNAs targeted to various critical regions of the viral genome are likely to have a strong therapeutic potential for interrupting multiple steps involved in the replication of HIV-1.[43] It has been found that under physiological salt conditions, binding of PNA to super coiled plasmid DNA is faster compared to linear DNA.[42] This result is relevant to the fact that the transcriptionally active chromosomal DNA usually is negatively supercoiled, so it can be better target for PNA binding *in vivo*. It has also been found that the binding of PNA to dsDNA is enhanced when the DNA is being transcribed. This transcription-mediated PNA binding occurs about threefold as efficiently when the PNA target is situated on the nontemplate strand instead of the template strand. As transcription mediates template strand-associated $(PNA)_2$/DNA complexes, which can arrest further elongation, the action of RNA polymerase results in repression of its own activity, *i.e*., suicide transcription.[44] These findings are highly relevant for the possible future use of PNA as an antigene agent. We wish to refer to reports describing the ability of PNA to activate transcription, although this is not actually related to its antigene effect. Møllegaard *et al*.[30] have efficiently demonstrated that the looped-out single-stranded structure formed as a result of strand invasion is also capable of acting as efficient initiation sites for *Escherichia coli* and mammalian RNA polymerases in which the polymerase might start transcription using the single-stranded loop as a template.[38] This is consistent with the affinity of RNA polymerase for single-stranded DNA and its ability to transcribe single-stranded DNA.

The nuclear localisation signal (NLS) of SV40 has been shown to translocate 17-mer anti-myc PNA over the plasma membrane into the cytosol and further convey into nuclei of Burkitt's lymphoma derived cell-lines. A 17-mer antigene PNA, that is complementary to a unique sequence located at the start of the second exon of c-myc, was delivered into BRG

and BJAB cells by both NLS peptide and peptide with a scrambled NLS sequence. However, the nuclear transport of PNA was achieved only with a PKKKRKV peptide that corresponds to the active/wild type NLS (NLSwt).[45] Inside the nuclei the rhodamine-labelled PNA–NLS was visualised as a small number of highly fluorescing bright spots associated with clumped chromatin material. Twenty four hours after application of 10 μM antimyc- NLSwt–PNA constructs, MYC expression was inhibited by 75% and cell viability decreased by 25%, respectively. MYC expression in treated cells decreased progressively and after 72 h the protein concentration was below the level of detection. The level of myc mRNA was reduced by 35% after 7 h of treatment and by 60% after 18 h, suggesting that MYC expression was also inhibited at the level of transcription. However, reduction of protein concentration upon PNA-NLSwt construct treatment seems to slightly precede the decrease in the mRNA concentration. This discrepancy can be explained by general difficulties in quantifying exactly the Western and Northern blot analyses. On the other hand, this hints that antimyc-PNA–NLSwt acts not only on a transcriptional, but on a translational level as well.

The potential applicability of receptor mediated intracellular translocation of PN (from cytosol into the nucleus) was demonstrated in prostatic carcinoma cells. Dihydrotestosterone coupled to anti-gene PNA induced nuclear uptake in LNCaP cells that express the androgen receptor gene (AR), but not in DU145 cells where its receptor gene is silent. The cellular/cytoplasmic uptake of rhodamine labelled anti-myc PNA is, however, detectable in both cell-lines, but in DU145 cells the uptake is strictly cytoplasmic only.[46] Coupling of dihydrotestosterone adds hydrophobicity to PNA oligomer molecules and that seems to facilitate the uptake of PNA by cells, as compared to unmodified PNA.

1.2.3.2 Antisense strategy

In the antisense strategy the target of the PNA strand is the *m*RNA (instead the antigene where the target is the DNA double strand). The basic mechanism of the antisense effect by oligodeoxynucleotides is considered to be either a ribonuclease H (RNase H) - mediated cleavage of the RNA strand in oligonucleotide-RNA heteroduplex or a steric blockage in the oligonucleotide - RNA complex of the translation machinery.[47] Oligodeoxynucleotide analogs such as phosphorothioates activate RNase H and thus hold promise of working as antisense agents.[48] However, they also exhibit some non-specificity in their action. PNA/RNA duplexes, on the other hand, cannot act as substrates for RNase H. Normally; the peptide nucleic acid antisense effect is based on the steric blocking of either RNA processing,

transport into cytoplasm, or translation. It has been concluded from the results of *in vitro* translation experiments involving rabbit reticulocyte lysates that both duplex- (mixed sequence) and triplex-forming (pyrimidine-rich) PNAs are capable of inhibiting translation at targets overlapping the AUG start codon.[47] Triplex-forming PNAs are able to hinder the translation machinery at targets in the coding region of mRNA. However, the translation elongation arrest requires a $(PNA)_2$–RNA triplex and thus needs a homopurine target of 10-15 bases. In contrast, duplex-forming PNAs are incapable of doing the same. Triplex-forming PNAs can inhibit translation at initiation codon targets and ribosome elongation at codon region targets.

Mologni et al. showed effects of three different types of antisense on the *in vitro* expression of PML/RARα gene.[62] The first one was complementary to the first AUG (initiation) site. The second could bind to a sequence in the coding region that includes the second AUG, the starting site for the synthesis of an active protein. The third PNA was targeted against the 59-untranslated region (UTR) of the *m*RNA, the point of assembly of the translation machinery. Together, these three PNAs could efficiently inhibit translation even at a concentration much below the critical concentration used for each individual. The result suggests that the PNA targeting of RNA molecules like PML/RARα requires the effective blocking of different sequences on the 59 part of the messenger. A 59-UTR PNA target can also be used as efficiently as an initiation (AUG) target to achieve an antisense activity of PNA, and a more effective translation inhibition can be achieved by combining PNA directed toward 59-UTR and AUG regions.

Triple helix-forming PNAs can also hinder the translation process. Bis-PNA or clamp-PNA structures are capable of forming internal triple helical constructs. In principle, if targeted against the coding region of *m*RNA, PNA_2/RNA triple helix-forming derivatives can also cause a stop in translation, which can be easily verified by the detection of a truncated protein.[47] However, this methodology, requires a sequence optimization for each new target. Recent studies show that *E. coli* cells are somewhat permeable for PNA molecules. Good and Nielsen [50a-b] have shown that it is possible to achieve PNA antisense effects in the 'leaky' mutant strains of E. coli. PNAs targeted against the AUG region of the *m*RNA corresponding to β-galactosidase and β-lactamase genes were indeed capable of down-regulating the expression of these two genes.[50a] Another study demonstrated the effect of two bis-PNAs, targeted against the homopurine stretches in *r*RNA, either in the peptidyl transferase center or in the α-sarcin loop, in inhibiting the ribosome function in a cell-free system.[50b] The

translation was arrested at submicromolar range of PNA concentration. The growth of a mutant strain of *E. coli*, namely, AS19, was also inhibited by using the same PNAs at low micromolar concentration.

1.2.3.3 Inhibition of replication

It is also possible by using PNA to inhibit the elongation of DNA primers by DNA polymerase. Further, the inhibition of DNA replication should be possible if the DNA duplex is subjected to strand invasion by PNA under physiological conditions or if the DNA is single stranded during the replication process. Efficient inhibition of extra chromosomal mitochondrial DNA, which is largely single-stranded during replication, has been demonstrated by Taylor *et al*.[51] The PNA-mediated inhibition of the replication of mutant human mitochondrial DNA is a novel (and also potential) approach toward the treatment of patients suffering from ailments related to the heteroplasmy of mitochondrial DNA. Here wild-type and mutated DNA are both present in the same cell. Experiments have shown that PNA is capable of inhibiting the replication of mutated DNA under physiological conditions without affecting the wild-type DNA in mitochondria.

1.2.3.4 Interaction of PNA with enzymes

It was observed that PNAs are able to interact with several enzymes.

- **RNase H**

  Despite their remarkable nucleic acid binding properties, PNAs are not generally capable of stimulating RNase H activity on duplex formation with RNA. However, recent studies have shown that DNA/PNA chimeras are capable of stimulating RNase H activity. On formation of a chimeric RNA double strand, PNA/DNA can activate the RNA cleavage activity of RNase H. Cleavage occurs at the ribonucleotide parts base paired to the DNA part of the chimera. Moreover, this cleavage is sequence specific in such a way that certain sequences of DNA/PNA chimeras are preferred over others.[52] They are also reported to be taken up by cells to a similar extent as corresponding oligonucleotides. Thus, PNA/DNA chimeras appear by far the best potential candidates for antisense PNA constructs.

- **Polymerase and reverse transcriptase**

In general, there is no direct interaction of PNA with either DNA polymerase or reverse transcriptase. However, different groups have shown indirect involvement of PNA in inhibiting these enzyme functions (activity) under *in vitro* conditions. For example, PNA oligomers are capable of terminating the elongation of oligonucleotide primers by either binding to the template strand or directly competing with the primer for binding to the template. Primer extension by MMLV reverse transcriptase has been shown to be inhibited by introducing a PNA oligomer.[37] In another experiment, Nielsen et al.[53] demonstrated that the primer extension catalyzed by *Taq*-polymerase can be terminated by incorporating a PNA oligomer [PNA-H (t) 10] into the system. The latter can bind to a (dA)10 sequence in the template and thereby terminate the primer extension. Moreover, uncharged PNA primers with only a single 59-amino-29,59- dideoxynucleoside at the carboxyl terminus can be recognized by the Klenow fragment for DNA pol I and VentDNA polymerase (*Thermococcus litoralis*), and a linear amplification is possible with the use of an excess of PNA-DNA primer and suitable thermo stable polymerases.[54] Moreover, the reverse transcription of gag gene of HIV I is also inhibited *in vitro* by PNAs.[55] The inhibition has been achieved by using a bis-PNA construct, which is more efficient than the corresponding mono PNA construct.[51] Also, the reverse transcription can be completely inhibited by a pentadecameric antisense PNA, using a molar ratio of 10:1 (PNA/RNA), without any noticeable RNase H cleavage of the RNA.[55]

- **Telomerase**

  Human telomerase, a ribonucleoprotein complex consisting of a protein with DNA polymerase activity and an RNA component, synthesizes $(TTAGGG)_n$ repeats at the 39 end of DNA strands. PNA oligomers that are complementary to the RNA primer binding site can inhibit the telomerase activity. Studies have shown that the telomerase inhibition activity of PNA is better than that of corresponding activity of phosphorothioate oligonucleotides. This is mainly due to a higher binding affinity of PNA compared to phosphorothioates.[56] Corey and co-workers have demonstrated an efficient inhibition of telomerase after lipid mediated delivery of template- and non template- directed PNA into the cell.[57]

1.2.3.5 Mutagen action of PNA

One consequence of the tight binding of triplex-forming oligonucleotides and PNAs to cellular homopurine DNA targets is that they can induce DNA repair pathways within the cell. Thus, the PNA_2/DNA complex can be interpreted by the cell to be a DNA lesion in need of repair. One possible outcome of this is the production of site-specific mutants at, or proximal to, the site of PNA binding.[58] Faruqi ad co-workers reported that PNAs with binding affinities of around 10^{-7} M were able to be taken up by streptolysin- O permeabilized murine fibroblast, bind to their target sites within SupF1 reporter gene integrated into the genome, and induce point mutations or single base deletions or insertions in the target sequence or within 5 bp of the site.[59] The frequency of mutagenesis observed with the PNAs was 8×10^{-4}, compared to a background mutagenesis frequency of 9×10^{-5}. Similar results have been obtained with tightly binding triplex-forming phosphorothioates, leading to the prediction that triplex complexes in general can induce transcription-coupled DNA repair pathways.[60] Presently, this mutagenic capacity is being developed as a technique to selectively mutagenize and repair single point mutations that are crucial in certain genetic diseases, including sickle cell disease.[31]

1.2.4. Bibliography

1. a) Ray, A.; Nordén, B. *The FASEB journal* **2000**, *14*, 1041-1060 b) He, L.; Hannon, G. J. *Nature Rev. Genet*. **2004**, *5*, 522-531 c) Calin, G. A.; Croce, C. M. *Nature Rev. Cancer* **2006**, *6*, 857-866 d) Cheng, C. J.; Bahal, R.; Babar, I. A.; Pincus, Z.; Barrera, F.; Liu, C.; Svoronos, A.; Braddock, D. T.; Glazer, P. M.; Engelman, D. M.; Saltzman, W. M.; Slack, F. J. *Nature* **2015**, *518*, 107-110 e) Bahal, R.; McNeer, N. A.; Quijano, E.; Liu, Y.; Sulkowski, P.; Turchick, A.; Lu, Y. C. Bhunia, D. C.; Manna, A.; Greiner, D. L.; Brehm, M. A.; Cheng, C. J.; Giráldez, F. L.; Ricciardi, A.; Beloor, J.; Krause, D. S.; Kumar, P.; Gallagher, P. G.; Braddock, D. T.; Saltzman, W. M.; Ly, D. H.; Glazer, P. M. *Nat. Commu.,* **2016**, *7*, 13304.
2. Nielsen, P. E. *et al*. *Proc. Natl. Acad. Sci. USA* **1991**, 3892-3895
3. Nielsen, P. E. *et al*. *Nucleic Acid Res*. **1993**, *21*, 5332-5336
4. Carlsson, C.; Jonsson, M.; Nordén, B.; Dulay, M. T.; Zare, R. N.; Noolandi, J.; Nielsen, P. E.; Tsui, L.-C.; Zielenski, *J. Nature (London)* **1996**, *380,* 207
5. Rose, D. *J. Anal. Chem.* **1993**, *65*, 3545-3549
6. Igloi, G. L. *Proc. Natl. Acad. Sci. USA* **1998**, *95,* 8562-8567

7. *BIAcore X Instrument Handbook* (**1996**) Preliminary Ed., Pharmacia Biosensor AB, Uppsala, Sweden
8. Jensen, K. K.; Örum, H.; Nielsen, P. E.; Nordén, B. *Biochemistry* **1997,** *36*, 5072-5077
9. Lu, C.; Czanderna, A. W. Eds (**1984**) *Applications of Piezoelectric Quartz Crystal Microbalances*, Elsevier, Amsterdam
10. Okahata, Y.; Matsunobo, Y.; Ijiro, K.; Mukae, M.; Murakami, A.; Makino, K. *J. Am. Chem. Soc.* **1992**, *114*, 8299-8300
11. Okahata, Y.; Niikura, K.; Sugiura, Y.; Sawada, M.; Morii, T. *Biochemistry* **1998**, *37*, 5666-5672
12. Niikura, K.; Matsuno, H.; Okahata, Y. *J. Am. Chem. Soc*. **1998**, *120*, 8537-8538
13. Wang, J.; Nielsen, P. E.; Jiang, M.; Cai, X.; Fernandes, J. R.; Grant, D. H.; Ozsoz, M.; Beglieter, A.; Mowat, M. *Anal. Chem*. **1997,** *69*, 5200-5202
14. Ross, P. L.; Lee, K.; Belgrader, P. *Anal. Chem.* **1997**, *69*, 4197-4202
15. Egholm, M. *Nature Biotechnol*. **1997**, *15*, 1346
16. Griffin, T. J.; Tang, W.; Smith, L.M. *Nature Biotechnol.* **1997,** *15*, 1368-1372
17. Wang, J.; Palecek, E.; Nielsen, P. E.; Rivas, G.; Cai, X.; Shirashi, H.; Dontha, N.; Luo, D.; Farias, P. A. M. *J. Am. Chem. Soc.* **1996**, *118*, 267-278
18. Harris, J. L.; Winssinger, N. *Chem. Eur. J*. **2005**, *11*, 6792-6801
19. Dall'Angelo, S. *Thesis in Industrial Chemistry* (**2005**), University of Milan, Italy
20. Brandt, O.; Hoheisel, J. *Trends in Biotechnology* **2004**, *22*(12), 617-622
21. Walsh, P. S.; Erlich, H. A.; Higuchi, R. *PCR Methods Appl.* **1992,** *1*, 241-250
22. Demers, D. B.; Curry, E. T.; Egholm, M; Sozer, A. C. *Nucleic Acids Res.* **1995**, *23*, 3050-3055
23. Misra, H. S.; Pandey, P. K.; Modak, M. J.; Vinayak, R.; Pandey, V. N. *Biochemistry* **1998**, *37*, 1917-1925
24. Koppitz, M.; Nielsen, P. E.; Orgel, L. E. *J. Am. Chem. Soc.* **1998**, *120*, 4563-4569
25. Perry-O'Keefe, H.; Yao, X.-W.; Coull, J. M.; Fuchs, M.; Egholm, M. *Proc. Natl. Acad. Sci. USA,* **1996**, *93*, 472-480
26. Veselkov, A. G.; Demidov, V.; Nielsen, P. E.; Frank-Kamenetskii, M. D. *Nucleic Acids Res.* **1996**, *24,* 2483-2487
27. Demidov, V.; Frank-Kamenetskii, M. D.; Egholm, M.; Buchardt, O.; Nielsen, P. E. *Nucleic Acids Res.* **1993**, *21*, 2103-2107

28. Lansdorp, P. M.; Verwoerd, N.P.; Van de Rijke, F. M.; Dragowska, V.; Little, M. T.; Dirks, R. W.; Raap, A.K.; Tanke, H. *J. Hum. Mol. Genet.* **1996**, *5,* 685-691
29. Örum, H.; Nielsen, P. E.; Jorgensen, M.; Larsson, C.; Stanley, C.; Koch, T. *BioTechniques* **1995**, *19*, 472-480
30. Mollegaard, N. E.; Buchardt, O.; Egholm, M.; Nielsen, P. E. Proc. *Natl. Acad. Sci. USA* **1994**, *91,* 3892-3895
31. Dean, D. A. *Advanced Drug Delivery Reviews* **2000**, *44*, 81-95
32. Wang, G.; Xu, X.; Pace, D. A.; Dean, D. A.; Glazer, P. M.; Chan, P.; Goodman, S. R.; Hassman, C. F.; Shokolenko, I. *Nucl. Acids Res.* **1999**, *27*, 2806-2813
33. Bastide, L.; Boehmer, P. E.; Villani,G.; Lebleu, B. *Nucl. Acids Res*. **1999**, *27*, 551-554
34. Pooga, M.; Land, T.; Bartfai, T.; Langel, Ü. *Biomolecular Engineering* **2001**, *17*, 183-192
35. Bentin, T.; Nielsen, P. E. *Biochemistry* **1996**, *35*, 8863-8869
36. Nielsen, P. E.; Egholm, M.; Buchardt, O. *Gene* **1994**, *149*, 139-145
37. Hanvey, J. C.; Peffer, N. C.; Bisi, J. E.; Thomson, S. A.; Cadilla, R.; Josey, J. A.; Ricca, D. J.; Hassman, C. F.; Bonham, M. A.; Au, K. G.; Carter, S. G.; Bruckenstein, D. A.; Boyd, A. L.; Noble, S. A.; Babiss, L. E. *Science,* **1992**, *258*, 1481-1485
38. Praseuth, D.; Grigoriev,M.; Guieysse, A. L.; Pritchard, L. L.; Harel-Bellan, A.; Nielsen, P. E.; Helene, C. *Biochim. Biophys. Acta.* **1996**, *1309*, 226-238
39. Tomac, S.; Sarkar, M.; Ratilainen, T.; Wittung, P.; Nielsen,P. E.; Nordén, B.; Gräslund, A. *J. Am. Chem. Soc.* **1996**, *118*, 5544-5552
40. Egholm, M.; Christensen, L.; Dueholm, K. L.; Buchardt, O.; Coull, J.; Nielsen, P. E. *Nucleic Acids Res.* **1995**, *23*, 217-222
41. Armitage, B.; Koch, T.; Frydenlund, H.; Örum, H.; Schuster, G. B. *Nucleic Acids Res*. **1998**, *26,* 715-720
42. Kuhn, H.; Demidov, V. V.; Frank-Kamenetskii, M. D.; Nielsen, P. E. *Nucleic Acids Res.* **1998**, *26*, 582-587
43. Lee, R.; Kaushik, N.; Modak, M. J.; Vinayak, R.; Pandey, V. N. *Biochemistry,* **1998**, *37*, 900-910
44. Larsen, H. J.; Nielsen, P. E. *Nucleic Acids Res*. **1996**, *24*, 458-463
45. Cutrona, G.; Carpaneto, E. M.; Ulivi, M.; Rondella, S.; Landt, O.; Ferrarini, M.; Boffa, L. C. *Nature Biotechnol.* **2000**, *18*, 300-303
46. Boffa, L. C.; Scarfi, S.; Mariani, M. R.; Damonte, G.; Allfrey, V. G.; Benatti, V.; Morris, P. L. *Cancer Research,* **2000**, *60*, 2258-2262

47. Knudsen, H.; Nielsen, P. E. *Nucleic Acids Res*. **1996,** *24,* 494-500
48. Nyce, J. W.; Metzger, W. J. *Nature,* **1997**, *385*, 721-725
49. Mologni, L.; leCoutre, P.; Nielsen, P. E.; Gambacorti-Passerini, C. *Nucleic Acids Res.* **1998**, *26*, 1934-1938
50. a) Good, L.; Nielsen, P. E. Proc. *Natl. Acad. Sci. USA* **1998**, *95*, 2073-2076. b) Good, L.; Nielsen, P. E. *Nature Biotechnol.* **1998**, *16*, 355-358
51. Taylor, R. W.; Chinnery, P. F.; Tumbull, D. M.; Lightowlers, R. N. *Nature Genet*. **1997**, *15*, 212-215
52. Uhlmann, E.; Peyman, A.; Breiphol, G.; Will, D. W. *Angew. Chem. Int. Ed.* **1998**, *37*, 2796-2823
53. Nielsen, P. E.; Egholm, M.; Berg, R. H.; Buchardt, O. *Anti-Cancer Drug Design* **1993**, *8*, 53-63
54. Lutz, M. J.; Benner, S. A.; Hein, S.; Breipohl, G.; Uhlmann, E. *J. Am. Chem. Soc.* **1997**, *119*, 3177-3178
55. Koppelhus, U.; Zachar, V.; Nielsen, P. E.; Liu, X.; Eugen-Olsen, J.; Ebbesen, P. *Nucleic Acids Res.* **1997,** *25*, 2167-2173
56. Norton, J. C.; Piatyszek, M. A.; Wright, W. E.; Shay, J. W.; Corey, D. R. *Nat. Biotech.* **1996**, *14*, 615-620
57. Hamilton, S. E.; Simmons, C. G.; Kathiriya, I. S.; Corey, D. R. Chem. Biol. 1999, 6, 343–351
58. Dean, D. A. *Adv. Drug. Del. Rev*. **2000**, *44,* 81-95
59. Faruqi, A. F.; Egholm, M.; Glazer, P. M. *Proc. Natl. Acad. Sci. USA* **1998**, *95*, 1398-1403
60. Wang, G.; Seidman, M. M.; Glazer, P.M. *Science* **1996**, *271*, 802–805

Chapter 1: Peptide Nucleic Acid (PNA)

Section 3: Chemical modifications of PNA

Section 3: Chemical modifications of PNA

The major limitations of the therapeutic applications of PNAs are their poor solubility in aqueous media due to self-aggregation and an insufficient cellular uptake. In order to improve PNA solubility in aqueous media, the cellular uptake, the binding selectivity towards RNA versus DNA, or to stabilise duplex or triplex structures, several analogues have been synthesised over the years.[1]

1.3.1. PNAs with Modified Nucleobases

Inhibition of gene expression by antisense or antigene approaches relies on the formation of stable duplex and triplex structures.[2, 3] In this context, the use of modified nucleobases represents an obvious way to control recognition between nucleic acids. The non-standard nucleobases employed so far with PNA are limited, compared with the repertoire of backbone modifications described. Structures of nucleobase-modified PNA are illustrated in Figure 1.14.

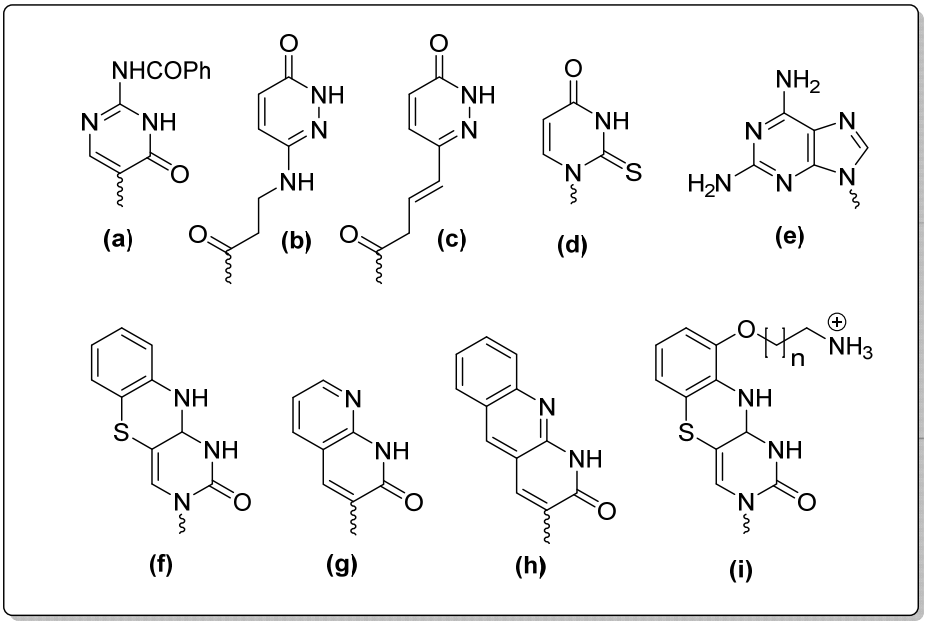

Figure 1.14: Structures of nucleobase-modified PNA.

Substitution of natural bases for analogues can be used for interfering with the hybridisation process; for example, N^4-benzoyl cytosine (Figure 1.14a) has been shown to cause inhibition of triplex formation, whereas E-base (Figure 1.14b), rationally designed to recognise T-A base pair, stabilises a triplex even when the target strand contains one or two pyrimidine residues.[4, 5] In fact, triplex formation is generally restricted to oligopurine strands whereas a

substantial destabilisation is observed when pyrimidine residues are introduced. However, the binding affinity of E•T-A triplet is far from optimal, which might partially be due to excessive flexibility of the linker between the backbone and the nucleobase. In order to address the issue of flexibility, a conformationally constrained E-base analogue (Figure 1.14c), was synthesised[6]. Surprisingly, no improvement was found, a result that could mean that local flexibility has only little influence on the thermodynamics of oligonucleotide hybridisation. As said, 2-Thiouracil (Figure 1.14d) along with 2, 6-diaminopurine (Figure 1.14e) was used as a non-natural base pair in PNA-DNA recognition and was shown, for the first time, to lead to a phenomenon termed as "double duplex invasion". Pyrimidines which have extended aromatic moieties as a means of increasing the stacking energy and hence the stability of the hybridised complexes represent another class of modified nucleobases. Incorporation of tricyclic phenothiazine (Figure 1.14f) as a substitute for cytosine and bicyclic/tricyclic naphthyridinones (Figure 1.14g and h) as substitutes for thymine showed a modest affinity increase, whereas tricyclic cytosine analogues based on the phenoxazine gave the highest increase in affinity and sequence specificity towards targets[7]. This result demonstrates that factors other than mere molecular stacking overlap, such as electronic factors, contribute to base pair stacking stabilities.

Interesting modification on nucleobases have also been carried out to yield fluorescent PNA monomers and oligomers (Figure 1.15).

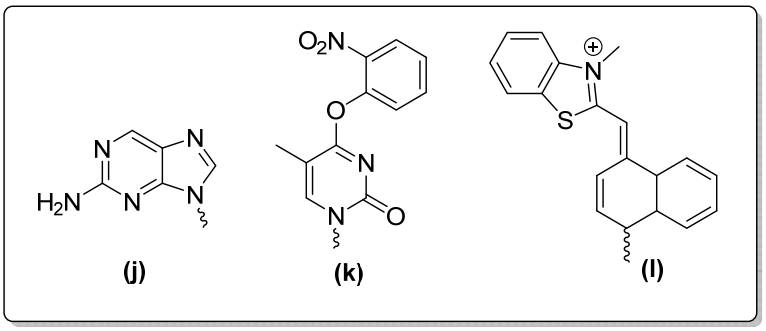

Figure 1.15: Structures of fluorescent nucleobase-modified PNA.

2-Aminopurine, being intrinsically fluorescent, can be used to study PNA‑DNA interaction dynamics[8]. O^4-(*o*-nitrophenyl) thymine (Figure 1.15-k) PNA monomer was reported as valuable intermediate for the introduction of fluorescent compounds into PNA oligomers[9]. Thiazole orange (Figure 1.15-l) is the first base to fulfil the demands desired for a fluorescent universal base[10]. Thanks to its remarkable base stacking ability, it pairs well against all four

canonical DNA bases maintaining duplex stability. In addition to this, the sensitivity of its fluorescence to a neighbouring base mismatch, it is suitable for homogeneous single-nucleotide-polymorphism detection[11].

1.3.2. PNAs with modified backbone

Since the first report of *aeg*PNA, many research groups have started the synthesis of backbone modified peptide nucleic acids in order to improve or modify the chemico-physical properties, in particular the solubility, and the binding affinity of classical PNA. Improvement of the aqueous solubility of PNAs has been achieved by the introduction of charges in the molecule, or by the introduction of ether linkages in the backbone. PNAs are endowed of positive charges by linking a terminal lysine residue[12] (Figure 1.16a) or by the introduction of a positive charge in the backbone, or by replacing the acetamide linker to the nucleobase by a flexible ethylene linker (Figure 1.16b) [13].

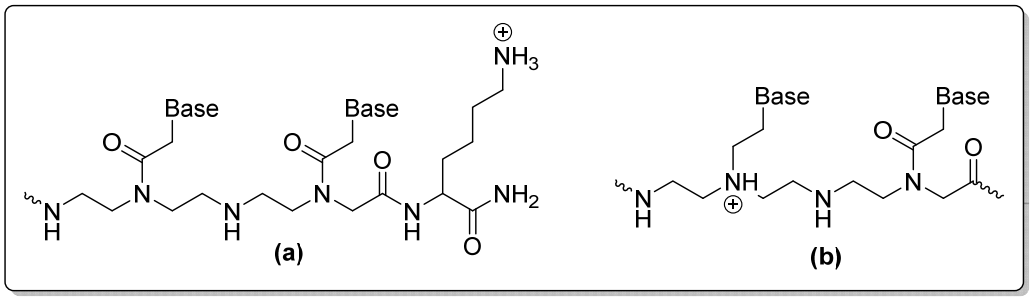

Figure 1.16: Positively charged modified backbone.

Cationic guanidinium linkages (Figure 1.17) have also recently been introduced into PNA and were found to improve its binding affinity with complementary nucleic acid sequences[14].

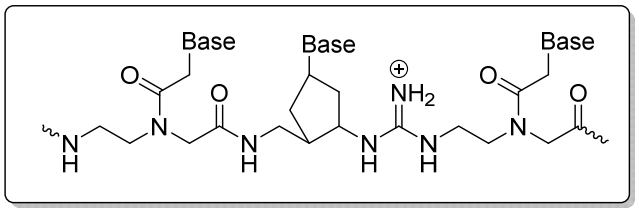

Figure 1.17: Positively charged guanidinium modified backbone.

Making the PNA anionic also aided in increasing its water-solubility as in the case of the phosphonate analogues (Figure 1.18), but was accompanied by a decrease in the binding affinity to complementary nucleic acid sequences [15-20].

Efimov *et al*.[15] have described the synthesis of homopyrimidine *p*PNA oligomers containing *N*-(2-hydroxyethyl) phosphonoglycine (*p*PNA-O), or *N*-(2-aminoethyl) phosphono glycine (*p*PNA-N). These oligomers did form complexes with complementary DNA/RNA, but with a much lower stability than PNA.

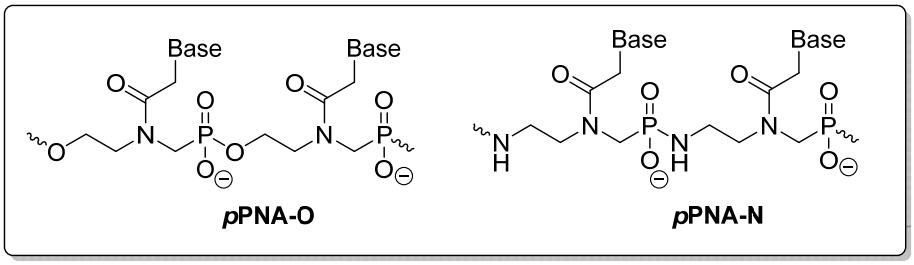

Figure 1.18: Anionic charged modified backbone.

Increased water solubility was also achieved by putting an ether linkage in the PNA backbone[20, 21] (Figure 1.19).

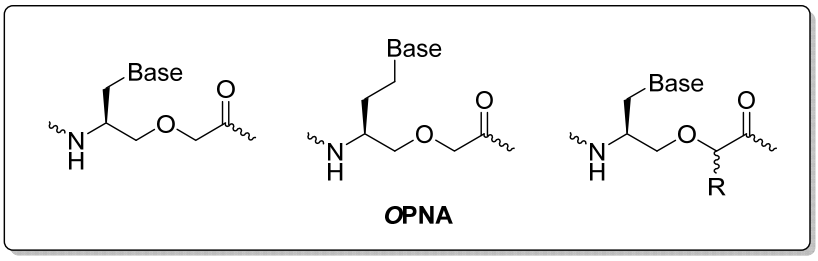

Figure 1.19: *O*-ether modified backbone.

In the attempt to make the backbone rigid, alkyl and cyclic substituents have been introduced[22,23]. 3-, 5- and 6-member rings have been appended in various position of the backbone. The rationale behind the design of such constrained PNA is to obtain a preorganised structure with high selectivity in the binding of DNA/RNA. As the presence of rotamers around the tertiary amide bond in *aeg*PNA interferes with the hybridisation process, it was postulated that connecting the nucleobase to the cycle inhibits the rotation, overcoming the problem of the rotamers. Examples of conformationally blocked PNA (Figure 1.20) are represented by the aminoprolyl PNA (*ap*-PNA), aminoethylprolyl PNA (*aep*-PNA), aminoethylpyrrolidinone PNA (*aepone*-PNA), pyrrolidine PNA, cyclopropane (cpr), cyclopentyl (cp) and cyclohexyl (ch) PNA.

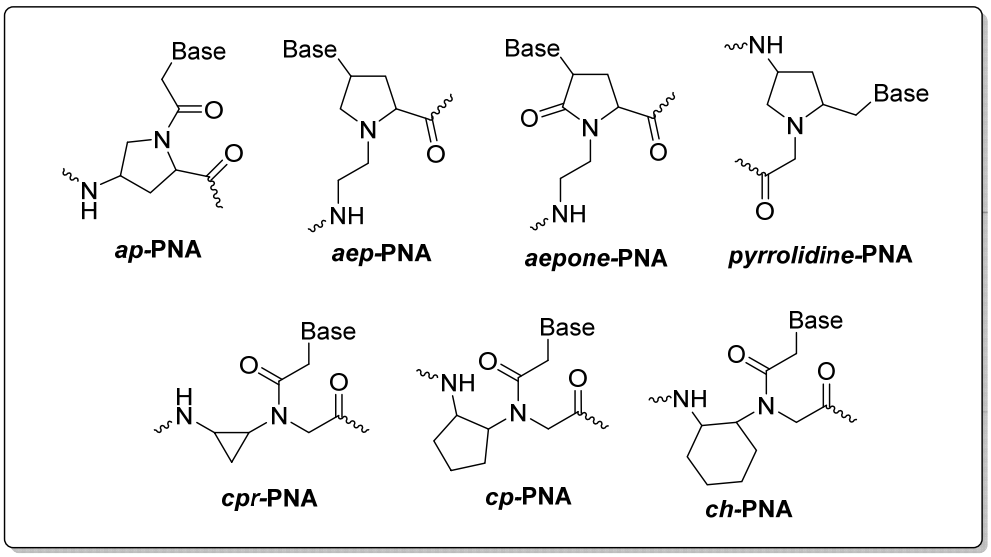

Figure 1.20: Rigid modified backbone.

Introduction of a single *ap*-PNA in a PNA sequence results in a stabilisation of the PNA/DNA duplex, whereas homothymine *ap*-PNA do not bind to the target sequence; stereochemistry affects the preference for parallel or antiparallel binding[24]. *Aep*-PNAs are obtained protecting the hydroxyproline carboxyl as an ester, derivatising the nitrogen with an ethylamine moiety and then replacing the OH with the nucleobase. These derivatives bear a positive charge; homothymine decamer binds polyadenilic acid to form 2:1 hybrids, with high affinity and specificity. When hybridised to DNA, they show higher affinity for the antiparallel hybridisation than for the parallel[25].#Aepone-PNAs also stabilise formation of triple helical structures with DNA partners, while destabilise triplexes formed with polyA[26]. (2R, 4S) Pyrrolidine-PNA oligomers form very stable hybrids with complementary DNA and RNA; protonation of the nitrogen does not affect the stability of the hybrids. On the contrary, (2S, 4S) isomers do not stabilise the formation of hybrids with DNA and RNA.[27] *Cp*-PNAs show higher affinity towards RNA than DNA; the (1R, 2S) enantiomers form higher affinity complexes with DNA than the (1S, 2R) enantiomers. Both stabilise PNA_2: DNA and PNA_2: RNA triplexes.[28] Cyclohexyl PNAs were synthesised in the forms (1S,2S), (1R,2R), (1S,2R), (1R,2S); although the presence of S,S isomers does not affect the thermal stability of DNA and RNA hybrids, introduction of R,R isomers results in a destabilisation of the PNA/DNA or RNA complexes. PNA including the (1R, 2S) isomer exhibits higher hybrid stability and ability to discriminate between DNA and RNA.[29]

1.3.3. PNAs with Fluorescent Probes

The introduction of fluorescent probes in biomolecules may constitute a valuable tool to study their structures and biological activity, opening the possibility to design new fluorescent bioactive molecules that can exploit their peculiar properties for diagnostics or therapeutic applications. For more than thirty years, the conjugation of fluorescent marker to DNA or proteins have been successfully applied and more recently also with PNAs.

In literature are now reported different examples of fluorescent PNAs and their cellular uptake, as well as their capability to hybridize specific DNA or RNA sequences, have been widely studied.

The introduction of a fluorescent molecule in the PNA oligomer can be achieved or by classical reaction in solution, or by solid phase reactions while the oligomer is still attached to the resin support.

In 1996 Kremsky *et al*[30] reported the Functionalisation of PNA oligomers with biotin and a fluorescein derivative, with the aim to set up a synthetic protocol to support specific markers in solid phase synthesis. Fluorescein is one of the most used fluorescent probe and finds wide applications in bio analytical chemistry, [31] molecular biology and pharmacokinetic studies.[32] As shown in (Figure 1.21), fluorescein itself cannot be directly used in solid phase synthesis (SPS), while its derivatives bearing a carboxylic group are suitable for classical peptide bond formation.

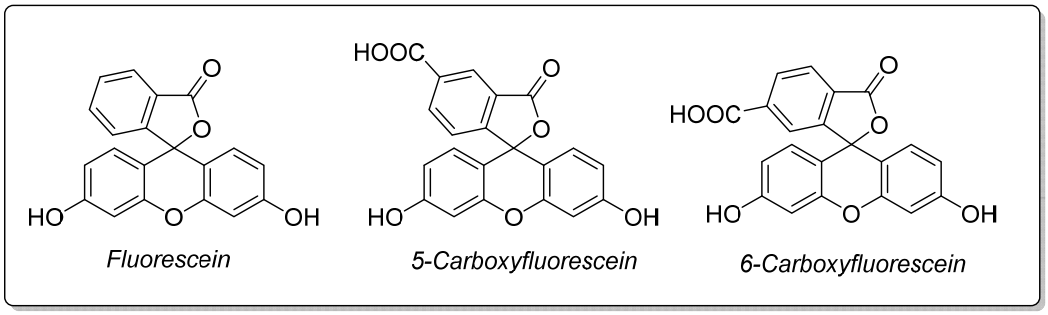

Figure 1.21: Fluorescein and its carboxy-derivatives.

Carboxy fluorescein derivatives, as pure isomer, are commercially available but are quite expensive; thus a mixture of the two isomers 5- and 6- carboxyfluorescein (61:39) were practically used in SPS.[33]

It's also commercially available the isothiocyanate derivative (FITC, Figure 1.22), that allows the outstanding reaction with free amino groups, by formation of stable thiourea bond.

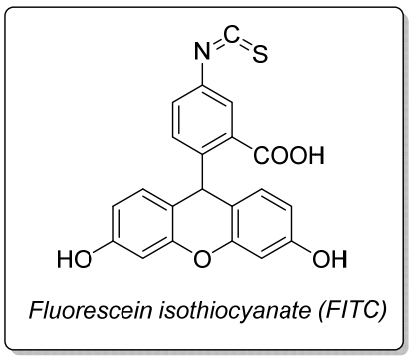

Figure 1.22: Fluorescein isothiocyanate (FITC)

In molecular biology, also rhodamine and its derivatives were widely used, as an alternative to fluorescein (Figure 1.23).

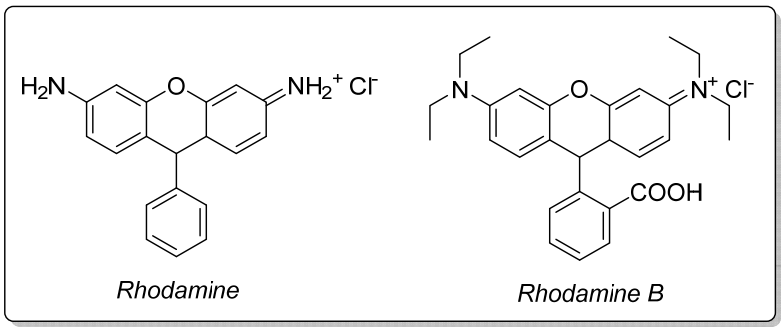

Figure 1.23: Rhodamine and Rhodamine B

More recently, Englund *et al*[34]. Have introduced in the PNA backbone a lysine-based monomer, exploiting the terminal ε-amino group to bind the 9-fluorenacetic acid as a fluorescent probe.

1.3.4. PNA Synthesis

1.3.4.1. Synthesis of PNA monomers

Although PNA monomers are commercially available, they are also relatively easy to synthesize from inexpensive starting materials (Scheme1.1).

As previously mentioned, PNA consists of repeating *N*-(2-aminoethyl) glycine units with a nucleobases attached on to it. The synthesis of the backbone unit can be achieved either *via* reductive amination of glycine ester with an *N*-protected amino acetaldehyde[35] or *via* an

alkylation's of mono-protected ethylenediamine with a bromoacetic acid ester[36]. Either route gives high yields of the desired intermediate.

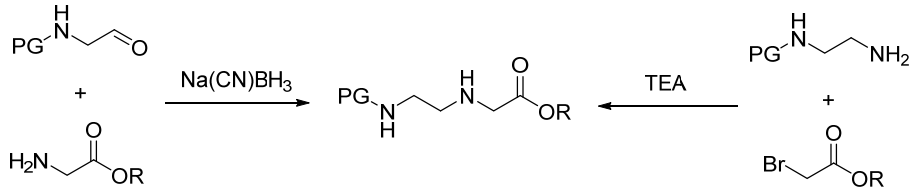

Scheme 1.1: Synthesis of protected (2-aminoethyl) glycine

In the next step, protected nucleobases *viz.,* adenine, guanine, cytosine, thymine or uracil are attached *via* an amide bond using a coupling agent, e.g., DCC[37] or HBTU[38] (Scheme 1.2).

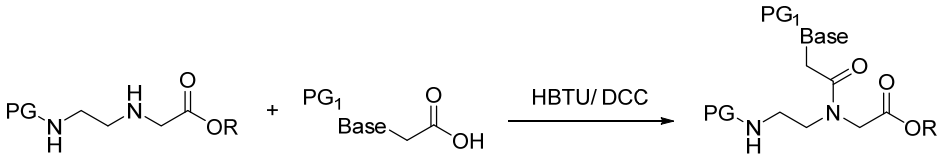

Scheme 1.2: Synthesis of *aeg* PNA monomers

PNA monomers can be assembled using synthetic methods developed for the peptide synthesis both in solid phase and in solution. Different synthetic strategies have been reported in the literature[35-38], but the most used are based on:

- Boc/Cbz protected monomers (Figure 1.24)
- Fmoc/Bhoc protected monomers

In our laboratories the first strategy is routinely used for the synthesis of PNA oligomers, both by manual as well as automated SPS, starting from commercially available *aeg*A **(1)**, *aeg*C **(2)** and *aeg*G **(3)** monomers, while *aeg*T **(4)** one is generally synthesized by ourselves in lab and its synthesis we will see in next chapter 2.

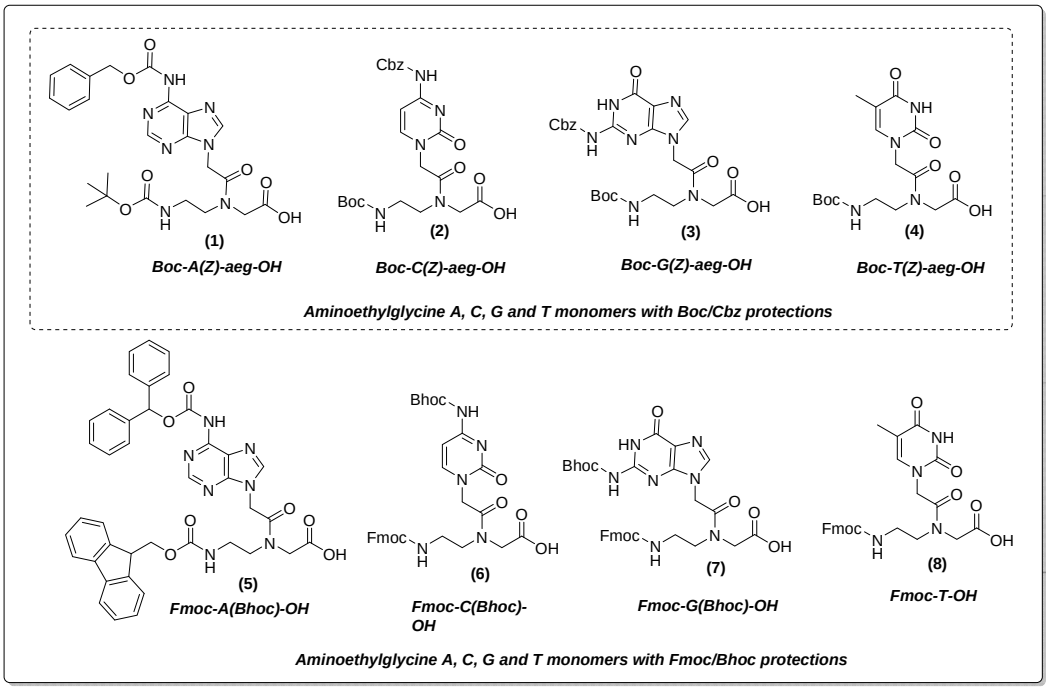

Figure 1.24: Aminoethylglycine A, C, G and T monomers with Boc/Cbz and Fmoc/Bhoc protections

1.3.4.2. Solid phase PNA synthesis

The assembly of PNA using the above described monomers is usually performed on a solid support, preferably *via* by manually or by automated synthesis

The solid support is usually functionalized polystyrene with a cleavable linker. The choice of the linker is very important and depends on the protecting group strategy used. For the Boc/Cbz strategy, the best linker is the MBHA (Figure 1.25-9), an acid labile linker that can be cleaved with a mixture of trifluoroacetic acid and trifluoromethanesulfonic acid. In the Fmoc/Bhoc strategy, an acid labile linker can be used, for example the Rink Amide (Figure 1.25-10). Best results in the Fmoc chemistry are achieved using a polyethylene glycol derivatized polystyrene resin (PEG-PS) that provides a "solution like" environment for the synthesis. The typical linkers used with this resin are the PAL or XAL linkers (Figure 1.25-11 and 12). The loading of the solid support can range from 30 μM/g to >1mM/g. Low loading resins are usually used in the synthesis of PNA-DNA chimera[36a].

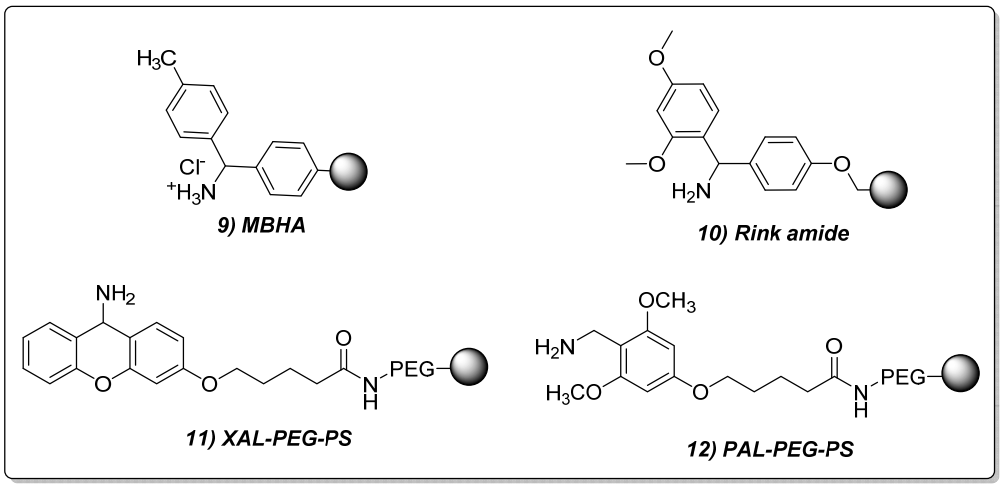

Figure 1.25: Most used solid phase supports for the synthesis of PNAs.

Independently from the strategy, the solid phase oligomers synthesis (Scheme 1.3) proceeds with the following standard synthetic steps:

1) Downloading*:* this step consists in the coupling of the first monomer or a properly protected-amino acid (*e.g.* PG_1-Lysine-*Nε*-PG_2, generally used to improve the solubility in water of the final oligomer), to the resin. This reaction is performed using a smaller amount of the monomer with respect to the loading of the resin, in order to avoid the interaction among the oligomer chains on a bead. A typical loading used in the PNA oligomers synthesis is 0.2 mmol/g.

2) Deprotection: to build the oligomer is necessary to remove the protecting group on the PNA monomer (or amino acid) attached on the resin. For the Boc/Cbz strategy, the Boc group is removed using trifluoroacetic acid (TFA) in presence of *m*-cresol (ratio 95:5). The *m*-cresol was added to function as a scavenger for the *tert*-butyl cations in order to avoid alkylation of the nucleobases.

3) Coupling: this step is the key step of the chain elongation. Using typical condensing agent (HBTU or HATU gave best results) the carboxylic acid function of a monomer is coupled with the amino group of the monomer attached on the resin and previously deprotected.

4) Capping*:* this step is performed in order to avoid that unreacted amino groups can react in the next coupling steps giving mistaken sequence that are more difficult to purify. The preferred capping reagent is acetic anhydride, which reacts very fast with the free amino groups.

Once the oligomer synthesis is completed, the chain is cleaved using the more appropriate reagent (for MBHA resin, TFA and trifluoromethanesulfonic acid (TFMSA) mixture in

presence of *m*-cresol and thioanisole). Usually, in the final cleavage also the protecting group of the exocyclic amino moieties of the nucleobases are also removed. At last, semi preparative HPLC purification were done to isolate the desired PNA oligomer.

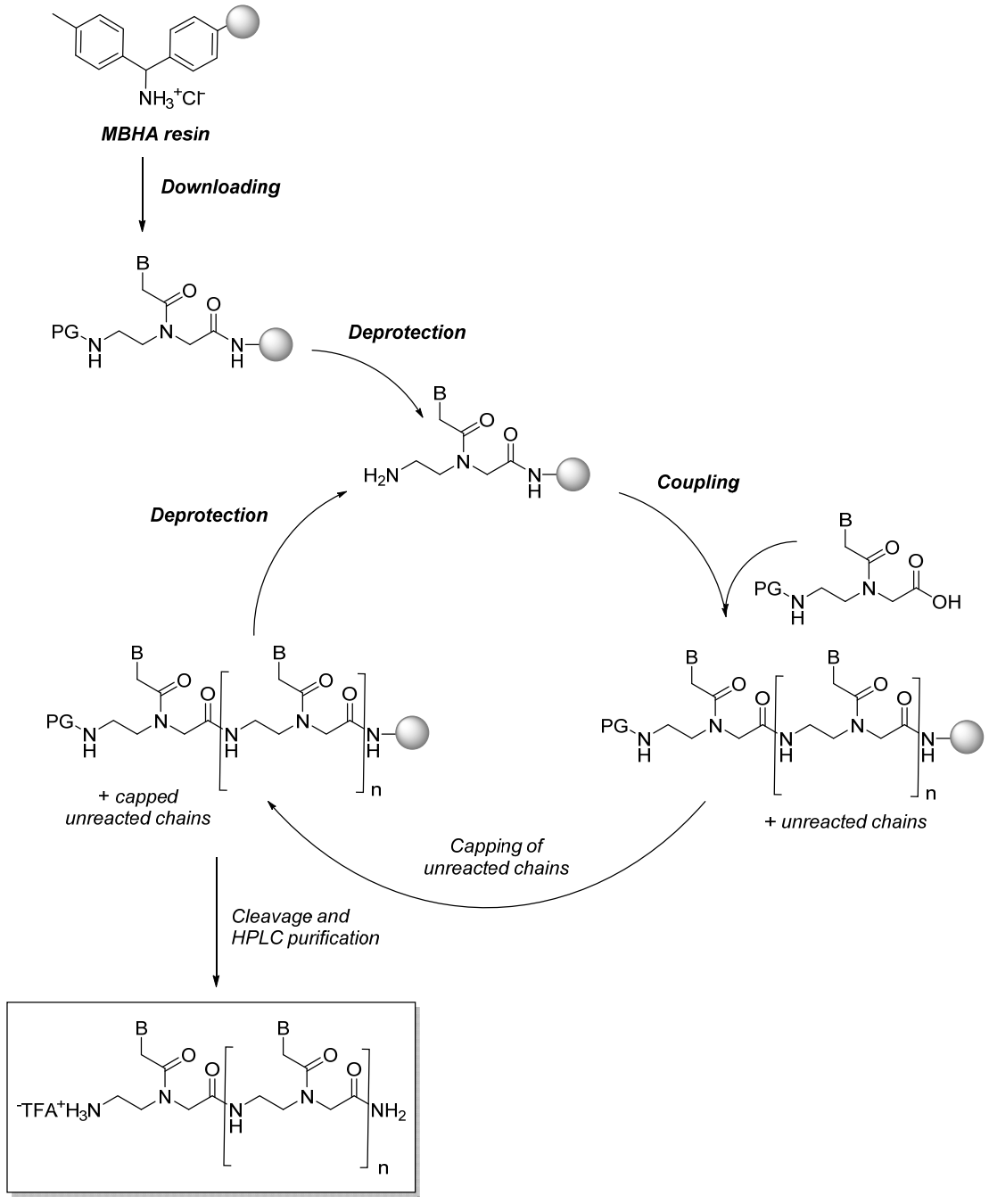

Scheme 1.3: Schematic representation of the solid phase PNA synthesis

The final acetylation is very useful in order to avoid undesired intramolecular side reaction (Scheme 1.4 and 1.5), because of the basicity of the terminal amino moiety and a favourable geometry for rearrangement, acyl migration of the nucleobase acetyl moiety to the *N*-terminal

Position (Scheme 1.4) is a common side reaction.

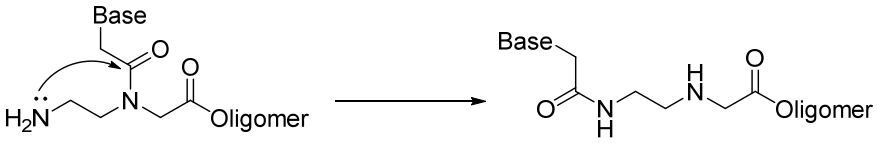

Scheme 1.4: undesired intramolecular side reaction

Another intramolecular side reaction in PNA synthesis is the attack of the primary amine at the *N*-terminal on the carbonyl group of the amide bond. In this case the *N*-terminal unit is lost and cleaved off in the form of a ketopiperazine derivative (Scheme 1.5).

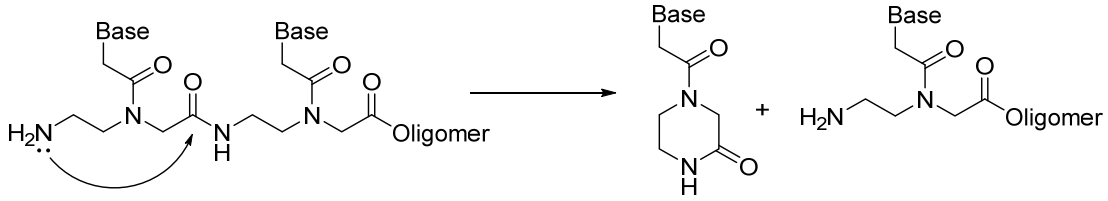

Scheme 1.5: undesired intramolecular side reaction

As mentioned above, HBTU and HATU gave the highest coupling yields in PNA synthesis. However, uronium salts react with primary amines to form guanidinium salts, and this reaction has been shown to cap free α-amines in peptide synthesis efficiently. The capped products are easily identified by mass spectroscopy by the presence of M+100 masses. The higher *p*Ka value of the 2-ethyl amine in PNA and the fact that it is less steric hindered makes PNA monomers even more prone to this reaction (Scheme 1.6). Therefore, pre-activation of the monomers and a slight excess or monomer over HATU are employed in the protocol.

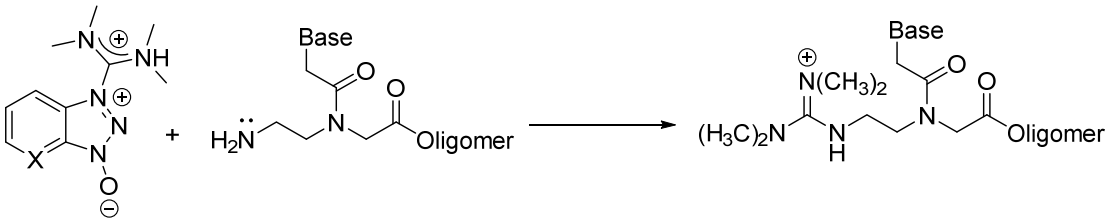

Scheme 1.6: Side reaction between condensing agent and *aeg*PNA monomer

1.3.5. Binding Affinity Evaluation of PNAs

Like other non-covalent structures, the DNA complexes (duplex or triplex) are unstable at high temperatures. When the temperature is increased gradually, this process of heat

denaturation, also called melting, begins in areas with a high A-T content. A-T base pairs can be separated more easily than G-C base pairs. The ***Melting Temperature*** (***Tm***) is defined as the temperature at which half of the DNA strands are in the double-helical state and half are in the single strand states (Figure 1.26).

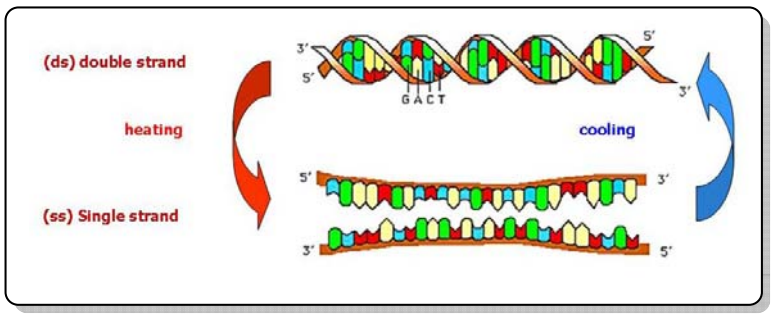

Figure 1.26: Thermal denaturation process of *ds*DNA

The best ways to determine the melting temperature and to evaluate the PNA/DNA interactions are by spectroscopic techniques, as described in the following paragraph, or by Differential Scanning Calorimetry (DSC).

1.3.7. Bibliography

1. Pensato, S.; Saviano, M.; Romanelli, A. *Expert Opin Biol Ther.* **2007**, *7,* 1219-32.

2. Uhlmann, E.; Peyman, A. *Chem. Rev.* **1990**, *90*, 543-584.

3. Doronina, S. O.; Behr, J. *Chem. Soc. Rev.* **1997**, *26,* 63-71.

4. Christensen, L.; Hansen, H. F.; Koch, T.; Nielsen, P. E. *Nucleic. Acids. Res*. **1998,** *26,* 2735-2739.

5. Eldrup, A.; Dahl, O.; Nielsen, P. *J. Am. Chem. Soc.* **1997**, *119*, 11116-11117.

6. Olsen, A. G.; Dahl, O.; Nielsen, P. E. *Bioorg Med Chem Lett*. **2004,** *14,* 1551-4.

7. a) Eldrup, A.; Nielsen, B.; Haaima, G.; Rasmussen, H.; Kastrup, J.; Christensen, C.; Nielsen, P. *Eur. J. Org. Chem.* **2001,** 1781-1790. b) Eldrup, A. B.; Christensen, C.; Haaima, G.; Nielsen, P. E. *J. Am. Chem. Soc.* **2002,** *124*, 3254-62. c) Rajeev, K.; Maier, M.; Lesnik, E.; Manoharan, M. *Org. Lett*. **2002**, *4*, 4395-4398.

8. Gangamani, B. P.; Kumar, V. A. *Chem. Commun.* **1997**, 1913-1914

9. De la Torre, B. G.; Eritja, R. *Bioorg. Med. Chem. Lett.* **2003,** *13*, 391-393

10. Kohler, O.; Seitz, O. *Chem. Comm*. **2003**, 2938-9.

11. a) Kohler, O.; Jarikote, D. V.; Seitz, O. *Chem Bio Chem.* **2005**, *6*, 69-77. b) Jarikote, D. V.; Kohler, O.; Socher, E.; Seitz, O. *Eur. J. Org. Chem*. **2005,** 3187-3195.

12. a) Nielsen, P. E.; Haaima, G.; Lohse, A.; Buchardt, O. *Angew. Chem. Int. Ed*. **1996**, *35,* 1939-1942. b) Sforza, S.; Haaima, G.; Marchelli, R.; Nielsen, P. E. *Eur. J. Org. Chem.* **1999**, 197-204.

13. Hyrup, B.; Egholm, M.; Buchardt, O.; Nielsen, P. E. *Bioorg. Med. Chem. Lett*. **1996**, *6*, 1083-1088.

14. Barawkar, D. A.; Bruice, T. C. *J. Am. Chem. Soc.* **1999,** *121*, 10418-10419.

15. Efimov, V. A.; Choob, M. V.; Buryakova, A. A.; Chakhmakhcheva, O. G. *Nucleosides, Nucleotides & Nucleic Acids.* **1998**, *17*, 1671 - 1679.

16. Efimov, V. A.; Buryakova, A. A.; Choob, M. V.; Chakhmakhcheva, O. G. *Nucleosides, Nucleotides & Nucleic Acids*. **1999,** *18*, 1393 - 1396.

17. Van der Laan, A. C.; Stromberg, R.; van Boom, J. H.; Kuyl-Yeheskiely, E.; Efimov, V. A.; Chakhmakhcheva, O. G. *Tetrahedron Lett*. **1996**, *37*, 7857-7860.

18. Peyman, A.; Uhlmann, E.; Wagner, K.; Augustin, S.; Breipohl, G.; Will, D. W.; Schafer, A.; Wallmeier, H. *Angew. Chem. Int. Ed.* **1996**, *35*, 2636-2638.

19. Kehler, J.; Henriksen, U.; Vejbjerg, H.; Dahl, O. *Bioorg. Med. Chem.* **1998**, *6*, 315-322.

20. Garcia-Echeverria, C.; Husken, D.; Chiesi, C. S.; Altmann, K. *Bioorg. Med. Chem. Lett.* **1997**, *7*, 1123-1126.

21. Kuwahara, M.; Arimitsu, M.; Sisido, M. *J. Am. Chem. Soc*. **1999,** *121*, 256-257.

22. Kumar, V.; Ganesh, K. *Acc. Chem. Res*. **2005**, *38*, 404-412.

23. Kumar, V. *Eur. J. Org. Chem*. **2002**, *2002*, 2021-2032.

24. Gangamani, B. P.; Decosta, M.; Kumar, V. A.; Ganesh, K. N. *Nucleosides, Nucleotides & Nucleic Acids*. **1999**, *18*, 1409-1411.

25. a) D'Costa, M.; Kumar, V.; Ganesh, K. *Org. Lett*. **1999**, *1*, 1513-1516. b) D'Costa, M.; Kumar, V.; Ganesh, K. *Org. Lett.* **2001**, *3*, 1281-1284.

26. Sharma, N. K.; Ganesh, K. N. *Chem Commun (Camb).* **2003**, 2484-5.

27. Puschl, A.; Tedeschi, T.; Nielsen, P. *Org. Lett*. **2000**, *2*, 4161- 4163.

28. a) Govindaraju, T.; Kumar, V.; Ganesh, K. *J. Org. Chem*. **2004**, *69*, 5725-5734 b) Govindaraju, T.; Kumar, V. A.; Ganesh, K. N. *Chem. Commun*. **2004**, 860-861 c) Myers, M. C.; Witschi, M. A.; Larionova, N. V.; Franck, J. M.; Haynes, R. D.; Hara, T.; Grajkowski, A.; Appella, D. H. *Org Lett.* **2003**, *5*, 2695-8. d) Englund, E. A.; Xu, Q.; Witschi, M. A.; Appella, D. H. *J. Am. Chem. Soc.* **2006**, *128*, 16456-7 e) Lagriffoule, P.; Eriksson, M.; Jensen, K. K.; Nielsen, P. E.; Wittung, P.; Norden, B.; Buchardt, O. *Chem. Eur. J.* **1997**, *3*, 912-919.

29. Corradini, R.; Sforza, S.; Tedeschi, T.; Marchelli, R. *Chirality.* **2007**, *19*, 269-294.

30. J.N. Kremsky, M. Pluskal, S. Casey, H. Perry-O'Keefe, S.A. Kates, N.D. Sinha, *Tetrahedron Lett.* **1996**, *37(25)*, 4313-4316.

31. a) F.V. Bright, *Anal. Chem.* **1988**, *60*, 1031A-1039A; b) R.P. Haughland, *Handbook of Fluorescent Probes and Research Chemicals* **1992**, Molecular Probes, Eugene, OR; c) M. Miki, *Eur. J. Biochem.* **1987**, *164*, 229-235.

32. M. Lu-Steffes *et al,. Clin. Chem.* **1982**, *28*, 2278-2282.

33. Adamczyk, M., Fishpaugh, J. R., Heuser, K. *J. Bioconjugate Chem.* **1997**, *8*, 253-255.

34. Englund, E.A., Appella, D. A, *Org. Lett.* **2005**, *7*, 3465-3467.

35. a) Salvi, J-P., Walchofer, N., Paris, J., *Tetrahedron Lett.,* **1994,** *35,* 1181-1184 b) Farese, A, Patino, N., Condom, R., Dalleu, S., Guedj, R. *Tetrahedron Lett.,* **1996**, *37*, 1413-1416 c) Falkiewicz, B., Kolodziejczyk, A. S, Lieberek, B, Wisniewski, K., *Tetrahedron* **2001**, *57*, 7909.

36. a) Van der Lann, A.C., Brill, R., Kuimelis, R.G., Kuyl-Yeheskiely, E., van Boom, J. H., Andrus, A., Vinayak, R., *Tetrahedron Lett*. **1997**, *38*, 2249-2252 b) Fader, L.D.,

Boyd, M., Tsantrizos, Y.S., *J. Org. Chem.,* **2001**, *66*, 3372-3379 c) Clivio, P., Guillaume, D., Adeline, M-T., Hamon, J., Riche, C., Fourrey, J-L., *J. Am. Chem. Soc.,* **1998,** *120*, 1157-1166 d) Efimov, V. A., Buryakova, A. A., Choob, M., Chakhmakhcheva, O. G., *Russ. J. Bioorg. Chem (Engl. Transl)* **1998,** *24,* 618-630.

37. Egholm, M., Nielsen, P.E., Buchardt, O., *J. Am. Chem. Soc,* **1992**, *114*, 9677-9678.

38. Thomson, S. A., Josey, J. A., Cadilla, R., Gaul, M.D., Hassman, C., Fred, *Tetrahedron,* **1995**, *51*, 6179-6194.

Chapter 1: Peptide Nucleic Acid (PNA)

Section 4: Aim of the thesis

1.4.1. Present Work

The preceding section has given an overview on the concept of peptide nucleic acids (PNAs) which are among the most interesting and versatile artificial structural mimic of nucleic acid (DNA). These are having the properties of natural oligonucleotides. The stability of PNA/DNA complexes makes PNAs powerful tools in antisense and antigene applications, and as markers in DNA screening assays. The major drawbacks of PNA are like poor water solubility, inefficient cell uptake, self-aggregation and uncertainty in directionality of binding restricts PNA extensive applications. Hence various modifications of PNA for improving the activity were attempted by different research groups, and these methods were described in section 3 of this chapter.

This research work concerns with the design, synthesis, characterization and analytical studies of newly modified Peptide Nucleic Acids (PNAs), [which is mimic of DNA and RNA] in non conventional manner for the applications in DNA interactions, RNA targeting and cellular imaging.

Moreover, in this thesis we introduce a very innovative and new technique for the interaction between PNA and DNA by using Stopped-flow spectroscopy. This technique has never been used so far to study the interaction between PNA/DNA strands in the formation of hybrids. Normally the affinity of PNA for DNA were detected by using melting temperature but sometimes this technique is not appropriate, especially if PNA contain some thermal sensitive functional groups. So, to overcome these obstacles we started this ingenious study of PNA-DNA interaction by using stopped-flow spectroscopy. We also design and synthesized PNA oligomers having magnetic and luminescent properties by the conjugation of iron oxide magnetic nanoparticles (MNPs) and by organometallic gold complexes which are, in principle, applicable for diagnostic and therapeutic purposes, miRNA targeting and cellular imaging.

Chapter 2 deals with the design and synthesis of newly modified lysine based Peptide Nucleic Acids (PNAs) decamer **(A)**, with the standard TCACTAGATG sequence of nucleobases and the corresponding fluorescent PNA-FITU (fluorescein isothiourea) decamer **(B)**. All these decamers were manually synthesized by SPPS using standard Boc-based chemistry (Figure 1.27)

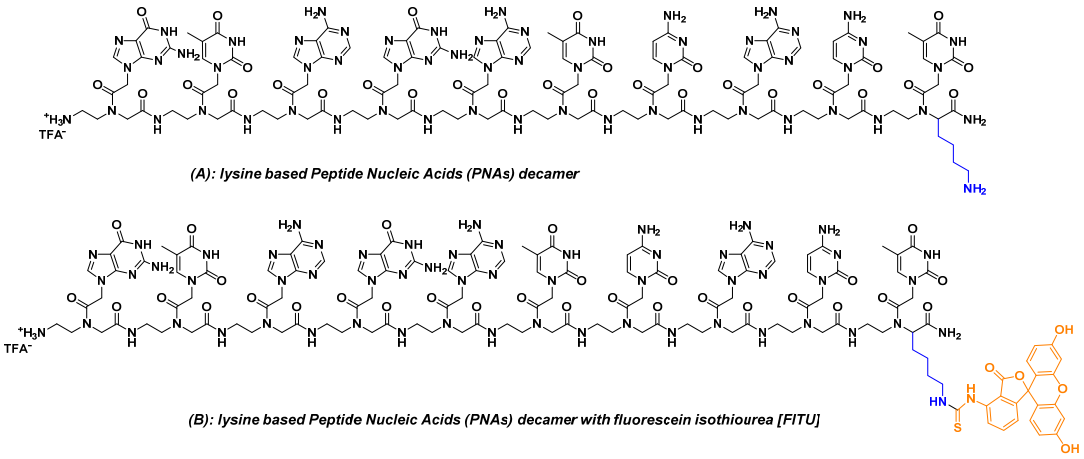

Figure 1.27: Synthesis of Peptide Nucleic Acids (PNAs) decamer **(A)** and **(B)**

The interaction of both decamers **(A)** and **(B)** with the complementary parallel and antiparallel DNA was followed by steady-state and stopped-flow fluorescence intensity. The kinetics of the PNA-DNA duplex formation has been studied. In particular, fluorescence stopped-flow technique has been exploited to compare the affinity of two PNA-DNA duplexes: using parallel and antiparallel DNA, such data would be very important for the evaluation and improvement of antisense reagents and of diagnostic probes based on PNA.

Chapter 3 deals with the design, synthesis and characterization of Peptide Nucleic Acids (PNA) and their conjugation with magnetic nanoparticles (MNPs) for the treatment in diagnostic and therapeutic purposes and the synthesis of Heterobifunctional Linker for the conjugation of PNA (Figure 1.28)

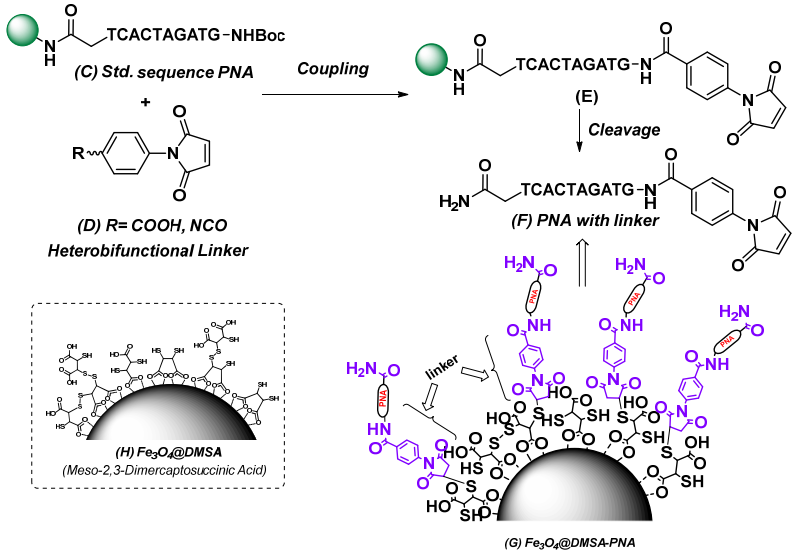

Figure 1.28: Functionalisation of magnetic nanoparticles with PNA through heterobifunctional linker.

However, MNPs-DMSA with functionasalizaion strategies for the specific purpose with polymers, antibodies, and cytokines has been reported. In order to take all these advantages, so we have been synthesised MNPs subsequently coated with DMSA with functionasalizaion strategies with PNA through heterobifunctional linker **(D)**. MNPs surface with amine (isocyanate) or carboxylic acid functional groups have been modified with heterobifunctional molecule and further reacted with Peptide nucleic acid (PNA). Taking the advantage of this approach here is the use of a linker molecule with PNA that anchored to MNPs. Amine-functionalized PNA were covalently attached to MNP-DMSA *via* an ethyl-3-(3-dimethylaminopropyl)-carbodiimide (EDC) or NHS mediated coupling reaction or by Michael addition of free thiol group attached to MNP-DMSA, on to the maleimide group **(G)**.

Chapter 4 deals with design and synthesis of modified Thymine monomer and PNA with simple organometallic Gold (I) complexes which is applicable for cellular imaging. Here we introduce Phosphine gold (I) on to the Thymine monomer **(K)** and homothymine decamer **(L)** (PNA) containing the triple bond at the terminal position (Figure 1.30). The development of gold (I)-acetylide complexes has led to several novel compounds. Most notably they have been investigated for their interesting photochemical properties or rich luminescence properties. Luminescence from gold-acetylide complexes typically results from "aurophilicity".

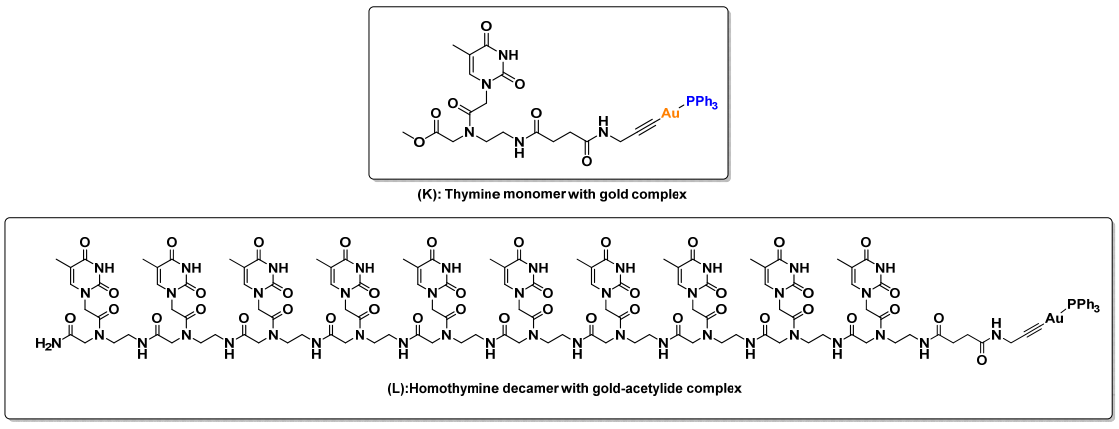

Figure 1.30: Thymine monomer **(K)** and homothymine 10-mer PNA **(L)** with gold complex

Taking all these advantages, we have successfully synthesized phosphine gold complex of thymine monomer in solution phase and studied its photoluminescence emission properties and which are applicable in cellular imaging. gold (I) complex which is never carried out in the field of conjugation with PNA.

Chapter 2: Design and synthesis of modified peptide nucleic acids (PNAs) with and without fluorescein isothiourea and its kinetic studies by using stopped-flow technique.

Section 1: Synthesis of aminoethylglycine PNA monomer and PNA decamers

2.1.1. Introduction

Peptide nucleic acid (PNA) is one of the most studied and interesting DNA mimic with great potential for biomedical applications, both in diagnostics and therapy[1]. The chemical structure of PNA is quite different with respect to that of natural nucleic acids in that its backbone is composed of *N*-(2-aminoethyl)glycine repeating units forming a pseudopeptide chain on which the four nucleobases like adenine or A, cytosine or C, guanine or G and thymine or T (Fig. 2.1). The neutral character of PNA molecules and the distance between two adjacent nucleobases (the same as that found in DNA and RNA) confer them stronger and more selective binding affinity for complementary nucleic acid (DNA and RNA) strands than natural nucleic acids[2].

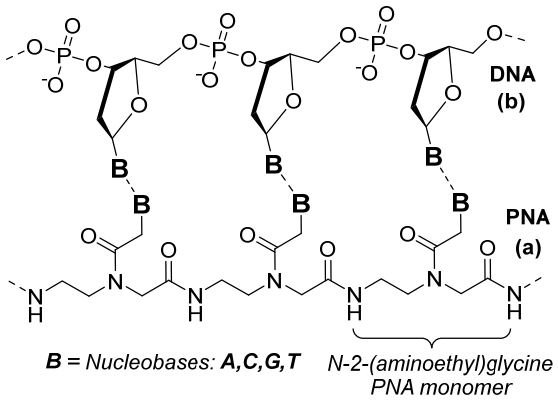

Figure 2.1: Peptide Nucleic Acid oligomer (a) with its complementary DNA (b)

Though in DNA-DNA duplexes the two strands are always in an antiparallel orientation (with the 5′-end of one strand opposed to the 3′- end of the other), PNA:DNA adducts can be formed in two different orientations, termed parallel (in which the terminal amino group of PNA is opposed to the 5′ end of DNA) and antiparallel (where, on the contrary, the amino group is opposed to the 3′ end of DNA). However, the antiparallel binding is favoured over the parallel one[3]. The binding of PNAs to DNA and RNA targets is stronger than that of DNA-DNA or RNA-RNA bindings[4]. This enhanced binding affinity is partially due to the uncharged property of the PNAs. Since PNAs are neutral in charge, the duplexes formed by PNA-DNA or PNA-RNA hybrids lack the electrostatic repulsion formed by DNA-DNA or RNA-DNA duplexes, resulting in a very stable duplex formation even at a relatively high temperature and a very high binding affinity.

One of the most popular, easy and reliable method to measure the stability of PNA-DNA hybrid systems is the melting temperature (T_m), that is the monitoring of the changes in UV

absorption at about 260 nm as a function of temperature[5]. The higher affinity of PNA-DNA binding is expressed by the larger melting temperature values of PNA-DNA hybrids with respect to those of DNA-DNA ones. In addition to melting temperature measurements, isothermal titration Calorimetry (ITC) [6] and atomic force microscopy (AFM) have been proposed as suitable methods[7].#But the thermodynamic data are obtained using a big quantity of materials failing to provide information on the kinetics of the interaction. Surface Plasmon Resonance (SPR)[8] and SPR-enhanced fluorescence spectroscopy[9] have been used to investigate also the kinetics of DNA-DNA and PNA-DNA interactions but every technique shows some advantages along with some drawbacks and a detailed description of the phenomenon is thus limited.

The stopped-flow absorbance spectroscopy and fluorescence intensity method[10] offers a powerful tool for a detailed kinetic analysis of interactions since it can monitor reactions continuously in real time and in a real physiological medium[11]. It has been used in the past to obtain a detailed understanding of locked nucleic acid (LNA) [11a] and PNA[12] as a trapping strand in helicase-catalyzed unwinding of oligonucleotide substrates. But fluorescence stopped-flow spectroscopy has never been used for a detailed PNA interaction study with parallel and antiparallel DNA with the aim of measuring the different affinities of the formed duplexes. Moreover, Gangamani *et al*. have previously demonstrated that intrinsic fluorescent PNA analogues can be used to monitor PNA self-melting and PNA-DNA duplex transitions without affecting or perturbing their structures.[13]

2.1.2. Objective

In the present work, the synthesis of newly modified lysine based Peptide Nucleic Acids (PNA) decamer **1**, with the TCACTAGATG sequence of nucleobases, and the corresponding fluorescent PNA-FITU (fluorescein isothiourea) decamer **2** were synthesized with standard manual Boc-based chemistry using MBHA resin loaded with the N(α)-Boc-N(ε)-Fmoc-*L*-lysine (Figure 2.2) The interaction of both decamers **1** and **2** with the complementary parallel and antiparallel DNA was followed by steady-state and stopped-flow fluorescence intensity. The kinetics of the PNA-DNA duplex formation has been studied. In particular, fluorescence stopped-flow technique has been exploited to compare the affinity of two PNA-DNA duplexes: using parallel and antiparallel DNA, such data would be very important for the evaluation and improvement of antisense reagents and of diagnostic probes based on PNA.

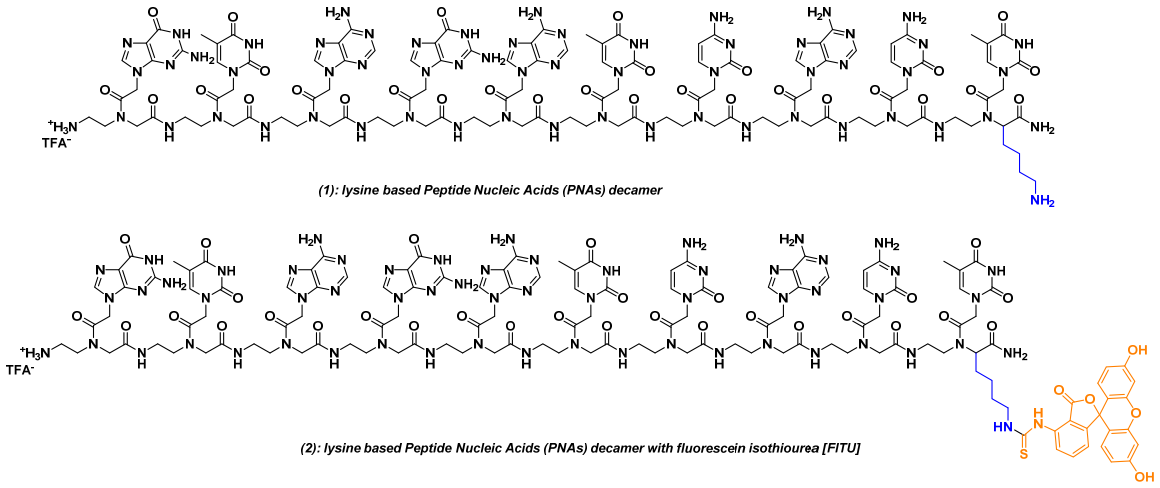

Figure 2.2: Synthesis of Peptide Nucleic Acids (PNAs) decamer **(1)** and **(2)**

The specific objectives of this chapter are

1. Solid phase synthesis of oligomers (PNAs) decamer **1** and corresponding fluorescent PNA-FITU decamer **2** by using standard manual Boc-based chemistry, using MBHA resin loaded with the N(α)-Boc-N(ε)-Fmoc-*L*-lysine (loading 0.2 mmol/g) and also synthesis of aminoethylglycine PNA monomer (Thymine monomer).

2. Cleavage from the solid support, purification and characterization of the oligomers

3. Kinetic studies of PNA oligomers **1** and corresponding fluorescent PNA-FITU decamer **2** with its complementary parallel and antiparallel DNA by steady-state and stopped-flow fluorescence instrument. This technique has never been used to study the interaction between Peptide Nucleic Acids (PNA) and DNA strands in the formation of hybrids.

2.1.2.1. Synthesis of aminoethylglycine PNA monomer (*aeg* T monomer)

The synthesis of unmodified *aeg*PNA monomers were carried out following the literature procedures[14]. The synthesis was started from the easily available ethylene diamine **3**, (Scheme 2.1). This was treated with di-*tert*-butyl dicarbonate to give the mono-protected derivative **4** and was obtained by using a large excess of ethylene diamine over the di-*tert*-butyl dicarbonate in high dilution conditions. The *di*-Boc derivative which was obtained as a minor product. The *N*-Boc-ethylenediamine **4** was then subjected to *N*-alkylation using methyl bromoacetate **5** and Triethyl amine in dry acetonitrile to yield the corresponding

methyl *N*-(2-Boc aminoethyl) glycinate **6,** which is the common intermediate or backbone for the preparation of all the PNA monomers in good yield. This methyl *N*-(2-Boc aminoethyl) glycinate **6** was further treated with thymine acetic acid **7** in presence of *N*-(3-Dimethylaminopropyl)-*N′*-ethylcarbodiimide hydrochloride (EDC.HCl) as a coupling agent in anhydrous acetonitrile, gives the corresponding *N*-(Boc-aminoethylglycyl)-thymine methyl ester **8** which was purified by using column chromatography with an excellent yield. The methyl ester **8** was hydrolyzed very efficiently with lithium hydroxide in methanol at rt followed by acidification by using 1M solution of $KHSO_4$ to give the corresponding acid **9** which was further used for solid phase synthesis and all the compounds exhibited ^{1}H and ^{13}C NMR spectra consistent with the reported data.[14]

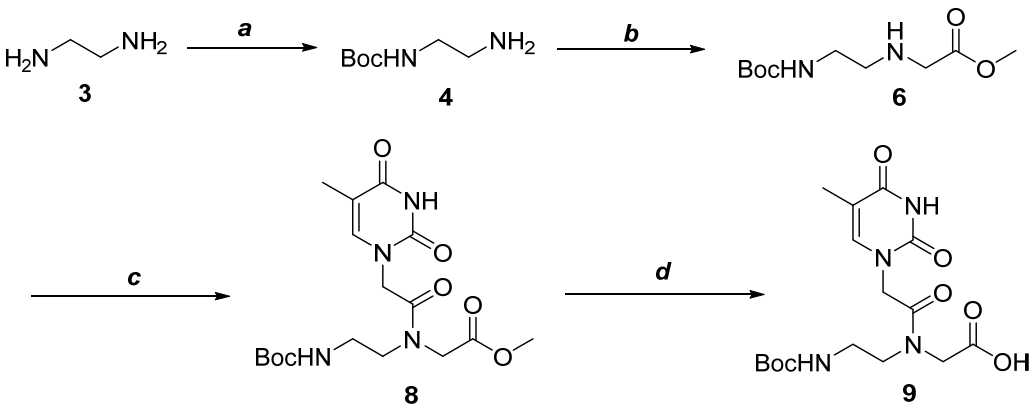

Scheme 2.1: Reagents and conditions: *a) $(Boc)_2O$, THF, 0 ^{o}C - rt, 12 hr, 95% b) methyl bromoacetate* ***(5)****, NEt_3, CH_3CN, rt, 3 hr, 40% c) Thymine acetic acid* ***(7)****, EDC.HCl, CH_3CN, rt, 3 hr, 82% d) $LiOH.H_2O$, MeOH, rt, 3 hr, 86%.*

2.1.3. General principle of Solid Phase Peptide Synthesis (SPPS)

The solid phase peptide synthesis method introduced by Merrifield,[15] offers great advantages in contrast to solution phase method. The fundamental promise of this technique involves the incorporation of *N*-*α*-amino acids into a peptide of any desired sequence with one end of the sequence remaining attached to a solid support matrix. After the desired sequence of amino acids has been obtained, the peptide can be removed from the polymeric support (Scheme 2.2). The solid support is a synthetic polymer that bears reactive groups such as $-NH_2$. These groups are made so that they can react easily with the carboxyl group of an *N*-*α*-protected amino acid, thereby covalently binding it to the polymer. The amino protecting group can then be removed and a second *N*-*α*-protected amino acid can be coupled to the attached amino acid. These steps are repeated until the desired sequence is obtained. At the end of the

synthesis, a different reagent is applied to cleave the bond between the C-terminal amino acid and the polymer support; the peptide is then released into solution and can be obtained from the solution.

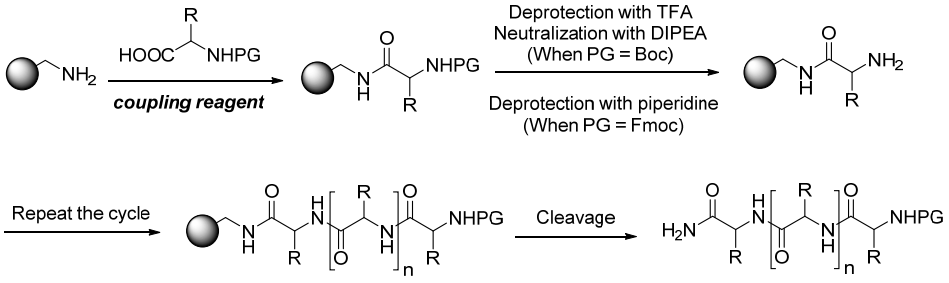

Scheme 2.2: General protocol for solid phase peptide synthesis.

2.1.3.1. Synthesis of PNA decamer (1)

As in the case of solid phase peptide synthesis, PNA synthesis is also done conveniently from the C- terminus to the N- terminus. For this, the monomeric units must have their amino functions suitably protected, with their carboxylic acid functions free. In present work the PNA decamer **1** (Scheme 2.2), with the TCACTAGATG sequence of nucleobases, and the corresponding fluorescent PNA-FITU decamer **2** (Scheme 2.3) were synthesized with standard manual Boc-based chemistry by using MBHA resin (4-methyl-benzhydryl amine) **3**.

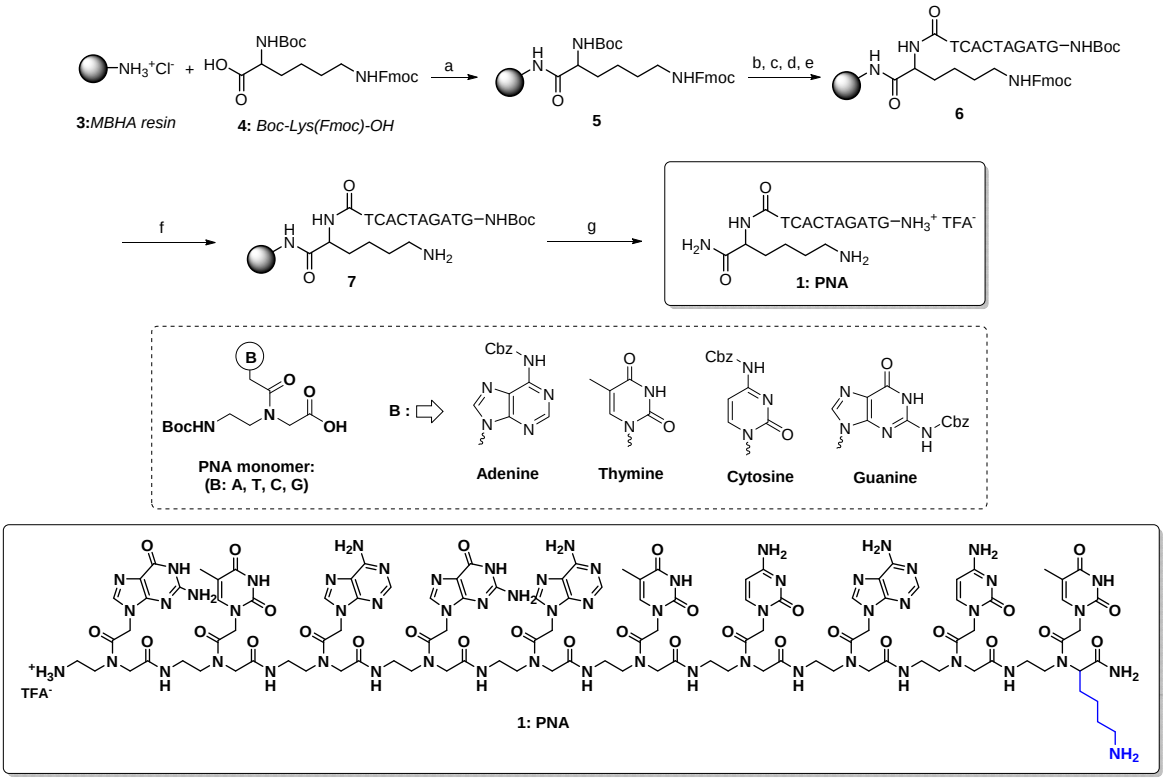

Scheme 2.2: Reagents and conditions: *a) HATU, DIPEA, NMP, 24 hr, rt; b) TFA/m-cresol, 95:5, 2 × 4 min, rt; c) CH_2Cl_2/DIPEA, 95:5, 2 × 2 min, rt; d) PNA monomer, HATU, DIPEA, NMP, 2 hr, rt; e) Ac_2O/Pyridine/NMP,1:25:25, 2 × 1 min, rt; f) 20% Piperidine in DMF, 2 × 20 min, rt; g) TFA/TFMSA/thioanisole/m-cresol 6:2:1:1 (v/v), 1 hr, rt.*

The synthesis was performed with standard manual Boc-based chemistry using MBHA resin **3** loaded with the N(*α*)-Boc-N(*ε*)-Fmoc-*L*-lysine monomer **4** by using HATU as a coupling reagent in order to obtain functionalized resin **5** with loading 0.2 mmol/g (Scheme 2.2). Then the tert-butyloxycarbonyl (Boc) group of the loaded lysine **5** was removed by treatment with 5% *m*-cresol in TFA to get an amine TFA salt which was neutralized by 5% DIPEA in dichloromethane. Then the free amine on resin was coupled with thymine monomer with DIPEA and HATU in NMP as a solvent. After coupling step resin were washed with NMP, and then treated with a solution of Ac_2O/pyridine/NMP (1:25:25, v/v). The cycles were repeated using the monomers like cytosine, adenine and guanine with the same protocol to afford the corresponding supported PNA 10-mer on resin **6**. Then, the Fmoc group was removed by treatment with a solution of 20% piperidine in DMF to give resin **7**, for which the presence of the free amino group was confirmed by the Kaiser test. Then the resin were cleaved by washing with TFA, and subsequently stirred with a mixture of TFA/TFMSA/thioanisole/*m*-cresol (6:2:1:1 v/v). The reaction mixture was filtered, and the filtrate were concentrated to by the addition of diethyl ether to afford white coloured crude PNA decamer **1**, which was purified by receive phase HPLC and analyzed by mass.

2.1.3.2. Purification of decamer (1) by reverse phase HPLC

The crude decamer **1** was purified by reverse phase semi preparative HPLC by column (tR = 6.2 min). The purity of the **1** was checked by LC-MS (Figure 2.3 and 2.4)

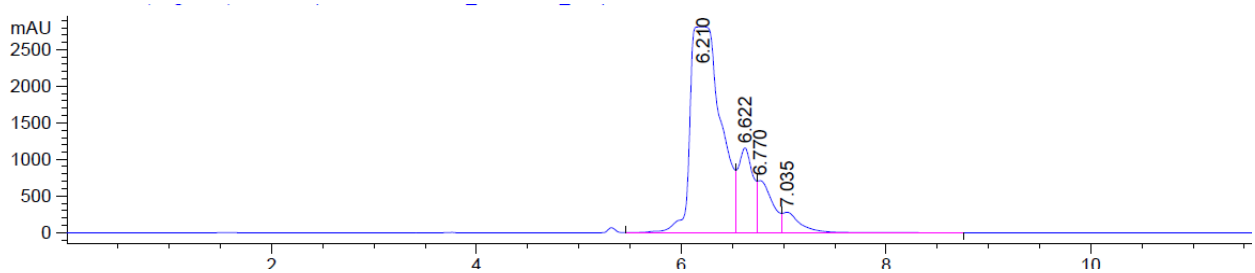

Figure 2.3: HPLC of decamer **1,** retention time 6.2 min.

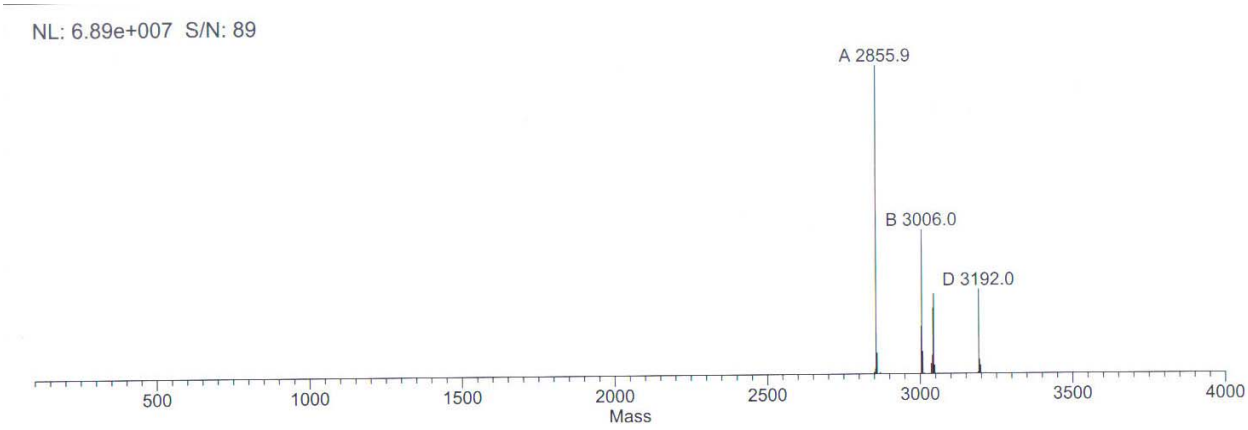

Figure 2.4: ESI-Mass analysis of decamer **1**, found *m/z*: $C_{114}H_{149}N_{60}O_{31}^{+}$: 2855.9

2.1.3.3. Synthesis of fluorescent PNA-FITU decamer (2)

The MBHA resin **7**, with the free amine group on lysine monomer was directly reacted with fluorescein isothiocyanate [FITC] with DIPEA in DMF to give resin **8**, (Scheme 2.3), which were tested by Kaiser Test.

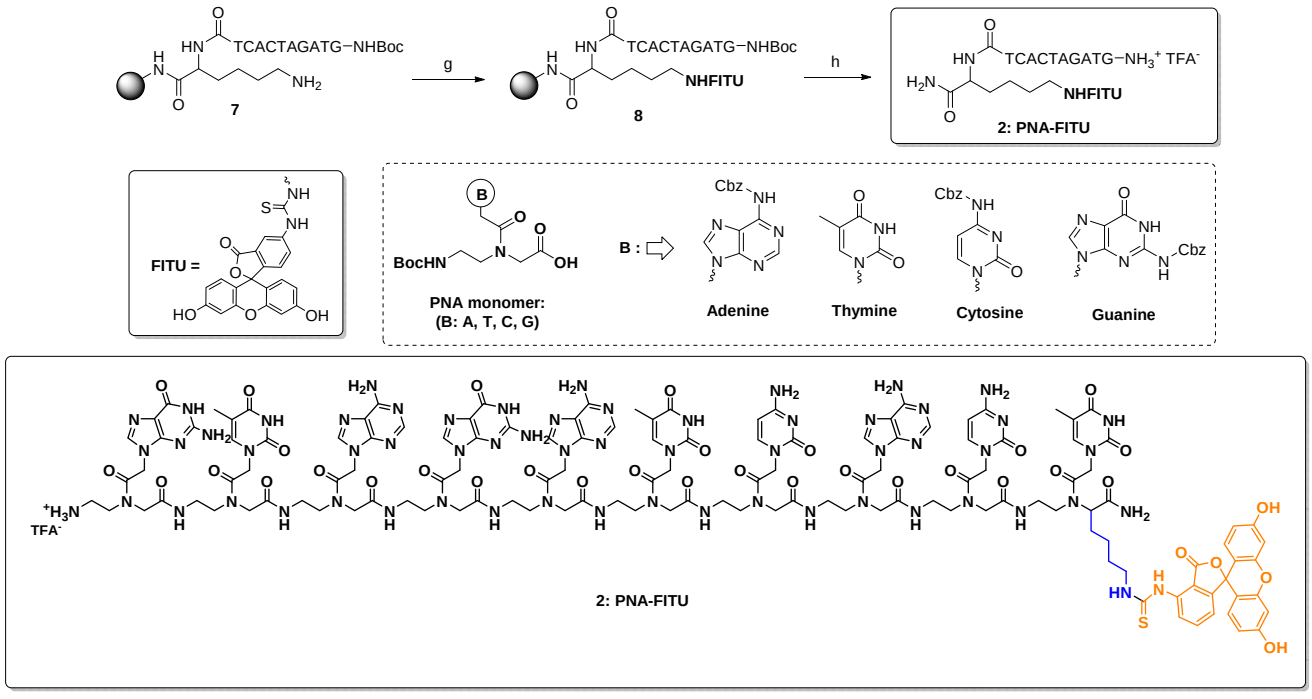

Scheme 2.3: Reagents and conditions: *g) FITC, DIPEA, DMF, 12 hr, rt; h) TFA/TFMSA/thioanisole/m-cresol 6:2:1:1 (v/v), 1 hr, rt.*

Then the resin were cleaved by washing with TFA and stirred with a mixture of TFA/TFMSA/thioanisole/*m*-cresol (6:2:1:1 v/v). The reaction mixture was filtered, the filtrate were concentrated and the residue taken up with diethyl ether to afford a yellow coloured crude fluorescent PNA-FITU decamer **2** which was purified by reverse phase HPLC and characterized by MALDI-TOF.

2.1.3.4. Purification of fluorescent PNA-FITU decamer (2) by reverse phase HPLC

The fluorescent PNA-FITU decamer **2** was purified by reverse phase semi preparative HPLC (tR = 12.9 min). The purity of **2** was checked by LC-MS (Figure 2.4 and 2.5)

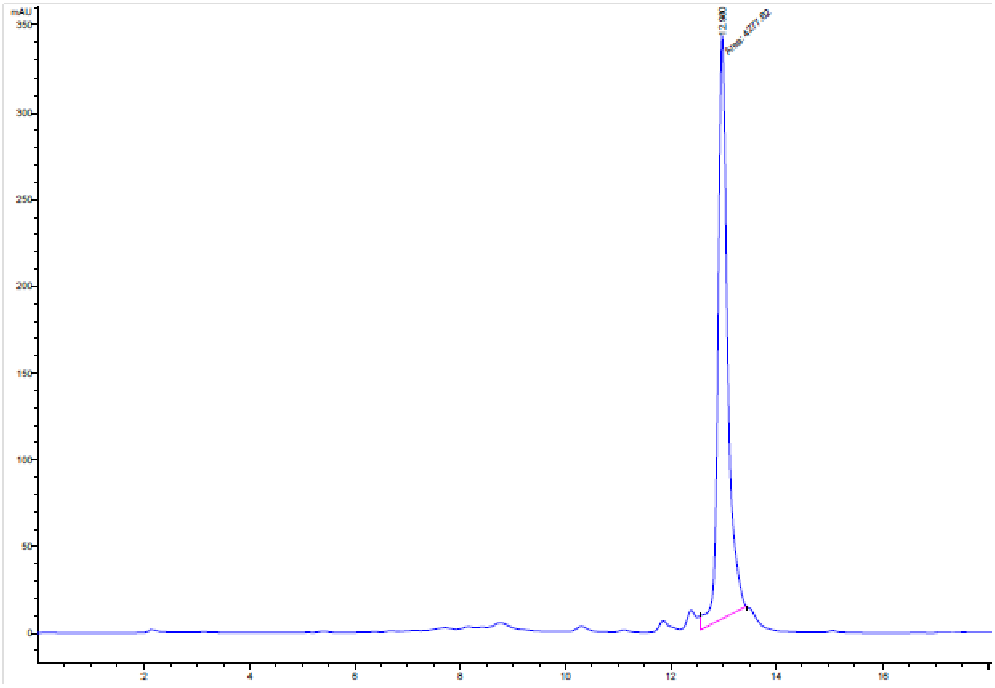

Figure 2.4: HPLC of fluorescent PNA-FITU decamer **2,** retention time 12.9 min.

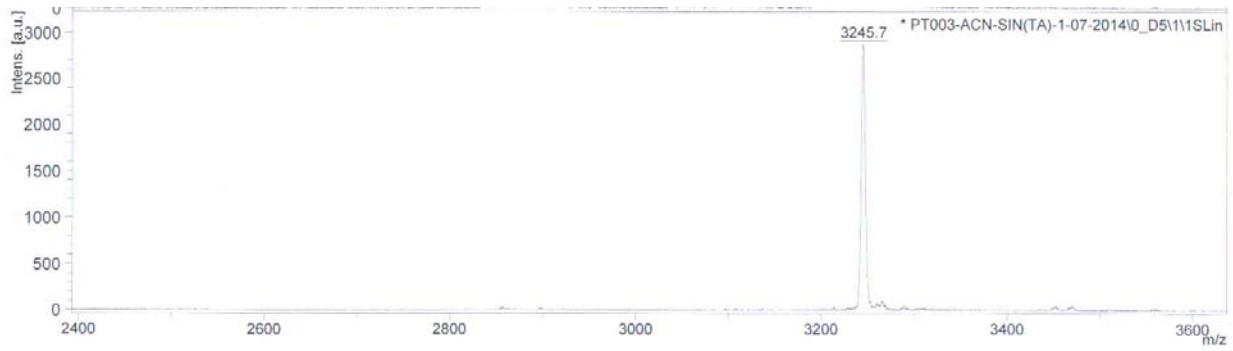

Figure 2.5: ESI-Mass analysis of fluorescent PNA-FITU decamer **2**, found *m/z*: $C_{135}H_{160}N_{61}O_{36}S^{+}$: 3245.7

2.1.4. Bibliography

1. Nielsen, P. E., Egholm, M., Berg, R. H., Buchardt, O. *Science*, **1991**, *254*, 1497-1500.

2. Egholm, M., Buchardt, O., Christensen, L., Behrens, C., Freier, S. M., Driver, D. *et al. Nature*, **1993**, *365*, 566-568.

3. Pellestor, F., Paulasova, P. *Eur. J. Hum. Genet.,* **2004**, *12*, 694-700.

4. Wang, G., Xu, X. S. *Cell Res.*, **2004**, *14*, 111-116.

5. Nielsen, P. E., *Peptide Nucleic Acids: Protocols and Applications, Horizon Bi, Wymondham, UK*, **2004**.

6. Schwarz, F. P., Robinson, S., Butler, J. M. *Nucleic Acids Res*., **1999**, *27*, 4792-4800.

7. Cao, M., Deng, L., Xu, H. *Colloids Surf. A Physicochem. Eng. Asp*. 2015, *470,* 46-51.

8. Ananthanawat, C., Hoven, V. P., Vilaivan, T., Su, X. *Biosens. Bioelectron*. **2011**, *26*, 1918-1923.

9. Kambhampati, D., Nielsen, P. E., Knoll, W. *Biosens. Bioelectron*. **2001**, *16*, 1109-1118.

10. Sujak, A.; Drepper, F.; Haehnel, W. *J. Photochem. Photobiol. B Biol.* **2004**, *74*, 135-143.

11. a) Barbero, N.; Napione, L.; Visentin, S.; Alvaro, M.; Veglio, A.; Bussolino, F. *Chem. Sci.* **2011**, *2*, 1804-1809 b) Dey, D.; Maiti, C.; Maiti, S.; Dhara. D. *Phys. Chem. Chem. Phys.* **2015**, *17*, 2366-2377.

12. Nanduri, B.; Eoff, R. L.; Tackett, J.; Raney, K. D. *Nucleic Acids Res.* **2001**, *29*, 2829-2835.

13. Gangamani, B. P.; Kumar, V. A.; Ganesh, K. N. *Chem. Commun.* **1997**, 1913-1914.

14. Dueholm, K. L., Egholm, M., Behrens, C., Christensen, L., Hansen, H. F., Vulpius, T. *J. Org. Chem.* **1994**, *59*, 5767-5773.

15. Merrifield, R. B. *J. Am. Chem. Soc*. **1963**, *85*, 2149-2154.

Chapter 2: Design and synthesis of modified peptide nucleic acids (PNAs) with and without fluorescein isothiourea and its kinetic studies by using stopped-flow technique.

Section 2: Kinetic studies of PNA: DNA duplexes by fluorescence Stopped-flow technique

2.2.1. Introduction to Fluorescence Stopped-flow spectroscopy

Fluorescence spectroscopy has been widely used to study ligand-protein interaction because of its simplicity and sensitivity. Fluorescence methods are particularly popular because they are well suited for protein-ligand interactions with dissociation constants in the range of 10^{-4} to 10^{-8} M, where some protein-nucleic acid dissociation constants fall. Many fluorescence parameters, such as anisotropy, intensity and energy transfer efficiency, are sensitive to formation of protein-ligand complexes and can be utilized to derive binding isotherms[1]. The change in fluorescence intensity on formation of a protein ligand complex is one of the simplest ways to measure binding of a ligand to a protein.

Stopped flow:

Stopped-flow technique is useful for studying fast reactions that have half-lives as short as a few milliseconds[2]. Many methods are available for measuring the equilibrium binding constant of a protein with a ligand, where the ligand can be a small molecule or another macromolecule such as a protein or nucleic acid. However, many biological processes are controlled not by equilibrium constants but by the kinetics of the interaction between protein and ligand and for this reason it is necessary to measure the association and dissociation rate constants in order to fully understand a system. Although this can be done using surface plasmon resonance techniques, and in certain cases by NMR measurements, rapid-reaction methods are generally the method of choice if a suitable intrinsic optical probe exists in the system or an extrinsic probe can be introduced.

In the stopped-flow technique[3], two solutions are rapidly mixed together and at any given point the age of the solution is defined by the flow rate and the volume between mixing and observation. However, by the use of a back syringe, the flow of mixed reactants is suddenly stopped and the reaction is followed in real time with a suitable detection system (Figure 2.l)

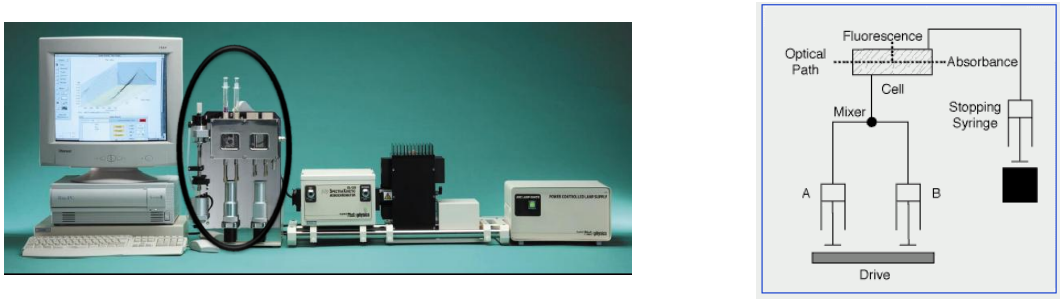

Figure 2.1: The stopped-flow instrument and its diagrammatic representation.

The stopped-flow absorbance spectroscopy and fluorescence intensity method[4] offers a powerful tool for a detailed kinetic analysis of interactions since it can monitor reactions continuously in real time and in a real physiological medium[5]. It has been used in the past to obtain a detailed understanding of locked nucleic acid (LNA) [6] and PNA[7] as a trapping strand in helicase-catalyzed unwinding of oligonucleotide substrates. But fluorescence stopped-flow spectroscopy has never been used for a detailed PNA interaction study with parallel and antiparallel DNA with the aim of measuring the different affinities of the formed duplexes. Moreover, Gangamani *et al*. have previously demonstrated that intrinsic fluorescent PNA analogues can be used to monitor PNA self-melting and PNA-DNA duplex transitions without affecting or perturbing their structures[8].

The objective of this work is to study PNA-DNA interaction from a kinetic point of view with a non-consuming and fast spectroscopic method. With this technique, with respect to steady-state spectroscopy, in a single experiment, the data that can be collected are many: a complete kinetic profile can be obtained as well as a thermodynamic description of the interaction.

2.2.2. Results and Discussion

PNA decamer **1** and fluorescein isothiocyanate (FITC) labelled PNA decamer **2** (PNA-FITU) were synthesized with a standard manual Boc-based chemistry (Section 1, Scheme 2.2 and 2.3). N(α)-Boc-N(ε)-Fmoc-*L*-lysine loaded MBHA resin (loading 0.2 mmol/g) was used to build the TCACTAGATG PNA decamer sequence. The (ε) amino group of the lysine was used as anchoring point for the FITC. Therefore, in decamer **1** the (ε) amino group of the lysine residue is present as a free amino moiety, while in decamer **2** it is conjugated with the FITC, becoming PNA-FITU (Fluorescein isothiourea).

The interaction of both decamers **1** and **2** with the complementary parallel and antiparallel DNA was followed by steady-state and stopped-flow fluorescence intensity.

2.2.2.1. Steady-state experiment

Preliminary UV-Vis and steady-state fluorescence experiments were performed in order to check the complex formation between PNA and DNA. The steady state experiment was performed by keeping PNA-FITU **2** concentration constant (0.2 μM) and titrating an increasing concentration of antiparallel DNA in the concentration range 1.6-16 μM in order

to reach saturation (Figure 2.2a). The fluorescence intensity maxima of the spectra were plotted against DNA concentration and the data were fitted to a rectangular hyperbola (Figure 2.2b) to get the thermodynamic binding constants[9, 10] and the spectra were obtained by exciting at 480 nm and collecting the spectra in the 480-650 nm range.

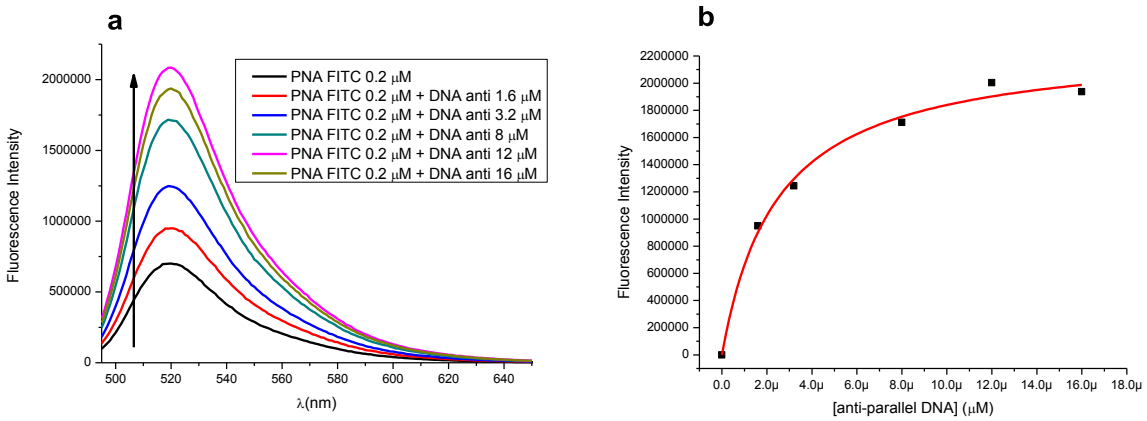

Figure 2.2: (a) Titration curves of the PNA-FITU vs antiparallel DNA interaction followed by steady-state fluorescence and (b) plot of the fluorescence intensity maxima (black squares) against DNA concentration and nonlinear fitting to hyperbole (red curve) to get the thermodynamic binding constants.

2.2.2.2. Stopped Flow experiment

However from the UV-Vis and steady-state fluorescence experiments conclude that fluorescent biolabeling did not interfere in the binding, so by taking this advantage we were studied the kinetic binding experiment by stopped flow fluorescence. The binding was investigated under pseudo-first order condition[11] ([DNA] ≫ [PNA-FITU]) by monitoring the fluorescence changes after the formation of the complex. The two interactions (PNA-FITU versus both parallel and antiparallel DNA) were studied by keeping PNA-FITU concentration fixed at 0.12 μM and changing the DNA concentration over the range 0.8-8 μM. Figure 2.3 shows that on mixing 0.12 μM PNA-FITU with 4 μM DNA (cell concentration) there is a decrease of the signal which reaches a plateau after few ms.

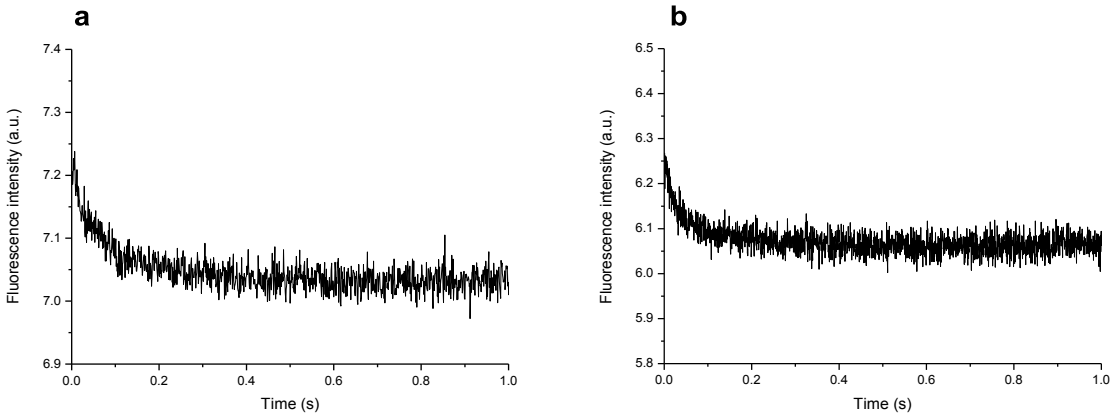

Figure 2.3: The stopped-flow fluorescence intensity record of the binding of 0.2 μM PNA-FITU to (a) 4 μM antiparallel DNA and (b) 4 μM parallel DNA. The reported concentrations are real cell concentrations.

Raw data were analyzed and plotted to a single exponential function providing the so called observed rate constant (k_{obs}). Figure 2.4 shows the dependence of the k_{obs} of DNA (both parallel and antiparallel) binding to PNA. The different behaviour when comparing parallel and antiparallel DNA is evident: in the case of antiparallel DNA binding to PNA-FITU, the k_{obs} evaluation is reproducible and the dependence with concentration is pronounced. Moreover, the repeatability is very good with a standard deviation for each concentration point being extremely small. A completely different scenario is recorded for parallel DNA where the fitting of the single curves to get k_{obs} is more difficult and the fitting to get any insight on the association and dissociation constants of the overall interaction results nearly impossible (Figure 2.4b). This suggests a weaker interaction of PNA-FITU with parallel DNA in agreement with the T_m measurements.

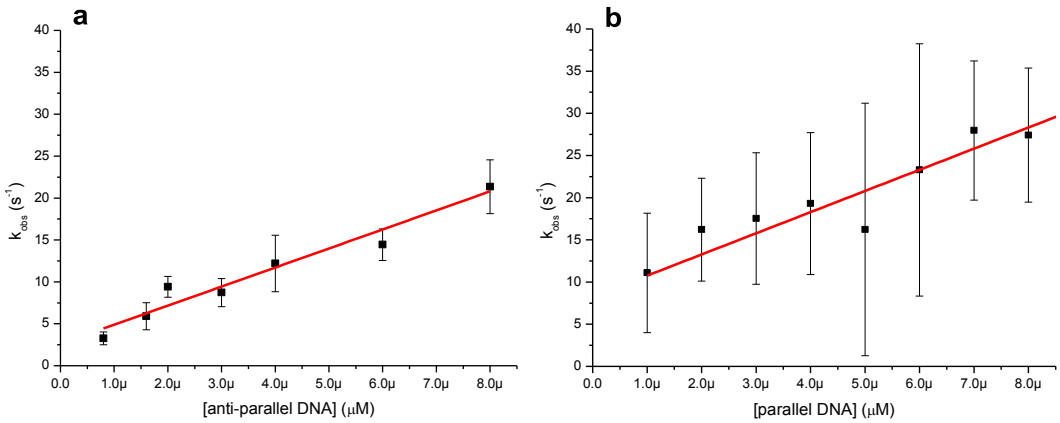

Figure 2.4: k_{obs} dependence for antiparallel DNA (a) and parallel DNA (b).

In any case, we can observe that k_{obs} dependence from (DNA) is, in term of slope of the line, comparable for both parallel and antiparallel DNA. The fact that the antiparallel DNA interaction is stronger and more reproducible is in agreement with the T_m measurements. For the PNA-FITU/antiparallel DNA interaction, the values of the kinetic parameters (k_{on} and k_{off}) can be calculated from the slopes and intercepts of the linear plots of k_{obs} versus increasing concentration of DNA (equation 2.1)[4a].

$$k_{obs} = k_{on}[DNA] + k_{off} \qquad \text{-----(2.1)}$$

The slope of the straight line is the k_{on} (second-order rate constant or rate constant of association process; units, $M^{-1}\ s^{-1}$) and the intercept on the ordinate is the k_{off} (first-order rate constant or rate constant of dissociation process; units, s^{-1}). For the PNA-FITU interacting with antiparallel DNA, the second-order rate constant k_{on} is $2.27 \cdot 10^6 \pm 1.12 \cdot 10^5\ M^{-1}\ s^{-1}$. As it can be seen, the intercept on the ordinate has a very small value ($2.62 \pm 0.56\ s^{-1}$). This means that the interaction is nearly completely shifted toward the formation of the complex. This interaction was also studied at higher concentrations of antiparallel DNA (up to 15 μM) to further monitor the interaction (Figure 2.5) and we are getting almost the same kinetic constants.

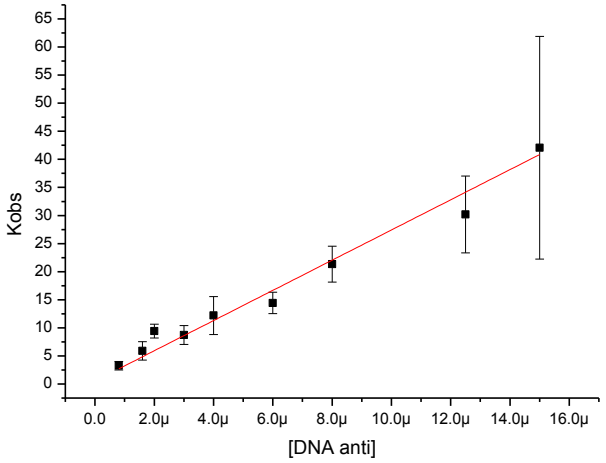

Figure 2.5: k_{obs} dependence for anti-parallel DNA in the 0.8-15 μM range.

2.2.2.3. Displacement experiment

Since the dissociation rate constant value seems to be small, the k_{off} obtained from the intercept cannot be consistent. To gain more information and to measure k_{off} value accurately, a displacement experiment was executed as proposed previously for a protein-protein interaction.[5a] Briefly, in the displacement experiment (Scheme 2.1), a solution containing

fluorescent PNA-FITU (PNA-fL) and DNA were mixed together. The concentration of PNA FITU chosen to get a saturation of DNA, and then a high concentration of unlabeled PNA (PNA-nfL) was added so that PNA-FITU dissociates from DNA and cannot re-associate.

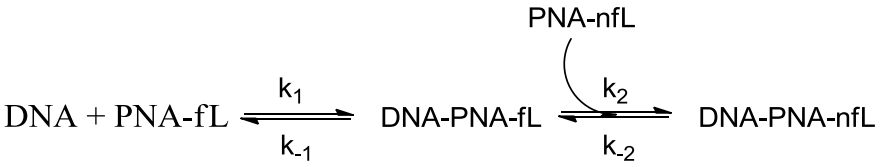

Scheme 2.1: Scheme of the displacement experiment

In this way the rate constant of the observed process were determined only by the k_{-1} in Scheme 2.1 which was measure directly by the displacement of PNA-FITU from its complex with DNA using an excess of unlabeled PNA. Experimentally, the increasing fluorescence intensity was monitored during the process and the corresponding record was fitted to give directly an average rate constant k_{off} value of 32.2 s^{-1} (Figure 2.6).

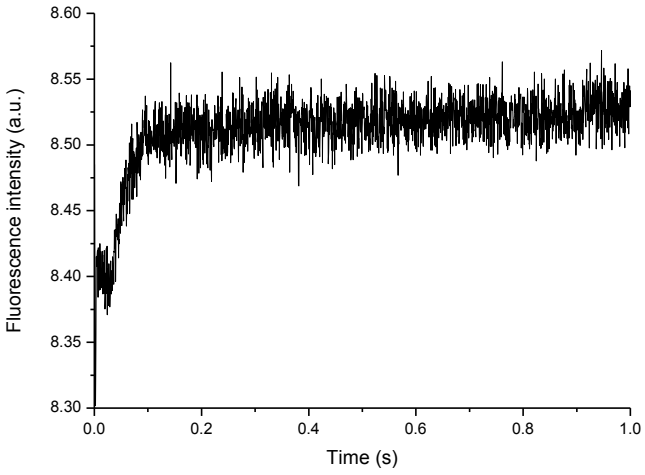

Figure 2.6: Displacement experiment: 50 μM of unlabelled PNA (PNA-nfL) is used to displace antiparallel DNA (1 μM) to PNA-FITU (PNA-fL, 1 μM).

This k_{off} value together with that obtained for the k_{on} allowed us to calculate the thermodynamic dissociation constant K_d (i.e. k_{off}/k_{on}) value of 14.2 μM for PNAFITU/ antiparallel DNA interaction, being in the same order of magnitude compared to the K_d obtained by steady-state fluorescence in the same buffer (2.5 μM) (Figure 2.2).

2.2.2.4. Temperature dependence experiment (T_m)

We also studied the temperature dependence experiment for the binding constants on our PNA-FITU **2** with its complimentary parallel and anti-parallel DNA. The same interaction experiments were repeated at 50 °C for both DNAs. The dependence of k_{obs} on parallel and antiparallel DNA concentration was again investigated in the range 0.8-8 μM (Figure 2.7).

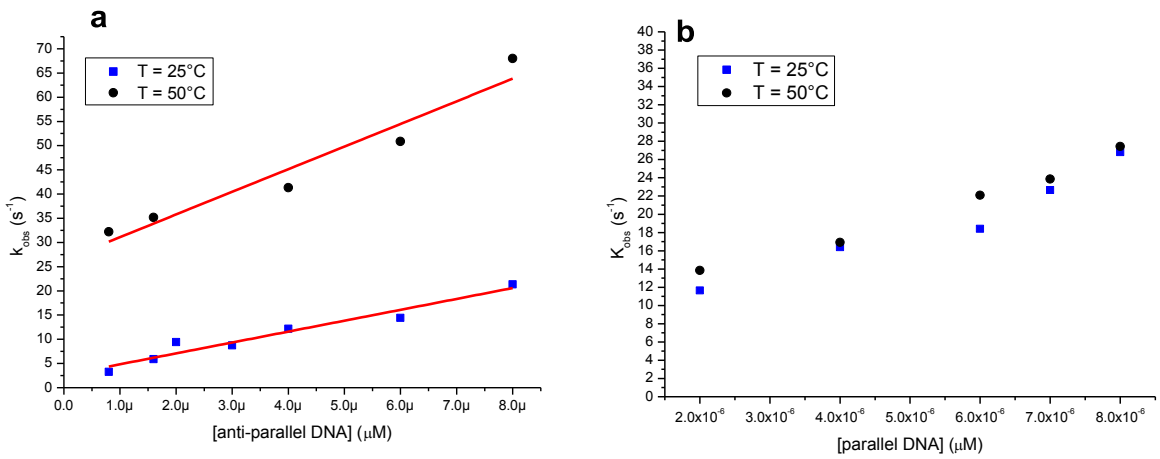

Figure 2.7: Temperature dependence of k_{obs} for (a) antiparallel DNA and (b) parallel DNA.

As is evident, in the case of parallel DNA, there is no temperature dependence of the interaction. On the contrary, the behaviour of PNA/antiparallel DNA interaction is different when working at 25 or 50 °C. In this case, it is possible to express numerically the strength of the two interactions (Table 2.1). As expected, the binding constant increases by increasing the working temperature.

Temperature (°C)	**K_a ($\cdot 10^4$) M^{-1}**	**K_d ($\cdot 10^{-6}$) M^{-1}**	**K_{on} ($\cdot 10^6$) M^{-1} s^{-1}**	**K_{off} s^{-1}**
25	7.05	14.18	2.27	32.2
50	17.69	5.65	4.67	26.4

Table 2.1: Thermodynamic and kinetic binding constants for PNA-FITU vs antiparallel DNA interaction at different temperatures.

2.2.3. Conclusion

In the present chapter, the PNA decamer **1**, with the TCACTAGATG sequence of nucleobases and the corresponding fluorescent PNA-FITU (fluorescein isothiourea) decamer **2** were synthesized with standard manual Boc-based chemistry.

The interaction of both decamers **1** and **2** with the complementary parallel and antiparallel DNA was followed by steady-state and stopped-flow fluorescence intensity and this has never been used or studied so far. In particular, fluorescence stopped-flow technique has been exploited to compare the affinity of two PNA-DNA duplexes: using parallel and antiparallel DNA, such data would be very important for the evaluation and improvement of antisense reagents and of diagnostic probes based on PNA.

Stopped-flow fluorescence showed the poor binding of PNA with its parallel DNA but was very useful for the determination of the binding constants for the PNA-antiparallel DNA interaction. The kinetic and thermodynamic constants obtained by stopped-flow fluorescence were in complete agreement with those obtained by steady-state measurements.

To conclude the stopped-flow has proved to be a reliable, non-consuming, in terms of time and sample, and fast method to discriminate the different behaviour between the parallel and antiparallel DNA. In the case of the interaction between PNA and antiparallel DNA, stopped-flow fluorescence has revealed its power, with respect to the melting temperature, in the possibility of working in a physiological environment with a real mimic of the interaction. All these kinetic studies with stopped-flow instrument have been done in collaboration with the University of Torino, Italy.

2.2.4. Experimental Section

2.2.4.1. General Materials and Methods

The thymine monomer *aeg*-(T) PNA-COOH was synthesized according to the literature[12]. The other three monomers containing the nucleobases C, G and A were purchased from ASM Research Chemicals and were used as such without further purification. 1-[bis(dimethylamino)methylene]-1*H*-1,2,3-triazolo[4,5-*b*]pyridinium 3-oxidhexafluoro phos - phate (HATU), fluorescein isothiocyanate isomer I (FITC), N(α)-Boc-N(ε)-Fmoc-*L*-lysine, trifluoroacetic acid (TFA), trifluoromethanesulfonic acid (TFMSA) and *m*-cresol were purchased from Aldrich. *N*-methyl-2-pyrrolidone (NMP), *N, N*-diisopropylethylamine (DIPEA) and thioanisole were purchased from Fluorochem. Polystyrene bead carrying 4-methylbenzhydrylamine hydrochloride salt groups (MBHA resin, 0.63 mmol/g) was purchased from VWR International. Parallel DNA (5′-3′ sequence: CATCTAGTGA) and antiparallel DNA (5′-3′ sequence: AGTGATCTAC) were purchased from Eurofins Genomics, Germany.

2.2.4.2. Experimental Techniques

UV-Vis measurements for the evaluation of the PNA-FITU concentration and the FITC labelled and unlabelled PNA-DNA interaction studies were recorded using a Varian cary 300 Bio UV-Visible Spectrophotometer. Steady state fluorescence measurements were recorded using a Fluorolog 2 from Jobyn Ivon. As a preliminary analysis for the stopped flow binding experiments, steady-state fluorescence spectra were recorded in the range of 495-650 nm upon excitation at 480 nm, at 25 °C, in order to investigate the binding of PNA-FITU to DNA.

Fluorescence kinetics measurements were recorded using an Applied Photophysics SX20 stopped-flow spectrometer fitted with a 515 nm cut-off filter between the cell and fluorescence detector and equipped with a thermostat bath. The excitation wavelength was 480 nm and slits widths of the excitation monochromator were 1.0 mm. Data acquisition, visualisation and analysis were provided by Pro-Data software from Applied Photophysics Ltd.

^{1}H and ^{13}C NMR spectra were recorded on Bruker 300 MHz and 70 MHz respectively. Chemical shifts (δ) are reported in parts per million relative to solvent peak. Many of the compounds described below showed many rotamers and consequently exhibit complex ^{1}H NMR patterns. Some of the signals in the ^{1}H NMR are therefore described as major (ma.) and minor (mi.) components; however, in many cases, some minor signals were obscured by the major signal of another proton. In such cases, only the major signal is reported or a range containing two or more CH_2. In some cases, the ^{13}C spectrum shows many peaks that cannot be distinguished in a small range: ov. Means 'overlapped'. Melting points of samples were determined in open capillary tubes with a Büchi Melting Point B-540 apparatus and (dec) indicates decomposition. The IR spectra were recorded on a Perkin-Elmer FTIR 4100. Mass spectra were obtained by LCMS techniques (a Thermo Scientific LCQ Advantage). TLC was performed using TLC glass plates pre-coated with silica gel (Merck). TLCs were visualized with UV light and/or either by charring in Ninhydrine solution or developing in I_2 chamber. Silica gel 60-120 and 100-200 mesh was used for column chromatography using ethyl acetate/hexane and dichloromethane/methanol mixture as elution solvent depending upon the compound polarity and chemical nature. Commercial reagents were generally used as received. Solvents used in organic reactions were distilled under an inert atmosphere. Unless

otherwise noted, all reactions were carried out at room temperature. Oligomers were characterized by RP HPLC, using C18 column and MALDI-TOF mass spectrometry.

All weightings of reagents were carried out with analytical balance Mettler Toledo AB135-S/FACT. Vials ALLTECH of 1.5 ml, 4 ml and 8 ml with frits of PTFE were used as reactor for manual solid phase synthesis. The **downloading** of the MBHA resin **3** was performed using the standard manual Boc-based chemistry and reported here:

1. Wash 0.1 gm MBHA resin twice in DCM and swell for 30 min.
2. Wash the resin with 5% DIPEA in DCM for 3 minutes.
3. Wash the resin twice in DCM. The resin is now neutralized.
4. Dissolve 0.20 mmol (amino acid or PNA monomer) in 0.5 mL NMP.
5. Add 0.4 mmol DIPEA to the monomer solution.
6. Dissolve 7.79 mg (0.19 mmol) HBTU in 0.5 mL NMP, and add this to the monomer solution.
7. Activate the monomer for 2 minutes.
8. Add the activated monomer solution to the neutralized resin.
9. Allow the reaction to proceed for 24 hour.
10. Filter the resin.
11. Wash the resin with 2 x NMP
12. Make 5 mL of capping solution using a 1:2:2 ratios of acetic anhydride, pyridine and NMP
13. Add the capping solution to the resin and allow the reaction to proceed for 1 hour. Successful capping will produce a negative Ninhydrine test.
14. Wash the resin with 2 x NMP
15. Wash the resin with 4 x DCM.
16. Wash the resin with2 mL of 5% DIPEA in DCM.

17. Wash the resin with 4 x DCM.

18. Dry the resin in vacuum.

The **cleavage** procedure to remove PNA oligomers from the MBHA resin is the following:

1. Wash the resin 2 x with TFA.

2. Make 1 mL of cleavage solution TFA/TFMSA/*m*-cresol/thioanisole 6:2:1:1.

3. Add the cleavage solution to the resin and allow the reaction to proceed for 1 hr on an orbital shaker.

4. Filter the resin and recover the solution in a centrifuge tubes

5. Wash the resin with TFA

6. Filter the resin and add this solution to the one recovered at point 4.

7. Repeat point 5 and 6 three times

8. Remove volatiles by nitrogen stream to afford black/brown oil.

9. Add cold diethyl ether to the tube and mix. A white precipitate forms.

10. Put the tube at -20°C for 1 hr to complete the precipitation.

11. Centrifuge and remove the solvent by pipetting the ether.

12. Wash the solid with fresh ether, mix, centrifuge and remove the solution.

13. Repeat point 12 four/five times

14. Dry the crude PNA first by nitrogen stream and then in vacuum.

HPLC of PNA oligomers were performed with a HPLC AGILENT 1100 Series, using an analytical column DISCOVERY® BIO WIDE PORE C18 (15 cm x 4.6 mm, 5 μM) and a semi preparative column DISCOVERY® BIO WIDE PORE C18 (25 cm x 10 mm, 10 μM).

MALDI-TOF spectra were recorded with a Bruker Daltonics Omniflex. Pulsed nitrogen lasers (337 nm) were used to generate ions that have been accelerated in a 20 kV field. The instrument was calibrated in the range from 0 to 20 KDa. Generally, Sinapinic acid and 2, 5-dihydroxybenzoic acid (DHB) matrixes were used.

A lyophilizer Telstar Cryodos were used to isolate pure PNA oligomers from aqueous solutions.

2.2.4.3. Experimental Procedures

***Tert-butyl* (2-aminoethyl) carbamate (4)**

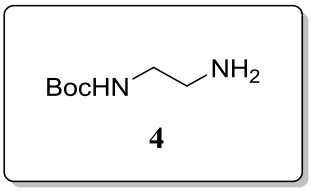

4

A solution of di-tert-butyl dicarbonate (0.5 g, 2.29 mmol) in THF (10 mL) was added over 30 min to a stirred, cooled solution of ethylene diamine **3** (0.46 mL, 6.87 mmol) in THF (10 mL) at 0 ^{o}C. After addition was complete, the reaction mixture was stirred in an ice bath for 30 min and then at room temperature for 12 h. After completion of reaction (monitored by TLC), solvents were removed under reduced pressure, the reaction mixture was diluted with brine (5 mL) and extracted with ethyl acetate (3 X 10 mL). The combined organic extracts were dried over anhydrous Na_2SO_4, filtered and concentrated under reduced pressure to afford compound **4** (0.350 gm, 95%) as a oily product, which were used without further purification.

Molecular formula: $C_7H_{16}N_2O_2$

R*f*: 0.2 (ethyl acetate)

^{1}H NMR (300 MHz, $CDCl_3$): δ 1.42 (s, 9H), 2.77 (t, 2H), 3.15 (m, 2H), 5 (bs, 1H).

^{13}C NMR (75 MHz, $CDCl_3$): δ 28.30, 41.67, 43.12, 79.09, 156.19

MS (ESI) *(m/z)*: 160 monoboc. + 260 diboc.$[M+Na]^+$

methyl (2-((tert-butoxycarbonyl)amino)ethyl)glycinate (6)

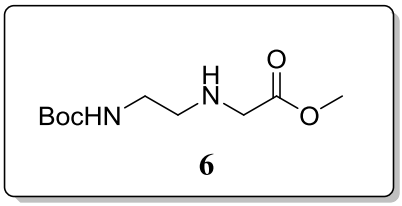

6

N-Boc-ethylene diamine **4** (8.5 gm, 55.31 mmol) was dissolved in acetonitrile (10 mL) to that solution triethylamine (5.9 gm, 58.64 mmol) were added dropwise, and then Methyl bromoacetate **5** (8.9 gm, 58.64 mmol) was added under vigorous stirring over 30 min. The reaction mixture was allowed to stir for another 2 hr. The progress of the reaction mixture was monitored by TLC. After completion of the reaction, mixture were reduced in on rota vapour to afford an yellow residue, which

was diluted in water (10 mL), The solution was cooled to 0-5 °C and the pH was adjusted to 10 – 10.5 with 2 M NaOH solution. The solution was extracted with DCM (2 X 10 mL). Again the pH of the water phase was adjusted to 11.2 with 2 M NaOH solution and then extracted with ethyl acetate (3 X 20 mL). The combined organic extracts were dried over anhydrous Na_2SO_4, filtered and concentrated under reduced pressure to afford crude compound **6**. The crude product was purified on flash chromatography (SiO_2, 3:7 EtOAc: Hexane) to **6** as a pale yellow oil in 40% yield.

Molecular formula: $C_{10}H_{20}N_2O_4$

R*f*: 0.3 (ethyl acetate)

^{1}H NMR (300 MHz, $CDCl_3$): δ 1.42 (s, 9H), 2.72 (t, 2H), 3.18 (q, 2H), 3.40 (s, 2H), 3.71 (s, 3H), 5.07 (bs, 1H).

^{13}C NMR (75 MHz, $CDCl_3$): δ 28.24, 39.93, 48.62, 50.04, 51.67, 77.00, 78.97, 156.00, 172.63

MS (ESI) *(m/z):* 255 $[M+Na]^+$

Methyl-N-(2-((tert-butoxycarbonyl)amino)ethyl)-N-(2-(5-methyl-2,4-dioxo-3,4-dihydropyrimidin-1(2H)-yl)acetyl)glycinate (8)

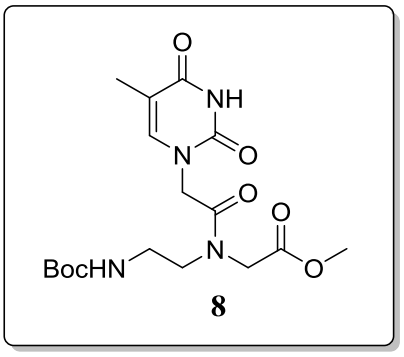

8

To a stirred solution of the compound **6** (0.74 g, 32.17 mmol) in acetonitrile (10 mL), Thymine acetic acid **7** (0.65 gm, 35.39 mmol) was added under nitrogen atmosphere and stir the reaction at room temperature for about 10 min., then EDC.HCl (0.7 g, 35.39 mmol) were added in portion-wise over a period of 30 min. The reaction mixture was allowed to stir for another 3 hr at room temperature. The progress of reaction was monitored by TLC. After completion of reaction solvent was removed under reduced pressure, the reaction mixture was diluted with brine (10 mL) and extracted with ethyl acetate (3 X 20 mL). The combined organic extracts were dried over anhydrous Na_2SO_4, filtered and concentrated under reduced pressure to afford crude compound **8,** which was purified on flash column chromatography (SiO_2) using ethyl acetate as a eluent to afford compound **8** as a white solid (1.02 gm, 82% yield); M.P.: 158 ^oC.

Molecular formula: $C_{17}H_{26}N_4O_7$

R*f*: 0.75 (ethyl acetate: methanol, 70:30)

IR ($CHCl_3$): 3421, 2360, 1756, 1698, 1666, 1474, 1426, 1255, 1210, 1016 cm^{-1}.

^{1}H NMR (300 MHz, $CDCl_3$): δ 1.45 (s, 9H), 1.91 (s, 3H), 3.35 (q, 2H), 3.54 (t, 2H), 3.76 (s, 3H), 4.07 (d, 2H), 4.58 (d, 2H), 5.56 (t, 1H), 6.97 (s, 1H), 8.81 (s, 1H)

^{13}C NMR (75 MHz, $CDCl_3$: mix of rotamers**):** δ 12.30, 28.40, 38.83, 47.74, 48.98, 50.30, 52.49, 77.00, 80.07, 110.79, 140.87, 151.00, 156.00, 164.01, 167.41, 170.11

MS (ESI) *(m/z):* 398 $[M+Na]^+$

N-(2-((tert-butoxycarbonyl)amino)ethyl)-N-(2-(5-methyl-2,4-dioxo-3,4-hydropyrimidin-1 (2H)-yl)acetyl)glycine (9) / [Boc-T-OH]

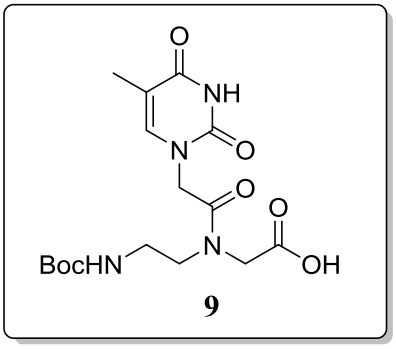

9

To a stirred solution of the compound **8** (1 gm, 26.35 mmol) in Methanol (10 mL), LiOH (0.55 gm, 13.18 mmol) was added and stir the reaction at room temperature for 3 hr. The progress of reaction was monitored by TLC. After completion of reaction solvent were removed under reduced pressure, to afford an yellow residue which was diluted with brine (10 mL) and extracted with DCM (3 X 10 mL). The solution was cooled to 0-5 °C and the pH was adjusted to 2 with 2 M $KHSO_4$ solution. The solution was extracted with ethyl acetate (3 X 20 mL). The combined organic extracts were dried over anhydrous Na_2SO_4, filtered and concentrated under reduced pressure to afford an crude acid **(9)**. To that acid add about 10 mL of diethyl ether and stir it for about 1 hr at room temperature, then filter the acid and wash it with diethyl ether 10 mL, and dried it on vacuum to afford **9** (0.9 gm, 86%) as a white solid. M.P.: 118-120 ^oC.

Molecular formula: $C_{16}H_{24}N_4O_7$

R*f*: 0.02 (ethyl acetate: methanol, 80:20)

IR (Nujol): 3420, 2361, 1653, 1541, 1456, 1251, 1006 cm^{-1}

^{1}H NMR (300 MHz, DMSO-d$_6$: mix of rotamers**):** δ 1.38 (s, 9H), 1.75 (s, 3H), 3.17 (m, 2H), 3.38 (t, 2H), 3.97 (d, 2H), 4.64 (d, 2H), 6.62 (s, 1H), 11.27 (s, 1H), 12.67 (bs, 1H)

^{13}C NMR (75 MHz, DMSO-d$_6$: mix of rotamers**):** δ 11.93, 28.17, 38.05, 39.51, 46.77, 47.54, 49.07, 78.05, 108.13, 142.02, 151.00, 155.75, 164.39, 167.17, 170.48

MS (ESI) *(m/z)*: 384 $[M+Na]^+$

Loading (0.2 mmol/gm) of N(*α*)-Boc-N(*ε*)-Fmoc-*L*-lysine monomer 4 on MBHA resin (5)

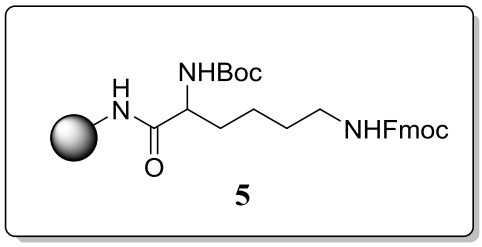

5

The MBHA resin **3** (0.4 gm) was washed with CH_2Cl_2 (2 x 5 mL) and activated by treatment with 5% DIPEA in CH_2Cl_2 for 5 min for 3 times; and then washed with CH_2Cl_2 (2 x 5 mL). In a vial, DIPEA (27 μL, 0.16 mmol) was added to a solution of N(*α*)-Boc-N(*ε*)-Fmoc-*L*-lysine monomer **4** (37.5 mg, 0.08 mmol) in NMP (1 mL); then, a solution of HBTU (30.3 mg, 0.08 mmol) in NMP (1 mL) in another vial and add this solution into the monomer solution, and activate the monomer solution for 2 minutes. This mixture was then added to the neutralized resin and at rt for 12 hr. The resin was washed with NMP (3 x 5 mL). A solution of Ac_2O/Py/NMP 1:2:2 (5 mL) was added to the resin (capping of unreacted amino groups) and left under stirring at rt for 1 h. After this time, the resin was washed with NMP (3 x 5 mL), CH_2Cl_2 (4 x 5 mL), 5% DIPEA in CH_2Cl_2 (2 x 5 mL) and again with CH_2Cl_2 (4 x 5 mL); and finally dried in vacuum to afford the MBHA resin downloaded with lysine monomer **5** (0.492 g); Kaiser Test: negative.

Synthesis of the resin supported TCACTAGATG sequence of nucleobases *aeg*-PNA decamer (6)

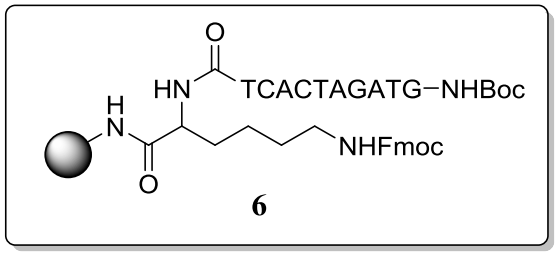

6

Solid phase synthesis was done by using standard manual Boc-based chemistry; resin **5** (100 mg, substitution with 0.2 mmol/gm) was placed in a reaction vessel (volume; 8 mL) and which was swollen with CH_2Cl_2 for 30 minutes, the Boc group of the loaded monomer was removed by treatment with TFA/*m*-cresol (95:5),

(3 mL, 2 x 4 min). The resin was washed with CH_2Cl_2 (2 x 5 mL) and then treated with CH_2Cl_2/DIPEA (95:5), (3 mL, 2 x 2 min). Then the resin was washed thoroughly with CH_2Cl_2 (2 x 5 mL). In a vial, DIPEA (35 µL, 0.2 mmol, 10 eq.) was added to a solution of *aeg*-(T) PNA-COOH monomer **9** (40.7 mg, 0.106 mmol, 5.3 eq.) in NMP (500 µL); then, a solution of HATU (38 mg, 0.1 mmol, 5 eq.) in NMP (500 µL) in another vial and add this solution into the monomer solution, and activate the monomer solution for 2 minutes. This mixture was then added to the neutralized resin and shaken for 2 hr at rt. After coupling step the resin was filtered, washed with NMP (3 x 5 mL) and CH_2Cl_2 (3 x 5 mL). Then resin treated with Ac_2O/Py/NMP; 1:25:25 capping solution twice for 1 min. and again washed the resin with CH_2Cl_2 (3 x 5 mL), NMP (3 x 5 mL) and CH_2Cl_2 (3 x 5 mL). The cycle was repeated using the required monomers like cytosine (53.4 mg), adenine (56 mg) and guanine (57.6 mg) with the same protocol and after the last coupling and capping the resin was washed with several times with NMP and CH_2Cl_2 and finally dried the resin under vacuum to afford the corresponding supported PNA decamer on resin **6** (146 mg).

Synthesis of the resin supported TCACTAGATG sequence of nucleobases *aeg*-PNA decamer (7)

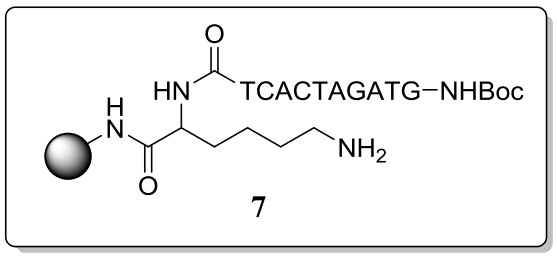

7

The Fmoc-*L*-lysine TCACTAGATG-NHBoc MBHA resin **6** (100 mg) was swollen with CH_2Cl_2 for 30 minutes. Then the Fmoc group was removed by treatment with a solution of 20% piperidine in DMF (2 mL, 3 x 20 min) the resin was filtered, washed with DMF (3 x 5 mL, 3 min) and CH_2Cl_2 (3 x 5 mL, 3 min) to afford an resin **7**, for which the presence of the free amino group was confirmed by the Kaiser test.

Synthesis of PNA Decamer (1)

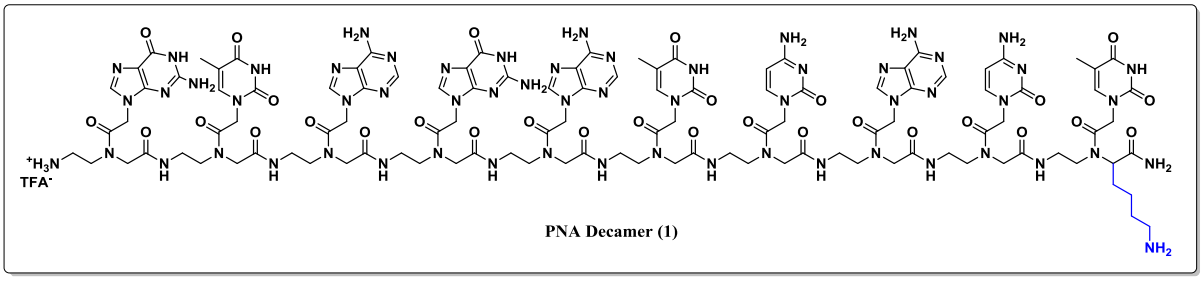

Cleavage: The resin **7** (100 mg) was washed with TFA (2 × 200 µL) and subsequently stirred for 1 hr with a mixture of TFA/TFMSA/thioanisole/*m*-cresol [6:2:1:1 v/v] (500 µL). The reaction mixture was filtered, and the resin washed with TFA (4 × 200 µL). The filtrate was concentrated under nitrogen flow and Et_2O (5 mL) was added to precipitate PNA as a white solid. Centrifugation of the slurry gave the product, which was washed with Et_2O (8 x 5 mL) and dried to afford the crude decamer **1** (28 mg). Purification of the crude PNA by RP-HPLC afforded the PNA 10-mer **1** (7.4 mg) as a white solid.

Retention time (analytic column 15 cm); gradient from 95% of H_2O/TFA 0.1% to 100% of AcCN/TFA 0.1%) = 6.2 min.

Maldi Tof MS: found *m/z*: 2855.9 [M] +, calculated for $C_{114}H_{149}N_{60}O_{31}^{+}$: 2855.83.

Synthesis of fluorescent PNA-FITU decamer (8)

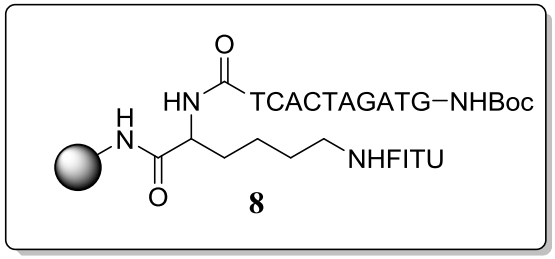

The MBHA resin **7** (100 mg) was washed with CH_2Cl_2 (2 x 5 mL), the free amine group on lysine, was directly reacted with fluorescein isothiocyanate [FITC]. In particular, a solution of DIPEA (34 µL, 0.2 mmol, 8 eq.) and FITC (38.60 mg, 0.099 mmol, 4 eq.) in DMF was added to the resin and shaken at room temperature for 12 h. Then the resin was washed with DMF (3 x 5 mL) and CH_2Cl_2 (3 x 5 mL) to afford resin **8**.

Synthesis of fluorescent PNA-FITU decamer (2)

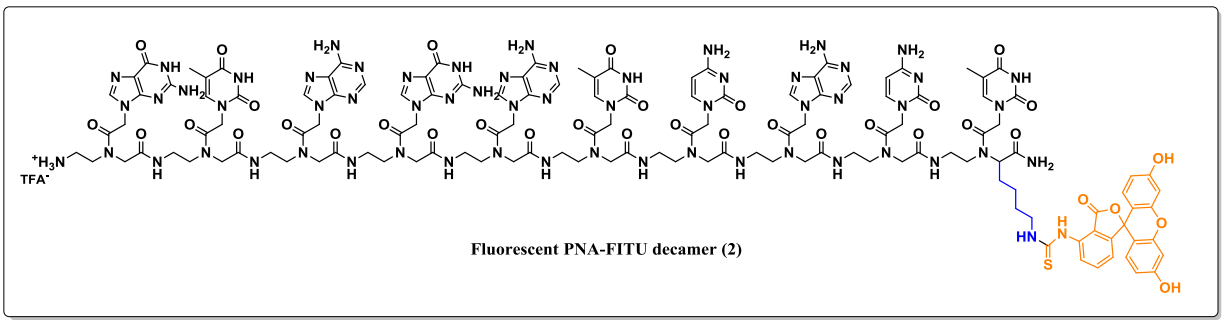

Cleavage: The resin **8** (100 mg) was washed with TFA (2 × 200 μL) and subsequently stirred for 1 hr with a mixture of TFA/TFMSA/thioanisole/*m*-cresol [6:2:1:1 v/v] (500 μL). The reaction mixture was filtered, and the resin washed with TFA (4 × 200 μL). The filtrate was concentrated under nitrogen flow and Et_2O (5 mL) was added to precipitate PNA as a white solid. Centrifugation of the slurry gave the product, which was washed with Et_2O (8 x 5 mL) and dried to afford the crude decamer **2** (26 mg). Purification of the crude PNA by RP-HPLC afforded the PNA-FITU decamer **2** (7 mg) as a yellow solid.

Retention time (analytic column 15 cm); gradient from 95% of H_2O/TFA 0.1% to 100% of AcCN/TFA 0.1%) = 12.9 min.

Maldi Tof MS: found *m/z*: 3245.7 $[M]^+$, calculated for $C_{135}H_{160}N_{61}O_{36}S^+$: 3245.22.

2.2.5. Bibliography

1. Ward, L. D. *Methods Enzymol.* **1985,** *117*, 400-414.

2. Harvey R. A.; Borcherdt W. O. *Anal. Chem*. **1972**, *44*, 1926-1928.

3. Eccleston, J. F.; Hutchinson, J. P.; Harding, S. E., Chowdhary, B. Z., *Eds.; Oxford University Press*. **2001**, 201-237.

4. a) Eccleston, J. F., Hutchinson, J. P., White, H. D. *Protein-Ligand Interactions, Structure and Spectroscopy: A Practical Approach, Oxford University Press*, **2001** b) Sujak, A., Drepper, F., Haehnel, W., *J. Photochem. Photobiol. B Biol*., **2004**, *74*, 135-143.

5. a) Barbero, N., Napione, L., Visentin, S., Alvaro, M., Veglio, A., Bussolino, F. et al., *Chem. Sci.* **2011**, *2*, 1804-1809 b) Dey, D., Maiti, C., Maiti, S., Dhara, D., *Phys. Chem. Chem. Phys*. **2015**, *17*, 2366-2377.

6. Christensen, U., Jacobsen, N., Rajwanshi, V. K., Wengel, J., Koch, T., *Biochem. J.*, **2001**, *354*, 481-484.

7. Nanduri, B., Eoff, R. L., Tackett, A. J., Raney, K. D., *Nucleic Acids Res.*,**2001**, *29*, 2829-2835.

8. Gangamani, B. P., Kumar, V. A., Ganesh, K. N., *Chem. Commun.*, **1997**, 1913-1914.

9. Baldassarre, F., Foglietta, F., Vergaro, V., Barbero, N., Capodilupo, A. L., Serpe, L. *et al., J. Photochem. Photobiol. B Biol.* **2016**, *158*, 16-22.

10. Copeland, R. A., *P R.A. rotein-Ligand Binding Equilibria, Wiley-VCH, Inc*., 2000.

11. Barbero, N.; Visentin, S.; Viscardi, G. *J. Photochem. Photobiol. A Chem.* **2015**, *299*, 38-43.

12. Dueholm, K. L., Egholm, M., Behrens, C., Christensen, L., Hansen, H. F., Vulpius, T. *et al*. *J. Org. Chem.* **1994**, *59*, 5767-5773.

Chapter 3: Design, synthesis and characterization of functionalized PNAs with heterobifunctional linker and their conjugation with magnetic nanoparticles (MNPs) for miRNA targeting.

Section 1: Introduction to Magnetic nanoparticles and its properties

3.1.1. Rationale

In the past decade, the non-coding microRNAs (miRNA) have emerged as a novel class of potent regulatory molecules that are found in a wide variety of organisms, able to modulate gene expression at the post-transcriptional level. They are responsible for regulating many biological processes including differentiation, apoptosis, proliferation and cell-fate determination. miRNAs are highly conserved in different animals, suggesting an early recruitment and a conserved role of these molecules in animal development. The dysregulation of miRNAs has been implicated in a variety of pathologies, such as inflammatory and autoimmune diseases, neurological disorders, as well as several types of cancer. Anti-miRNA platforms highly effective in *in-vitro* cell assays have been reported, but translation to the clinic is hampered by poor *in-vivo* stability of nucleic acids and ineffective uptake of nucleic acids by target cells.

The aim of this research is to overcome these obstacles by designing, producing and *in-vivo* testing new miRNA targeting materials constituted by chemically modified Peptide Nucleic Acids (PNAs, synthetic mimics of natural DNA and RNA)[1]. PNAs allow combining the versatility of synthetic materials with the effectiveness of the natural nucleic acids targeting, arising from the Watson-Crick base-pairing scheme. Moreover, PNAs are insensitive to enzymatic biodegradation by nucleases or peptidases and have outstanding chemical and thermal stability.

3.1.2. Scientific background: MicroRNAs

MicroRNAs (miRNAs or miRs) are a family of small (19-25 nucleotides in length) noncoding RNAs, which in the past decade have emerged as a novel class of potent regulatory molecules that are found in a wide variety of organisms, able to modulate gene expression at the post-transcriptional level[2]. They are responsible for regulating many biological processes including differentiation, apoptosis, proliferation and cell-fate determination. The dysregulation of miRNAs has been demonstrated to be associated with a variety of pathologies, such as inflammatory and autoimmune diseases, neurological disorders, as well as several types of cancer[3]. The inhibition of miRNAs using antisense oligonucleotides is an effective technique for the characterization and subsequent therapeutic targeting of miRNA function.

Moreover, PNAs are resistant to nucleases, which is an essential characteristic for a miRNA inhibitor that will be exposed to serum and cellular nucleases. A few reports on the inhibition of the function of some miRNAs have been published[4, 5]. However, *in vivo* applications of PNAs are hindered by poor cellular uptake, endosomal entrapment[6] and poor solubility in aqueous media due to the neutral chemical structure and self-aggregation. In order to solve these drawbacks many modifications of the original PNA backbones have been proposed, in particular by linking PNA to a polylysine or a polyarginine tail[5].

MNPs provide biocompatible and biodegradable nanovectors, which can be functionalized with proper drugs or targeting molecule, to obtain a theranostic nano-device for clinical uses. A great interest is at present devoted to multifunctional nanostructured magnetic particles in different areas of biomedicine[7].

3.1.3. Introduction to magnetic nanoparticles (MNPs)

Magnetic nanoparticles (MNPs) are a class of nanoparticles which can be manipulated using magnetic fields. The particles are made of magnetic elements such as iron, nickel and cobalt or their chemical compounds. During the past decade magnetic nanoparticles have been intensively studied, not only for general scientific interest but also due to the large number of their possible applications, such as catalysis[8], biomedicine[9], magnetic resonance imaging[10], data storage[11] and environmental remediation.

The physical and chemical properties of magnetic nanoparticles largely depend on the synthesis method and on their chemical structure. In most cases, their size range from 1 to 100 nm, that is the size range necessary for them to display superparamagnetism[12]. In a more general way, the properties of the nanocrystals strongly depend upon the dimension of the nanoparticles. Therefore it is important to control their proprieties and studies related to fluid stability, control of surfactants, particle sizes, materials, and physical behaviour are essential to understand ferrofluid behaviour to improve applications or develop new nanoparticles (Figure 3.1).

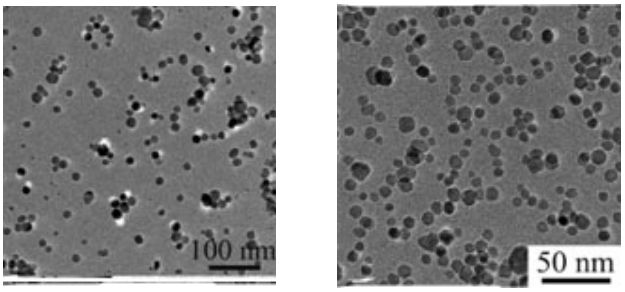

Figure 3.1: TEM imaging of iron nanoparticles.

MNPs possessing appropriate physicochemistry and tailored surface properties have been extensively investigated for various applications such as drug delivery, hyperthermia, magnetic resonance imaging (MRI), tissue engineering and repair, biosensing, biochemical separations, and bioanalysis. In the field of disease therapy, the development of "theranostics", which facilitates simultaneous drug delivery and imaging, represents an important breakthrough of MNP technology.[13] Currently, various clinical trials are in progress to investigate the potential of different magnetic nanosystems for pharmaceutical and biomedical applications.[14, 15, 16]

3.1.3.1. Synthesis

Several chemical methods can be used to synthesize magnetic nanoparticles for medical applications: micro emulsions, sol-gel syntheses, sonochemical reactions, hydrothermal reactions, hydrolysis and thermolysis of precursors, flow injection syntheses, and electrospray syntheses.[17] Iron oxides (either Fe_3O_4 or γ Fe_2O_3) are usually prepared by an aging stoichiometric mixture of ferrous and ferric salts in aqueous medium. The chemical reaction of Fe_3O_4 formation may be written as scheme 3.1.

$$Fe_2^{+} + 2Fe_3^{+} + 8OH^{-} \longrightarrow Fe_3O_4 + 4H_2O$$

Scheme 3.1

According to the thermodynamics of this reaction, complete precipitation of Fe_3O_4 should be expected at a pH ranging between 8 and 14, with a stoichiometric ratio of 2:1 (Fe^{3+}/Fe^{2+}) in a non-oxidizing oxygen environment.[18]

3.1.3.2. Stabilization of Magnetic Nanoparticles

The stabilization of the iron oxide particles is crucial to obtain magnetic colloidal ferrofluids that are stable against aggregation in a biological medium as in a magnetic field. The stability of a magnetic colloidal suspension results from the equilibrium between attractive and repulsive forces. Theoretically, four kinds of forces can contribute to the interparticle potential in the system. Van der Waals forces induce strong short-range isotropic attractions. For magnetic suspensions, magnetic dipolar forces between two particles must be added. These forces induce anisotropic interactions, which are found to be globally attractive if the

anisotropic interparticle potential is integrated over all directions. Finally, steric repulsion forces have to be taken into account for non-naked particles.

In iron oxide, the surface iron atoms act as Lewis acids and coordinate with molecules that donate lone-pair electrons. Therefore, in aqueous solutions, the Fe atoms coordinate with water, which dissociates readily to leave the iron oxide surface hydroxyl functionalized. These hydroxyl groups are amphoteric and may react with acids or bases.[19]

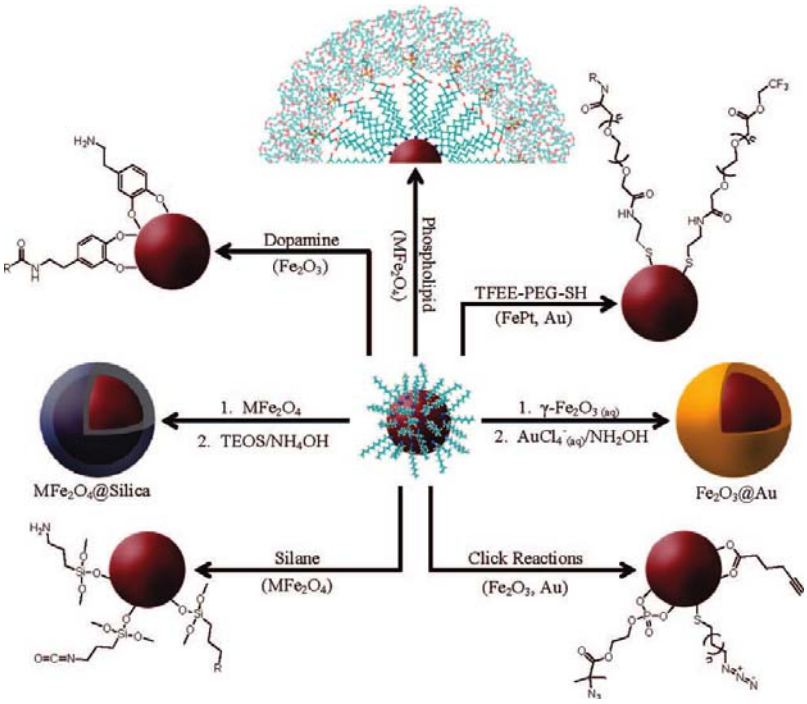

Figure 3.2: Stabilization of iron nanoparticles.

Depending on the pH of the solution, the surface of the magnetite will be positive or negative. The isoelectric point is observed at pH 6.8[20] around this point [point of zero charge (PZC)], the surface charge density (Σ) is too small and the particles are no longer stable in water and flocculate.

The main ways used to stabilize the iron oxide nanoparticles use to build around the particles a secondary core-shell made of small molecules, polymers or a second metal (Figure 3.2).

3.1.3.3. Surface Functionalization

The design of improved and multifunctional nanoparticles is a huge challenge. A very intensive investigation has been conducted to search for new strategies to prepare magnetic nanoparticles with tailor-made properties for pharmaceutical applications, especially for

targeted drug delivery, biomedical imaging, biosensing, hyperthermia, or nanothermometry. DMSA coated nanoparticles have also been used as a basic core for further functionalizations.

There are several ways and methods to conjugate some drug to the MNPs. In the last decade functionalization have mainly be made using amine, carboxylic acid, thiol, carbonyl group etc linked by covalent bonds. The best procedure is to stabilize the nanoparticles with some ligands having with a specific functional group in the end and then to use this group to form the bioconjugates with the specific drug (Figure 3.3).

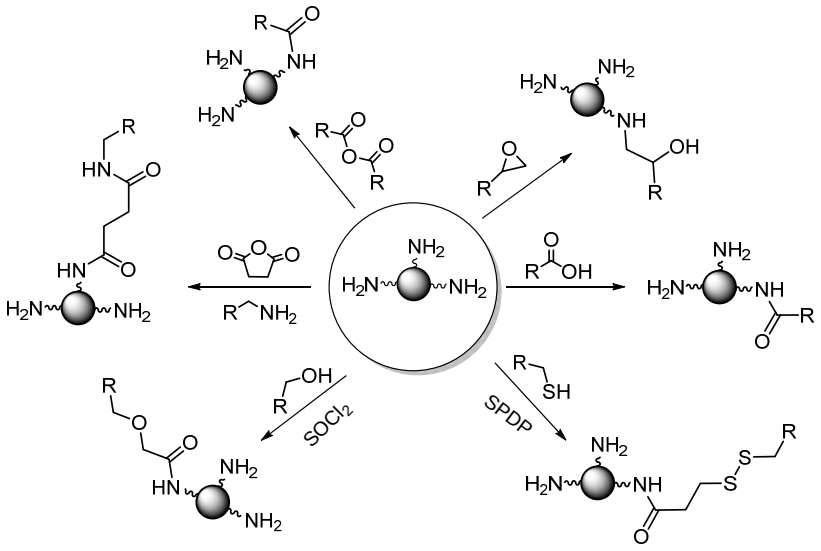

Figure 3.3: Post-synthesis functionalization of iron nanoparticles.

In this way, one peptide or protein could be attached to the nanoparticles thanks to a simple chemical interaction with the surface anime of the nanoparticles.

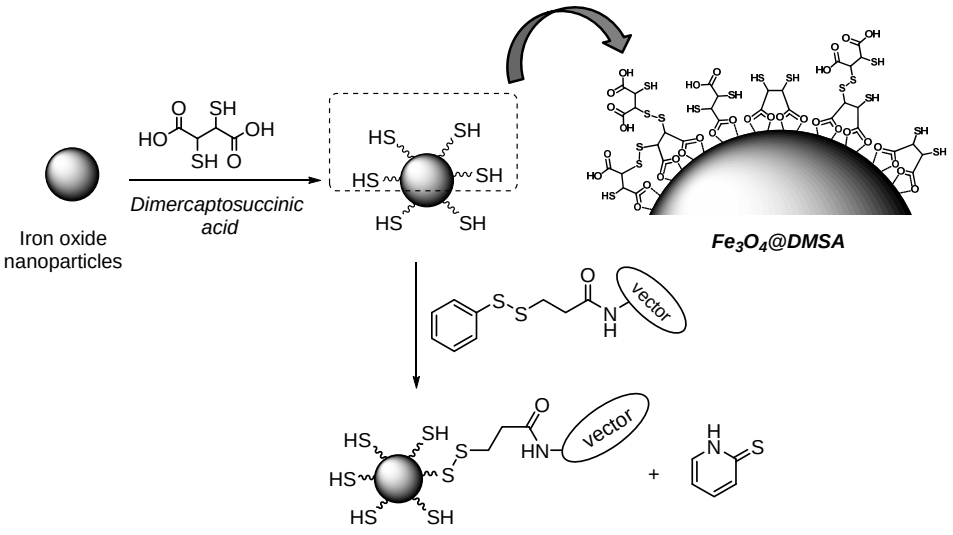

Figure 3.4: Thiol chemistry: post-synthesis functionalization of iron nanoparticles.

Another using the thiol chemistry or the well know reaction call click-chemistry (Figure 3.4 and 3.5).

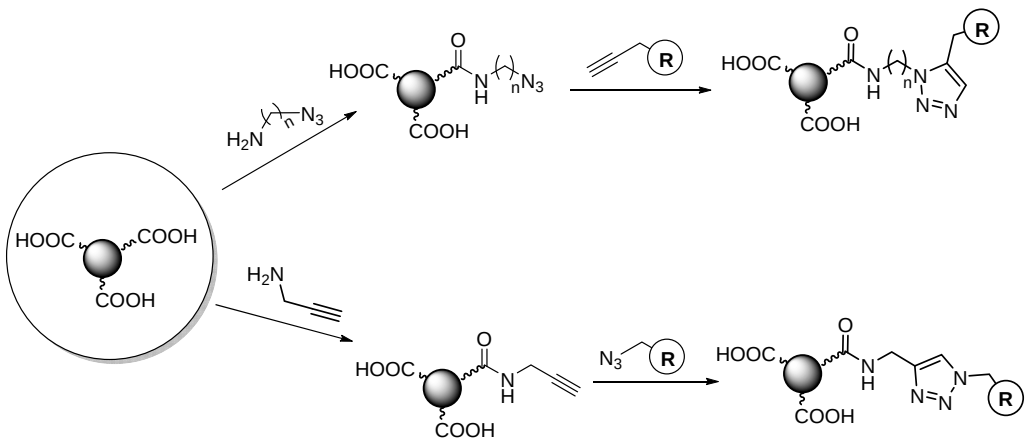

Figure 3.5: Click-chemistry, post-synthesis functionalization of iron nanoparticles.

3.1.3.4. Biomedical applications

Magnetic nanoparticles are already applied in biotechnology and nanomedicene. Some formulations have been clinically approved for medical imaging and therapeutic applications. Some of them include formulations of iron oxide nanoparticles like for liver and spleen imaging [21].

3.1.3.4.1. Disease therapy

MNPs are promising stimuli-sensitive drug carriers because of their magnetic field responsiveness, an applied extracorporeal magnetic field can concentrate these nano devices at the desired site, keeping them in place for a given period of time until the encapsulated drug is released, thereby minimizing the drug-associated side effects due to nonspecific distribution.[22] Alternatively, the heat generation property of the MNPs under the influence of an external AMF may contribute to an additional therapeutic mechanism called hyperthermia.

In vitro

In vitro use of MNPs has proven to be very useful tools for magnetic separation techniques in clinical use and have replaced other separation technologies. This is particularly true concerning immunomagnetic cell separation and purification, as solid phase for immunoassays for isolation, purification and recognition of proteins[23]. In addition they are

used for molecular biology, where they were shown to be useful for the isolation, purification, hybridization, synthesis and as markers for DNA/RNA.[24] The isolation and detection of microorganisms is easily possible using MNPs[23], as well as an efficient gene transfer of nucleotides or gene sequences into cells.

In vivo

Magnetic nanoparticles (usually Fe_2O_3 and Fe_3O_4) are quite useful for *in vivo* applications, as they do not retain any magnetism after removal of the magnetic field. They are specially suitable for therapy. One major hurdle that underlies the use of nanoparticles therapy is the problem of getting the particles to a particular site in the body. A potential benefit of using magnetic nanoparticles is the use of localized magnetic field gradients to attract the particles to a chosen site, to hold them there until the therapy is complete and then to remove them. This involves some fairly advanced design of systems for producing these fields. Additionally, such equipment should ideally contain other molecules to show that the particles have been actually located in the appropriate region of the body.[25] The particles may be injected intravenously, and then blood circulation would be used to transport the particles to the region of interest for treatment. Alternatively, in many cases the particles suspension would be injected directly into the general area when treatment is desired. Either of these routes has the requirement that the particles do not aggregate and block their own spread. Nanoparticles of about 5-10 nm diameter should form the ideal particles for most forms of therapy but that there will also be problems of formulating the particle concentrations and suspending media to obtain best distributions. Nanotechnology has reached a stage that makes it possible to produce, characterize and specifically tailor the functional properties of nanoparticles for clinical applications.

3.1.3.4.2. Magnetic resonance imaging

Magnetic Resonance Imaging (MRI), or nuclear magnetic resonance imaging (NMRI), is primarily a medical imaging technique commonly used in radiology to visualize the internal structure and function of the body. Clinical diagnostics with MRI (magnetic resonance imaging) has become a popular non-invasive method for diagnosing many pathologies, because of the different relaxation times of hydrogen atoms in different tissue. The increase the diagnostic sensitivity and specificity many contrast agent are used, one of most used are the MNPs and SPIONs because they ability to modify the relaxation time of the protons.[26]

3.1.2. Objective:

In the present work we focused our attention on to the design, synthesis and characterization of functionalized Peptide Nucleic Acids **9** (PNAs) with heterobifunctional linker and their conjugation with magnetic nanoparticles **10** (MNPs) for miRNA targeting. The MNPs bound to PNA can be exploited both as contrast agents for magnetic resonance imaging (MRI) and as sources of local overheating through the application of an alternating magnetic field (Magnetic Fluid Hyperthermia, MFH). Moreover, the microRNAs targeting ability of these tools for selectively delivering magnetic nanoparticles and destroying, by hyperthermia, targeted cells in multicellular organisms. However, synthesis of MNPs has been done by in collaboration with Dr. Daniela Maggioni & group (CARIPLO Project), University of Milan, Italy.

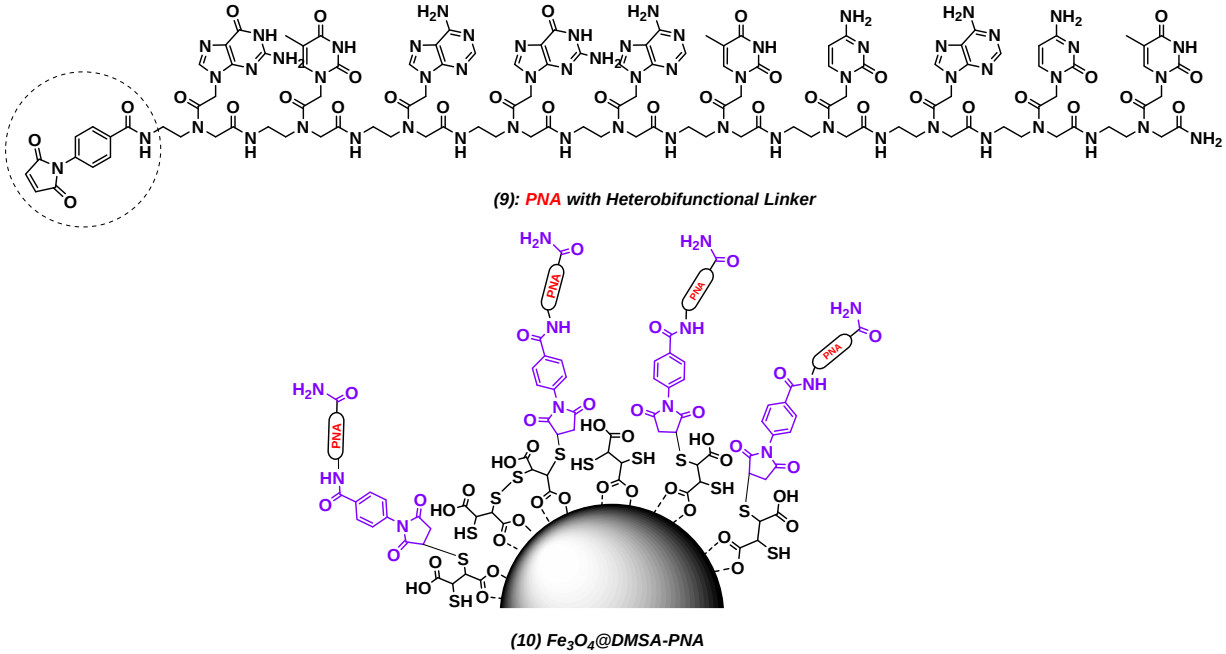

Figure 3.6: (9) PNA with Heterobifunctional Linker and (10) Fe_3O_4 on DMSA-PNA.

3.1.5. Results and discussion

We planned to synthesized (*p*-Maleimido) phenyl isocyanate (PMPI) **15** as a heterobifunctional linker, because it contains highly reactive isocyanate functional group which could be useful for the formation of urea bond with terminal free amino group from PNA oligomer and other is activated alkene which were used as Micheal acceptor, free thiol

groups from DMSA coated MNP. So, (PMPI) **15** were easily synthesized as reported in literature[27] and its synthesis is shown in Scheme 3.2.

3.1.5.1. Synthesis of heterobifunctional linker

So for this we started our synthesis from cheap and commercially available *p*-amino benzoic acid **11**. (*p*-Maleimido) benzoic acid (PMBA) **12** was synthesized by the condensation reaction of maleic anhydride with *p*-amino benzoic acid **11** (PABA) followed by cyclodehydration using acetic anhydride and sodium acetate in three step procedure with 60% yield. This (*p*-Maleimido) benzoic acid (PMBA) **12** is directly converted into the corresponding (*p*-maleimido)benzoyl chloride (PMB-Cl) **13** by refluxing in thionyl chloride to obtained acyl chloride almost a quantitative yield, which was reacted with sodium azide in order to form the PMB-azide **14** in 67% yield after chromatographic purification. Then, the labile PMB-azide **14** undergoes a Curtius rearrangement in anhydrous toluene affording the desired (*p*-Maleimido) phenyl isocyanate (PMPI) **15** in quantitative yield.

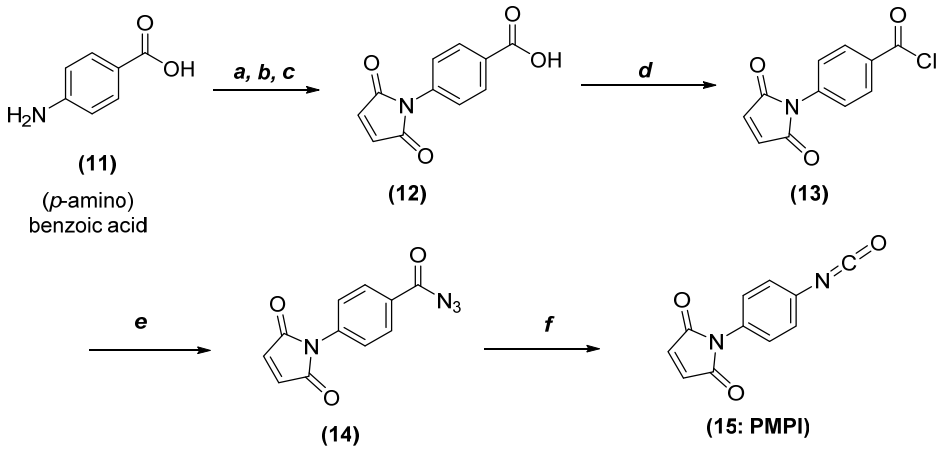

Scheme 3.2: Reagents and conditions: *a) maleic anhydride, Acetone/MeOH, 20 mins, rt; b) Ac_2O, NaOAc, 2 hr, 50 ^oC; c) H_2O, 2.5 hr, 70 ^oC, 50%; d) $SOCl_2$, DCM, reflux, 2 hr, quant.; e) NaN_3, Acetone, 0 ^oC - rt, 4 hr, 70%; f) Toluene, reflux, 1.5 hr, quant.*

After successfully synthesized heterobifunctional linker, next job was link this linker **15** having isocyanate group as a electrophile with free amino group as a nucleophile at the terminal position of the decamer (PNA) **16**. So accordingly we plan to synthesize PNA decamer **16**.

3.1.5.2. Synthesis of PNA decamer (16)

PNA decamer **16**, with the TCACTAGATG sequence of nucleobases were synthesized. The synthesis was performed with standard manual Boc-based chemistry using MBHA resin **3,** firstly loaded with Thymine monomer **9** by using HBTU as a coupling reagent in order to obtain functionalized resin **17** with loading 0.2 mmol/g (Scheme 3.3). Then the tert-butyloxycarbonyl (Boc) group of the loaded monomer **17** was removed by treatment with 5% *m*-cresol in TFA to get an amine TFA salt which was neutralized by 5% DIPEA in dichloromethane. Then the free amine on resin was coupled with next cytosine monomer with DIPEA and HATU in NMP as a solvent. After coupling step resin were washed with NMP, and then treated with a solution of Ac_2O/pyridine/NMP (1:25:25, v/v). The cycles were repeated using the monomers like adenine, cytosine, thymine and guanine (TCACTAGATG sequence) with the same protocol to afford the corresponding supported PNA 10-mer on resin **16**, which were tested by Kaiser Test. Then small amount (~5 mg) of the resin were cleaved by washing with TFA, and subsequently stirred with a mixture of TFA/TFMSA/thioanisole/*m*-cresol (6:2:1:1 v/v). The reaction mixture was filtered, and the filtrate were concentrated to by the addition of diethyl ether to afford white coloured crude PNA decamer **18**, which was analyzed by mass.

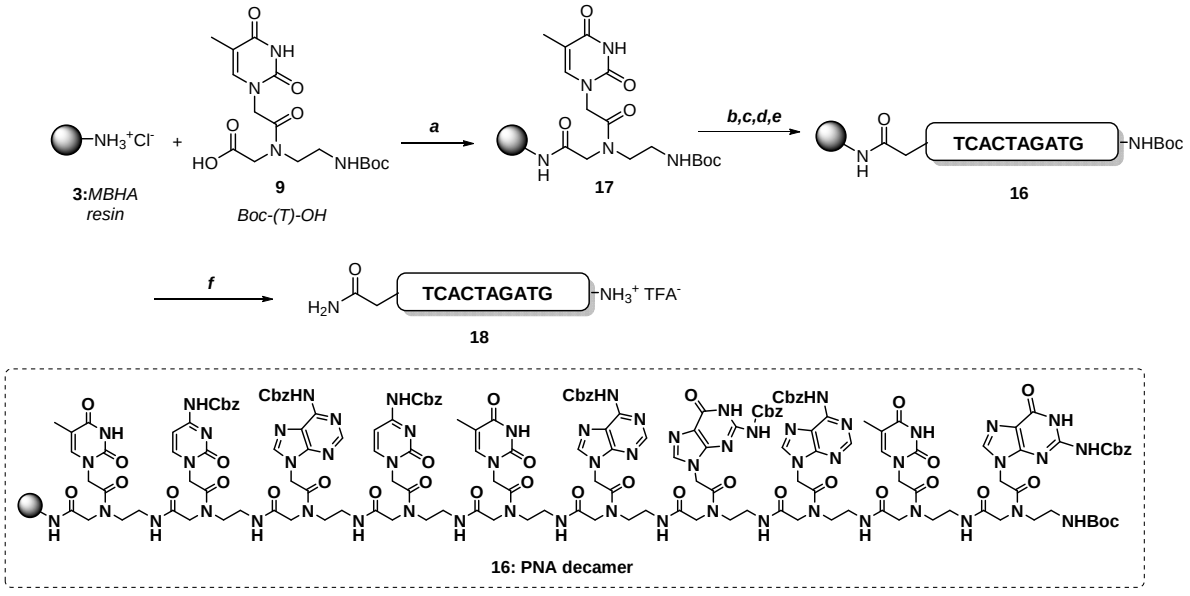

Scheme 3.3: Reagents and conditions: *a) HBTU, DIPEA, NMP, 24 hr, rt; b) TFA/m-cresol, 95:5, 2 × 4 min, rt; c) CH_2Cl_2/DIPEA, 95:5, 2 × 2 min, rt; d) PNA monomers, HATU, DIPEA, NMP, 2 hr, rt; e) Ac_2O/Pyridine/NMP 1:25:25, 2 × 1 min, rt; f) TFA/TFMSA/thioanisole/m-cresol 6:2:1:1 (v/v) 1 hr, rt.*

3.1.5.3. Synthesis of PNA-linker for the conjugation to magnetic nanoparticle (MNP)

After synthesizing heterobifunctional linker (PMPI) **15**, our next target is to attached this linker **15** to the standard sequence of decamer (PNA) **16** [Figure 3.7]; through the reaction of isocyanate group from linker with the terminal amino group of PNA decamer.

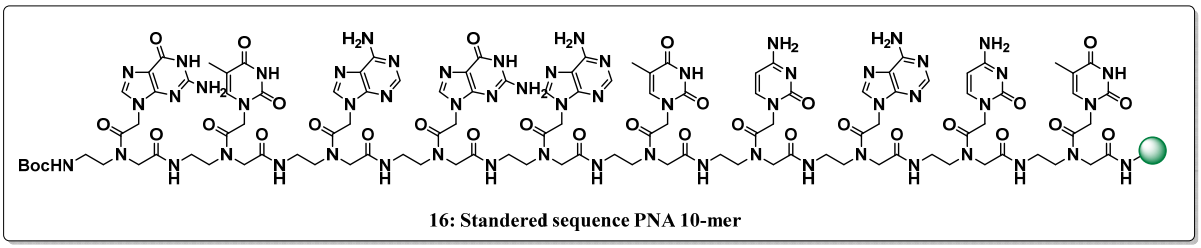

Figure 3.7: Standard sequence of decamer (PNA)

For this, firstly we tried reaction of PMPI **15** on single adenine monomer **20** (which were loaded on MBHA resin) by using solid phase methodology, through the Boc-strategy to afford urea **21**, which on after classical cleavage conditions afford **22**. We performed several coupling reactions but unfortunately, we are getting only 10 to 12% yield of compound **22**, which means compound **22** was never obtained as a pure single product, and which were confirmed by HPLC and mass (Scheme 3.4).

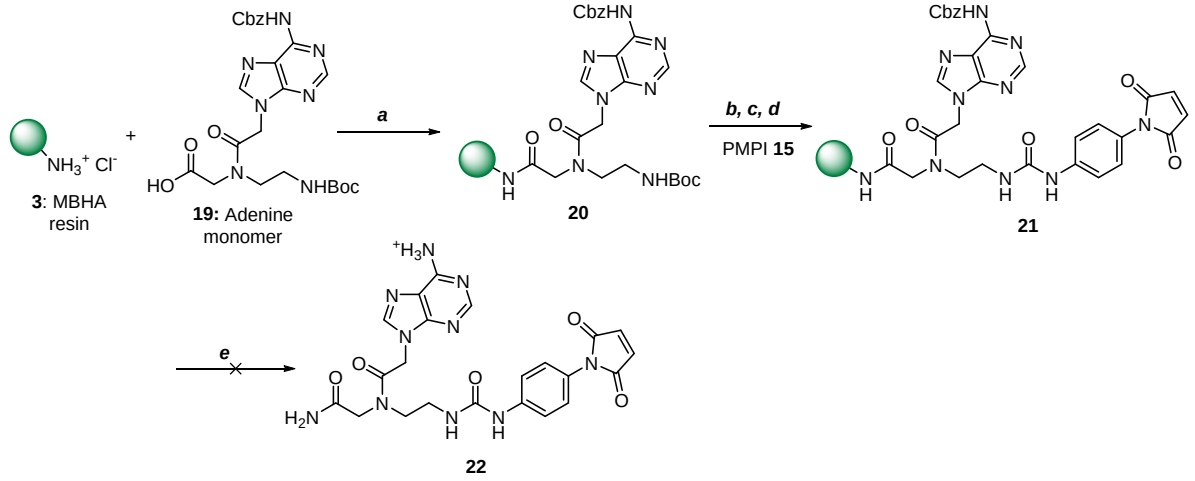

Scheme 3.4: Reagents and conditions: *a) HBTU, DIPEA, NMP, 24 hr, rt; b) TFA/m-cresol, 95:5, 2 × 4 min, rt; c) CH_2Cl_2/DIPEA, 95:5, 2 × 2 min, rt; d) PMPI (**15**), DIPEA, NMP; 2 hr, rt; e) TFA/TFMSA/thioanisole/m-cresol 6:2:1:1 (v/v), 1 hr, rt.*

Here we performed several coupling reaction conditions based on similar types of literature reports[28], with downloading of monomer on MBHA resin like 0.2 and 0.67 mmol/gm and

also screened solvents like NMP and DMF, but unfortunately we are not getting desired product **22** instead we get complex compound which were characterized by NMR and mass (Table 3.1)

Table 3.1: Coupling conditions for the synthesis of urea **22** by using SSPS, through the Boc-strategy.

Entry	*aeg*-A monomer (20)	PMPI (15)	Base	Solvent	Result (%)
1	*(0.02 mmoles)*	(1.5 eq.)	DIPEA (10 eq.)	NMP	Not well characterized
2	*(0.67 mmoles)*	(5 eq.)	DIPEA (10 eq.)	NMP	10% product formation **(22)**
3	*(0.67 mmoles)*	(5 eq.)	DIPEA (10 eq.)	DMF	12% product formation **(22)**

We are also tried the same reaction in solution phase. Accordingly, the synthesis began with the esterification of the commercially available adenine monomer **19** with K_2CO_3 and MeI in acetone to afford an ester **23** in 92% yield. This compound **23** was then subjected with TFA in dichloromethane for the deprotection of -Boc group to afford a crude **24** which were used for the next reaction without further purification. This compound **24** was treated with PMBI **15** in dichloromethane but unfortunately here also we are getting only 30% of compound **25** (Scheme 3.5).

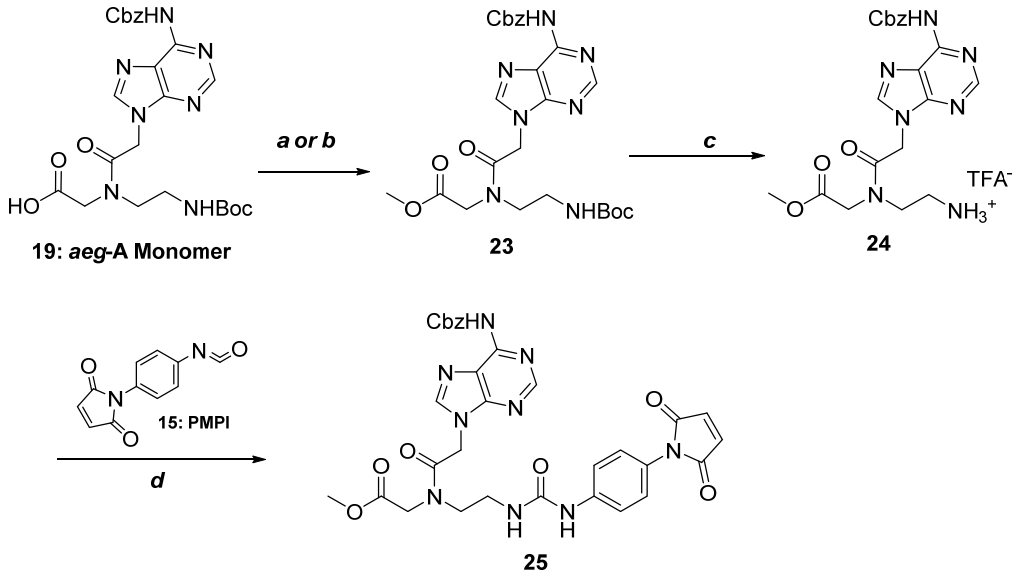

Scheme 3.5: Reagents and conditions: *a) DMAP, DCC, DCM, 0 ^{o}C-rt, 3 hr, 60%; b) K_2CO_3, MeI, Acetone, 0 ^{o}C-rt, 12 hr, 92%; c) TFA, DCM, 0 ^{o}C-rt, 2 hr, 85%; d) PMPI* ***(15)****, DIPEA, DCM, rt, 12 hr, 34%.*

In both the cases means in solid phase (Scheme 3.4) as well as in solution phase (Scheme 3.5) we are getting a desired products **22** and **25** with low yields.

So we planned and designed new strategy for the conjugation of linker to PNA **16**, and prepared the more simple linker, for this we used (*p*-maleimido) benzoic acid (PMBA) **12**, which is the precursor of the PMPI **15** and equally economically also important. So in the test reaction acid **12** was coupled with the terminal amino group of PNA monomer **19** in presence of HATU as a coupling agent in NMP to afford monomer **26** which, after cleavage gave the maleimido modified PNA monomer **27**. Finally, the structure of compound **27** was confirmed by mass analysis (Scheme 3.6).

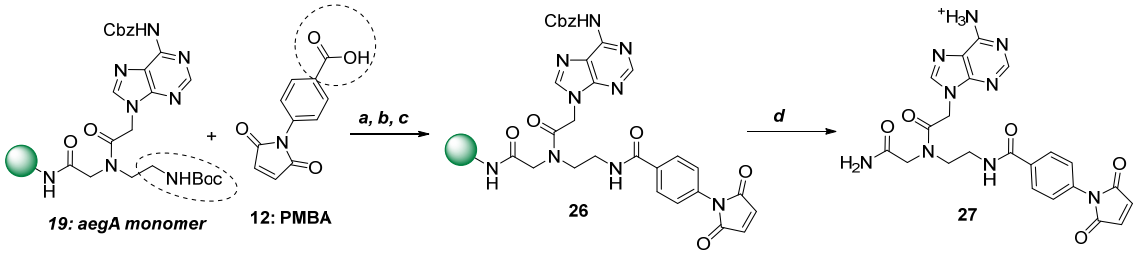

Scheme 3.6: Reagents and conditions: *a) TFA/m-cresol, 95:5, 2 × 4 min, rt; b) CH_2Cl_2/DIPEA, 95:5, 2 × 2 min, rt; c) PMBA* ***(12)****, HATU, DIPEA, NMP; 2 hr, rt; d) TFA/TFMSA/thioanisole/m-cresol 6:2:1:1 (w/w), 1 hr, rt.*

We got the desired product **27** by using this new strategy. We implement the same strategy with the standard sequence of decamer **16** (synthesized in lab by manually using Boc strategy) with PMBA **12** by using HATU as a coupling agent in presence of DIPEA in NMP to afford **28**, which was confirmed by Kaiser Test. After cleavage from the resin, PNA oligomer **9** (Scheme 3.7) was obtained as white solid and its MW was confirmed by Q-Tof mass analysis.

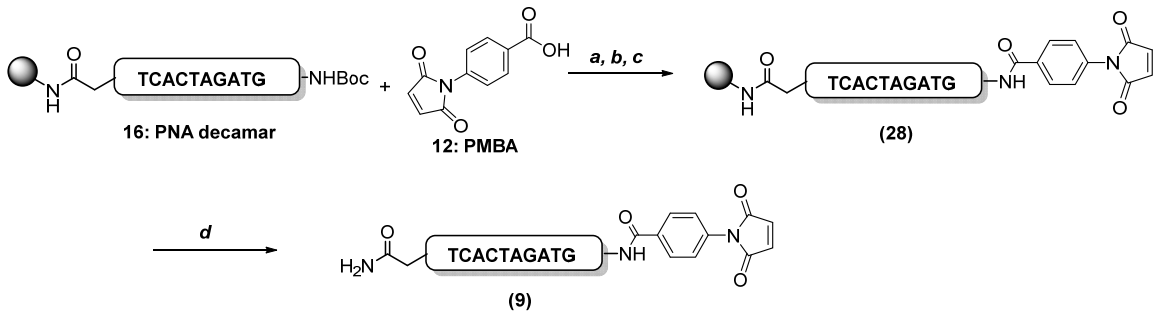

Scheme 3.7: Reagents and conditions: *a) TFA/m-cresol, 95:5, 2 × 4 min, rt; b) CH_2Cl_2/DIPEA, 95:5, 2 × 2 min, rt; c) PMBA* ***(12)****, HATU, DIPEA, NMP; 2 hr, rt; d) TFA/TFMSA/thioanisole/m-cresol 6:2:1:1 (w/w), 1 hr, rt.*

3.1.5.4. Purification of decamer (9) by reverse phase HPLC

The crude decamer **9** was purified by reverse phase semi preparative HPLC by column (tR = 12.2 min). The purity of the **9** was checked by LC-MS (Figure 3.8 and 3.9)

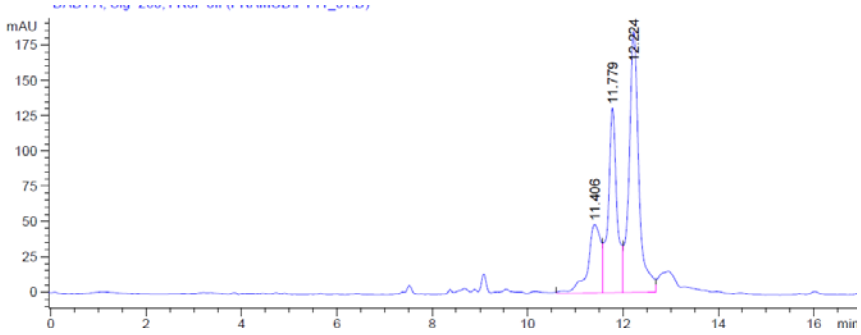

Figure 3.8: HPLC of decamer **9,** retention time 12.2 min.

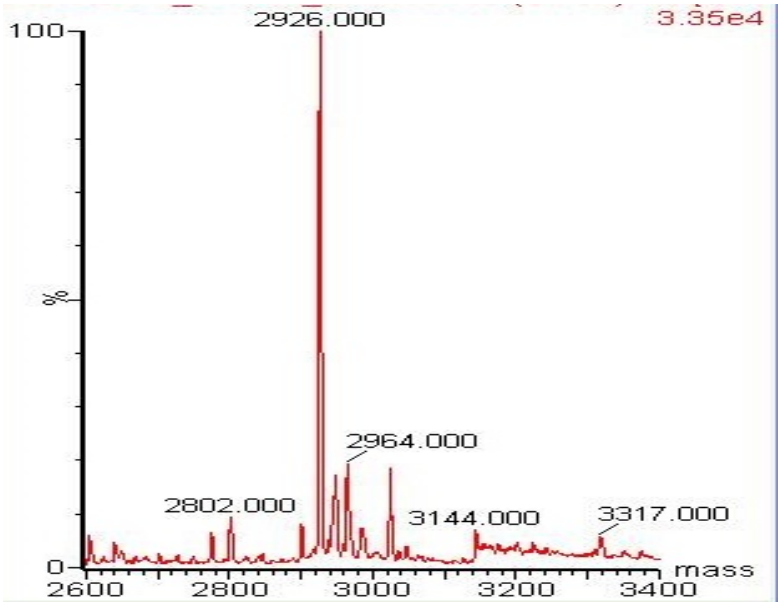

Figure 3.9: ESI-Mass analysis of decamer **9**, found *m/z*: $C_{119}H_{141}N_{59}O_{33}$: 2926.00

3.1.5.5. Functionalisation of nanoparticles with PNA-maleimide-*(MNP-DMSA-PNA: 10)*

Once we have successfully synthesized and characterized oligomer **9**, Michael addition of free thiol groups from DMSA-MNP **29** (Figure 3.10) onto the PNA-malemide (oligomer **9**) was realized in the presence of water, under sonication for 6 hr (Scheme 3.8). The loading of PNA onto MNP was confirmed by elemental analysis and zeta potential (Figure 3.11)

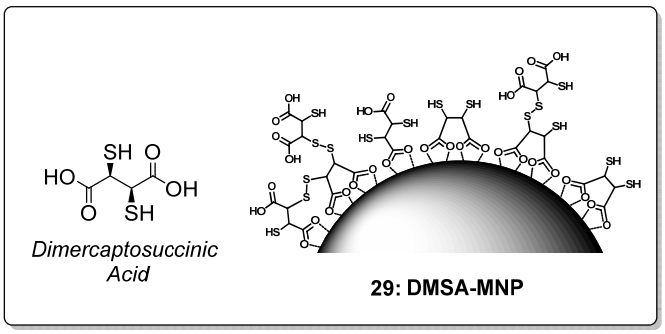

Figure 3.10: MNP surface functionalized with *meso*-2,3-dimercaptosuccinic acid (MNP-DMSA)

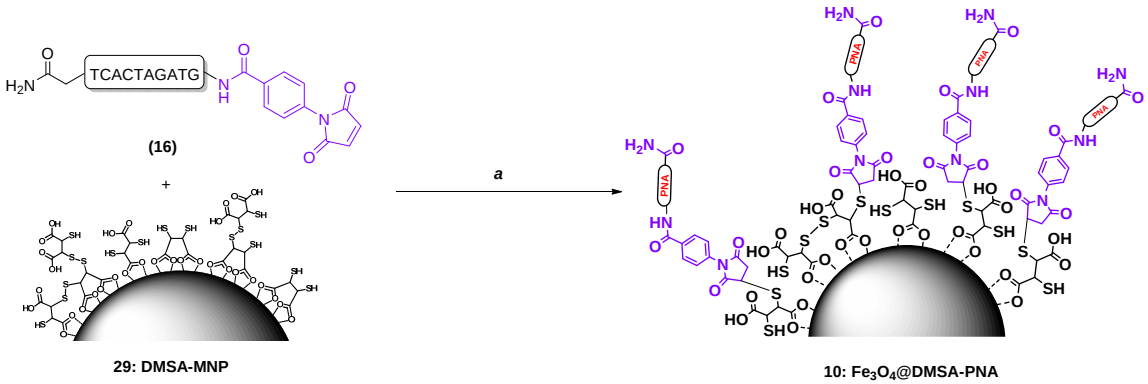

Scheme 3.8: Reagents and conditions: *a) H_2O, sonication, r.t., 4 hr.*

Zeta potential measurements in acetone, showed a decrease in negative superficial charge, from -34.2 ± 0.3 mV to -20.1 ± 1.4 mV. This change is coherent with the bonding of PNA oligomer.

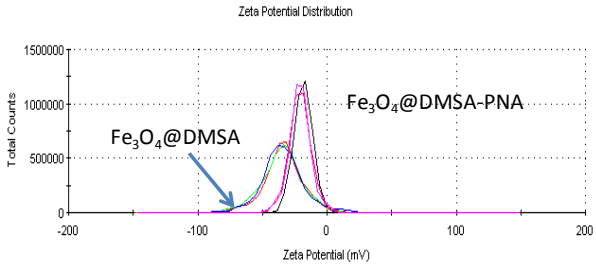

Figure 3.11: Zeta potential distribution of the two nanoparticles

Finally, ζ-potential measurements on the Fe_3O_4@DMSA-Mal-PNA colloid (Fig.3.11) showed a decrease of the negative surface charge with respect to Fe_3O_4@DMSA, from -34.2 ± 0.3 mV to -20.1 ± 1.4 mV, in line with the bonding of a positively charged species such as PNA to the negatively charged native nanoparticles.

We also tried another strategy for the functionalisation of nanoparticle with PNA **18** (without linker). DMSA-MNP **29** is having free thiol and carboxylic group.

3.1.5.6. Functionalisation of nanoparticles with PNA by EDC/NHS coupling

By taking advantage of the presence of the free carboxylic group in DMSA, we planned to coupled it with free the amino group on PNA decamer **18** by using EDC.HCl as a coupling reagent under sonication (Scheme 3.9)

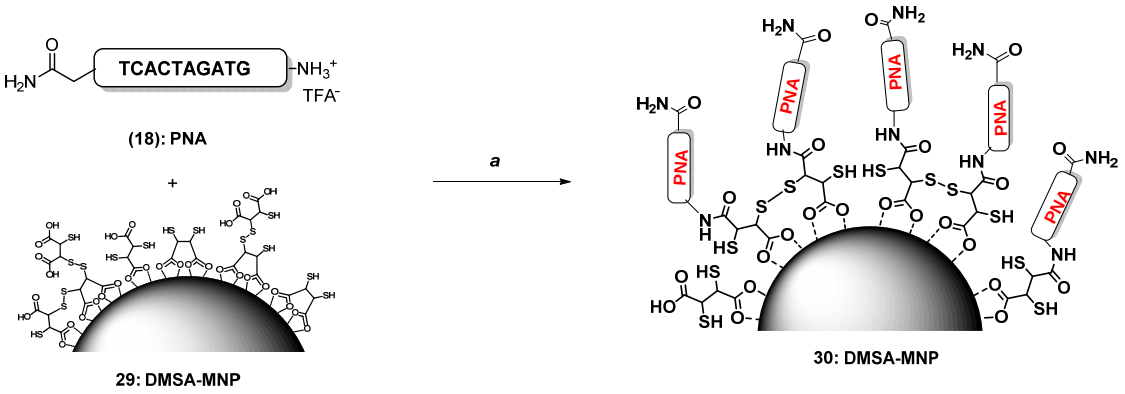

Scheme 3.9: Reagents and conditions: *a) EDC.HCl, NHS, CH_3CN, sonication, rt., 2 hr.*

Unfortunately, after addition of the EDC.HCl the nanoparticles become a colloid and loses its stability, likely due to the shielding of the nanoparticle negative surface charge by the positively charged EDC. From the FT-IR spectra of the obtained MNP, we found bands not attributable to those of PNA (1645 vs 1685 and 1130-1054 vs 1207-1140), which suggest

that they can come from EDC. (Figure 3.12). Also elemental analysis confirmed this hypothesis (Table 3.2).

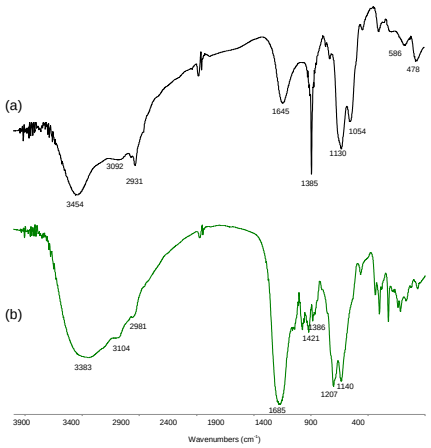

Figure 3.12: FTIR spectra of (a) MNP with PNA; (b) PNA in solid (KBr pellets).

Table 3.2: Elemental analysis of the MNP

	MNP@DMSA	MNP@PNA (30)	PNA (18)
C%	3.36	8.03	47.57
H%	0.75	1.73	5.03
N%	---	2.16	29.79
C/N	---	2.16	1.60

Synthesis of DMSA-MNP **29,** MNP **10** and MNP **30** has been done by our collaborator Dr. Daniela and co-workers, University of Milan, Italy.

3.1.6. Conclusion

A novel and effective strategy for binding PNA oligomers onto the surface of magnetic iron oxide nanoparticles has been developed. All the requirements that stimulated this work have been fulfilled, and some of the drawbacks shown by previous literature reports have been overcome. The control of the size of the magnetic core for the diagnostic and therapeutic applications is ensured by the use of thermal decomposition synthetic route. The desired water solubility and the colloidal stability are provided by the coating with DMSA. The stable linking of MNP to PNA oligomers is given by the efficient Michael addition of

maleimide-functionalized PNAs to the SH groups of DMSA grafted to the nanoparticle surface.

The approach here described, therefore, produces multimodal hybrid organic-inorganic nanomaterials, that can act as dual (T_1 and T_2) MRI contrast agents, as efficient hyperthermia promoters and as PNA carriers. To fully exploit the theranostic potential of these nanohybrids, future work will explore the replacement of the standard PNA sequence, here used for setting the method, with PNA oligomers designed for targeting specific non-coding microRNAs (miRNA), [2] whose dysregulation has been implicated in a variety of pathologies, such as inflammatory and autoimmune diseases, neurological disorders, as well as several types of cancer.[3]

3.1.7. Bibliography

1. Nielsen, P. E., Egholm, M., Berg, R. H., Buchardt, O. Science, **1991**, *254*, 1497-1500.

2. (a) He, L., Hannon, G. J. *Nat Rev Genet* **2004**, *5*, 522-531 (b) Krol, J., Loedige, I., Filipowicz, W. *Nat Rev Genet* **2010**, *11*, 597–610.

3. Iorio, M. V., Croce, C. M. *A comprehensive review, EMBO Molecular Medicine,* **2012**, *4*, 143-159.

4. Fabani, M. M., Abreu-Goodger, C., Williams, D., Lyons, P. A., Torres, A. G., Smith, K. G. C., Enright, A. J., Gait, M. J., Vigorito. E. *Nucleic Acids Research*, **2010**, *38*, 4466-4475.

5. Gambari, R., Fabbri, E., Borgattia, M.,.Lampronti, I, Finotti, A,.Brognara, E., Bianchi, N., Manicardi, A., Marchelli, R., Corradini. R. *Biochem Pharmacol,* **2011**, *82*, 1416-1429.

6. Nielsen, P. E. *Quarterly Reviews of Biophysics*, **2005**, *38*, 345-350.

7. (a) Roca, A. G., Costo, R., Rebolledo, A. F., Veintemillas-Verdaguer, S., Tartaj, P., González-Carreño, T., Morales, M. P., Serna, C. *J. Phys D: Appl Phys,* **2009**, *42*, 224002 (b) Berry, C. C. *J.Phys. D: Appl Phys*, **2009**, *42*, 224003 (c) Pankhurst, Q. A., Thanh, N. T. K., Jones, S. K., Dobson, J. *J. Phys D: Appl Phys*, **2009**, *42*, 224001.

8. Lu, A. H., Schmidt, W., Matoussevitch, N., Bonnemann, H., Spliethoff, B., Tesche, B., Bill, E., Kiefer, W., Schuth, F. *Angewandte Chemie-International Edition* **2004**, *43*, 4303.

9. Gupta, A. K., Gupta, M. *Biomaterials*, **2005**, *26*, 3995.

10. Mornet, S., Vasseur, S., Grasset, F., Veverka, P., Goglio, G., Demourgues, A., Portier, J., Pollert, E., Duguet, E. *Progress in Solid State Chemistry* **2006**, *34*, 237.

11. Hyeon, T. *Chemical Communications* **2003**, 927.

12. Lu, A. H., Salabas, E. L., Schuth, F. *Angewandte Chemie-International Edition* **2007**, *46*, 1222.

13. Shubayev, V. I.; Pisanic, T. R., II; Jin, S. *Adv. Drug Delivery Rev*. **2009**, *61*, 467.

14. Laurent, S.; Forge, D.; Port, M.; Roch, A.; Robic, C.; Elst, L. V.; Muller, R. N. *Chem. Rev.* **2008**, *108*, 2064

15. Gupta, A. K.; Gupta, M. *Biomaterials* **2005**, *26*, 3995

16. Duran, J. D. G.; Arias, J. L.; Gallardo, V.; Delgado, A. V. *J. Pharm. Sci.* **2008**, *97*, 2948.

17. (a) Chin, A. B., Yaacob, I. I. *Journal of Materials Processing Technology* **2007**, *191*, 235 (b) Albornoz, C., Jacobo, S. E., *Journal of Magnetism and Magnetic Materials* **2006**, *305*, 12 (c) Kim, E. H., Lee, H. S., Kwak, B. K., Kim, B. K. *Journal of Magnetism and Magnetic Materials* **2005**, *289*, 328 (d) Wan, J. X., Chen, X. Y., Wang, Z. H., Mu, L., Qian, Y. T. *Journal of Crystal Growth* **2005**, *280*, 239 (e) Kimata, M., Nakagawa, D., Hasegawa, M. *Powder Technology* **2003**, *132*, 112 (f) Salazar-Alvarez, G., Muhammed, M., Zagorodni, A. A. *Chemical Engineering Science* **2006**, *61*, 4625 (g) Basak, S., Chen, D. R., Biswas, P. *Chemical Engineering Science* **2007**, *62*, 1263.

18. Sjogren, C. E., Johansson, C., Naevestad, A., Sontum, P. C, BrileySaebo, K., Fahlvik, A. K. *Magnetic Resonance Imaging* **1997**, *15*, 55.

19. Lefebure, S., Dubois, E., Cabuil, V., Neveu, S., Massart, R. *Journal of Materials Research* **1998**, *13*, 2975.

20. Bacri, J. C., Perzynski, R., Salin, D., Cabuil, V., Massart, R. *Journal of Magnetism and Magnetic Materials* **1990**, *85*, 27.

21. Singh, A., Sahoo, S. K. *Drug Discovery-Today*, **2013**, *19*, 474-481.

22. (a) Dobson, J. *Drug Dev. Res.* **2006**, *67*, 55 (b) Alexiou, C.; Jurgons, R.; Schmid, R. J.; Bergemann, C.; Henke, J.; Erhardt, W.; Huenges, E.; Parak, F. *J. Drug Targeting* **2003**, *11*, 139 (c) Arias, J. L. *Molecules* **2008**, *13*, 2340.

23. Gruttner, C.; Teller, J. *Journal of Magnetism and Magnetic Materials* **1999**, *194*, 8.

24. (a) Olsvik, O.; Popovic, T.; Skjerve, E.; Cudjoe, K. S.; Hornes, E.; Ugelstad, J.; Uhlen, M. *Clinical Microbiology Reviews* **1994**, *7*, 43 (b) Strom, V.; Hultenby, K.; Gruttner, C.; Teller, J.; Xu, B.; Holgersson, J. *Nanotechnology* **2004**, *15*, 457.

25. Berry, C. C.; Curtis, A. S. G. *Journal of Physics D-Applied Physics* **2003**, *36*, R198.

26. Chambon, C.; Clement, O.; Leblanche, A.; Schoumanclaeys, E.; Frija, G. *Magnetic Resonance Imaging* **1993**, *11*, 509.

27. Annunziato, M. E.; Patel, U. S.; Ranade, M.; Palumbo, P. S. *Bioconjugate Chem.,* **1993**, *4*, 212-218.

28. (a) Guillier, F.; Orain, D.; Bradley, M. *Chem. Rev.* **2000**, *100*, 2091-2157 (b) Boeijen, A.; Ameijde, J.; Liskamp, Rob M. J. *J. Org. Chem.* **2001,** *66*, 8454-8462 (c) Casassus, C. D.; Pulka, K.; Claudon, P.; Guichard, G. *Org. Lett.*, **2012**, *14*, 3130-3133.

Chapter 3: Design, synthesis and characterization of functionalized PNAs with heterobifunctional linker and their conjugation with magnetic nanoparticles (MNPs) for miRNA targeting.

Section 2: Experimental Section

3.2.1. Experimental Section

3.2.1.1. General Materials and Methods

The monomers containing the nucleobases C, G and A were purchased from ASM Research Chemicals and were used for the synthesis of PNA decamer, as such without further purification. The thymine monomer *aeg*-(T) PNA-COOH was synthesized in lab. (Chapter 2, section 2). 1-[bis(dimethylamino)methylene]-1*H*-1,2,3-triazolo[4,5-*b*]pyridinium 3-oxidhexafluoro phos- phate (HATU), trifluoroacetic acid (TFA), trifluoromethanesulfonic acid (TFMSA), *m*-cresol and *p*-amino benzoic acid were purchased from Aldrich. *N*-methyl-2-pyrrolidone (NMP), *N, N*-diisopropylethylamine (DIPEA) and thioanisole were purchased from Fluorochem. Polystyrene bead carrying 4-methylbenzhydrylamine hydrochloride salt groups (MBHA resin, 0.63 mmol/g) was purchased from VWR International.

3.2.1.2. Experimental Techniques

^{1}H and ^{13}C NMR spectra were recorded on Bruker 300 MHz and 70 MHz respectively. Chemical shifts (δ) are reported in parts per million relative to solvent peak. Many of the compounds described below showed many rotamers and consequently exhibit complex ^{1}H NMR patterns. Some of the signals in the ^{1}H NMR are therefore described as major (ma.) and minor (mi.) components; however, in many cases, some minor signals were obscured by the major signal of another proton. In such cases, only the major signal is reported or a range containing two or more CH_2. In some cases, the ^{13}C spectrum shows many peaks that cannot be distinguished in a small range: ov. Means ‘overlapped’. Melting points of samples were determined in open capillary tubes with a Büchi Melting Point B-540 apparatus and (dec) indicates decomposition. The IR spectra were recorded on a Perkin-Elmer FTIR 4100. Mass spectra were obtained by LCMS techniques (a Thermo Scientific LCQ Advantage). TLC was performed using TLC glass plates pre-coated with silica gel (Merck). TLCs were visualized with UV light and/or either by charring in Ninhydrine solution or developing in I_2 chamber. Silica gel 60-120 and 100-200 mesh was used for column chromatography using ethyl acetate/hexane and dichloromethane/methanol mixture as elution solvent depending upon the compound polarity and chemical nature. Commercial reagents were generally used as received. Solvents used in organic reactions were distilled under an inert atmosphere.

Unless otherwise noted, all reactions were carried out at room temperature. Oligomers were characterized by RP HPLC, using C18 column and MALDI-TOF mass spectrometry.

All weightings of reagents were carried out with analytical balance Mettler Toledo AB135-S/FACT. Vials ALLTECH of 1.5 ml, 4 ml and 8 ml with frits of PTFE were used as reactor for manual solid phase synthesis.

HPLC of PNA oligomers were performed with a HPLC AGILENT 1100 Series, using an analytical column DISCOVERY® BIO WIDE PORE C18 (15 cm x 4.6 mm, 5 μm) and a semi preparative column DISCOVERY® BIO WIDE PORE C18 (25 cm x 10 mm, 10 μm).

MALDI-TOF spectra were recorded with a Bruker Daltonics Omniflex. Pulsed nitrogen lasers (337 nm) were used to generate ions that have been accelerated in a 20 kV field. The instrument was calibrated in the range from 0 to 20 kDa. Generally, Sinapinic acid and 2, 5-dihydroxybenzoic acid (DHB) matrixes were used.

A lyophilizer Telstar Cryodos were used to isolate pure PNA oligomers from aqueous solutions.

3.2.1.3. Experimental Procedures

4-(2,5-dioxo-2,5-dihydro-1H-pyrrol-1-yl)benzoic acid (12)

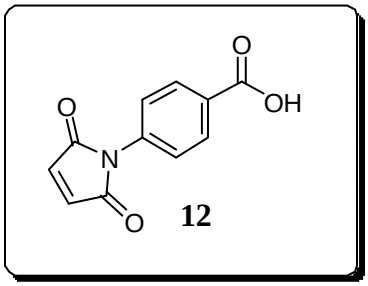

12

Commercially available *p*-aminobenzoic acid, PABA **11** (4.36 gm, 31 mmol, 1 eq.) was suspended in 30 ml of acetone and solubilized by the addition of 5 ml of methanol. A solution of maleic anhydride (3.66 gm, 37 mmol, 1.2 eq.) in 10 ml of acetone was added dropwise and the resulting precipitate stirred for 20 min. The material was suction filtered, washed with acetone and vacuum-dried to afford a yellow powder (5.9 gm). This material was dissolved in acetic anhydride (13 mL), treated with sodium acetate (1.1 gm), and then heated with stirring at 50 °C for 2 hr. The volatiles were then removed in vacuo, and the resulting residue was taken up in 150 mL of water and heated at 70 °C for 2.5 hr. The resulting white precipitate was suction filtered, washed with water and vacuum-dried to afford compound **12** crude product, which was purified on flash column chromatography (SiO_2) using 10% MeOH in DCM as a eluent to afford compound **12** as a white solid (3.5 gm, 50%); M.P.: 234 ^{o}C.

Molecular formula: $C_{11}H_7NO_4$

R*f*: 0.7 (DCM: Methanol, 90:10)

IR ($CHCl_3$): 3583, 3178, 2360, 1710, 1603, 1516, 1420 cm^{-1}.

^{1}H NMR (300 MHz, $CDCl_3$ + DMSO-d_6): δ 6.82 (s, 2H), 7.36 (d, J = 9 Hz, 2H), 8.02 (d, J = 9 Hz, 2H)

^{13}C NMR (75 MHz, $CDCl_3$+ DMSO-d_6): δ 118.88, 126.28, 130.05, 130.51, 134.92, 135.58, 166.88, 169.67

MS (ESI) *(m/z)*: 218 $(M+1)^+$

4-(2,5-dioxo-2,5-dihydro-1H-pyrrol-1-yl)benzoyl chloride (13)

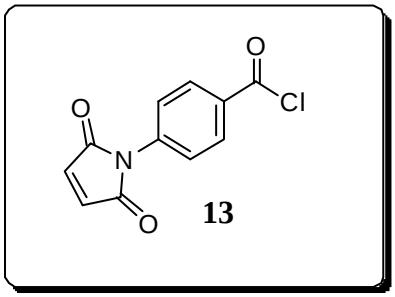

13

p-Maleimidobenzoic acid, PMBA **12** (500 mg, 2.30 mmol) was suspended in 2 mL of DCM and then 10 mL of thionyl chloride were added, leading to a yellowish solution. After refluxing for 2 hr and the progress of the reaction was monitored by TLC, the solution were vacuum dried to afford a yellow powder as desired product **13** (540 mg, quantitative yield), which were used without further purification. M.P.: 158 ^oC.

Molecular formula: $C_{11}H_6ClNO_3$

R*f*: 0.6 (ethyl acetate: Hexane, 50:50)

IR ($CHCl_3$): cm^{-1} 3473, 3107, 1772, 1713, 1599.

^{1}H NMR (300 MHz, $CDCl_3$+DMSO-d_6): δ 6.93 (s, 2H), 7.65 (d, J = 8.7 Hz, 2H), 8.25 (d, J = 8.7 Hz, 2H),

^{13}C NMR (75 MHz, CDC_{l3}+DMSO-d_6): δ 120.00, 127.20, 130.95, 131.39, 135.53, 143.31, 164.89, 168.07, 170.55

4-(2,5-dioxo-2,5-dihydro-1H-pyrrol-1-yl)benzoyl azide (14)

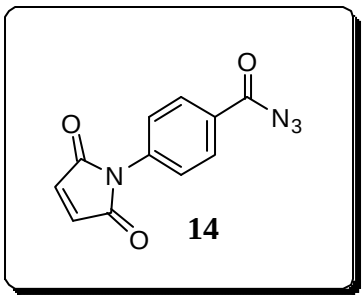

14

To a stirred suspension of compound **13** (500 mg, 2.12 mmol, 1 eq.) in 5 mL of acetone at 0 °C, solid NaN_3 (690 mg, 10.60 mmol, 5 eq.) was added in three portions. The suspension was stirred at 0 °C and then raised to room temperature. The progress of the reaction was monitored by TLC. After stirring at rt for 4 hr, the solvent were removed in vacuo, and the resulting orange/reddish residue was chromatographed with DCM as eluent. The product **14** is isolated upon evaporation of solvent to afford an pale yellow fluffy needles (359 mg, 70%).

Molecular formula: $C_{11}H_6N_4O_3$

R*f*: 0.6 (ethyl acetate: Hexane, 50:50)

IR ($CHCl_3$): cm^{-1} 3111, 2137, 1717, 1692, 1604, 1509, 1460, 1376.

^{1}H NMR (300 MHz, $CDCl_3$): δ 6.91 (s, 2H), 7.55 (d, J = 8 Hz, 2H), 8.15(d, J = 8 Hz, 2H)

^{13}C NMR (75 MHz, $CDCl_3$+DMSO-d_6): δ 124.76, 128.66, 129.68, 134.06, 136.29, 168.30, 171.02

1-(4-isocyanatophenyl)-1H-pyrrole-2, 5-Dione (15)

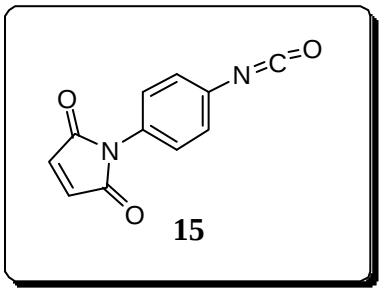

15

A solution of compound **14** (300 mg, 1.24 mmol) in dry toluene (10 mL) is refluxed under nitrogen for 1.5 hr. The progress of the reaction was monitored by TLC, after completion of the reaction evaporate the reaction mixture on to the rota vapour. This quantitatively affords compound **15** as a yellow solid (265 mg). *[This compound should be stored in a sealed vial, protected from light and moisture, in a freezer];* M.P.: 121-123 °C.

Molecular formula: $C_{11}H_6N_2O_3$

R*f*: 0.5 (ethyl acetate: Hexane, 40:60)

^{1}H NMR (300 MHz, $CDCl_3$): δ 6.87 (s, 2H), 7.17-7.20 (d, J = 9 Hz, 2H), 7.33-7.36 (d, J = 9 Hz, 2H)

^{13}C NMR (75 MHz, $CDCl_3$): δ 125.34, 127.04, 128.67, 132.93, 134.25, 169.19

MS (ESI) *(m/z):* 215 (M+1).

Loading (0.2 mmol/gm) of Thymine monomer 9 on MBHA resin (17)

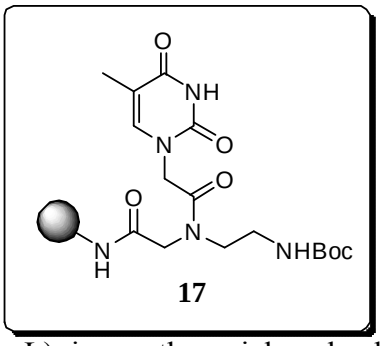

17

The MBHA resin **3** (0.3 gm) was washed with CH_2Cl_2 (2 x 5 mL) and activated by treatment with 5% DIPEA in CH_2Cl_2 for 5 min for 3 times; and then washed with CH_2Cl_2 (2 x 5 mL). In a vial, DIPEA (21 μL, 0.12 mmol) was added to a solution of Thymine monomer **9** (23.06 mg, 0.06 mmol) in NMP (1 mL); then, a solution of HBTU (22.78 mg, 0.06 mmol) in NMP (1 mL) in another vial and add this solution into the monomer solution, and activate the monomer solution for 2 minutes. This mixture was then added to the neutralized resin and at rt for 12 hr. The resin was washed with NMP (3 x 5 mL). A solution of Ac_2O/Py/NMP 1:2:2 (5 mL) was added to the resin (capping of unreacted amino groups) and left under stirring at rt for 1 hr. After this time, the resin was washed with NMP (3 x 5 mL), CH_2Cl_2 (4 x 5 mL), 5% DIPEA in CH_2Cl_2 (2 x 5 mL) and again with CH_2Cl_2 (4 x 5 mL); and finally dried in vacuum to afford the MBHA resin downloaded with Thymine monomer **17** (0.352 gm); Kaiser Test: negative.

Synthesis of the resin supported TCACTAGATG sequence of nucleobases *aeg*-PNA decamer (16)

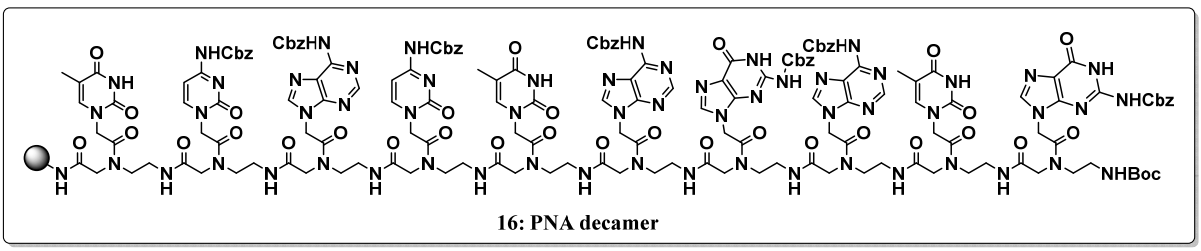

16: PNA decamer

Solid phase synthesis was done by using standard manual Boc-based chemistry; resin **17** (100 mg, substitution with 0.2 mmol/g) was placed in a reaction vessel (volume; 8 mL) and which was swollen with CH_2Cl_2 for 30 minutes, the Boc group of the loaded monomer was removed by treatment with TFA/*m*-cresol (95:5), (3 mL, 2 x 4 min). The resin was washed with CH_2Cl_2 (2 x 5 mL) and then treated with CH_2Cl_2 /DIPEA (95:5), (3 mL, 2 x 2 min). Then the resin was washed thoroughly with CH_2Cl_2 (2 x 5 mL). In a vial, DIPEA (35 µL, 0.2 mmol, 10 eq.) was added to a solution of *aeg*-(C) PNA-COOH monomer (53.37 mg, 0.106 mmol, 5.3 eq.) in NMP (500 µL); then, a solution of HATU (38 mg, 0.1 mmol, 5 eq.) in NMP (500 µL) in another vial and add this solution into the monomer solution, and activate the monomer solution for 2 minutes. This mixture was then added to the neutralized resin and shaken for 2 hr at rt. After coupling step the resin was filtered, washed with NMP (3 x 5 mL) and CH_2Cl_2 (3 x 5 mL). Then resin treated with Ac_2O/Py/NMP; 1:25:25 capping solution twice for 1 min. and again washed the resin with CH_2Cl_2 (3 x 5 mL), NMP (3 x 5 mL) and CH_2Cl_2 (3 x 5 mL). The cycle was repeated using the required monomers like cytosine (53.4 mg), adenine (56 mg) and guanine (57.6 mg) with the same protocol and after the last coupling and capping the resin was washed with several times with NMP and CH_2Cl_2 and finally dried the resin under vacuum to afford the corresponding supported PNA decamer on resin **16** (146 mg).

Synthesis of PNA Decamer (18)

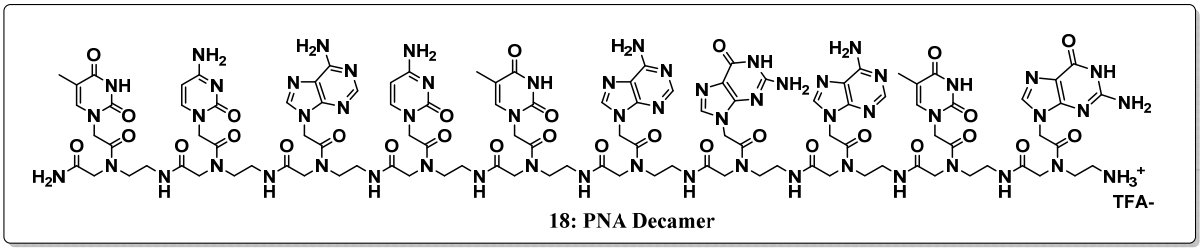

18: PNA Decamer

Cleavage: The resin **16** (5 mg) was washed with TFA (2 × 100 µL) and subsequently stirred for 1 hr with a mixture of TFA/TFMSA/thioanisole/*m*-cresol [6:2:1:1 v/v] (500 µL). The reaction mixture was filtered, and the resin washed with TFA (2 × 100 µL). The filtrate was concentrated under nitrogen flow and Et_2O (5 mL) was added to precipitate PNA as a white solid. Centrifugation of the slurry gave the product, which was washed with Et_2O (5 x 5 mL) and dried to afford the crude decamer **18**.

Retention time (analytic column 15 cm); gradient from 95% of H_2O/TFA 0.1% to 100% of AcCN/TFA 0.1%) = 10.2 min.

Maldi Tof MS: found *m/z:* 2726 [M] +, calculated for $C_{108}H_{137}N_{58}O_{30}^{+}$: 2726.10

Loading (0.67 mmol/gm) of Adenine monomer 19 (*aeg*-A-PNA) on MBHA resin 3.

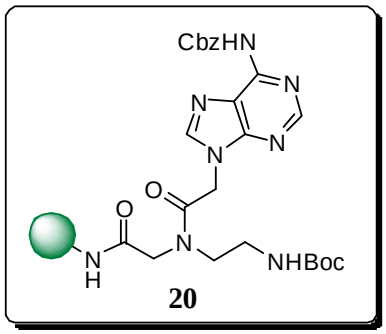

20

The MBHA resin **3** (200 mg) was washed with CH_2Cl_2 (2 x 5 mL) and activated by treatment with 5% DIPEA in CH_2Cl_2 for 5 min for 3 times; and then washed with CH_2Cl_2 (2 x 5 mL). In a vial, DIPEA (47 µL, 0.268 mmol) was added to a solution of Adenine monomer **19** (70.7 mg, 0.134 mmol) in NMP (1 mL); then a solution of HBTU (51 mg, 0.134 mmol) in NMP (1 mL) in another vial and add this solution into the monomer solution, and activate the monomer solution for 2 minutes. This mixture was then added to the neutralized resin and at rt for 12 hr. The resin was washed with NMP (3 x 5 mL). A solution of Ac_2O/Py/NMP 1:2:2 (5 mL) was added to the resin (capping of unreacted amino groups) and left under stirring at rt for 1 hr. After this time, the resin was washed with NMP (3 x 5 mL), CH_2Cl_2 (4 x 5 mL), 5% DIPEA in CH_2Cl_2 (2 x 5 mL) and again with CH_2Cl_2 (4 x 5 mL); and finally dried in vacuum to afford the MBHA resin downloaded with Adenine monomer **20** (263 mg); Kaiser Test: negative.

Synthesis of 21:

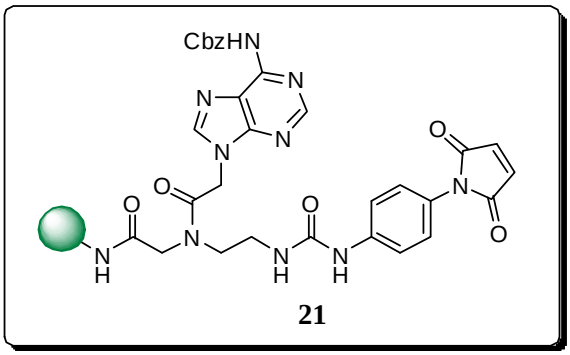

21

The resin **20** (85 mg, substitution with 0.67 mmol/g) was placed in a reaction vessel (volume; 8 mL) and which was swollen with CH_2Cl_2 for 30 minutes, the Boc group of the loaded monomer was removed by treatment with TFA/*m*-cresol (95:5), (3 mL, 2 x 4 min). The resin was washed with CH_2Cl_2 (2 x 5 mL), DMF (2 x 5 mL) and then treated with CH_2Cl_2 /DIPEA (95:5), (3 mL, 2 x 2 min). Then the

resin was washed thoroughly with CH_2Cl_2 (2 x 5 mL). In a vial, (60.93 mg, 0.284 mmol) of **15** PMPI in DMF (500 µL). Then in another vial, DIPEA (70 µL, 0.4 mmol, 7 eq.) with DMF (500 µL), add this solution of DIPEA into the resin, followed by PMPI solution and allowed the reaction for 12 hr at room temperature. After this the resin was filtered, washed with DMF (2 x 5 mL) and CH_2Cl_2 (2 x 5 mL) and finally dried the resin under vacuum to afford the corresponding supported PNA urea on resin **21** (95 mg). Kaiser Test: negative

Synthesis of 22:

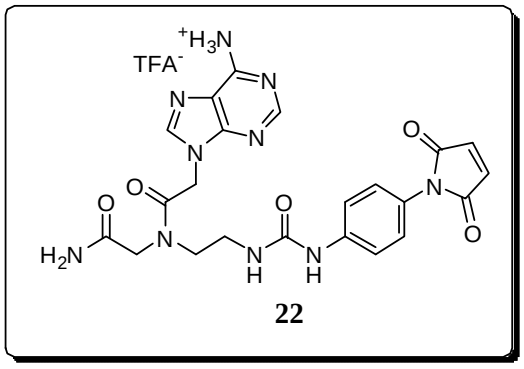

22

Cleavage: The resin **21** (95 mg) was washed with TFA (2 × 100 µL) and subsequently stirred for 1 hr with a mixture of TFA/TFMSA/thioanisole/*m*-cresol [6:2:1:1 v/v] (500 µL). The reaction mixture was filtered, and the resin washed with TFA (2 × 100 µL). The filtrate was concentrated under nitrogen flow and Et_2O (5 mL) was added to precipitate monomer as a white solid. Centrifugation of the slurry gave the product, which was washed with Et_2O (5 x 5 mL) and dried to afford the white coloured compound **22** (39 mg)

Retention time (analytic column 15 cm); gradient from 95% of H_2O/TFA 0.1% to 100% of AcCN/TFA 0.1% for 30 min.) = 8.1 min and 9.2 min.

Maldi Tof MS: found *m/z:* 507 $[M]^+$ + 631, calculated for $\mathbf{C_{22}H_{23}N_{10}O_5^+}$: 507.18

Methyl-N-(2-(6-(((benzyloxy)carbonyl)amino)-9H-purin-9-yl)acetyl)-N-(2-((tert butoxycarbonyl)amino)ethyl)glycinate (23)

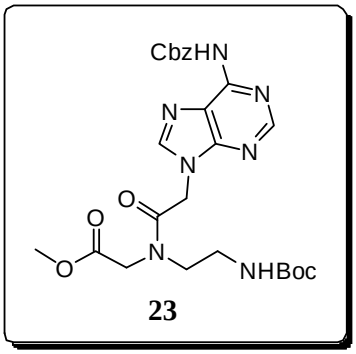

23

To the stirred solution of acid **19** (100 mg, 0.189 mmol) in anhydrous DCM (5 mL) and methanol (0.5 mL), DMAP (23 mg, 0.189 mmol) were added and stirred the reaction for 10 min at 0 ^oC. DCC (47 mg, 0.227 mmol) was added slowly and the resultant solution was stirred for 3 hr at room temperature. The

progress of the reaction was monitored by TLC. Filter the reaction mixture on to the filter paper and evaporate all the solvent under reduced pressure. The residue were diluted with 5 mL of Water and extracted with ethyl acetate (3×10 mL) and again washed with saturated solution of citric acid, then with saturated solution of $NaHCO_3$ and brine. The organic layers were dried over anhydrous Na_2SO_4, filtered and concentrated under reduced pressure to afford crude ester **23** which was purified by column chromatography using MeOH: DCM (10:90) to afford pure compound **23** (65 mg, 60%)

Molecular formula: $C_{25}H_{31}N_7O_7$

R*f*: 0.6 (MeOH: DCM, 10:90)

^{1}H NMR (300 MHz, $CDCl_3$): δ 1.42 (s, 9H), 3.39 (q, 2H), 3.64 (t, 2H), 3.73(s, 3H), 4.07 (d, 2H), 5.14 (d, 2H), 5.29 (s, 2H), 5.63 (bs, 1H), 7.35-7.44 (m, 5H), 8.06 (s, 1H), 8.74 (s, 1H).

MS (ESI) (*m/z*): 541 $(M+Na)^+$

2-(2-(6-(((benzyloxy)carbonyl)amino)-9H-purin-9-yl)-N-(2-methoxy-2-oxoethyl)acetamido)ethan-1-aminium (24)

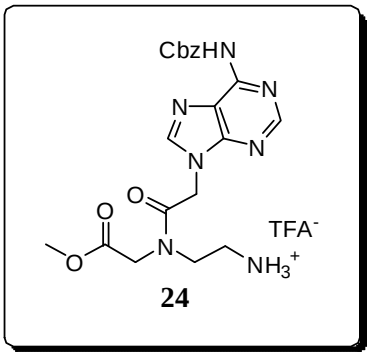

24

The compound **23** (85 mg, 0.157 mmol) was dissolved in minimum volume of DCM (5 mL) and TFA (1 mL) was added slowly at 0 ^oC. Reaction mixture was allowed to stir for 2 hr at room temperature. The progress of the reaction was monitored by TLC. After completion of the reaction saturated solution of $NaHCO_3$ solution was added to the reaction mixture for neutralization and then the aqueous layer was extracted repeatedly with DCM (2 x 10 mL). The organic layers were dried over anhydrous Na_2SO_4, filtered and concentrated under reduced pressure to afford the free amine **24** (60 mg, 85%) which was used without further purification.

Molecular formula: $C_{20}H_{24}N_7O_5^+$

R*f*: 0.3 (MeOH: DCM, 10:90)

^{1}H NMR (300 MHz, $CDCl_3$): δ 2.76 (t, 2H), 3.38(q, 2H), 3.60 (s, 3H), 3.79 (d, 2H), 4.30(d, 2H), 5.10 (d, 12H), 5.30 (s, 2H), 7.31-7.34 (m, 5H), 8.18 (d, 1H), 8.73 (s, 1H).

Methyl-N-(2-(6-(((benzyloxy)carbonyl)amino)-9H-purin-9-yl)acetyl)-N-(2-(3-(4-(2,5-dioxo-2,5-dihydro-1H-pyrrol-1-yl)phenyl)ureido)ethyl)glycinate (25)

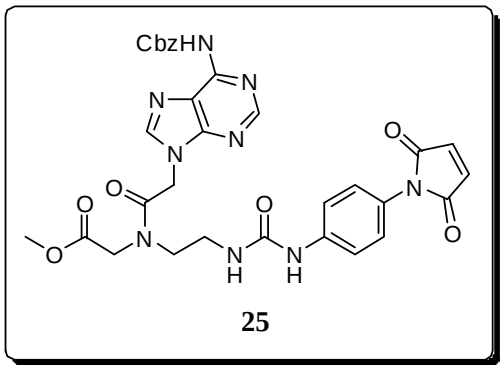

25

To the stirred solution of PMPI **15** (41 mg, 0.191 mmol) in anhydrous DCM (5 mL), compound **24** (60 mg, 0.136 mmol) were added followed by the addition of DIPEA (35 µL, 0.191 mmol) at room temperature, and stirred the reaction for 12 hr under nitrogen atmosphere. The progress of the reaction was monitored by TLC; evaporate all the solvent under reduced pressure. The residue were diluted with 5 mL of Water and extracted with ethyl acetate (3 x 10 mL) and brine. The organic layers were dried over anhydrous Na_2SO_4, filtered and concentrated under reduced pressure to afford **25.**

*Note: This compound **25** was not well characterized by mass as well as ^{1}H-NMR.*

Synthesis of 26:

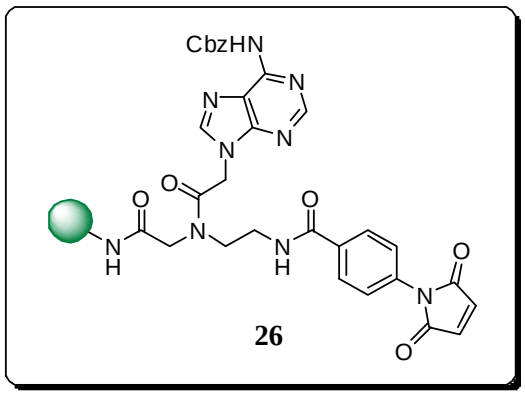

26

The resin **20** (50 mg, substitution with 0.67 mmol/g) was placed in a reaction vessel (volume; 8 mL) and which was swollen with CH_2Cl_2 for 30 minutes, the Boc group of the loaded monomer was removed by treatment with TFA/*m*-cresol (95:5), (2 mL, 2 x 4 min). The resin was washed with CH_2Cl_2 (2 x 5 mL), NMP (2 x 5 mL) and then treated with CH_2Cl_2 /DIPEA (95:5), (1 mL, 2 x 2 min). Then the resin was washed thoroughly with CH_2Cl_2 (2 x 5 mL). In a vial, DIPEA (62 µL, 0.354 mmol, 10 eq.) was added to a solution of PMBA **12** (40 mg, 0.184 mmol, 5.2 eq.) in NMP (500 µL); then, a solution of HATU (67.3 mg, 0.177 mmol, 5 eq.) in NMP (500 µL)

in another vial and add this solution into the acid solution, and activate the acid solution for 2 minutes (yellow coloured solution). This mixture was then added to the neutralized resin and shaken for 2 hr at room temperature. After coupling step the resin was filtered, washed with NMP (3 x 5 mL) and CH_2Cl_2 (3 x 5 mL) and finally dried the resin under vacuum to afford the corresponding supported PNA monomer on resin **26** (61 mg). Kaiser Test: negative

Synthesis of 27:

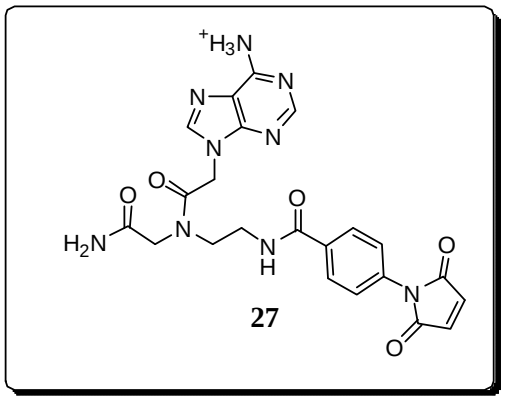

Cleavage: The resin **26** (61 mg) was washed with TFA (2 × 100 µL) and subsequently stirred for 1 hr with a mixture of TFA/TFMSA/thioanisole/*m*-cresol [6:2:1:1 v/v] (500 µL). The reaction mixture was filtered, and the resin washed with TFA (2 × 100 µL). The filtrate was concentrated under nitrogen flow and Et_2O (5 mL) was added to precipitate monomer as a white solid. Centrifugation of the slurry gave the product, which was washed with Et_2O (5 x 5 mL) and dried to afford the white coloured compound **27** (7.5 mg)

Retention time (analytic column 15 cm); gradient from 95% of H_2O/TFA 0.1% to 100% of AcCN/TFA 0.1% for 30 min.) = 8.8 min.

ESI-MS: found *m/z*: 492.30 $[M]^+$, calculated $C_{22}H_{22}N_9O_5^+$: 492.17

Synthesis of PNA decamer with linker (28):

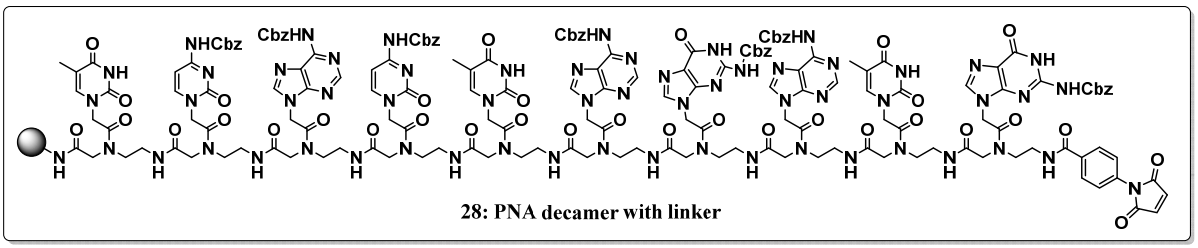

The resin **16** (102 mg, substitution with 0.2 mmol/g) was placed in a reaction vessel (volume; 8 mL) and which was swollen with CH_2Cl_2 for 30 minutes, the Boc group of the loaded

monomer was removed by treatment with TFA/*m*-cresol (95:5), (3 mL, 2 x 4 min). The resin was washed with CH_2Cl_2 (2 x 5 mL), NMP (2 x 5 mL) and then treated with CH_2Cl_2 /DIPEA (95:5), (3 mL, 2 x 2 min). Then the resin was washed thoroughly with CH_2Cl_2 (2 x 5 mL). In a vial, DIPEA (36 µL, 0.204 mmol, 10 eq.) was added to a solution of PMBA **12** (24.36 mg, 0.112 mmol, 5.5 eq.) in NMP (500 µL); then, a solution of HATU (38.78 mg, 0.102 mmol, 5 eq.) in NMP (500 µL) in another vial and add this solution into the acid solution, and activate the acid solution for 2 minutes (yellow coloured solution). This mixture was then added to the neutralized resin and shaken for 2 hr at room temperature. After coupling step the resin was filtered, washed with NMP (3 x 5 mL) and CH_2Cl_2 (3 x 5 mL) and finally dried the resin under vacuum to afford the corresponding supported PNA decamer on resin **28** (110 mg). Kaiser Test: negative.

Synthesis of PNA decamer with linker (9):

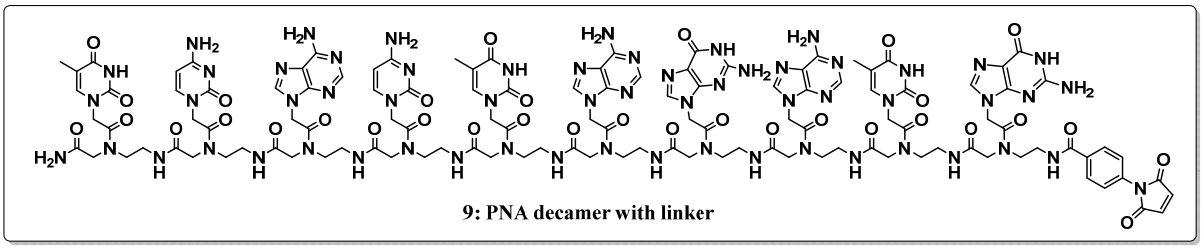

9: PNA decamer with linker

Cleavage: The resin **28** (110 mg) was washed with TFA (2 × 100 µL) and subsequently stirred for 1 hr with a mixture of TFA/TFMSA/thioanisole/*m*-cresol [6:2:1:1 v/v] (500 µL). The reaction mixture was filtered, and the resin washed with TFA (2 × 100 µL). The filtrate was concentrated under nitrogen flow and Et_2O (5 mL) was added to precipitate monomer as a white solid. Centrifugation of the slurry gave the product, which was washed with Et_2O (5 x 5 mL) and dried to afford the white coloured PNA decamer **9** (17 mg)

Retention time (analytical column 15 cm); gradient from 95% of H_2O/TFA 0.1% to 100% of AcCN/TFA 0.1% for 60 min.) = 12.2 min.

Q-TOF/MS: found *m/z*: 2926.00 $[M+1]^+$, calculated $C_{119}H_{141}N_{59}O_{33}$: 2925.12

Functionalisation of nanoparticles with PNA-maleimide-*(MNP-DMSA-PNA: 10)*

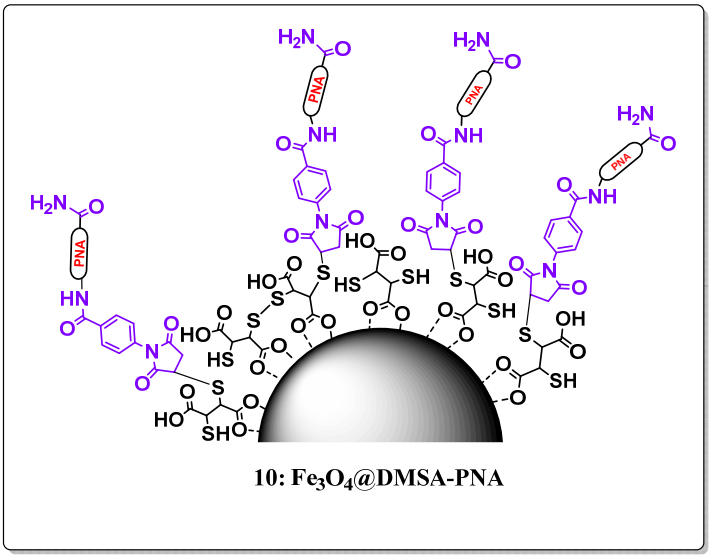

A suspension of 5 mL of Fe_3O_4@DMSA (0.56 mg/mL Fe = 0.77 mg Fe_3O_4 /ml) was added to a solution of 5 mg of PNA dissolved in 0.5 mL of milliQ water under inert atmosphere. The pH of the reaction mixture was adjusted to 7 and the reaction carried out under ultrasonic irradiation for 4 hr at room temperature. The nanoparticles were then collected with a permanent magnet, re-suspended in 5 mL water and centrifuged (3 x, 15 min at 7197 rcf). The isolated magnetic nanoparticles **10** were then stored under nitrogen atmosphere.

MNP Fe_3O_4@DMSA:

Elemental analysis = C 3.36% H 0.75% N NOT DETECTED;

Total DMSA= 12.742% w/w.

Z potential in acetone = -34.2 ± 0.3 mV

MNP Fe_3O_4@DMSA + PNA maleimmide

Elemental analysis = C 10.23% H 1.40% N 3.97%

Total PNA =14.063%

Z potential in acetone = -20.1 ± 1.4 mV

Functionalisation of nanoparticles with PNA-maleimide-*(MNP-DMSA-PNA: 30)*

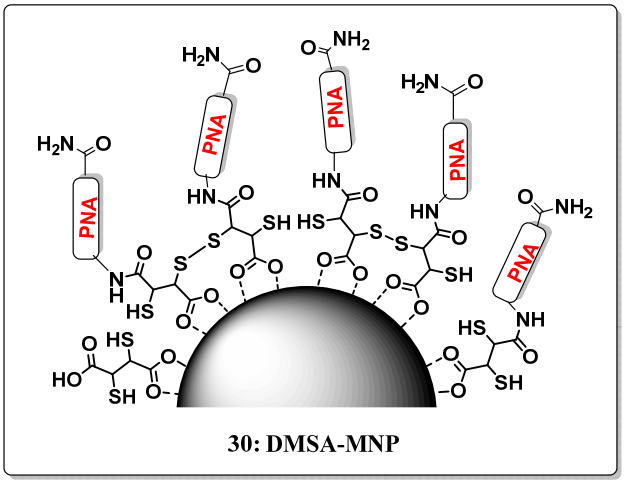

The MNP@DMSA carboxyl groups were first activated by adding 12.4 mg EDC (0.065 mmol) and 46 mg NHS (0.4 mmol) to 5 mL of MNP8@DMSA water suspension (0.8 mg/mL Fe_3O_4). The addition of EDC apparently destabilized a lot the nanoparticle colloid, resulting in a visible aggregation. The suspension pH was then changed to 4.5 by careful addition of HCl 0.1 or 1 M and the activation reaction continued for 2 hr in an ultrasonic bath. Then the activated MNP were added dropwise to a solution of 5 mg PNA **18** dissolved in 0.5 mL of CH_3CN and 1 mL of phosphate buffer (pH 8, 5 mM). The suspension pH was adjusted to 8 by careful addition of NaOH solution. The reaction mixture was first placed in an ultrasonic bath and left under ultrasonic irradiation for 2 hr at room temperature and then left on a shaking plate overnight. The nanoparticles were then purified via centrifugation with water (3 x, 15 min, 7550 rcf) and subsequently collected in a Schlenk flask under inert atmosphere.

Elemental analysis: **MNP Fe_3O_4@DMSA** = C 3.36%; H 0.7%

Elemental analysis: **MNP Fe_3O_4@DMSA** = C 8.03%; H 1.73%; N 2.16%

Elemental analysis: **PNA 18 =** C 47.57%; H 5.03%; N 29.79%

Chapter 4: Design and synthesis of modified thymine monomer PNA and homothymine decamer PNA sequence with gold (I) complexes for cellular imaging.

Section 1:Synthesis of modified thymine PNA monomer and PNA decamer

4.1.1. General Introduction: Gold Chemistry

Gold is highly regarded and holds a very special position among the metals in the periodic table (Figure 4.1) for at least three millennia; it has been known as the most noble metal, referring to its resistance towards most corrosive forces. It has also been dubbed "King of the Metal" due to its monetary value. Gold is robust; it is mechanically ductile and soft, and has a attractive colour and glittering appearance. It is held to be an ideal construction material for objects of culture and art, for jewellery and for coin currency. In more recent periods, its high electrical and thermal conductivity has made gold metal also an important material: first for the electrical and then for the electronics industry.[1] Gold is not simply a homologue of the other two coinage metals in the periodic table, copper and silver, but showed entirely different oxidation states and oxidation potentials, coordination numbers and coordination geometries.[2]

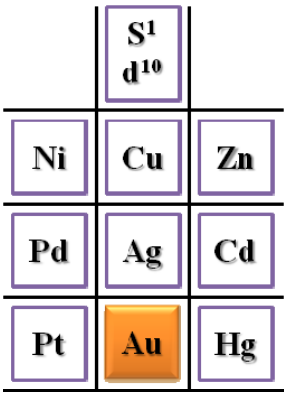

Figure 4.1: Position of gold metal in the periodic table of the elements.

Historically, gold was desirable metal because of its resistance to oxidation and excellent conductivity. Within the last 30 years however, chemists have had to readjust their perspective as a myriad of gold chemistry has emerged.[3-6] As an organometallic metal centre, gold typically prefers the +1 or +3 oxidation state with the former being the more common. The overwhelming majority of neutral gold(I) complexes are two coordinate, linear species. This preference for linear geometry has been attributed to a small energy gap between s, p and d states which results in proficient s/d or s/p hybridizations.[3] The linear gold(I) complexes are $14e^-$ and thus electron deficient. Consequently, when sterics permit, these complexes have been observed to act as soft Lewis acids and can coordinate a third and fourth ligand.[3, 7] Gold(I) complexes generally form, two coordinate species with a linear

geometry of two donor atoms or ligands. The ligands can be neutral (L) or anionic (X^-), thus forming species of these general types; [L-Au-X], [L-Au-L] $^+$ or [X-Au-X]$^-$.[8]

The development of gold(I)-acetylide complexes has led to several novel compounds.[9-14] Most notably they have been investigated for their interesting photochemical properties. Luminescence from gold-acetylide complexes typically results from "aurophilicity" or the presence of weak molecular interactions between two gold centers.[9, 12, 14]

The rich gold acetylide chemistry has grown to include σ [15a, 16-18] and π[19, 20] bound complexes. LAu–C≡C–R complexes (where L is a $2e^-$ donor, typically a tertiary phosphine) have classically been prepared by reaction of [Au-Cl-L] with a terminal alkyne in the presence of a strong base (Figure 4.2-A) [17,22,23] while η^2- C_2R_2 complexes have typically been accessible from complexes of [Au-X-L] where L is a volatile ligand such as SMe_2 (DMS)[21]or tetrahydrothiophene (THT) as shown in (Figure 4.2-B).[19]

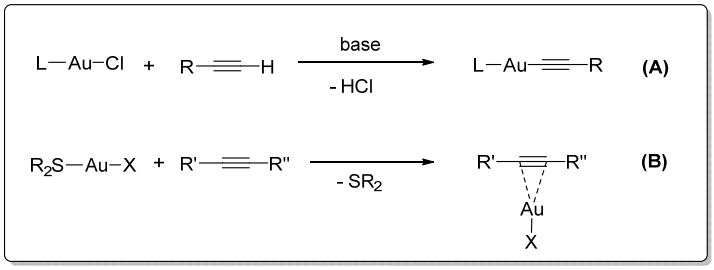

Figure 4.2: Gold(I)-acetylide complexes

4.1.2. Synthesis of gold(I)-acetylide complexes: A literature survey

There are numerous literature reported so far with different reaction conditions for the conjugation of gold(I) with acetylide or a triple bond.[24] In 2000 Dyson *et al.*[25] has been reported the mononuclear phosphane Au(I) acetylides **1-6** were treated with the [AuCl(PR'$_3$)] complex (PR_3' corresponding to the water-soluble phosphanes PTA and DAPTA) with terminal acetylenes in the presence of a base (KOH in methanol) (Scheme 4.1).

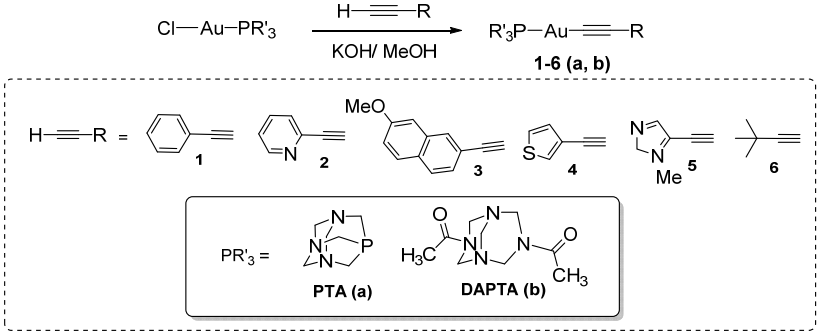

Scheme 4.1: Synthesis of Mononuclear Alkynyl gold(I) derivatives

In 2007 Laguna *et al*[26] and co-workers also reported a different variety of gold(I) complexes containing the water-soluble phosphine ligands TPPMS, TPPDS and TPPTS (mono-, di- and tri-sulfonated triphenyl phosphine) were prepared by under basic condition by using NaOH with different gold(I) alkynyl complexes [AuC≡CR(TPPTS)] (Scheme 4.2)

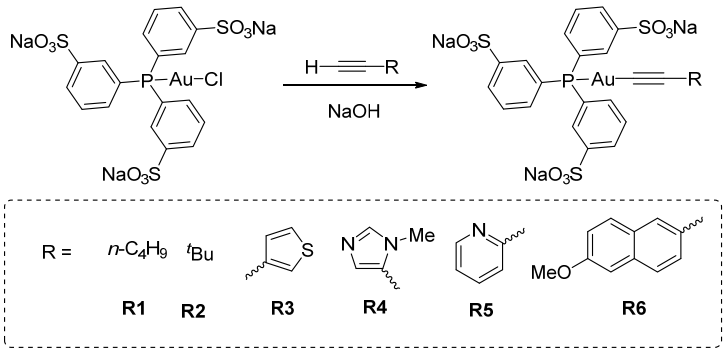

Scheme 4.2: Synthesis of Alkynyl gold(I) derivatives

N-Heterocyclic carbene (NHC) gold acetylide complexes have also been reported. The first synthesis of these complexes by Singh *et al*. involved the use of ethyl magnesium chloride to obtain the desired product (Scheme 4.3) path I.[27] This method was however, only used to make the terminal acetylide species. A more general approach was reported by Fujimura *et al*. who disclosed a synthetic scheme involving phosphine substitution by a stronger s-donating NHC ligand (Scheme 4.3- (3)). More recently Gray has reported the reaction of [AuCl(NHC)] with sodium tert-butoxide and alkynes to form the desired gold acetylides complexes.[28]

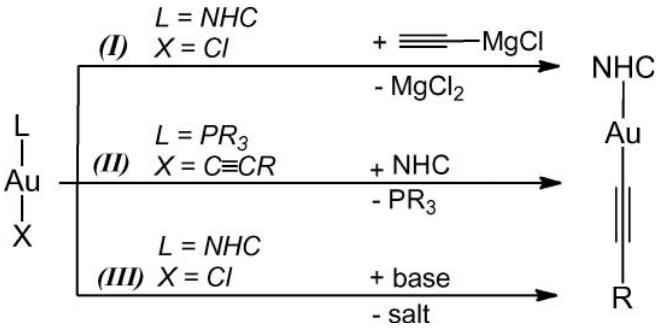

Scheme 4.3: General methods for the preparation of (NHC)AuC≡CR.

In 2006 Barnard *et al* [29] reported the synthesis and structures of a family of fascinating dinuclear Au(I)–carbene complexes **7** and **8**. These complexes have demonstrated significant

antimitochondrial activity and interestingly the cyclophane ligand framework allows fine control over the intramolecular distance between the gold atoms. Compound **7** supports a short Au···Au interaction of 3.0485(3) Å and is luminescent, whereas compound **8**, with a significantly longer Au···Au distance (3.7917(4) Å), is not (Figure 4.3)

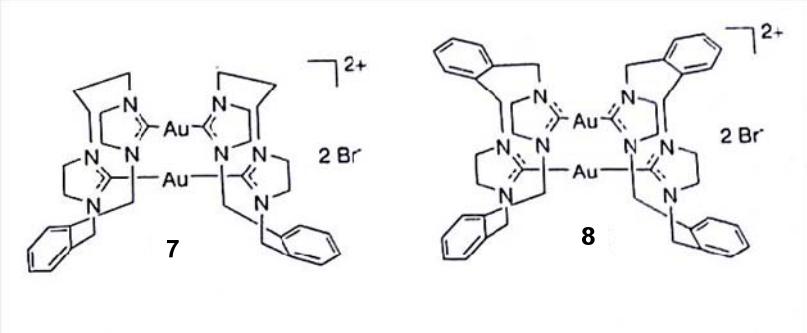

Figure 4.3: N-Heterocyclic carbene (NHC) gold acetylide complexes

Very recently in 2015 Hikisz *et al*[30] has reported gold(I) complexes of alkynyl chromones **9**, **10** and flavone **11** were synthesized and characterized in presence of DIPEA and triphenyl phosphine gold chloride (Scheme 4.4)

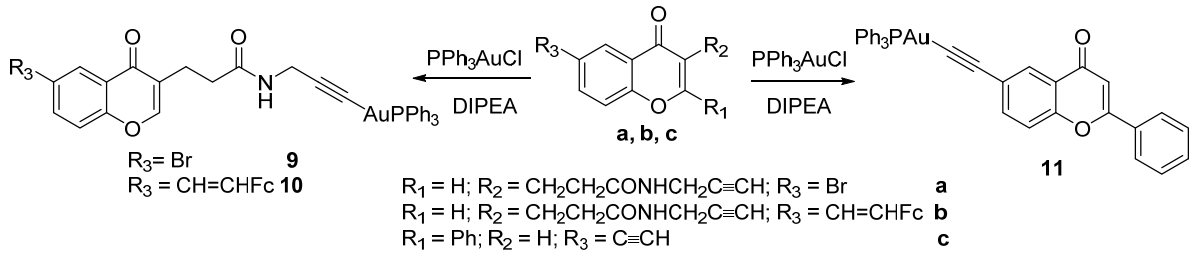

Scheme 4.4: Synthesis of gold(I)-complexes of alkynyl chromones and flavones.

All these complexes were evaluated as anticancer and antibacterial agents against four human cancer cell lines and four pathogenic bacterial strains.

Moreover in 2012 and 2014 Chao *et al*[31] reported synthesis of mononuclear gold(I) acetylide complexes with urea and with amide group by using KF as base in presence of PPh_3AuCl as a gold precursor (Scheme 4.5). Gold(I) acetylide complex with an amide group has been reported as an anion sensor.

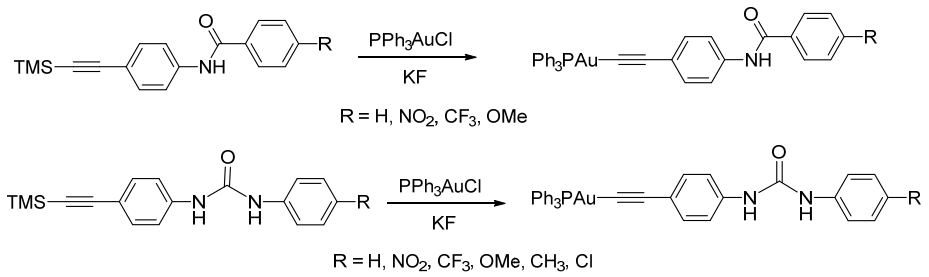

Scheme 4.5: Synthesis of mononuclear gold(I) acetylide complexes

4.1.3. Applications of gold(I) alkynyl systems

Gold(I) alkynyl complexes present a growing research field with respect to their very wide range of applications in different areas such as luminescence, molecular recognition, optical switches, electronics and catalysis. Biological applications are also being developed in the recent years, where these complexes are used as therapeutic agents against different illnesses such as cancer cells or malaria. Last from 15 years, there has been a growing interest in metal alkynyl complexes and their potential applications in molecular electronics and materials science.[32,33] In particular, gold(I) derivatives are especially interesting due to their rich luminescence properties. The preference of gold(I) for a linear coordination geometry, together with the linearity of the acetylide unit and its π-unsaturated nature have made the alkynylgold(I) complexes attractive building blocks for organometallic oligomeric and polymeric materials which may possess unique properties such as optical non-linearity, electrical conductivity, and liquid crystallinity.[34]

Alkynyl gold(I) derivatives with phosphine ligands have been investigated for their interesting photochemical properties or rich luminescence properties due to intermolecular interaction between Au atoms (aurophilic interaction).

Luminescence property:

Luminescence is one of the most studied and denoted properties and applications of gold(I) alkynyl complexes. The luminescence of gold(I) acetylide was first reported by Che in 1993[35] and has been extensively studied by his group and also by Yam's group.[36] More recently, these properties have found interest in the use of the systems in a wide range of different applications. In general, two different emission bands are observed between 400 and 600 nm whose large Stokes shifts with respect to absorption bands (250–350 nm) are used to assign a triplet parentage for the emissions. The heavy-atom effect induced by the introduction of the

$AuPR_3$ moiety into the organic alkynyl backbone, improves the possibility to observe triplet emission at ambient temperature.

Catalytic applications:

At the beginning of the last century, organic chemists began to use transition-metal catalysts to form carbon-carbon and carbon-heteroatom bonds. Although gold was considered to be an inert metal for a long time, its ability to behave as a soft Lewis acid has been recognized recently.[37]

Therapeutic applications:

Throughout prehistory and ancient history, most major civilizations attributed medicinal character to gold.[38] In fact, gold complexes have been extensively studied due to the clinically established antiarthritic properties of Au(I) thiolates, such as sodium aurothiomalate (Myocrisin), aurothioglucose (Solganal) and [(1-thio-β-D-glucopyranose-2,3,4,6-tetraacetato-*S*)(triethylphosphane) gold] (Auranofin). Although rheumatoid arthritis is the most well known disease treated with gold derivatives, asthma, pemphigus (an autoimmune disease of the skin) and HIV have also been investigated in this field and more recently, successful results are being obtained against malaria and cancer.[39]

4.1.4. Objective

The development of gold(I) acetylide complexes has led to several novel compounds.[13, 40] most notably they have been investigated for their interesting photochemical properties or rich luminescence properties. Luminescence from gold-acetylide complexes typically results from "aurophilicity".

Taking all these advantages, in the present work we have planned to design and synthesize a gold(I) complex (Figure 4.4), which was never reported in the literature, to carry out studies in the field of conjugation of PNA with luminescent probes for cellular imaging. This target molecule can be considered a potential "dual-action" compound, composed of two specific parts having a different role, i.e. the PNA and the luminescent linear complex of gold.

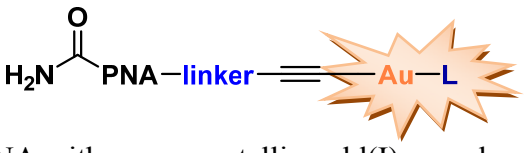

Figure 4.4: Conjugates of PNA with organometallic gold(I) complex

In particular, the complex of gold (I) conjugate acts as potentially luminescent probe but has also features as pharmacological agent and anticancer. So for this, we planned to introduce phosphine gold(I) chloride **12** onto PNA decamer **13** containing the triple bond at the terminal position (Figure 4.5)

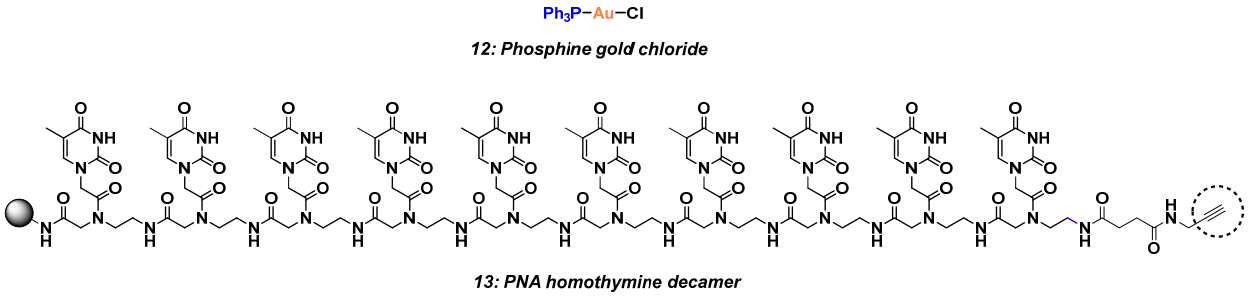

Figure 4.5: Phosphine gold(I) chloride **12** and PNA decamer **13**

4.1.5. Results and discussion

We decided to start our synthesis from single thymine PNA monomer in solution.

4.1.5.1. Synthesis of thymine monomer PNA gold(I)-acetylene

The synthesis started from the thymine monomer precursor **14** (for preparation refer chapter 2, section 1). This thymine monomer **14** was subjected to TFA in dichloromethane for the deprotection of Boc group to afford **15,** which was used for the next reaction without purification. The crude compound **15** was then treated with DIPEA followed by the addition of succinic anhydride in DMF to afford acid **16** which was purified by methanol. Its ^{1}H-NMR spectrum showed peaks as multiplets at δ 2.27 to 2.43 for four protons and one singlet at δ 12.05 for one proton and peaks at δ 171.66 and 173.84 in its ^{13}C-NMR spectrum corresponded to amide and acid carbonyl group. Further peak at *m/z* 398 $[M+1]^{+}$ in its mass spectrum confirmed the formation of acid **16**. The acid **16** was reacted with DIPEA and propargyl amine in the presence of EDC.HCl as a coupling agent in DMF to furnish compound **17** in 77% yield after chromatographic purification. Its ^{1}H-NMR spectrum showed peak as singlet at δ 3.08 for one proton corresponding to terminal alkyne and peaks at δ 3.81 to 3.84 for two protons and peaks at δ 73.00 and 81.38 in its ^{13}C-NMR spectrum corresponding to alkyne. Further peak at *m/z* 435 $[M+1]^{+}$ in its mass spectrum confirmed the formation of **17** compound. The compound **17** was then reacted with different bases in presence of phosphine gold chloride **12** for the formation of compound **18** (Scheme 4.6)

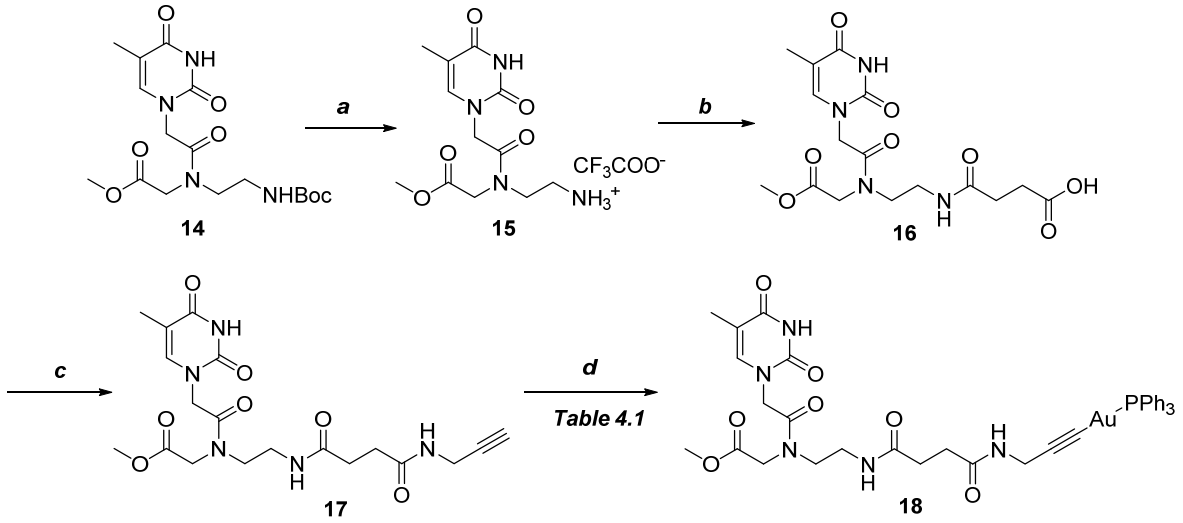

Scheme 4.6: Reagents and conditions: *a) 20% TFA, DCM, 0 ^oC - rt, 12 hr, 96%; b) succinic anhydride, DIPEA, DMF, 0 ^oC - rt, 12 hr, 70%; c) propargyl amine, EDC.HCl, DMF, rt., 12 hr, 82% ; d) Phosphine gold chloride* ***(12)****, base, rt. (Table 4.1)*

In order to introduce the phosphine gold moiety under basic conditions on to the acetylene compound **17**, several different conditions were screened, as shown in Table 4.1. In almost all conditions reported in Table 4.1, entry 1-3, we do not get the desired product **18**, instead we recovered the starting compound **17**. It was observed that treatment of compound **17** with 5 eq. of sodium acetate at ambient temperature, gave the gold complex in only 10% (Table 4.1, entry 4).

Whereas, **17** on treatment with strong base (KO^tBu) at room temperature led to the formation of gold complex **18** in 24% yield (Table 4.1, entry 5). ^1H NMR spectrum showed absence of signal that appeared at δ 3.06 (t, 1 H), as a triplet integrating for one protons (acetylene proton) and the downfield shifting of the multiplet at δ 7.45-7.55 for the fifteen protons indicating the presence of a phosphine group (-PPh_3). ^{13}C NMR spectra of compound **18** displayed downfield signals at δ 128.39 to 134.30 indicating the presence of a phosphine group (-PPh_3). Further peak at *m/z* 893 $[M+Na]^+$; in its mass spectrum confirmed the formation of **18** compound.

Table 4.1: bases and solvents for the formation of Compound **18**

Entry	Base	Solvent	Result (18) %	Analysis
1	NaOMe (1.5 eq.)	MeOH	-	starting recovered
2	NEt_3 (1.5 eq.)	DCM/MeOH	-	starting recovered
3	NaOAc (1.5 eq.)	DCM/MeOH	-	starting recovered
4	NaOAc (5 eq.)	DCM/MeOH	10%	-
5	**KOtBu (4 eq.)**	**MeOH**	**24%** *(after purification)*	**^{1}H/^{13}C-NMR, ESI**

We also designed and synthesized **18** by another alternative strategy (Scheme 4.7)

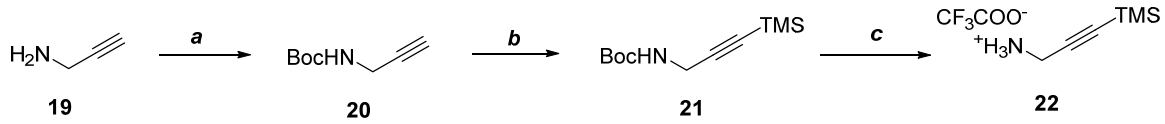

Scheme 4.7: Reagents and conditions: *a) $(Boc)_2O$, $THF:H_2O$, 0 °C – rt, 2 hr, 34%; b) n-BuLi, TMSCl, THF, -78 °C, 2 hr, 58%; c) 20% TFA, DCM, rt, 1 hr, quant.*

For the synthesis of thymine PNA monomer gold complex **18**, we started our synthesis from commercially available propargyl amine **19** which was protected with Boc anhydride to afford compound **20** in 34%. The alkyne functionality of compound **20** was protected with TMS by using trimethyl silyl chloride in presence of *n*-BuLi to afford **21** in 57% yield. Compound **22** was subjected to N-Boc deprotection by TFA in dichloromethane at room temperature to get product **22** in quantitative yield. This compound **22** were used as coupling partner for the next reaction. (Scheme 4.8)

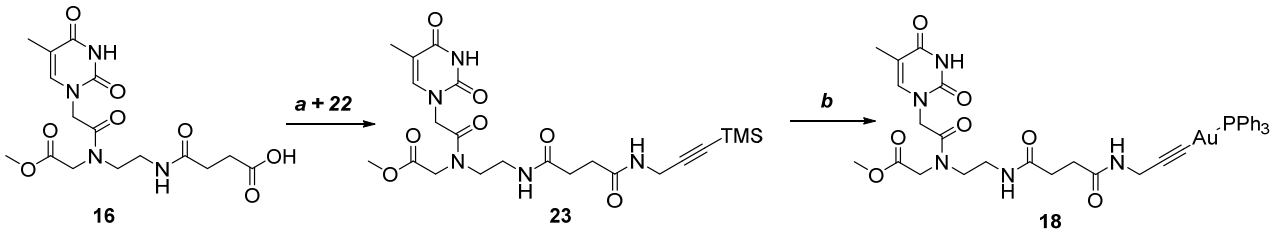

Scheme 4.8: Reagents and conditions: *a) **22**, EDC.HCl, HOBt, DIPEA, DMF, rt, 12 hr, 48%; b) PPh_3AuCl **12**, KF, DCM/MeOH, rt, 12 hr, 54%.*

The thymine monomer of acid **16** were coupled with amine salt **22**, in presence of DIPEA, EDC.HCl and HOBt as coupling reagent in DMF as solvent to afford **23** in 48% yield. Its ^{1}H-NMR spectrum showed peak as singlet at δ 0.15 for nine proton corresponds to trimethylsilyl

group and peak at δ -0.37 in its ^{13}C-NMR spectrum corresponds to the TMS group, while peaks at δ 88.01 and 101.22 corresponded to alkyne. Further peak at *m/z* 507 $[M+1]^+$ in its mass spectrum confirmed the formation of **23** compound.

The structure of compound **23** was fully assigned by using 2D NMR experiments like COSY and HSQC. Partial COSY indicating correlation between the protons only; which was suggested confirmation of compound **23.** (Figure 4.6)

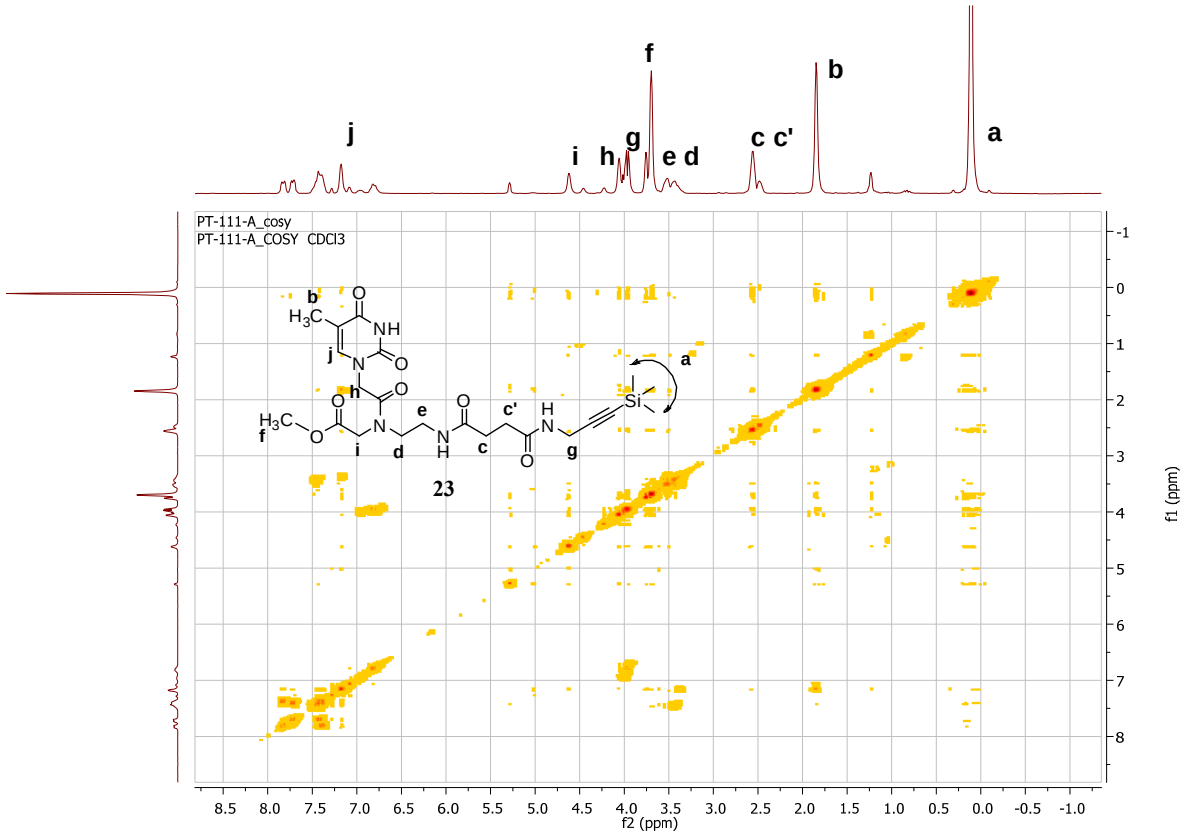

Figure 4.6: COSY-NMR spectrum of compound **23** in $CDCl_3$.

While in the HSQC spectrum, indicating correlation between the protons and carbons; Its ^{1}H-NMR spectrum showed peak as singlet at δ 0.15 for nine proton corresponds to trimethylsilyl group and peak at δ -0.37 in its ^{13}C-NMR spectrum corresponds to the TMS group; and ^{1}H-NMR spectrum showed peak as multiplets at δ 3.98-4.05 for four protons which corresponds to $-CH_2$ *(g)* protons and which correlates with its ^{13}C carbon at δ 30.09.

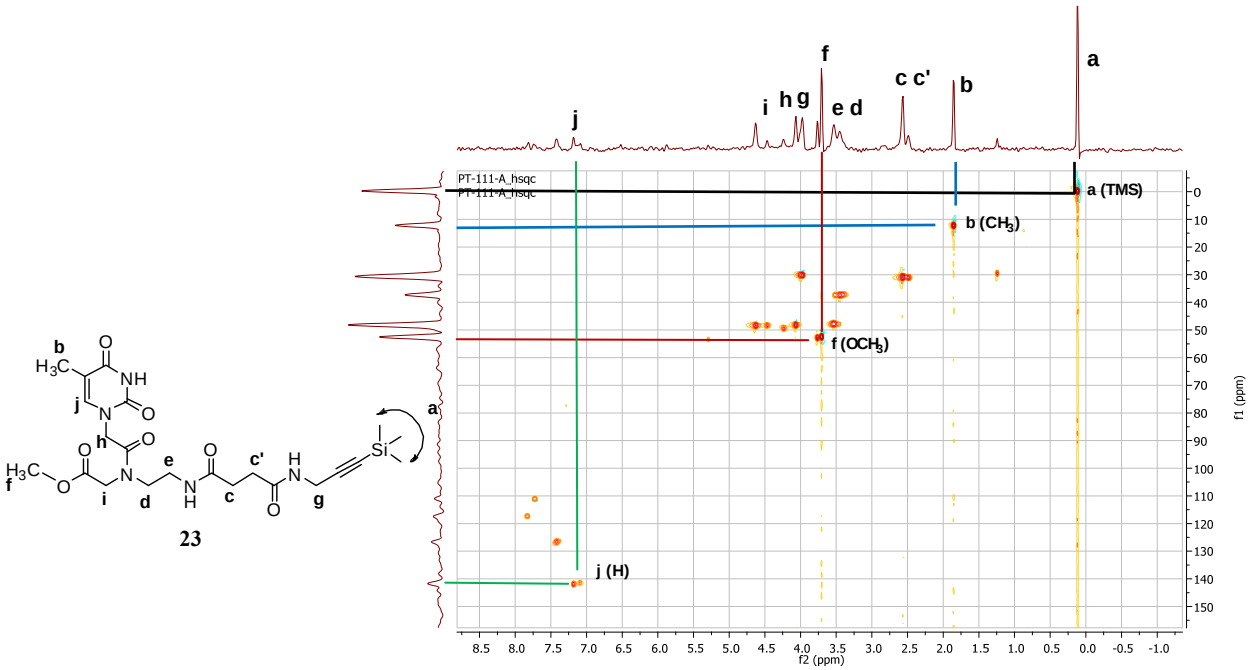

Figure 4.7: HSQC-NMR spectrum of compound **23** in $CDCl_3$

The 2D-NMR experimental study strongly supported the structure of compound **23**.

The compound **23** was subjected with KF and phosphine gold chloride **12** in methanol at room temperature to furnish gold(I) acetylene thymine PNA monomer **18** in 54% yield. (Scheme 4.8) ^{1}H NMR spectrum showed absence of signal that appeared at δ 0.15 for nine proton corresponds to trimethylsilyl group and the downfield shifting of the multiplet at δ 7.45-7.55 for fifteen protons indicating the presence of a phosphine group (-PPh_3). ^{13}C NMR spectra of compound **18** displayed downfield signals at δ 128.39 to 134.30 indicating the presence of a phosphine group (-PPh_3). Further peak at *m/z* 893 $[M+Na]^+$; in its mass spectrum confirmed the formation of **18** compound.

We also tried another alternative strategy for the synthesis of gold(I) acetylene thymine PNA monomer **18**. As we have compound **21** in our hand, which was subjected with KF and phosphine gold chloride **12** in methanol at room temperature to furnish gold(I) acetylene compound **24** in 73% yield (Scheme 4.9).

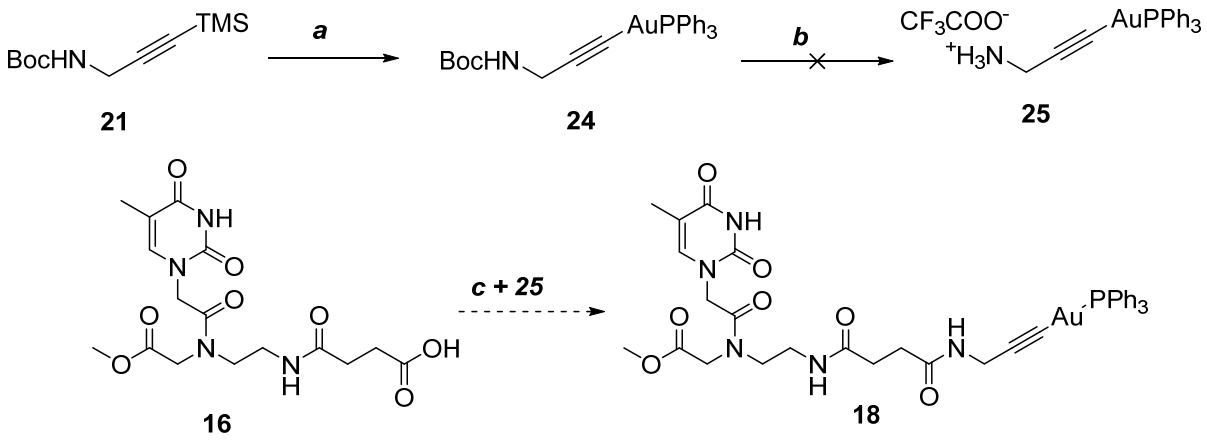

Scheme 4.9: Reagents and conditions: *a) PPh_3AuCl* ***12****, KF, DCM/MeOH, rt, 12 hr, 73%; b) 20% TFA, DCM, rt, 1 hr, quant.; c)* ***25****, EDC.HCl, HOBt, DIPEA, DMF, rt.*

The Boc group of compound **24** was removed by TFA in dichloromethane at room temperature but failed to obtain compound **25.**

The compound **18** shows some good and interesting photoluminescence emission properties on its solid state than in solution state.

4.1.5.2. Optical characterization and photoluminescence emission of compound 18

The gold complex **18** appears as a white microcrystalline solid, soluble in most organic solvents, like DCM, THF and DMSO and less soluble in water or buffer solutions. The spectroscopic and photo physical data of the Au(I)-acetylide complex are reported in figures 4.6 to 4.8 and Table 4.2

Figure 4.6 reports the quantitative absorption spectrum of **18** measured in a dichloromethane solution at 10^{-5} M concentration. Up to 300 nm the spectra accounts for optical transitions characterized by extinction coefficient over 10^4 $M^{-1}cm^{-1}$,which are typical of almost pure π-π* excitations of the conjugated framework.

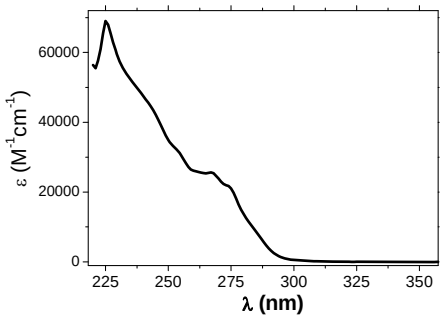

Figure 4.6: Absorption spectra of **18** in DCM solution (10^{-5} M).

Sample **18** is not emissive in diluted solution at room temperature or at low temperature in 77 K rigid matrix of 2MeTHF or MeOH/EtOH 1:1 v/v mixture.

On the contrary, according to literature[41] in aggregate form as a neat microcrystalline solid, sample **18** displays at room temperature, a clear orange-red emission as shown in Figure 4.7. The solid sample was excited both at 250 nm and 300 nm and in both cases it displays an emission with maximum at 655 nm (Figure 4.7) and FWHM (full width half maxima) of 5200 cm^{-1}. The excitation spectra of the sample, green line in figure 4.7 (inserted figure), shows a sharp peak at 310 nm and absorption onset at 370 nm. Compared to the solution room temperature analysis this new low energy band could be ascribed to the absorption of the aggregated form of sample **18** and tentative attributed to a transition deriving from Au(I)-Au(I) interactions. The sample, in the solid state is characterized by a quite high emission quantum efficiency (QY). A luminescence QY of 5% is measured by means of absolute methods and the emission is characterized by a microsecond, bi-exponential, decay rate with a short lifetime component of 1.9 µs (33% relative contribution) and a longer one of 14.0 µs (67% relative contribution). The microsecond lifetime regime is typical of heavy metal perturbed phosphorescence emissions.

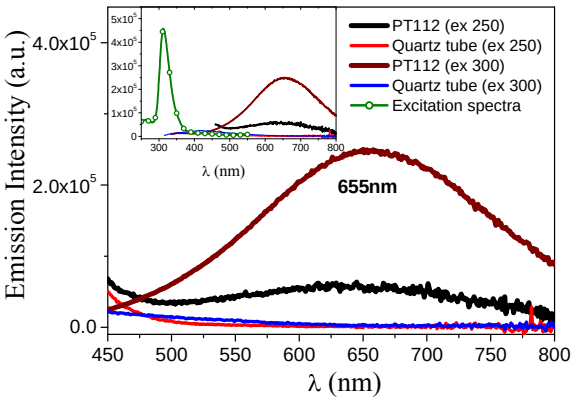

Figure 4.7: Emission spectrum of **18** solid sample at two different excitations, black line at 250 nm and deep red one at 300 nm. For comparison the baselines observed for the quartz sample holder, excited at the same wavelength (red and blue lines), are reported. Inset reposts the excitation spectra of the solid sample.

Moreover by considering (i) the structure of sample **18** (and the absence of significant chromogenic moieties other than the phenyl groups of PPh_3 and the Au(I)-acetylide)[42], (ii) the lack of emission in fluid solution (indeed consequence of the previous consideration), (iii) the broad, featureless emission and its large Stocks shift from the excitation maximum; (iv) the relatively long radiative lifetime; we can confidently attribute the emission reported in figure 4.7 to a phosphorescent process involving metal-metal Au(I)-Au(I) interactions in the solid state. It means that upon aggregation staking can take place between molecules providing new Metal-Metal "d" states which are responsible for the 655 nm emission.

The fact that in the solid state of the sample **18** Au complex emits with good quantum efficiency is, by itself, interesting because it means that the complex can be used as a luminescent "off-on" probe. In fact the complex evolve from a non emissive species (isolated molecules) to a red emissive one (aggregate) upon careful induced aggregation from its homogeneous solution. Similarly to previous literature studies[43], we investigate the aggregation induced emission of sample **18** in a mixed solvent system. Due to the poor solubility in water we engineered the experiment and studied the aggregation phenomena in a DMSO (good solvent for sample **18**) / water solvent system. DMSO represents also a good solvent choice since it has good biocompatibility with cells and is suitable for with in vitro experiments.[44]

We prepared a mother solution of sample **18** in DMSO (C_M=1.12 mM). 0.1 mL of the mother solution was diluted during the experiment to a final volume of 2 mL; hence the concentrations of 56 μM (similar to literature reported value43) were studied. Figure 4.8 reports the aggregation induced luminescence enhancement of sample 18 at different DMSO/H_2O ratio (range 40/60 up to 5/95).

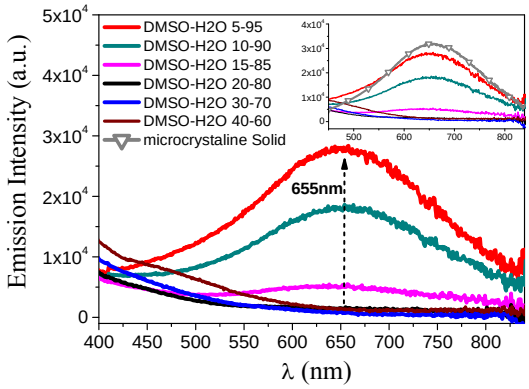

Figure 4.8: Emission spectra of sample **18** (56 μM) in DMSO/H_2O mixture between 400 nm and 840 nm (with excitation at 300 nm).

The Au(I)-acetylide complex is as expected, non emissive in pure DMSO solution and analogously no emission is detected up to a water content of 80%. In figure 4.8 is clearly evident the raise of a broad band peaking around 655 nm at the 15/85 DMSO/H_2O mixture; this signal becomes more intense increasing the water content (see 5/95). In the inset of Figure 4.8 is reported, together with the titration curves, the emission spectra of the Au(I) complex as neat solid which nicely match the emission detected in solution.

The lifetime of the emission signal in the 5/95 DMSO/H_2O mixture shows a bi-exponential character with a short decay component of 2.0 μs (38%) and a longer one of 15.4 μs (62%). It is interesting to note that these photo physical data perfectly match with those measured for the pure solid sample **18**; therefore indicating that the signal recorded in solution belongs to a gold self-aggregate analogue to the solid aggregate previously described in figure 4.7

In table 4.2 are reported the photophysical data measured for sample **18** microcrystalline solid sample and those measured in the DMSO/H_2O solvent mixture. Both at 10/90 and 15/85 DMSO/H_2O solvent ratio the measured lifetimes are in good agreement with those of the parent solid aggregate indicating the same origin. To note that even though an emission signal is not clearly perceivable in figure 4.83 at the 20/80 ratio, nonetheless a decay lifetime of about 3.9 μs can be measured indicating probably the incipient formation of micro aggregates that later evolve to give the broad orange-red emission.

Table 4.2: Photophysical data measured for sample **18** microcrystalline solid sample and the DMSO/H_2O solvent mixtures.

Expt.	Quantum yield (φ)	T (%) [μS] (ex.300 nm to ex.600 nm)
Sample 18 [Au(I) complex]	0.05	1.9 (33); 14.0 (67)
DMSO/H_2O system	-	
5/95	-	2.0 (38); 15.6 (62)
10/90	-	1.62 (41); 13.50 (59)
15/85	-	0.47 (50); 7.26 (50)
20/80	-	3.9 (100)
30/70	-	-
40/60	-	-

So in conclusion, we used a physical media (solvent/non-solvent) to induce aggregation and we proved that this interaction cause the formation of a new emissive system. In principle any conditions that may allow for the same type of metal-metal interaction (formation of Au(I)-Au(I) system) may lead to the same red emission and therefore the molecule **18** can behave as a "off-on" probe or shows photoluminesecent property and can be applicable for cellular imaging.

We have successfully synthesized thymine monomer gold(I)-acetylene **18** with triphenyl phosphine ligand (PPh_3). So we planned to use trisulfonated triphenylphosphane (TPPTS) as a ligand and designed a new route for the synthesis of gold(I)-acetylene complex **31** (Scheme 4.10)

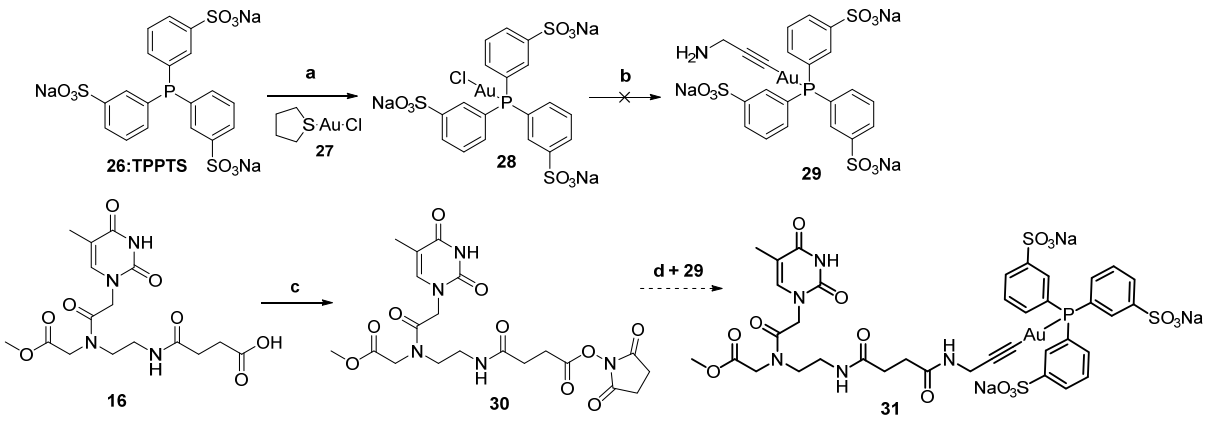

Scheme 4.10: Reagents and conditions: *a) **27**, AcCN, H_2O, rt, 2 hr, quant.; b) propargyl amine, rt, 12 hr; c) NHS, EDC.HCl, DIPEA, DMF, rt, 12 hr, 85%; d) **29**, DMF, rt.*

We started our synthesis from commercially available *m*-trisulfonated-triphenylphosphane (TPPTS) **26** with chloro(tetrahydrothiophene)gold(I) complex **27** (which is prepared in lab) under degassed solvent system AcCN:H2O to afford gold(I) complex **28** in quantitative yield. The compound **28** was subjected with propargyl amine and KOH under degassed MeOH:DMF solvent system at room temperature, but failed to obtained compound **29**. The thymine monomer of acid **16** was also reacted with NHS in presence of DIPEA and EDC.HCl as coupling reagent in DMF as solvent to afford **30** in 85% yield.

We tried the same reaction condition and did the reaction two times for the formation of compound **29**; which was reported in literature[43]; but we failed to obtained compound **29**.

We decided to change to our protocol for the formation of compound **31,** as we already synthesized the thymine monomer **18** by using TMS strategy, we applied the same conditions for the synthesis of compound **31** (Scheme 4.11)

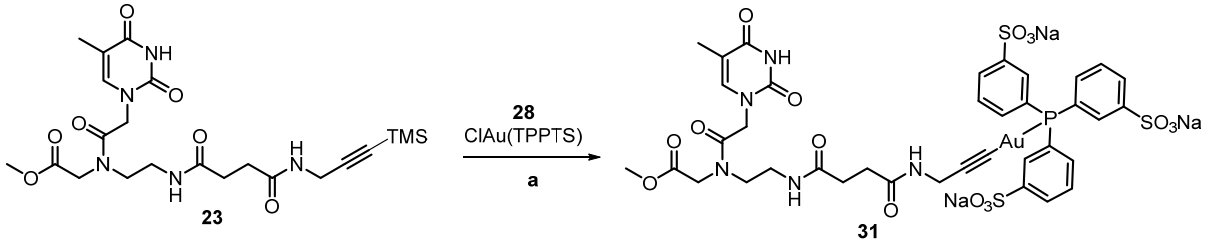

Scheme 4.11: Reagents and conditions: *a) **28**: ClAu(TPPTS), KF, DCM/MeOH, rt, 12 hr, quant.*

The compound **23** was subjected with KF and *m*-trisulfonated-triphenylphosphane gold chloride **28** in methanol at room temperature to furnish gold(I) acetylene thymine PNA monomer **31** in quantitative yield. ^{1}H NMR spectrum showed absence of signal that appeared at δ 0.15 for nine proton corresponds to trimethylsilyl group. Further peak at *m/z* 1199 $[M+K]^{+}$; in its mass spectrum confirmed the formation of **31** compound.

After successful synthesis of gold(I) complexes **18** and **31** with thymine monomer in solution phase; we planned to introduce the same strategy with homothymine PNA oligomer on solid phase.

4.1.5.3. Synthesis of gold complex with homothymine PNA decamer on solid support

The synthesis was performed with standard manual Boc-based chemistry using MBHA resin **32**, firstly loaded with Thymine monomer **33** by using HBTU as a coupling reagent in order to obtain functionalized resin **34** with loading 0.2 mmol/g (Scheme 4.12).

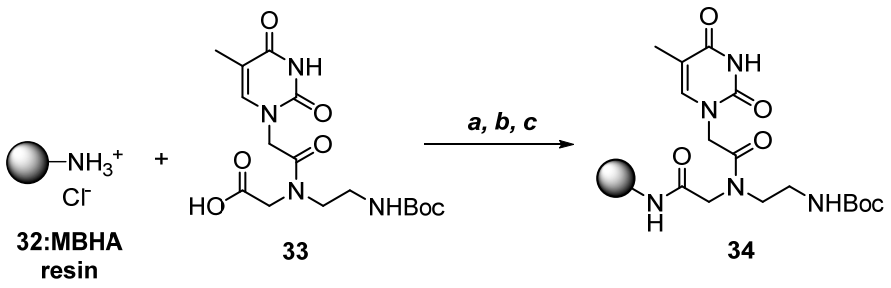

Scheme 4.12: Reagents and conditions: *a) CH_2Cl_2/DIPEA, 95:5, 2 × 2 min, rt; b) **33**, HBTU, DIPEA, NMP, 24 hr, rt; c) Ac_2O/Pyridine/NMP 1:25:25, 2 × 1 min, rt.*

Then the *tert*-butyloxycarbonyl (Boc) group of the loaded monomer **34** was removed by treatment with 5% *m*-cresol in TFA to get an amine TFA salt which was neutralized by 5% DIPEA in dichloromethane. Then the free amine on resin was coupled with next thymine monomer **33** with DIPEA and HATU in NMP as a solvent. After coupling step resin were washed with NMP, and then treated with a solution of Ac_2O/pyridine/NMP (1:25:25, v/v). The cycles were repeated eight more times by using the thymine monomer only with the same protocol to afford the corresponding supported homothymine PNA decamer on resin **35** (Scheme 4.13). Then the resin **35** (5 mg) were cleaved by washing with TFA, and subsequently stirred with a mixture of TFA/TFMSA/thioanisole/*m*-cresol (6:2:1:1 v/v) to get **35'** and characterized by analytical HPLC with retention time 11.84 min. and also confirmed by Q-Tof mass analysis *m/z* $C_{110}H_{144}N_{41}O_{40}^{+}$: 2680.00

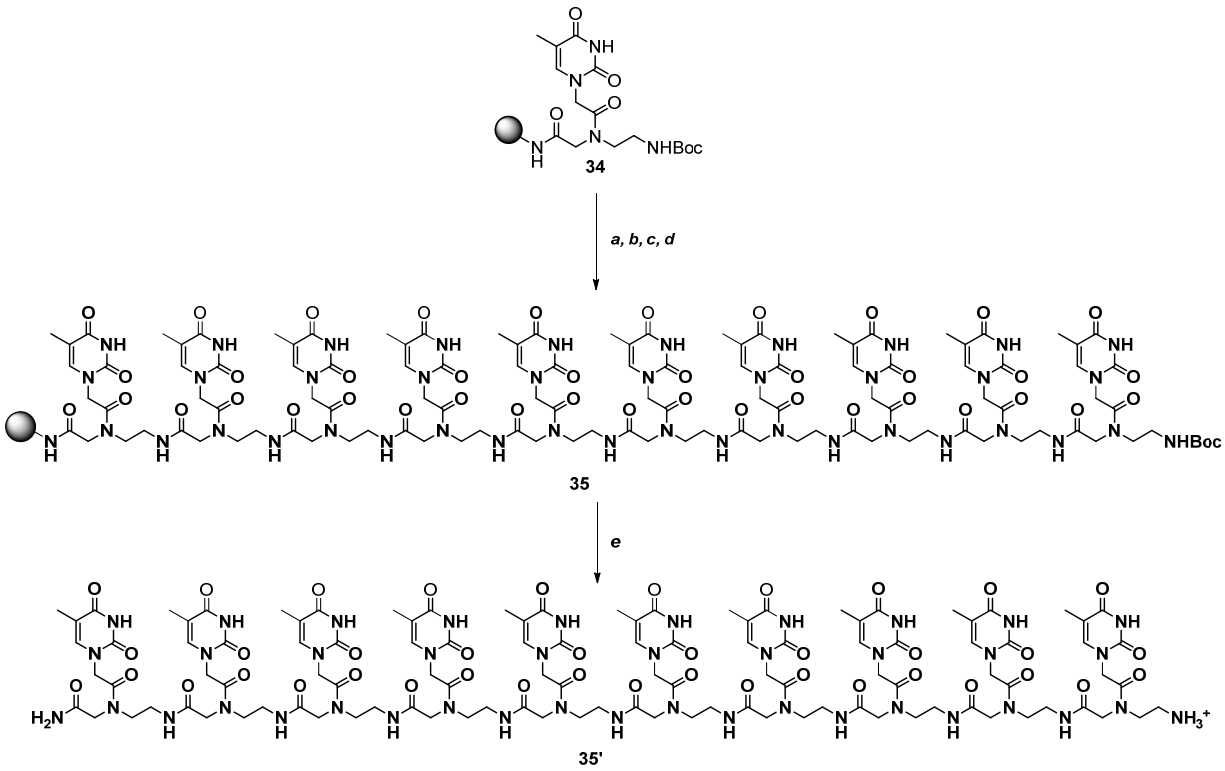

Scheme 4.13: Reagents and conditions: *a) TFA/m-cresol, 95:5, 2 × 4 min, rt; b) CH_2Cl_2/DIPEA, 95:5, 2 × 2 min, rt; c)* ***33****: thymine monomer, HATU, DIPEA, NMP, 2 hr, rt; d) Ac_2O/Pyridine/NMP 1:25:25, 2 × 1 min, rt.; e) TFA/TFMSA/thioanisole/m-cresol 6:2:1:1 (v/v), 1 hr, rt.*

4.1.5.4. Analytical HPLC and Q-Tof mass: Homothymine PNA decamer (35')

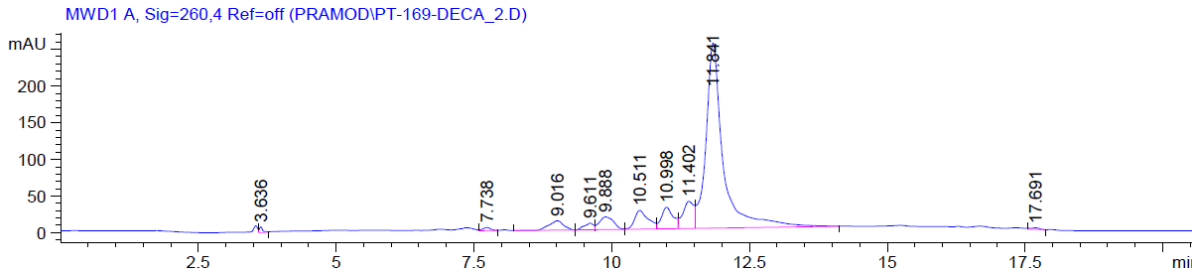

Figure 4.9: Analytical HPLC of homothymine PNA decamer **35',** retention time 11.84 min.

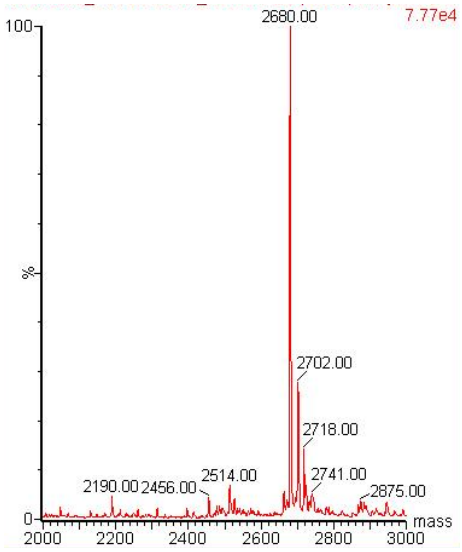

Figure 4.10: Q-Tof/Mass analysis of homothymine decamer **35'**, $C_{110}H_{144}N_{41}O_{40}^{+}$: 2680.00

After successfully synthesizing homothymine decamer **35**, Boc group were removed by treatment with 5% *m*-cresol in TFA to get an amine TFA salt which was neutralized by 5% DIPEA in dichloromethane. Then the free amine on resin was coupled with propargyl acid **36** with DIPEA and HATU in NMP as a solvent for 2 hr at room temperature. After coupling step, the resin was washed with NMP and DCM for several times to afford the corresponding resin **37** (Scheme 4.14).Then the resin was cleaved by washing with TFA, and subsequently stirred with a mixture of TFA/TFMSA/thioanisole/*m*-cresol (6:2:1:1 v/v). The reaction mixture was filtered, and the filtrate were concentrated to by the addition of diethyl ether to afford white coloured crude PNA decamer **38**, which was analyzed by mass and HPLC.

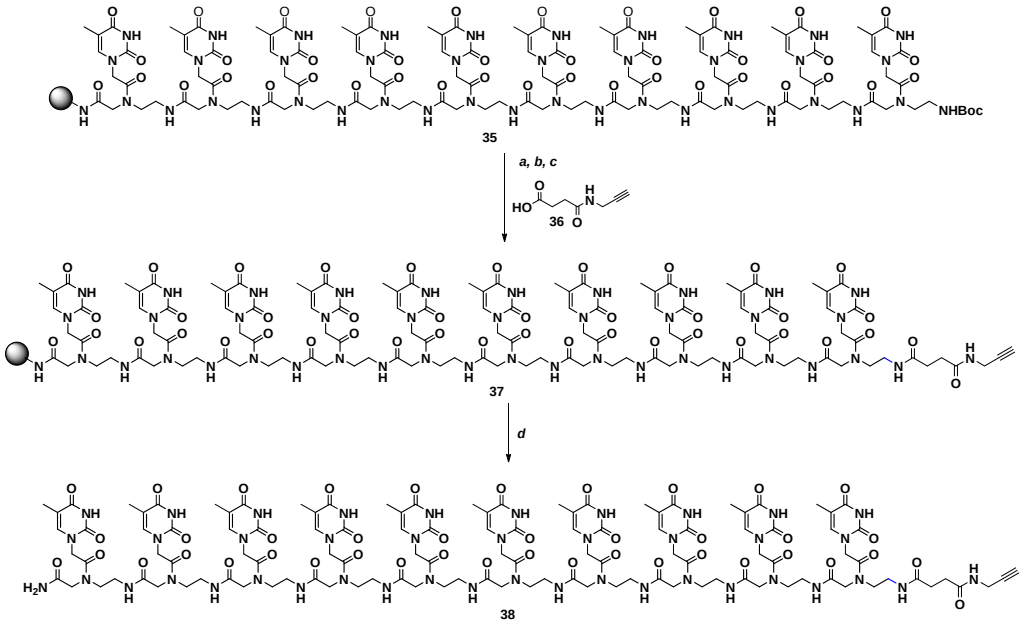

Scheme 4.14: Reagents and conditions: *a) TFA/m-cresol, 95:5, 2 × 4 min, rt; b) CH_2Cl_2/DIPEA, 95:5, 2 × 2 min, rt; c)* ***36****, HATU, DIPEA, NMP, 2 hr, rt; d) TFA/TFMSA/thioanisole/m-cresol 6:2:1:1 (v/v), 1 hr, rt.*

4.1.5.5. Analytical HPLC and Q-Tof mass: PNA decamer (38)

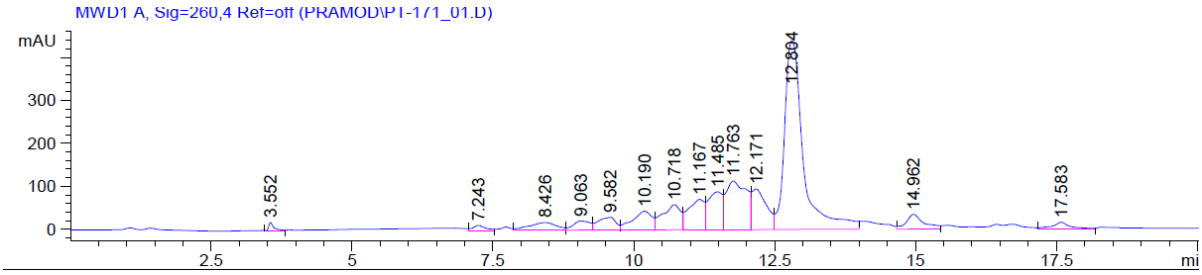

Figure 4.11: Analytical HPLC of PNA decamer **38,** retention time 12.80 min.

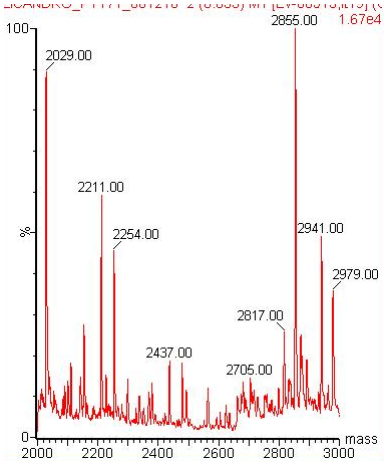

Figure 4.12: Q-Tof/Mass analysis of PNA decamer **38**, $C_{117}H_{150}N_{42}O_{42}$: 2855 $[M+K]^+$

The PNA decamer **38** was subjected to KO^{t}Bu and phosphine gold chloride **12** in methanol at room temperature; however, in these conditions the formation of gold(I) acetylene PNA decamer **39** was not observed, as revealed by the MALDI-Tof analysis (Scheme 4.15)

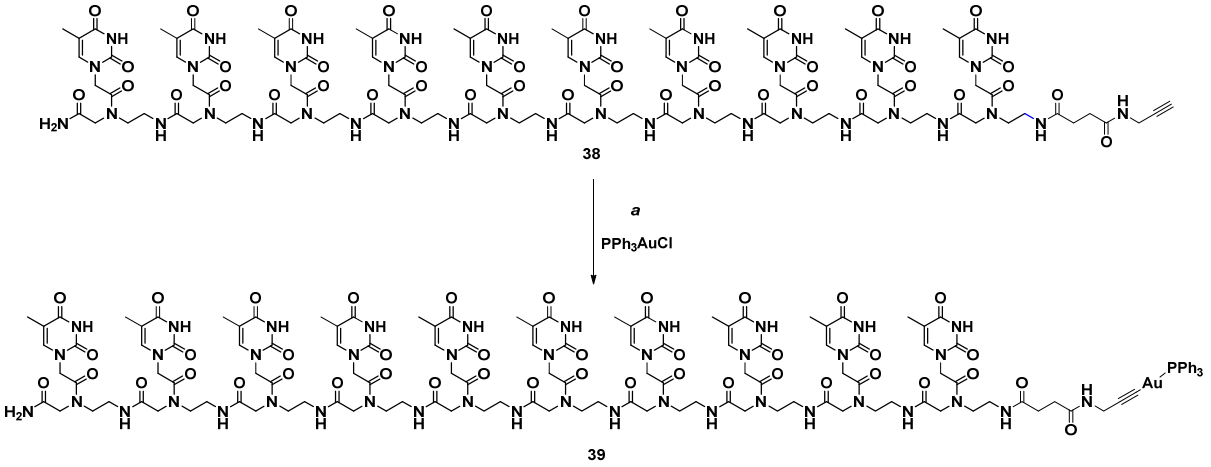

Scheme 4.15: Reagents and conditions: *a) PPh_3AuCl **12**, KO^{t}Bu, DCM/MeOH, rt, 12 hr*.

MALDI-TOF: *m/z*: $C_{135}H_{164}AuN_{42}O_{42}P$ calculated 3273.14; found 1657.39 and 2837.8

4.1.6. Bibliography

1. Schmidbaur, H. Gold, *Progress in Chem., Biochem. and Tech.,* Wiley, **1999.**

2. (a) Puddephatt, R. J. *The Chemistry of Gold, Elsevier,* **1978** (b) Rapson, W. S.; Groenewald, T. *Gold Usage, Academic Press:* **1978** (c) Schmidbaur, H. *Gold Bull*. **1990**, *23*, 11-21.

3. (a) Shapiro, N. D.; Toste, F. D.; *Synlett,* 675 (b) Belmont, P.; Parker, E; *Eur. J. Org. Chem.*, **2009**, 6075-6089 (c) Gimeno, M. C.; Laguna, A.; *Chem. Rev.,* **1997**, *97*, 511-522.

4. Shaw, C. F.; *Chem. Rev.,* **1999**, *99*, 2589-2600.

5. Hashmi, A. S. K.; Chem. Rev., **2007**, *107*, 3180-3211.

6. (a) Min, B. K.; Friend, C. M.; *Chem. Rev*., **2007**, *107*, 2709-2724 (b) Arcadi, A.; *Chem. Rev.,* **2008**, *108*, 3266-3325.

7. Patil, N. T.; Yamamoto, Y.; *Chem. Rev.,* **2008**, *108*, 3395-3442.

8. Hess, B. A. *Relativistic Effects in Heavy-Element Chemistry and Physics, Wiley:* **2003**.

9. Flugge, S.; Anoop, A.; Goddard, R.; Thiel W.; Furstner, A. *Chemistry (Weinheim an der Bergstrasse, Germany),* **2009**, *15*, 8558-8565.

10. Shapiro, N. D.; Toste, F. D.; *Proc. Natl. Acad. Sci. U. S. A.*, **2008**, *105*, 2779-2782.

11. Wong, W.Y.; *Comments Inorg. Chem.,* **2005**, *26*, 39-74.

12. Wong, W.Y.; Choi, S. W. K.; *J. Chem. Soc., Dalton Trans.*, **1996**, 4227-4232.

13. Payne, N. C.; Ramachandran, R.; Treurnicht, I.; Puddephatt, R. J. *Organometallics,* **1990**, *9*, 880-882.

14. Feilchenfeld, H; Weaver, M. J.; *J. Phys. Chem*., **1989**, *93*, 4276-4282.

15. (a) Hunks, W. J.; MacDonald, M. A.; Jennings, M. C.; Puddephatt, R. J. *Organometallics*, **2000**, *19*, 5063-5070 (b) Schmidbaur, H. *Gold Bull*., **1990**, *23*, 11-21.

16. Schuh, E.; Valiahdi, S. M.; Jakupec, M. A.; Keppler, B. K.; Chiba, P.; Mohr, F. J. *Chem. Soc., Dalton Trans.,* **2009**, 10841-10845.

17. Cross, R. J.; Davidson, M. F.; McLennan, A. J. *J. Organomet. Chem.,* **1984**, *265*, C37-C39.

18. Johnson, A.; Puddephatt, R. J. *J. Chem. Soc., Dalton Trans.,* **1977**, 1384-1388.

19. Schulte, P.; Behrens, U. *Chem. Commun.,* **1998**, 1633–1634.

20. (a) Wu, J.; Kroll, P.; Dias, H. V. R. *Inorg. Chem.,* **2009**, *48*, 423-425 (b) Liau, R. Y.; Schier, A.; Schmidbaur, H. *Organometallics*, **2003**, *22*, 3199–3204.

21. Lang, H.; Kohler, K.; Zsolnai, L. *Chem. Commun.,* **1996**, 2043–2044.

22. Chao, H. Y.; Lu, W.; Li, Y.; Chan, M. C. W.; Che, C. M.; Cheung, K. K.; Zhu, N. *J. Am. Chem. Soc.*, **2002**, *124*, 14696–14706.

23. Whittall, I. R.; Humphrey, M. G.; Houbrechts, S.; Persoons, A.; Hockless, D. C. R. *Organometallics*, **1996**, *15*, 5738–5745.

24. (a) Vicente, J.; Chicote, M. T.; Abrisqueta, M. D.; *Organometallics*, **1997**, *16*, 5628-5636 (b) Ronald, J; Davidson, M. F.; *Chem, Soc , Dalton Trans,* **1986**, 411-414.

25. Vergara, E.; Cerrada, E.; Casini, A.; Zava, O.; Laguna, M. Dyson, P. J. *Organometallics*, **2010**, *29*, 2596–2603.

26. Sanz, S.; Jones, L. A.; Mohr, F.; Laguna, M. *Organometallics*, **2007**, *26*, 952-957.

27. Singh, S.; Kumar, S. S.; Jancik, V.; Roesky, H. W.; Schmidt, H. G.; Noltemeyer, M. *Eur. J. Inorg. Chem.,* **2005**, 3057–3062.

28. Partyka, D. V.; Gao, L.; Teets, T. S.; Updegraff, J. B.; Deligonul, N.; Gray, T. G. *Organometallics*, **2009**, *28*, 6171–6182.

29. Barnard, P. J.; Wedlock, L. E.; Baker, M. V.; Berners Price, S .J.; Joyce, D. A.; Skelton, B. W.; Steer, J. H. *Angew. Chem. Int. Ed.* **2006,** *45*, 5966 –5970.

30. Hikisz, P.; Szczupak, L.; Chyla, A. K.; Guspiel, A.; Oehninger, L.; Ott, I.; Therrien, B.; Solecka, J.; Kowalski, K. *Molecules*, **2015**, *20*, 19699–19718.

31. (a) Zhou, Y. P.; Zhang, M.; Li, Y. H.; Guan, Q. R.; Wang, F.; Lin, Z. J.; Lam, C. K.; Feng, X. L.; Chao, H. Y. *Inorg. Chem*. **2012**, *51*, 5099−5109 (b) Shi, H. Y.; Qi, J.; Zhao, Z. Z.; Feng, W. J.; Li, Y. H.; Sun, L.; Lin, Z. J.; Chao, H. Y. *New J. Chem.,* **2014**, *38*, 6168-6175.

32. Yam, V. W. W.; *J. Organomet. Chem.,* **2004**, *689*, 1393.

33. (a) Long, N. J.; Williams, C. K. *Angew. Chem., Int. Ed*., **2003**, *42*, 2586 (b) Cadierno, V.; Gamasa, M. P.; Gimeno, *J. Organometallics*, **1998**, *17*, 697 (c) Roidl, G.; Enkelmann, V.; Adams, R. D.; Bunz, U. H. F. *J. Organomet. Chem.,* **1999,** *578*, 144.

34. (a) Whittall, I. R.; Humphrey, M. G.; Samoc, M.; Davies, B. L. *Angew. Chem., Int. Ed. Engl*., **1997**, *36*, 370 (b) Whittall, I. R.; McDonagh, A. M.; Humphrey, M. G.; Samoc, M. *Adv. Organomet. Chem.*, **1999**, *43*, 349 (c) Alejos, P.; Coco, S.; Espinet, P. *New J. Chem.*, **1995**, *19*, 799.

35. Li, D.; Hong, X.; Che, C. M.; Lo, W. C.; Peng, S. M. *J. Chem. Soc., Dalton Trans.,* **1993**, 2929.

36. Chao, H. Y.; Lu, W.; Li, Y.; Chan, M. C. W.; Che, C. M.; Cheung, K. K.; Zhu, N. *J. Am. Chem. Soc.*, **2002**, *124*, 14696.

37. Skouta, R.; Li, C. J. *Tetrahedron,* **2008**, *64*, 4917.

38. Shaw, C. F. *Chem. Rev.,* **1999**, *99*, 2589.

39. Schuh, E.; Valiahdi, S. M.; Jakupec, M. A.; Keppler, B. K.; Chiba, P.; Mohr, F. *Dalton Trans.,* **2009**, 10841.

40. Yam, V. W.W.; Choi, S.W.K. *J. Chem. Soc., Dalton Trans.,* **1996**, 4227-4232.

41. Sugimoto, N.; Tamai, S.; Fujisawa, K.; Tsutsumi, O. *Mol. Cryst. Liq. Cryst.,* **2014**, *601*, 97-106.

42. Li, D.; Hong, X.; Che, C. M.; Lo, W. C.; Peng, S. M. *J. Chem. Soc., Dalton Trans.,* **1993**, 2929-2932 (here it would not be expected luminescence from the free, isolated molecule itself since: PPh_3 will not act as suitable chromophore; the propargylamide unit, bound to Au(I), has not, as well, sufficient degree of conjugation to provide emission)

43. Kemper, B.; Hristova, Y. R.; Tacke, S.; Stegemann, L.; Bezouwen, L.; Stuart, M. C. A.; Klingauf, J.; Strassertbd, C. A.; Besenius, P. *Chem. Commun*., **2015**, *51*, 5253-5256.

44. Wang, H.; Zhong, C. Y.; Wu, J. F.; Huang, Y. B.; Liu, C. B. *Journal of Controlled Release*, **2010**, *143*, 64–70.

Chapter 4: Design and synthesis of modified thymine monomer PNA and homothymine decamer PNA sequence with gold(I) complexes for cellular imaging.

Section 2: Experimental

4.2.1. Experimental Section

4.2.1.1. General Materials and Methods

The monomers containing the nucleobases C, G and A were purchased from ASM Research Chemicals and were used for the synthesis of PNA decamer, as such without further purification. The thymine monomer *aeg*-(T) PNA-COOH was synthesized in lab. (Chapter 2, section 2). 1-[bis(dimethylamino)methylene]-1*H*-1,2,3-triazolo[4,5-*b*]pyridinium 3-oxidhexafluoro phosphate (HATU), trifluoroacetic acid (TFA), trifluoromethanesulfonic acid (TFMSA), *m*-cresol, phosphine gold chloride and Triphenylphosphine-3,3′,3″-trisulfonic acid trisodium salt (TPPTS) were purchased from Aldrich. *N*-methyl-2-pyrrolidone (NMP), *N, N*-diisopropylethylamine (DIPEA) and thioanisole were purchased from Fluorochem. Polystyrene bead carrying 4-methylbenzhydrylamine hydrochloride salt groups (MBHA resin, 0.63 mmol/g) was purchased from VWR International.

4.2.1.2. Experimental Techniques

^{1}H, ^{13}C and ^{31}P NMR spectra were recorded on Bruker 300 MHz and 70 MHz respectively. Chemical shifts (δ) are reported in parts per million relative to solvent peak. Many of the compounds described below showed many rotamers and consequently exhibit complex ^{1}H NMR patterns. Some of the signals in the ^{1}H NMR are therefore described as major (ma.) and minor (mi.) components; however, in many cases, some minor signals were obscured by the major signal of another proton. In such cases, only the major signal is reported or a range containing two or more CH_2. In some cases, the ^{13}C spectrum shows many peaks that cannot be distinguished in a small range: ov. Means ‘overlapped’. Melting points of samples were determined in open capillary tubes with a Büchi Melting Point B-540 apparatus and (dec) indicates decomposition. The IR spectra were recorded on a Perkin-Elmer FTIR 4100. Mass spectra were obtained by LCMS techniques (a Thermo Scientific LCQ Advantage). TLC was performed using TLC glass plates pre-coated with silica gel (Merck). TLCs were visualized with UV light and/or either by charring in Ninhydrine solution or developing in I_2 chamber. Silica gel 60-120 and 100-200 mesh was used for column chromatography using ethyl acetate/hexane and dichloromethane/methanol mixture as elution solvent depending upon the compound polarity and chemical nature. Commercial reagents were generally used as received. Solvents used in organic reactions were distilled under an inert atmosphere.

Unless otherwise noted, all reactions were carried out at room temperature. Oligomers were characterized by RP HPLC, using C18 column and MALDI-TOF mass spectrometry.

All weightings of reagents were carried out with analytical balance Mettler Toledo AB135-S/FACT. Vials ALLTECH of 1.5 ml, 4 ml and 8 ml with frits of PTFE were used as reactor for manual solid phase synthesis.

HPLC of PNA oligomers were performed with a HPLC AGILENT 1100 Series, using an analytical column Phenomenex Luna (15 cm x 4.6 mm, 5 μm) and a semi preparative column Phenomenex Luna C18 (25 cm x 10 mm, 10 μm).

MALDI-TOF spectra were recorded with a Bruker Daltonics Omniflex. Pulsed nitrogen lasers (337 nm) were used to generate ions that have been accelerated in a 20 kV field. The instrument was calibrated in the range from 0 to 20 kDa. Generally, Sinapinic acid and 2, 5-dihydroxybenzoic acid (DHB) matrixes were used.

A lyophilizer Telstar Cryodos were used to isolate pure PNA oligomers from aqueous solutions.

4.2.1.3. Experimental Procedures

2-(N-(2-methoxy-2-oxoethyl)-2-(5-methyl-2,4-dioxo-3,4-dihydropyrimidin-1(2H)-yl)acetamido)ethan-1-aminium salt (15)

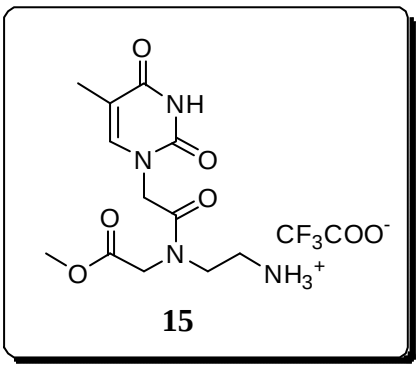

15

The compound **14** (1 gm, 2.509 mmol) was dissolved in DCM (10 mL) and 20% TFA (2 mL) was added slowly at 0 ^{o}C. Reaction mixture was allowed to stir for 2 hr at room temperature. The progress of the reaction was monitored by TLC. After completion of the reaction; reaction mixture were evaporated on rota vapour to afford pale yellowish white residue of free amine salt **15** in quantitative yield; which was used without further purification.

Molecular formula: $C_{12}H_{19}N_4O_5^+$

R*f*: 0.2 (MeOH: DCM, 50:50)

^{1}H NMR (300 MHz, MeOD-d_4 mix of rotamers**):** δ 1.88 (s, 3H); 3.15-3.31 (m, 4H); 3.70-3.76 (m, 4H); 3.83 (s, 3H); 4.18_{mi} - 4.39_{ma} (d, 2H); 4.60_{ma} - 4.75_{mi} (d, 2H); 7.29_{ma} - 7.37_{mi} (s, 1H)

4-((2-(N-(2-methoxy-2-oxoethyl)-2-(5-methyl-2,4-dioxo-3,4-dihydropyrimidin-1(2H)-yl)acetamido)ethyl)amino)-4-oxobutanoic acid (16)

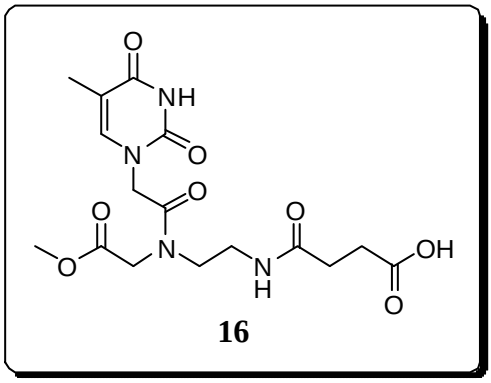

16

A mixture of succinic anhydride (2.42 gm, 24.18 mmol) and DIPEA (4.2 mL, 24.18 mmol) was added to a solution of **15** (1 gm, 2.42 mmol) in dry DMF (20 mL) at 0 °C. The reaction mixture was kept at room temperature and stirred it for overnight. Then, the solvent (dark brown colour) was evaporated at reduced pressure and the crude product was precipitated from MeOH and recovered by filtration to afford **16** (0.680 gm, 71%) as white solid. M.P.: 216 °C.

Molecular formula: $C_{16}H_{22}N_4O_8$

R*f*: 0.2 (ethyl acetate: methanol, 80:20)

FT-IR (Nujol): ν_{max}/cm^{-1} 3316, 2925, 1698, 1662, 1556, 1463, 1375

^{1}H NMR (300 MHz, DMSO-d_6: mix of rotamers**):** δ 1.75 (s, 3H), 2.27-2.43 (m, 4H), 3.14-3.41 (m, 4H), 3.31 (s, 3H), 3.63_{ma} - 3.72_{mi} (d, 2H), 4.07_{ma} - 4.31_{mi} (d, 2H), 4.47_{mi} - 4.64_{ma} (d, 2H), 7.27_{mi} - 7.33_{ma} (d, 1H), 7.80_{mi} - 7.95_{ma} (t, 1H), 11.26 (s, 1H), 12.05 (s, 1H, -COOH)

^{13}C NMR (75 MHz, DMSO-d_6: mix of rotamers**):** δ 11.87, 28.90, 29.84, 36.92, 46.69, 47.70, 48.70, 51.75, 52.24, 108.01, 142.17, 150.97, 164.36, 167.39, 169.55, 171.66, 173.84

MS (ESI) *(m/z)*: 398 $[M+1]^+$ and $[M+Na]^+$

Methyl-N-(2-(5-methyl-2,4-dioxo-3,4-dihydropyrimidin-1-(2H)-yl)acetyl)-N-(2-(4-oxo-4-(prop-2-yn-1-ylamino)butanamido)ethyl)glycinate (17)

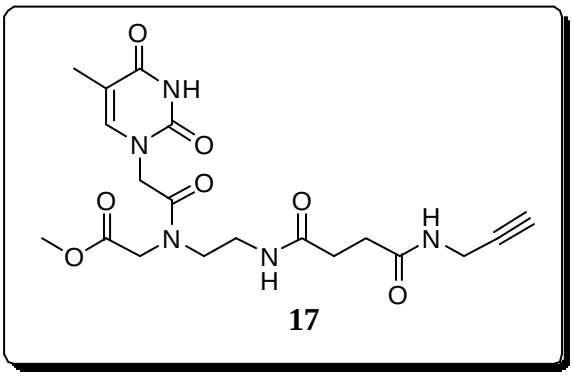

17

EDC.HCl (216 mg, 1.13 mmol) and propargyl amine (42 µL, 1.13 mmol) were added to a solution of compound **16** (150 mg, 0.37 mmol) in dry DMF (5 mL). The mixture was stirred at room temperature for overnight. The solvent were removed under vacuum and the crude product was purified by column chromatography on silica gel (ethyl acetate/MeOH 8:2) yielding **17** (135 mg, 82%) as white solid. M.P.: 192 °C.

Molecular formula: $C_{19}H_{25}N_5O_7$

R*f*: 0.6 (ethyl acetate: methanol, 80:20)

FT-IR (Nujol): ν_{max}/cm^{-1} 3294, 2936, 2724, 1716, 1674, 1643, 1536, 1213.

^{1}H NMR (300 MHz, DMSO-d$_6$ mix of rotamers**):** δ 1.75 (s, 3H); 2.29 - 2.34 (m, 4H); 3.04 - 3.28 (m, 4H); 3.62_{ma} - 3.71_{mi} (d, 2H); 3.81- 3.83 (m, 2H); 4.06_{ma} - 4.30_{mi} (d, 2H); 4.47_{mi} - 4.64_{ma} (d, 2H); 7.27_{mi} - 7.36_{ma} (d, 1H); 7.78_{mi} - 7.93_{ma} (t, 1H); 8.25 (s, 1H); 11.27 (s, 1H)

^{13}C NMR (75 MHz, DMSO-d$_6$ mix of rotamers**):** δ 12.05, 27.93, 30.20, 30.42, 37.00, 46.81, 47.90, 51.97, 52.43, 73.00, 81.38, 108.25, 142.43, 151.17, 164.64, 167.59, 169.78, 171.38, 172.22

MS (ESI) *(m/z)*: 435 $[M+1]^+$ and $[M+Na]^+$

Tert-butyl prop-2-yn-1-ylcarbamate (20)

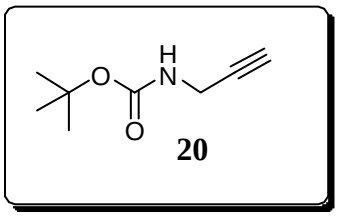

20

A solution of propargyl amine **19** (0.4 gm, 7.26 mmol) in 25% THF-H_20 (20 mL) was treated with aq. saturated $NaHCO_3$ (0.4 mL) followed by the dropwise addition of di-tertbutyl dicarbonate (1.47 gm, 7.99 mmol) and the mixture was stirred at room temperature for 5 hr. The progress of the reaction was moniterd by TLC. The reaction mixture was concentrated, extracted with ethyl acetate (3 x 10 mL) and washed with brine (5 mL). The combined organic extracts were dried over anhydrous Na_2SO_4, filtered and concentrated under reduced pressure to afford crude compound **20,** which was purified on

flash column chromatography (SiO_2) using EtOAc: Hexane (20:80) as a eluent to afford compound **20** as a white solid (0.395 gm, 35% yield) or Recrystallization in hexane to afforded **20**.

Molecular formula: $C_8H_{13}NO_2$

R*f*: 0.4 (EtOAc: Hexane; 30:70)

FT-IR (Nujol): ν_{max}/cm^{-1} 3461, 2359, 1725, 1556

^{1}H NMR (300 MHz, $CDCl_3$): δ 1.46 (s, 9H); 2.22 (t, 1H); 3.92 (s, 2H), 4.70 (bs, 1H)

^{13}C NMR (75 MHz, $CDCl_3$): δ 28.23, 30.25, 71.13, 79.94, 80.04, 155.23

Tert-butyl (3-(trimethyl silyl)prop-2-yn-1-yl) carbamate (21)

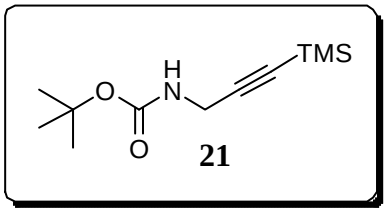

21

A solution of *n*-BuLi in hexane (1.6 M, 1.2 mL) was added to a solution of N-t-butoxycarbonylprop-2-ynylamine **20** (150 mg, 0.1 mmol) in THF (5 mL) at -78 ^oC. After 15 minutes a solution of Trimethyl silyl chloride (0.25 mL, 1.93 mmol) in THF (5 mL) was added dropwise. The mixture was stirred for an additional 1 hr at room temperature, the progress of the reaction was monitored by TLC after which a solution of AcOH (2 mL, 0.25M) was added and stirred the reaction for additional 1 hr at room temperature, the solution was concentrated under reduced pressure and extracted with ethyl acetate (3 x 10 mL). The combined organic extracts were dried over anhydrous Na_2SO_4, filtered and concentrated under reduced pressure to afford crude compound **21,** which was purified on flash column chromatography (SiO_2) using EtOAc: Hexane (20:80) as a eluent to afford compound **21** as a white solid (125 mg, 58% yield) or Recrystallization in hexane to afforded **21**.

Molecular formula: $C_{11}H_{21}NO_2Si$

R*f*: 0.5 (EtOAc: Hexane; 20:80)

FT-IR (Nujol): ν_{max}/cm^{-1} 3431, 2360, 1719, 1645

^{1}H NMR (300 MHz, $CDCl_3$): δ 0.15 (s, 9H); 1.44 (s, 9H); 3.93 (s, 2H); 4.73 (bs, 1H)

^{13}C NMR (75 MHz, $CDCl_3$): δ -0.23, 28.31, 31.40, 79.89, 87.94, 101.80, 155.15

MS (ESI) *(m/z)*: 227 $[M+Na]^+$

3-(trimethylsilyl)prop-2-yn-1-aminium 2,2,2-trifluoroacetate (22)

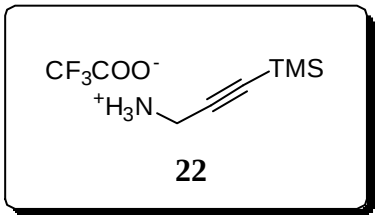

22

The compound **21** (50 mg, 0.219 mmol) was dissolved in DCM (5 mL) and 20% TFA (0.4 mL) was added slowly at room temperature reaction mixture was allowed to stir for 1 hr. The progress of the reaction was monitored by TLC. After completion of the reaction; reaction mixture were evaporated on rota vapour to afford pale yellowish residue of free amine salt **22** in quantitative yield; which was used without further purification.

Molecular formula: $C_8H_{14}F_3NO_2Si$

R*f*: 0.02 (EtOAc: Hexane; 30:70)

^{1}H NMR (300 MHz, $CDCl_3$): δ 0.16 (s, 9H); 3.78 (s, 2H); 8.19 (bs, 2H)

Methyl-2,2-dimethyl-14-(2-(5-methyl-2,4-dioxo-3,4-dihydropyrimidin-1(2H)-yl)acetyl)-7,10-dioxo-6,11,14-triaza-2-silahexadec-3-yn-16-oate (23)

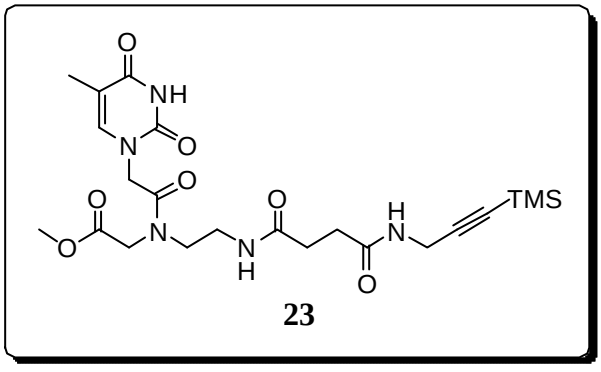

23

To a stirred solution of the compound **16** (102 mg, 0.256 mmol) in anhydrous DMF (5 mL), HOBt (47 mg, 0.307 mmol) and EDC.HCl (76 mg, 0.385 mmol) were added at 0 ^oC. Then a solution of compound **22** (62 mg, 0.256 mmol) in DMF (1 mL) was added dropwise followed by addition of DIPEA (30 µL, 1.28 mmol). The reaction mixture was stirred for an additional 12 hr at room temperature, the progress of the reaction was monitored by TLC. The solution was concentrated under reduced pressure and extracted with ethyl acetate (3 x 10 mL). The combined organic extracts were dried over anhydrous Na_2SO_4, filtered and concentrated under reduced pressure to afford crude compound **23,** which was purified on flash column

chromatography (SiO_2) using DCM: MeOH (90:10) as a eluent to afford compound **23** as a white solid (52 mg, 48% yield)

Molecular formula: $C_{22}H_{33}N_5O_7Si$

R*f*: 0.4 (DCM: MeOH: 90:10)

^{1}H NMR (300 MHz, $CDCl_3$ mix of rotamers**):** δ 0.15 (s, 9H); 1.89 (s, 3H); 2.53-2.60 (m, 4H); 3.46-3.57 (m, 4H); 3.74_{ma}-3.80_{mi} (s, 3H); 3.98-4.05 (m, 4H); 4.07_{ma}-4.23_{mi} (d, 2H); 4.47_{mi}-4.62_{ma} (d, 2H); 6.59 (bs, 1H); 7.09_{mi}-7.19_{ma} (s, 1H); 7.44 (s, 1H); 9.44 (bs, 1H)

^{13}C NMR (75 MHz, $CDCl_3$ mix of rotamers**):** δ -0.31, 12.15, 30.09, 30.70, 30.97, 37.35, 47.89, 48.11, 48.29, 52.40, 88.01, 101.22, 110.24, 117.23, 141.75, 151.44, 164.68, 167.72, 170.12, 172.08, 173.32

MS (ESI) *(m/z)*: 507 $[M+1]^+$ and $[M+Na]^+$

Synthesis of Thymine monomer PNA with gold complex (18)

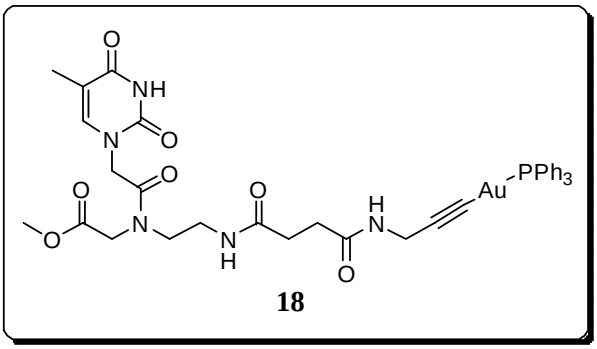

18

To a stirred solution of the compound **17** (50 mg, 0.114 mmol) in anhydrous methanol (5 mL) with a foil covered round bottomed flask. KO^{t}Bu (26 mg, 0.23 mmol) and [AuCl(PPh_3)] **12** (68.2 mg, 0.14 mmol) were added under nitrogen atmosphere for 12 hr at room temperature. The progress of reaction was monitored by TLC. After completion of reaction solvent were removed under reduced pressure, to afford an yellow coloured residue which was purified on flash column chromatography (SiO_2) using DCM/MeOH (95:05) as a eluent to afford compound **18** as a white solid (23 mg, 24% yield)

Or

To a mixture of Ph_3PAuCl **12** (48 mg, 0.098 mmol) and compound **23** (50 mg, 0.098 mmol) in anhydrous CH_2Cl_2 was added KF. $2H_2O$ (12 mg, 0.196 mmol) in methanol (1 mL) dropwise. The mixture was stirred overnight in the dark. After completion of reaction, solvent were removed under reduced pressure, to afford an yellow coloured residue which was

purified on flash column chromatography (SiO_2) using DCM/MeOH (95:05) as a eluent to afford compound **18** as a white solid (48 mg, 54% yield)

Molecular formula: $C_{37}H_{39}AuN_5O_7P$

R*f*: 0.5 (DCM: Methanol, 95: 05)

^{1}H NMR (300 MHz, $CDCl_3$ mix of rotamers**):** δ 1.86 (s, 3H); 2.46 – 2.56 (m, 4H); 3.44 - 3.54 (m, 4H); 3.74_{ma} - 3.76_{mi} (s, 3H); 4.04_{ma} - 4.06_{mi} (d, 2H); 4.11_{ma} - 4.22_{mi} (m, 2H); 4.48_{mi} – 4.65_{ma} (d, 2H); 6.41 (s, 1H); 7.05_{mi} - 7.19_{ma} (s, 1H); 7.42 – 7.55 (m, 15H); 9.03 (bs, 1H)

^{13}C NMR (75 MHz, $CDCl_3$ mix of rotamers**):** δ 12.30, 29.65, 30.64, 31.05, 31.54, 37.23, 48.41, 52.56, 53.39, 83.43, 99.25, 110.42, 128.39, 128.56, 129.10, 129.24, 131.68, 134.12, 134.30, 141.56, 151.29, 164.00, 167.70, 170.40, 171.52,172.84

^{31}P[1H] NMR ($CDCl_3$): δ_P = +43.23 ppm

MS (ESI) *(m/z)*: 893 $[M+Na]^+$; 721.71 $[PPh_3AuPPh_3]$

Synthesis of gold(I) acetylene complex (24)

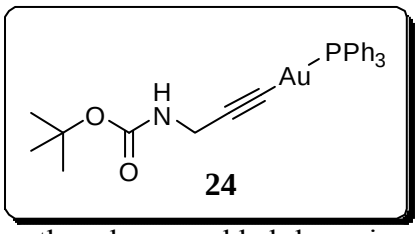

24

To a stirred solution of the compound **21** (50 mg, 0.219 mmol) in anhydrous DCM (5 mL), $[AuCl(PPh_3)]$ **12** (108 mg, 0.219 mmol) were added under nitrogen atmosphere and a solution of KF (25 mg, 0.439 mmol) in 1 mL of methanol were added dropwise and stirred it for 12 hr at room temperature. The progress of reaction was monitored by TLC. After completion of reaction solvent were removed under reduced pressure to afford an yellow coloured residue which was purified on flash column chromatography (SiO_2) using EtOAc: Hexane (30:70) as a eluent to afford compound **18** as a white solid (101 mg, 73% yield)

Molecular formula: $C_{26}H_{27}AuNO_2P$

R*f*: 0.4 (EtOAc: Hexane (30:70)

^{1}H NMR (300 MHz, $CDCl_3$ mix of rotamers**):** δ 1.46 (s, 9H); 4.11 (d, 2H); 4.72 (bs, 1H); 7.45-7.56 (m, 15H)

MS (ESI) *(m/z)*: 613 $[M+Na]^+$

Chloro(tetrahydrothiophene)gold(I) complex (27)

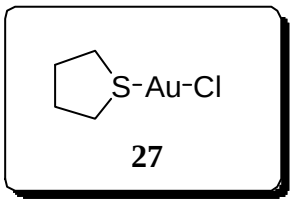

27

Potassium tetrachloroaurate(III) (0.4 gm, 0.0105 mmol) was dissolved in water (5 mL) at 0 ^oC. To this solution tetrahydrothiophene (0.3 mL, 0.0317 mmol) was added dropwise. After stirring for 0.5 hr, the pale-white solid was filtrated off, washed with water and diethyl ether, and dried under vacuum. The resulting chloro(tetrahydrothiophene)gold(I) complex **27** was used for the next step without further purification.

Molecular formula: C_4H_8AuClS

^{1}H NMR (300 MHz, $CDCl_3$): δ 2.23 (bs, 2H); 3.40 (bs, 2H)

Synthesis of (PPh_3)AuCl Complex (12)

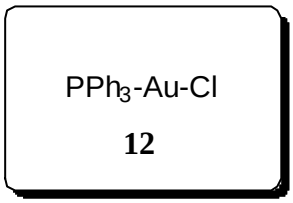

12

To a stirred solution of chloro(tetrahydrothiophene)gold(I) **27** (100 mg, 0.31 mmol) in CH_2Cl_2 (5 mL) was added dropwise a solution of the triphenyl phosphine (PPh_3) (82 mg, 0.31 mmol) in CH_2Cl_2 (3 mL) at room temperature for overnight, the solvent was removed under reduced pressure to give (PPh_3)AuCl complex **12** as a white solid in quantitative yield.

Molecular formula: $C_{18}H_{15}AuClP$

^{1}H NMR (300 MHz, $CDCl_3$): δ 7.48- 7.57 (m, 15H)

^{31}P[1H] NMR ($CDCl_3$): δ_P = +35.19 ppm

Synthesis of (TPPTS)AuCl Complex (28)

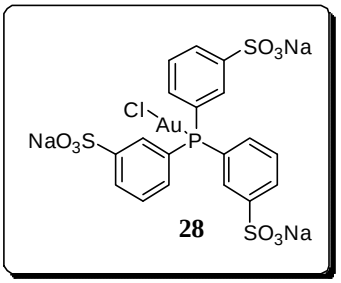

28

To a solution of ClAu(THT) **27** (40 mg, 0.124 mmol) in 6 mL degassed CH_3CN, was added *m*-trisulfonated-triphenylphosphane

(TPPTS) (71 mg, 0.124 mmol) under an argon atmosphere. 6 mL of degassed H_2O were added to dissolve the TPPTS completely. After stirring for 2 hr at room temperature under argon, CH_3CN and tetrahydrothiophene were removed on the rota vapour. The aqueous solution was then lyophilised on the freeze dryer to obtain a white solid **28** in quantitative yield.

Molecular formula: $C_{18}H_{12}AuClNa_3O_9PS_3$

^{1}H NMR (300 MHz, DMSO-d_6): δ 7.42 - 7.61 (m, 3H); 7.62 – 7.79 (m, 3H); 7.83 – 7.86 (m, 6H)

^{31}P[1H] NMR (DMSO-d_6): δ_P = +35.20 ppm

MS (ESI) *(m/z)*: 823 $[M+Na]^+$

2, 5-dioxopyrrolidin-1-yl 4-((2-(N-(2-methoxy-2-oxoethyl)-2-(5-methyl-2,4-dioxo-3,4-dihydropyrimidin-1(2H)-yl)acetamido)ethyl)amino)-4-oxobutanoate (30)

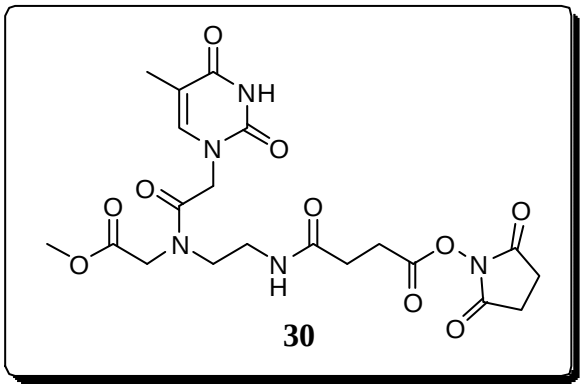

30

To a stirred solution of the compound **16** (100 mg, 0.251 mmol) in anhydrous DMF (5 mL), EDC.HCl (105 mg, 0.627 mmol) and DIPEA (0.13 mL, 0.753 mmol) were added at room temperature. *N*-Hydroxy succinimide (72 mg, 0.627 mmol) was added onto the reaction mixture and stirred it for 12 hr at room temperature, the progress of the reaction was monitored by TLC. The solution was concentrated under reduced pressure to afford crude compound **30,** which was directly purified on flash column chromatography (SiO_2) using DCM: MeOH (90:10) as a eluent to afford compound **30** as a white solid (106 mg, 85% yield)

Molecular formula: $C_{20}H_{25}N_5O_{10}$

R*f*: 0.4 (MeOH: DCM; 10:90)

^{1}H NMR (300 MHz, $CDCl_3$ mix of rotamers**):** δ 1.89 (s, 3H); 2.64 (s, 2H); 2.80 (s, 2H); 2.88 (s, 3H); 2.95 (s, 3H); 3.63 (t, 2H); 3.73 (s, 3H); 3.80 (s, 2H); 4.14_{ma} – 4.16_{mi} (d, 2H); 4.35_{mi} – 4.46_{ma} (d, 2H); 6.96 (s, 1H); 8.02 (s, 1H); 8.76 (bs, 1H)

Synthesis of Complex (31)

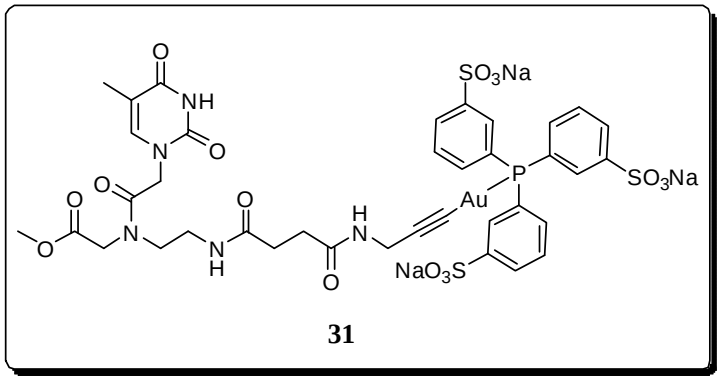

31

To a mixture of (TPPTS)AuCl **28** (17.65 mg, 0.022 mmol) and compound **23** (11.20 mg, 0.022 mmol) in anhydrous CH_2Cl_2 was added KF. $2H_2O$ (3 mg, 0.044 mmol) in methanol (0.5 mL) dropwise. The mixture was stirred at room temperature for overnight in the dark. After completion of reaction, solvent were removed under reduced pressure, to afford an yellow coloured residue which was then lyophilised on the freeze dryer to obtain a light organge solid **31** in quantitative yield.

Molecular formula: $C_{37}H_{36}AuN_5Na_3O_{16}PS_3$

^{1}H NMR (300 MHz, DMSO-d6 mix of rotamers**):** δ 1.75 (s, 3H); 2.27 – 2.41 (m, 4H); 2.74 – 2.99 (m, 4H); 3.62 (s, 3H); 3.69 - 3.87 (d, 2H); 4.05_{ma} – 4.32_{mi} (d, 2H); 4.55_{mi} – 4.70_{ma} (d, 2H); 6.53 (s, 1H); 7.37 – 7.42 (m, 16H); 11.25 (bs, 1H)

MS (ESI) *(m/z)*: Q-Tof: calculated: 1199.04; found 1238.39 $[M+K]^+$

4-oxo-4-(prop-2-yn-1-ylamino)butanoic acid

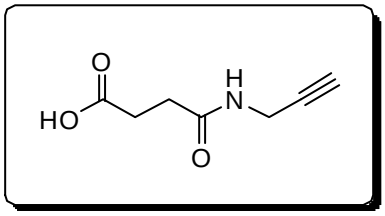

A solution of succinic anhydride (300 mg, 2.99 mmol), propargylamine (29 μL, 4.49 mmol) and 4-DMAP (330 mg, 2.69 mmol) in CH_2Cl_2 (10 mL) was stirred for 3 hr at room temperature. Then, the mixture was washed with a solution of 5% Na_2CO_3 (10 mL). The aqueous layer was acidified with a 1 N HCl solution and then extracted with ethyl acetate (3 X 10 mL). The combined organic extracts were dried over anhydrous Na_2SO_4, filtered and concentrated under reduced pressure to afford compound **XX** (465 mg, 88%).

Molecular formula: $C_7H_9NO_3$

R*f*: 0.5 (CH_2Cl_2/MeOH/AcOH)

FT-IR (Nujol): ν_{max}/cm^{-1} 3293, 2724, 1698, 1634, 1555,

^{1}H NMR (300 MHz, $CDCl_3$): δ 2.31- 2.32 (m, 2 H); 2.40-2.42 (m, 2H), 3.08 (s, 1H); 3.82 (s, 2H); 8.29 (s, 1H); 12.07 (s, 1H)

^{13}C NMR (75 MHz, $CDCl_3$): δ 27.84, 28.92, 29.71, 72.99, 81.26, 170.76, 173.80

MS (ESI) *(m/z)*: 155 $[M+Na]^+$

Loading (0.2 mmol/gm) of thymine monomer 33 on MBHA resin (34)

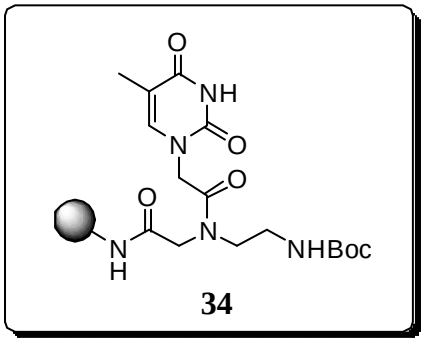

34

The MBHA resin **32** (0.2 gm) was washed with CH_2Cl_2 (2 x 5 mL) and activated by treatment with 5% DIPEA in CH_2Cl_2 for 5 min for 3 times; and then washed with CH_2Cl_2 (2 x 5 mL). In a vial, DIPEA (14 μL, 0.08 mmol) was added to a solution of thymine monomer **33** (15.38 mg, 0.04 mmol) in NMP (1 mL); then, a solution of HBTU (15.17 mg, 0.04 mmol) in NMP (1 mL) in another vial and add this solution into the monomer solution, and activate the monomer solution for 2 minutes. This mixture was then added to the neutralized resin and shakes it on orbital shaker for 12 hr. The resin was washed with NMP (3 x 5 mL). A solution of Ac_2O/Py/NMP 1:2:2 (5 mL) was added to the resin (capping of unreacted amino groups) and left under stirring at rt for 1 hr. After this time, the resin was washed with NMP (3 x 5 mL), CH_2Cl_2 (4 x 5 mL), 5% DIPEA in CH_2Cl_2 (2 x 5 mL) and again with CH_2Cl_2 (4 x 5 mL); and finally dried in vacuum to afford the MBHA resin downloaded with thymine monomer **34** (0.242 gm); Kaiser Test: negative.

Synthesis of homo-thymine decamer (35) on solid phase

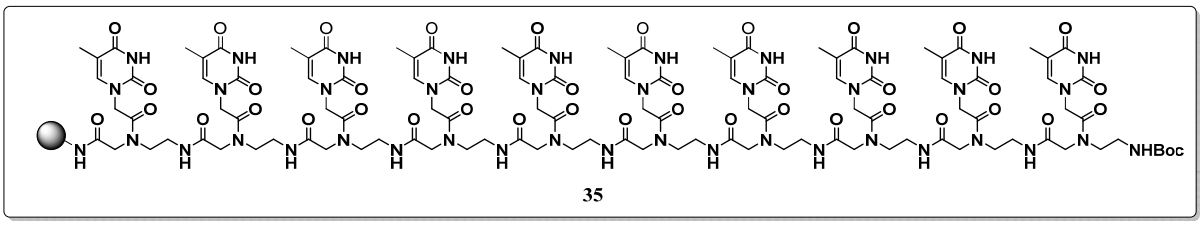

35

The resin **34** (100 mg, substitution with 0.2 mmol/g) was placed in a reaction vessel (volume; 8 mL) and which was swollen with CH_2Cl_2 for 30 minutes, the Boc group of the loaded monomer was removed by treatment with TFA/*m*-cresol (95:5), (3 mL, 2 x 4 min). The resin

was washed with CH_2Cl_2 (2 x 5 mL) and then treated with CH_2Cl_2/DIPEA (95:5), (3 mL, 2 x 2 min). Then the resin was washed thoroughly with CH_2Cl_2 (2 x 5 mL). In a vial, DIPEA (35 µL, 0.2 mmol, 10 eq.) was added to a solution of Thymine monomer **33** (40.7 mg, 0.106 mmol, 5.3 eq.) in NMP (500 µL); then, a solution of HATU (38 mg, 0.1 mmol, 5 eq.) in NMP (500 µL) in another vial and add this solution into the monomer solution, and activate the monomer solution for 2 minutes. This mixture was then added to the neutralized resin and shaken for 2 hr at room temperature. After coupling step the resin was filtered, washed with NMP (3 x 5 mL) and CH_2Cl_2 (3 x 5 mL). Then resin treated with Ac_2O/Py/NMP; 1:25:25 capping solution twice for 1 min. and again washed the resin with CH_2Cl_2 (3 x 5 mL), NMP (3 x 5 mL) and CH_2Cl_2 (3 x 5 mL). The cycle was repeated using thymine monomer **33** with the same protocol and after the last coupling and capping the resin was washed with several times with NMP and CH_2Cl_2 and finally dried the resin under vacuum to afford the corresponding supported PNA homothymine decamer on resin **35** (138 mg).

Short cleavage: The resin **35** (5 mg) was washed with TFA (2 × 100 µL) and subsequently stirred for 1 hr with a mixture of TFA/TFMSA/thioanisole/*m*-cresol [6:2:1:1 v/v] (300 µL). The reaction mixture was filtered, and the resin washed with TFA (4 × 100 µL). The filtrate was concentrated under nitrogen flow and Et_2O (5 mL) was added to precipitate PNA as a white solid. Centrifugation of the slurry gave the product, which was washed with Et_2O (8 x 5 mL) and dried to afford the crude homothymine decamer **35'** as a white solid.

Retention time (analytic column 15 cm); gradient from 95% of H_2O/TFA 0.1% to 100% of AcCN/TFA 0.1%) = 11.84 min.

Maldi Tof MS: found *m/z*: 2680.00 $[M]^+$, calculated for $C_{110}H_{144}N_{41}O_{40}^+$: 2679.05

Synthesis of homo-thymine decamer with terminal alkyne (37) on solid phase

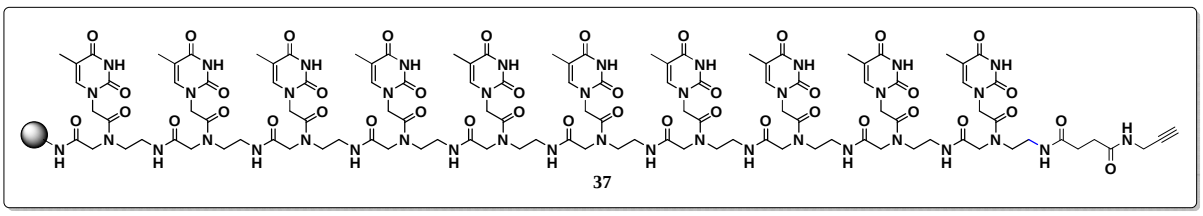

37

The resin **35** (50.5 mg) was placed in a reaction vessel (volume; 8 mL) and which was swollen with CH_2Cl_2 for 30 minutes, the Boc group of the loaded homothymine decamer was

removed by treatment with TFA/*m*-cresol (95:5), (2 mL, 2 x 4 min). The resin was washed with CH_2Cl_2 (2 x 5 mL) and then treated with CH_2Cl_2/DIPEA (95:5), (2 mL, 2 x 2 min). Then the resin was washed thoroughly with CH_2Cl_2 (2 x 5 mL). In a vial, DIPEA (18 µL, 0.101 mmol, 10 eq.) was added to a solution of propargyl acid **36** (8.6 mg, 0.055 mmol, 5.5 eq.) in NMP (500 µL); then, a solution of HATU (19.20 mg, 0.055 mmol, 5 eq.) in NMP (500 µL) in another vial and add this solution into the monomer solution (propargyl acid), and activate the monomer solution for 2 minutes. This mixture was then added to the neutralized resin and shaken for 2 hr at room temperature. After coupling step the resin was filtered, washed with NMP (3 x 5 mL) and CH_2Cl_2 (3 x 5 mL) and finally dried the resin under vacuum to afford the corresponding supported resin of PNA homothymine decamer **37** (58 mg).

Synthesis of homo-thymine decamer with terminal alkyne (38)

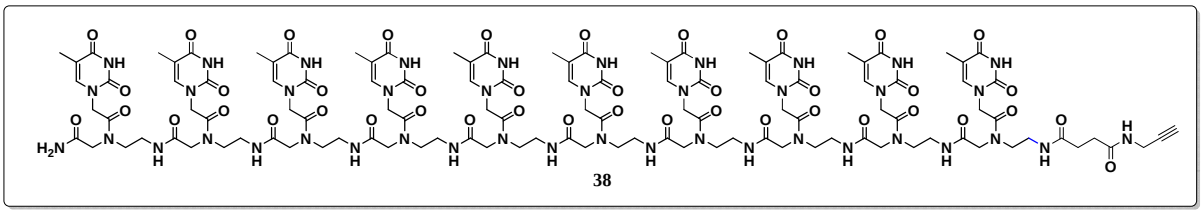

38

Cleavage: The resin **37** (58 mg) was washed with TFA (2 × 200 µL) and subsequently stirred for 1 hr with a mixture of TFA/TFMSA/thioanisole/*m*-cresol [6:2:1:1 v/v] (500 µL). The reaction mixture was filtered, and the resin washed with TFA (4 × 200 µL). The filtrate was concentrated under nitrogen flow and Et_2O (5 mL) was added to precipitate PNA as a white solid. Centrifugation of the slurry gave the product, which was washed with Et_2O (8 x 5 mL) and dried to afford the crude homothymine decamer **38** (14.5 mg). Purification of the crude PNA by RP-HPLC afforded the homothymine decamer **38** as a white solid.

Retention time (analytic column 15 cm); gradient from 95% of H_2O/TFA 0.1% to 100% of AcCN/TFA 0.1%) = 12.80 min.

Maldi Tof MS: found *m/z:* 2816.09 $[M]^+$, calculated for $C_{117}H_{150}N_{42}O_{42}$: 2855 $[M+K]^+$

List of Publications

1. “Is it possible to study the kinetic parameters of interaction between PNA and parallel and antiparallel DNA by stopped-flow fluorescence?” N. Barbero, S. Cauteruccio, **P. Thakare**, E. Licandro, G. Viscardi, S. Visentin; *Journal of Photochemistry & Photobiology, B: Biology* **2016**,*163*, 296-302.

2. “Fischer carbene mediated covalent grafting of a peptide nucleic acid on gold surfaces and IR optical detection of DNA hybridization with a transition metal carbonyl label”; Pratima Srivastava, Mahsa Ghasemi, Namrata Ray, Amitabha Sarkar, Jana Kocabova, Stepanka Lachmanova, Magdalena Hromadova, Souhir Boujday, Silvia Cauteruccio, **Pramod Thakare**, Emanuela Licandro, Celine Fosse, Michele Salmain; *Applied Surface Science*, **2016**, *385*, 47 55

3.“Superparamagnetic Iron Oxide Nanoparticles Functionalized by Peptide Nucleic Acids”; Marco Galli, Andrea Guerrini, Silvia Cauteruccio, **Pramod Thakare**, Davide Dova, Francesco Orsini, Paolo Arosio, Claudio Carrara, Claudio Sangregorio, Alessandro Lascialfari, Daniela Maggioni, Emanuela Licandro; *Journal of Material Chemistry B.(communicated)*

Erratum